SPACE-TIME TURBO CODING FOR CDMA MOBILE COMMUNICATIONS

D.J. van Wyk

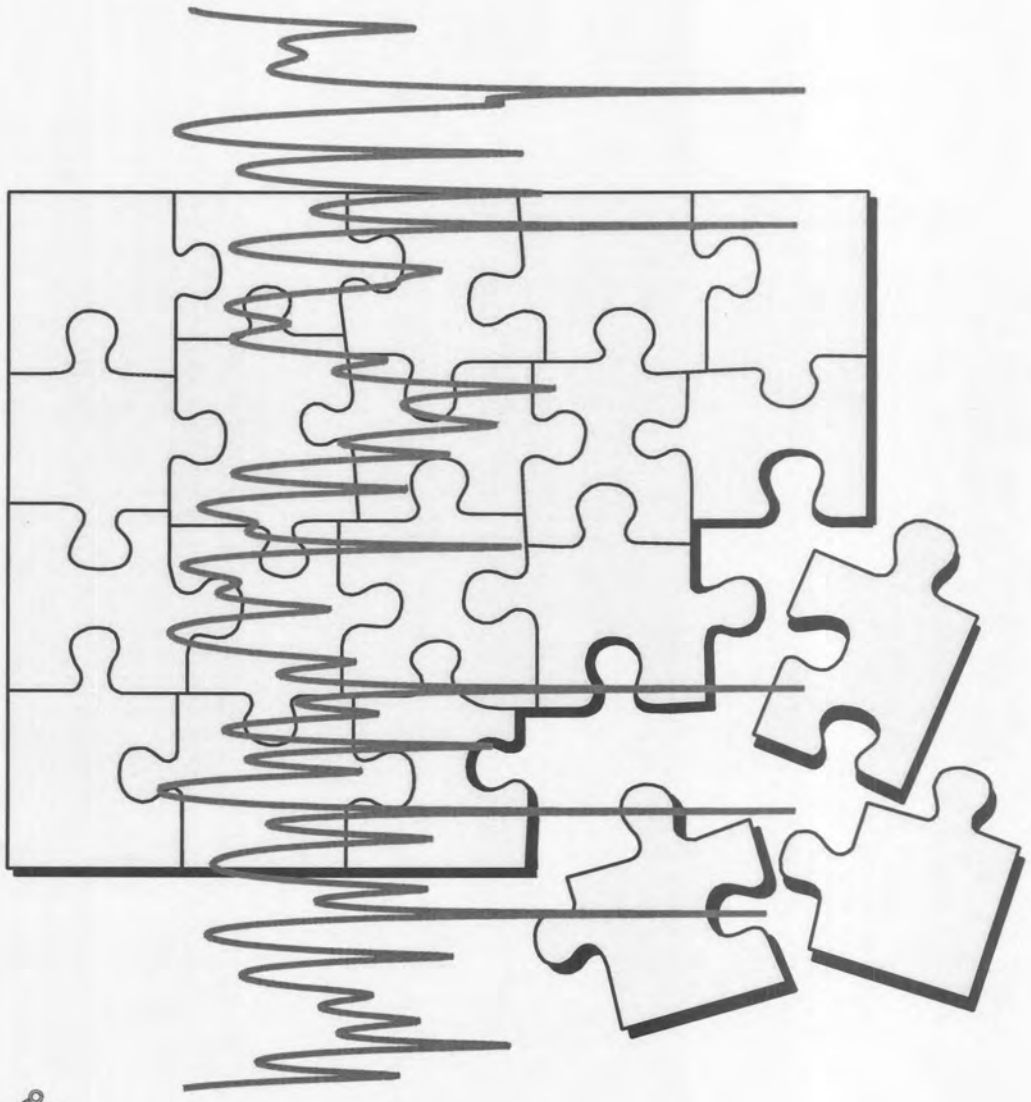

University of Pretoria

SPACE-TIME TURBO CODING FOR CDMA MOBILE COMMUNICATIONS

by

Daniël Jacobus van Wyk

Doctoral thesis submitted as partial fulfilment
of the requirements for degree

Doctor of Philosophy

in

Electrical and Electronic Engineering

in the

Faculty of Engineering, Built Environment and
Information Technology

at the

University of Pretoria

August 2000

Dedication

This thesis is dedicated to my wife, Daleen, for all her love, patience, and support, and for all the sacrifices that she has made so that I could complete this research.

It is also dedicated to my son NW, for the joy that he has brought to my life, and to my parents for all of their love and support of me in all of my endeavors.

SPACE-TIME TURBO CODING FOR CDMA MOBILE COMMUNICATIONS

Daniël Jacobus van Wyk

Department of Electrical and Electronic Engineering

Faculty of Engineering, Built Environment and Information Technology

University of Pretoria

Degree: Philosophiae Doctor

Supervisor: Prof. L.P. Linde

SUMMARY

Against the background of the rapid evolution of mobile communication systems in the areas of service provision and capacity enhancement described above, the main focus of the research is on coded space-time processing techniques. The use of space-time processing is an attractive solution because it can mitigate the effects of multipath fading as well as suppress co-channel interference, therefore, significantly improving system performance. The topics are presented in the context of designing mobile communication systems where the two core areas of spatial processing and error coding are to be integrated in an optimum way. Of particular importance in this thesis, will be those CDMA based solutions for the mobile sector and the new performance analysis issues that need to be addressed as a result of the introduction of heterogeneous services and service environments into a single, mobile cellular access network. Furthermore, novel applications of turbo transmit and receive antenna diversity and beamforming techniques to mobile cellular access networks aimed at increasing the efficiency of such networks are considered. The thesis has the following goals:

- To establish a general spatial/temporal channel model for use in the evaluation of coded space-time processing concepts applied to CDMA networks.
- To analyze the performance of uncoded cellular CDMA systems incorporating space-time techniques using analytical methods in a number of realistic application scenarios.
- To design, implement and evaluate coding strategies for incorporation into the space-time CDMA systems. This objective can be broken down into the following items:
  - Space-time coding systems when considering multiple transmit antennas for the downlink.
  - Coded space-time systems when considering multiple receive antennas for the uplink.
- To establish the performance of coded space-time CDMA cellular networks under realistic scenarios.

This thesis introduces many (some novel) space-time turbo coded techniques to increase the downlink capacity of a cellular CDMA network using multiple transmit antennas. For improving the uplink capacity, coded space-time diversity and beamforming techniques, employing multiple receive antennas, are considered. In order to quantify the performance improvements that may be achieved, a framework for the evaluation of

these systems are constructed. Using this framework the BEP of all the space-time coding systems are derived analytically, and evaluated under identical propagation scenarios. The results presented show that the use of space-time turbo coded processing is an attractive solution since it can improve system performance significantly under conditions of multipath fading for both the uplink and downlink. It is shown that the two core areas of spatial processing and channel coding can be integrated in an optimum way to increase the capacity of existing cellular CDMA networks.

Key Words: Mobile Digital Wireless Communication, Multiple-Access Communication, Error Correction Coding, Multiple Transmit and Receive Antenna, Space-Time Diversity and Beamforming, Turbo Transmit Diversity.

Department of Electrical and Electronic Engineering University of Pretoria

UNIVERSITEIT VAN PRETORIA
UNIVERSITY OF PRETORIA
YUNIBESITHI YA PRETORIA

SPACE-TIME TURBO CODING FOR CDMA MOBILE COMMUNICATIONS

Daniël Jacobus van Wyk

Departement Elektriese en Elektroniese Ingenieurswese

Fakulteit Ingenieurswese, Bou-omgewing en Inligtingtegnologie

Universiteit van Pretoria

Graad: Philosophiae Doctor

Studieleier: Prof. L.P. Linde

OPSOMMING

Gemeet teen die agtergrond van die snelle ontwikkeling van mobiele kommunikasiestelsels en dienste, asook die fisiese beperkings gestel deur beskikbare bandwydte en seindrywing, ondersoek die proefskrif ruimte-tyd kodeerde prosesseringstegnieke vir huidige en toekomstige multi-gebruiker CDMA sprei-spektrum kommunikasiestelsels. Die gebruik van ruimte-tyd prosessering is uiters geskik vir mobiele kommunikasie aangesien dit die effekte van multipad voortplanting en ko-kanaalsteurings teen kan werk. In die proefskrif word die twee kern areas van ruimte prosessering en foutkorreksiekodering optimaal geintegreer. Die proefskrif het die volgende doelwitte:

- Om 'n algemene ruimte/tyd kanaalmodel op te stel waarmee die voorgestelde foutkorreksie kodeerde ruimte-tyd prosesseringskonsepte en algoritmes teen evalueer kan word. Laasgenoemde kanaalmodel sluit ook ruimte-tyd korrelasie modelering in.
- Om die verwerrigting van ongekodeerde ruimte-tyd sellulêre CDMA kommunikasiestelsels te evalueer deur middel van analitiese metodes onder realistiese toepassingskondisies.
- Om die ontwerp, implementering en verwerrigtinganalises van ruimte-tyd kodeerde sellulêre CDMA kommunikasiestelsels uit te voer vir insluiting in huidige en toekomstige CDMA kommunikasiestelsels. Hierdie doelwit word verder onderverdeel:
  - Ruimte-tyd koderingstelsels wanneer multi-antenna elemente by die basisstasie-sender vir seintransmissie in die voorwaartse pad beskikbaar is.
  - Gekodeerde ruimte-tyd stelsels wanneer multi-antenna elemente by die basisstasie-ontvanger vir seinontvangs in die tru-waartse pad beskikbaar is. Hier word gekyk na beide ontvanger diversiteit en antenna patroonvorming.
- Om die verwerrigting van ruimte-tyd kodeerde sellulêre CDMA kommunikasiestelsels te evalueer deur middel van analitiese metodes onder realistiese toepassingskondisies.

Hierdie proefskrif stel verskeie (sommige uniek) ruimte-tyd turbo gekodeerde tegnieke voor vir die kapasiteitverbetering van sellulêre CDMA kommunikasiestelsels in die voorwaarste pad wanneer van multi-anttena elemente vir seintransmissie gebruik gemaak word by die basisstasie. Om die kapasiteit in die

tru-waartse pad te verbeter word foutkorreksie kodeerde diversiteit en patroonvormingstegnieke voorgestel vir implementering by die ontvanger basisstasie. Die navorsingsresultate dui daarop dat die voorgestelde ruimte-tyd kodeerde prosesseringstegnieke uitstekend geskik is vir die verbetering van beide die voorwaartse en tru-waartse paaie. Die proefskrif lê hiermee die grondslag vir die ontwerp en evaluasie van ruimte-tyd prosesseringstegnieke vir toekomstige CDMA sellulêre kommunikasienetwerke.

Sleutelwoorde: Mobiele Syferkommunikasie, Multi-Gebruiker Kommunikasie, Foutkorreksiekodering, Multi-Versend en Ontvangs Antennas, Ruimte-Tyd Diversiteit en Antenna Patroonvorming, Turbo Versend Diversiteit.

Department of Electrical and Electronic Engineering University of Pretoria

PREFACE

I would like to thank my Creator, to Him all the praise !

The research work contained in this thesis has been carried out at the University of Pretoria in the Department of Electrical and Electronic Engineering.

I am indebted to many people for their advice and assistance towards the successful completion of this thesis.

In particular to my supervisor, Prof. Louis Linde for directing this research and his constant and enthusiastic encouragement. I am immensely thankful for his support and guidance which started while I was still an undergraduate student. His superb supervision and most professional approach, in every way, has benefited me tremendously.

The discussions I have had with Dr. Ian Oppermann stimulated many of the ideas presented in this thesis. I would also like to thank him for the tremendous support, and enthusiasm over the past few years. I also thank him for the great opportunity to go to Sydney as a research fellow of Southern Poro Communications.

I would also like to express my deepest appreciation to Dr. Pieter van Rooyen and Dr. Michiel Lötter for the invaluable discussions and suggestions throughout the course of my research. I have had the pleasure to work with them during the writing of our book on "Space-time processing for CDMA". Without this project, my journey towards this thesis would have been even more difficult.

To my research colleagues and friends Dr. Jack Glass, Dr. Rupert Herzog, Dr. Matt Valenti, Dr. Giorgio Tarrico, Jacques Cilliers, Etiënne Pretorius and Momin Jamil my sincere thanks. A special word of gratitude is expressed to Etiënne for the many hours of discussions on CDMA and coding. We have made such a great team and I sincerely hope that we can work together again in future.

Special thanks go to Dr. Ian Oppermann, Dr. Matt Valenti and Dr. Khaled B. Letaief who provided the most comprehensive proofreading of the thesis that I have received.

For financial assistance and unique opportunities I thank the University of Pretoria and CSIR Defencetek. For the time granted me to finish the research and the frequent words of encouragement, I thank my colleagues at CSIR Defencetek.

To my parents, parents in-law and sisters for their unselfish support. Finally, I would also express my deepest gratitude to my wife Daleen and son NW, for their continuous support and love. I dedicate this thesis to them.

CONTRIBUTIONS

Most of the results presented in this thesis have been published or have been submitted for publication in international conferences and journals. During the research which has lead to this thesis, the following publications have been prepared. In addition an international patent was filed (see 18) and a book by Kluwer Academic Publishers (KAP) was published (see 23).

1 D.J. van Wyk & L.P. Linde (November, 1996) Hybrid block-convolutional rate-1/2 coding strategy for constant envelope (CE)Q^2PSK. In: IEE Electronics Letters, vol. 32, no. 24, pages 2204-2206.

2 D.J. van Wyk, M.P. Lötter, L.P. Linde & P.G.W. van Rooyen (September, 1997) A multiple trellis coded Q^2PSK system for wireless local loop. In: Proceedings of IEEE International Symposium on Personal Indoor and Mobile Radio Communications, Helsinki, Finland, pages 624-628.

3 B. Westra, D.J. van Wyk, J.E. Cilliers & L.P. Linde (September, 1997) Performance evaluation of multi-level four-dimensional Q^2PSK in Gaussian noise. In: South African Symposium on Signal Processing, Stellenbosch, South Africa, pages 141-146.

4 D.J. van Wyk & L.P. Linde (October, 1997) A multiple trellis coded Q^2PSK system for personal communication. In: Proceedings of IEEE International Conference on Universal Personal Communication, San Diego, California, U.S.A., pages 259-263.

5 D.J. van Wyk & L.P. Linde (March, 1998) Rate-1/2 trellis coding for Q^2PSK operating on the Rician fading channel. In: Transactions of the SAIEE, pages 33-39.

6 J.E. Cilliers, L.P. Linde & D.J. van Wyk (September, 1998) A syncronous Q^2PSK DS-CDMA system: System conceptualisation, implementation and performance analysis. In: Proceedings of IEEE International Symposium on Spread-Spectrum Techniques and Applications, Sun City, South Africa, pages 4-8.

7 D.J. van Wyk & L.P. Linde (September, 1998) Turbo-Coded/Multi-antenna diversity combining scheme for DS/CDMA systems. In: Proceedings of IEEE International Symposium on Spread-Spectrum Techniques and Applications, Sun City, South Africa, pages 18-22.

8 D.J. van Wyk & L.P. Linde (September, 1998) A Turbo Coded DS/CDMA system with embedded Walsh-Hadamard codewords: Coder design and performance evaluation. In: Proceedings of IEEE International Symposium on Spread-Spectrum Techniques and Applications, Sun City, South Africa, pages 359-363.

9 M.Jamil, L.P. Linde, J.E. Cilliers & D.J. van Wyk (September, 1998) Comparison of complex spreading sequences based on filtering methods and mean square correlation characteristics. In: Transactions of the SAIEE, pages 98-112.

10 D.J. van Wyk & L.P. Linde (September, 1998) Design and performance evaluation of a turbo/Walsh-Hadamard coded QPSK DS/CDMA system. In: Transactions of the SAIEE, pages 120-130.

11 D.J. van Wyk, L.P. Linde & P.G.W. van Rooyen (June, 1999) On the performance of a turbo-coded/multi-antenna transmission diversity scheme for DS/CDMA systems with adaptive channel estimation. In: International Conference on Telecommunications, Cheju, Korea.

12 D.J. van Wyk & L.P. Linde (June, 1999) Multiple trellis coded Q^2PSK: Code design and performance study on fading channels. In: Transactions of the South African Institute of Electrical Engineers, pages 90-98.

13 D.J. van Wyk, I.J. Oppermann & L.P. Linde (September, 1999) Low rate coding considerations for space-time coded DS/CDMA. In: Proceedings of IEEE Vehicular Technology Conference, Amsterdam, The Netherlands, pages 2520-2524.

14 D.J. van Wyk, I.J. Oppermann, E. Pretorius & P.G.W. van Rooyen (September, 1999) On the construction of layered space-time coded modulation STCM codes employing MTCM code design techniques. In: Proceedings of IEEE Vehicular Technology Conference, Amsterdam, The Netherlands, pages 2969-2973.

15 M.Jamil, L.P. Linde & D.J. van Wyk (September, 1999) An analysis of the effects of filtering on the correlation characteristics of 4-phase sequences for CDMA applications. In: Proceedings of IEEE Africon, pages 227-232.

16 D.J. van Wyk, I.J. Oppermann, & L.P. Linde (November, 1999) Performance tradeoff among spreading, coding and multiple-antenna transmit diversity for high capacity space-time coded DS/CDMA. In: Proceedings of MILCOM, Atlantic City, New Jersey, U.S.A., Session 14-1.

17 D.J. van Wyk, & L.P. Linde (November, 1999) Fading Correlation and its effect on the capacity of space-time turbo coded DS/CDMA systems. In: Proceedings of MILCOM, Atlantic City, New Jersey, U.S.A., Session 18-4.

18 D.J. van Wyk and P.G.W. van Rooyen (February, 2000). Super-orthogonal turbo transmit diversity. Preliminary International Patent. Sony Laboratories, Japan.

19 D.J. van Wyk, I.J. Oppermann, P.G.W. van Rooyen & L.P. Linde (February, 2000). Space-time coded transmit diversity for CDMA. A submission to the IEEE Transactions on Communication.

20 D.J. van Wyk, M.P. Lötter, P.G.W. van Rooyen & L.P. Linde (February, 2000). On the performance of coded space-time receive diversity and beamforming for CDMA communications. A submission to the IEEE Transactions on Communication.

21 M. Jamil, K. Kryzmien, D.J. van Wyk & L.P. Linde (February, 2000). Performance analysis of constant envelope quadriphase sequences for CDMA. A submission to the IEEE ISSSTA'00.

22 D.J. van Wyk, P.G.W. van Rooyen & L.P. Linde (February, 2000). On the performance of super-orthogonal turbo transmit diversity for cellular CDMA. A submission to the IEEE ISSSTA'00.

23 P.G.W. van Rooyen, M.P. Lötter & D.J. van Wyk (February, 2000) Space-Time Processing for CDMA mobile communications, Kluwer Academic Publishers.

24 D.J. van Wyk, P.G.W. van Rooyen & L.P. Linde (February, 2000). On turbo transmit diversity for cellular CDMA. A submission to the International Turbo Coding Symposium 2000.

25 D.J. van Wyk, J.E. Cilliers & F. Lessing (February, 2000). On the detection and characterization of covert radio signals. Accepted for publication in MCF&EW Seminar.

26 D.J. van Wyk & L. Botha (March, 2000). Wideband CDMA for wireless communication systems. In: Elektron Journal, pages 16-19.

27 J.E. Cilliers, D.J. van Wyk & L.P. Linde (April, 2000). Performance of multi-dimensional QPSK under CDMA multiuser interference conditions. In preparation.

28 I.J. Oppermann & D.J. van Wyk (April, 2000). Space-time convolutional coded CDMA employing an LMMSE receiver. In preparation.

LIST OF ABBREVIATIONS

2G	second generation
3G	third generation
ACTD	Alamouti code transmit diversity
AS-TDTD	antenna-selection time-division transmit diversity
AWGN	additive white Gaussian noise
BEP	analytical bit error probability
BER	bit error rate
BCH	Bose and Ray-Chaudhuri codes
BPSK	binary phase-shift keying
BRAN	broadband radio access channel
BSS	base station subsystem
CC	convolutional coded
CDS	circular disk of scatterers
CDSM	circular disk of scatterers model
CDMA	code-division multiple-access
CDTD	code-division transmit diversity
CIR	carrier-to-interference ratio
CL-AS	closed-loop antenna-selection
CLPC	closed-loop power control
cpdf	conditional probability distribution function
CSI	channel state (or side) information
dB	decibel
DECT	digital enhanced cordless telephone
DOA	direction-of-arrival
DS	direct-sequence
DTD	delay transmit diversity
EEP	error-event path
EFD	effective fading distribution
EGC	equal gain combining
EMF	estimated matched filter
ESM	effective scatterer model
ETSI	European telecommunications standards institute
FDD	frequency-division duplex
FDMA	frequency-division multiple-access
FEC	forward error correction
FIR	finite impulse response
FPLMTS	future personal land mobile telephone system

GAA	Gaussian angle of arrival (model)
GFD	Gaussian fading distribution
GS	Gaussian scatterer model
GSM	global system for mobile communications (formerly: Groupe Spécial Mobile)
HDD	hard decision decoding
IIR	infinite impulse response
IMT-2000	international mobile telecommunications for the 21st century
IN	intelligent network
IP	internet protocol
IPI	inter-path-interference
IRWEF	input redundancy weight enumerating function
ISI	inter-symbol interference
IS-54	interim standard 54
IS-95	interim standard 95
ITU	international telecommunications union
LAN	local area network
LMS	least mean squares
LMMSE	least mean minimum square error
LOS	line of sight
LSED	layered squared Euclidean distance
LSEDP	layered squared Euclidean distance product
MACH	multiple-access channel
MAI	multiple-access intereference
MAP	maximum a posteriori
MF	matched filter
MFD	maximum free distance
MIMO	multiple input/multiple output
MISO	multiple input/single output
ML	maximum likelihood
MLSD	maximum likelihood sequence detection
MLSE	maximum likelihood sequence estimation
MM	multi media
MMSE	minimum mean square error
MPSK	multiple phase-shift keying
MRC	maximal ratio combining
MSE	mean square error
MTCM	multiple trellis-coded modulation
MU	multiuser
MUD	multiuser detection (or demodulation)
MUSIC	multiple signal classification

NLMS	normalized LMS
NLOS	non line of sight
NO-CDTD	non-orthogonal (delayed) CDTD
O-CDTD	orthogonal code-division transmit diversity
OTD	orthogonal transmit diversity
OVSF	orthogonal variable spreading factor
PCTTD	parallel-concatenated turbo transmit diversity
pdf	probability distribution function
PCS	personal communication system/service
PN	pseudo-noise
PSA	pilot symbol assisted
PSK	phase-shift keying
QoS	quality-of-service
QPSK	quadrature phase-shift keying
Q^2PSK	quadrature-quadrature phase-shift keying
RCCC	rate-compatible convolutional codes
RF	radio frequency
RMS	root mean square
RS	Reed-Solomon codes
RSC	recursive systematic convolutional
RSC&WH	recursive systematic convolutional and Walsh-Hadamard
RR-TDTD	round-robin time-division transmit diversity
SC	selection combining
SCTTD	serial-concatenated turbo transmit diversity
SDD	soft-decision decoding
SDMA	space division multiple access
SIMO	single input/multiple output
SINR	signal-to-interference-noise ratio
SISO	single (soft) input/single (soft) output
SNR	signal-to-noise ratio
SOCC	super-orthogonal convolutional code
SOTC	super-orthogonal turbo code
SOTTD	super-orthogonal turbo transmit diversity
SOVA	soft-output Viterbi algorithm
SS	spread-spectrum
STCM	space-time coded modulation
STTCM	space-time turbo coded modulation
SU	single user

TCM	trellis coded modulation
TCS	trellis coded spreading
TD-CDMA	time division CDMA
TDD	time-division duplex
TDMA	time-division multiple-access
TDTD	time-division transmit diversity
T/F/C	time, frequency and code
T-MTCM	turbo multiple trellis coded modulation
TOA	time of arrival
TPC	transmit power control
TTCM	turbo trellis coded modulation
TTD	turbo transmit diversity
TU	typical urban
UHF	ultra high frequency
ULA	uniform linear array
UMTS	universal mobile telephone system
UTRA	UMTS terrestrial radio access
VSF	variable spreading factor
WEF	weight enumerating function
WH	Walsh-Hadamard
WLL	wireless local loop
WSS	wide-sense stationary
WCDMA	wideband code-division multiple-access

LIST OF SYMBOLS

arg	argument
max	maximum
$\{-1, 1\}$	binary set
$\|\| \cdot \|\|$	Euclidean distance
$(\cdot)^H$	Hermitian
A_d^C	number of codewords of weight d
$A_{i,d}^C$	number of codewords of weight d for input weight i
$A^C(I, D)$	weight enumerating function
$A^{C_i}(I, D)$	weight enumerating function inner code
$A^{C_o}(I, D)$	weight enumerating function of outer code
$A_{gff/gfb}$	feedforward and feedback generator polynomial
A_k	received amplitude
$a_k(t)$	binary spreading waveform
β_k	received signal strength in volts
$\beta_l^{(k)}(i)$	strength of specific multipath
$\mathbf{b}$	vector of data bits
$\hat{\mathbf{b}}$	specific version of $\mathbf{b}$
$\mathbf{b}_i$	vector of bits for interval i
$b_k(t)$	binary data sequence
$b_i^{(k)}$	bit for user k, symbol interval i
$\tilde{\mathbf{b}}_i^{(k)}$	vector of bits up until user k symbol interval i
$\hat{\mathbf{b}}(s)$	bit estimate vector for stage s
$\hat{\mathbf{b}}_{ML}$	maximum likelihood estimate of $\mathbf{b}$
$\mathcal{BW}$	total signal bandwidth
$\mathcal{BW}_{ch}$	coherence bandwidth
C_i	inner code
C_o	outer code
C_{tot}	total capacity
$\mathbf{c}_n$	codeword
d	Hamming weight
d_{free}	free distance
$d_i^{(k)}$	element for user k symbol interval i of $\mathbf{D}$
$d^{(j)}(t)$	reference signal for user j
$\mathbf{D}$	code matrix
δ	scalar difference
$\text{erfc}(x)$	complimentary error function of x
$E(\mathbf{y})$	expected value of $\mathbf{y}$

E_b	energy per bit
$E_{d\|i}$	expectation w.r.t. distribution $\rho(d \mid i)$
$E_{P_{ACTD}}(\mathbf{X}, \mathbf{Y})$	product distance for ACTD
$E_{P_{DTD}}(\mathbf{X}, \mathbf{Y})$	product distance for DTD
$E_{P_{OTD}}(\mathbf{X}, \mathbf{Y})$	product distance for OTD
E_s	energy per symbol
$e_i^{(k)}$	estimation error
η	noise vector for Rake combined case
$\hat{\eta}$	noise vector from decorrelator
$\eta_n^{(j)}(i)$	noise sample
η_m	bandwidth efficiency
η_ζ	vector of noise samples
f_d	maximum doppler shift
$\Phi_S(t)$	characteristic function of S
$\mathbf{G}_e$	equal gain combining matrix
$\mathbf{G}_R$	Rake combining matrix
$\mathbf{G}_s$	selection diversity combining matrix
$g(t)$	chip waveform
g_{ff}	feedforward
g_{fb}	feedback
$\Gamma(\cdot)$	Gamma function
γ_0	interference
γ_{0c}	interference under conditions coding
γ_b	average SNR per bit
γ_k	average SNR per diversity branch
$\mathbf{h}^{(k)}(t, \tau)$	channel impulse response
$h_i^{(k)}(\tau)$	multipath channel response
$\mathbf{I}$	identity matrix
I_{mai_n}	multiple access interference
I_{ni_n}	AWGN interference
I_{si_n}	self interference
i	symbol interval index
$J_0(\cdot)$	Bessel function
j	user index
k	user index or number of coder input bits
k_i	number of inner coder input bits

k_o	number of outer coder input bits
$\mathcal{K}_k$	Rice factor
K	number of active users
K_{cc}	convolutional code constraint length
K_{tc}	turbo code constraint length
K_{oc}	orthogonal code constraint length
κ	multiplicity factor
l	multipath index
L_p	number of multipath
L_R	number of RAKE taps
L_{min}	length of shortest error event path
L_{WH}	length of Hadamard codeword
λ	branch metrics of soft-input trellis decoder
m	Nakagami-m fading parameter
m_0	Nakagami parameter of main received path
M_D	number of diversity antennas
M_B	number of beamforming antennas
M_R	number of receive antennas
M_T	number of transmit antennas
n_l	path loss exponent
n	symbol index or number of coder output bits
n_i	number of inner coder output bits
n_o	number of outer coder output bits
$\mathbf{n}(t)$	Gaussian noise in received signal
$n(t)$	complex envelope of the noise process
$n_m(t)$	Gaussian noise process for antenna element m
N	processing gain
N_{cc}	convolutional code interleaver size (trellis decoder decoding depth)
N_{tc}	turbo code interleaver size (trellis decoder decoding depth)
N_0	two-sided noise spectral density
Ω_k	average power of received path
ω_c	carrier frequency
$p_{R_s,\phi}(R_s,\phi)$	pdf of scatterers
$p_{\Phi_0}(\phi_0)$	pdf of the angular distribution of users
$P(\mathbf{b}\|\mathbf{y})$	probability of $\mathbf{b}$ given $\mathbf{y}$
$p(\mathbf{y}\|\mathbf{b})$	pdf of $\mathbf{y}$ given $\mathbf{b}$
$P(\mathbf{b})$	probability of $\mathbf{b}$
$p_S(s)$	pdf of S
P_k	received power
P_e	bit error probability

$P_d(c-\hat{c})$	probability of codeword error
P_w	word error probability
π	interleaver
π^{-1}	de-interleaver
q	multipath index
$Q(\cdot)$	Q-function
$\mathbf{r}(t)$	received signal
$\mathcal{R}^{(kj)}$	spatial correlation between user k and reference user
R_{k1}	periodic correlation between user k and reference user
$\hat{R}_{k1}$	aperiodic correlation between user k and reference user
R_c	overall code rate
R_o	outer code rate
R_i	inner code rate
R	mobile to base station distance
R_D	scatterer radius
R_0	cut-off rate of channel
R_r	radius of cells
R_{xx}	correlation of real components
R_{xy}	correlation between real and imaginary components
$\mathbf{R}_\zeta$	correlation matrix for matched filtered statistic
ρ_{ij}	fading correlation constant between transmissions i and j
ρ	average spatial correlation
$S_n^{(j)}$	desired received signal
$\sigma^2_{\text{mai}_n}$	MAI variance
$\sigma^2_{\text{si}_n}$	self interference variance
$\sigma^2_{\text{ni}_n}$	AWGN variance
σ_T	total interference variance
σ^2	noise variance
σ	noise process standard deviation
σ_s	standard deviation of scatterers
$s(t)$	received signal power envelope
$s_k(t)$	transmitted signal for user k
t	time
$\overline{\tau}_m$	mean excess delay
τ_0	minimum path delay

$\tau_l^{(k)}(t)$	propagation delay of path l from user k
τ_m	maximum excess delay
τ	delay
$\tau_l^{(k)}$	time delay for specific multipath
θ_k	carrier phase
T_c	chip period
T_s	symbol period
T_{samp}	sampling period
$T(L, I, D, J)$	transfer function i.t.o. path length, input weight, output weight and remergings with zero state
$T_{l,i,d,j}$	number of paths of length l, input weight i, output weight d, and j remergings with zero state
$\mathbf{u}$	output of linear detector
U_s	RAKE output
v	mobile speed
V	system load
$\varphi_l^{(k)}(i))$	phase shift for specific multipath
ϖ_l	width of peak l
$\mathbf{w}_q^{(j)}$	weight vector
X_{ck}	in-phase Gaussian random variable
X_{sk}	quadri-phase Gaussian random variable
x	encoded bit
ζ	vector of matched filter outputs
$\zeta_{m_D}^{(j)}(i)$	detector output on m_Dth diversity branch
Z	number of constituent RSC encoders utilized in turbo encoder

1 INTRODUCTION

"Imagination is more important than knowledge, for knowledge is limited while imagination embraces the entire world."

– Albert Einstein

During the past ten years, there has been an explosive growth of personal and mobile wireless services whose ultimate goal is to support universal personal and multimedia services without regards to mobility and location. These future services are intended to provide image, video and local area network applications requiring high-speed data transmission that may be more than 1000 times faster than present systems [1]. Current development trends in telecommunications are driven by user requirements, which include access to a diverse range of services for anyone, anywhere, anytime and at the lowest possible cost. In an ideal world, this would ultimately lead to one worldwide mobile solution, using one radio-access network and one single core network. Physical limits imposed by the mobile radio channel cause performance degradation and make it very difficult to achieve high bit rates at low error rates over time dispersive wireless channels.

In order to understand the importance of this thesis, the contributions are sketched against the background of an ever increasing user population that is placing increasingly stringent demands on existing and planned communication networks for high quality flexible services.

Smart antennas have recently been proposed for wireless communications [2, 3, 4, 5]. The use of multiple element antenna arrays is an attractive solution because they can mitigate the effects of multipath fading as well as suppress co-channel interference, thereby significantly improving system performance. These antenna arrays may be employed either at the transmitter or the receiver. In a cellular radio system, it is generally most practical to employ an antenna array at the base station rather than at the mobile terminals. Then, in transmitting from the mobile to the base station (uplink channel), receiver diversity is achieved through a multiple receive antenna array, while in transmitting from the base station to the mobiles (downlink channel), transmit diversity is achieved through a multiple transmit antenna array. To further improve system performance, both spatial (multiple antennas) and temporal (multipath combining and coding) processing can be combined so that both the time and space or angular domains can be efficiently

exploited. This joint space-time processing can be adopted at both the base stations and mobile stations to improve the system performance and capacity by orders in magnitude [6, 7].

In this thesis, the focus is on coded transmit diversity and its achievable performance when used in cellular CDMA systems. Transmitter diversity has traditionally been viewed as more difficult to exploit than receiver diversity, in part because of the challenging signal design problem: the transmitter is permitted to generate a different signal at each antenna element. The addition of coding complicates the signal design problem, but increases the transmitter diversity degrees of freedom, and also the potential of optimal space-time coded diversity gain.

In this chapter, a brief introduction into some of the newest developments in mobile communications is presented. Specific emphasis is placed on the infra-structural evolution of second generation mobile communication networks to third generation mobile communication networks. Then, the goals and specific contributions of this thesis are listed in Section 1.2. The basic definitions and operating principles of antenna arrays and coded space-time processing for spread spectrum code division multiple access (CDMA) are presented in Section 1.3, as a basis for the work covered in this thesis. Finally, the organization of this thesis is described in Section 1.4.

1.1 OVERVIEW

1.1.1 From Second Generation to Third Generation

Mobile communications at the beginning of the 21th century is characterized by a diverse set of applications using many incompatible standards. In order for today's mobile communications to become truly personal communications in this century, it will be necessary to consolidate the standards and applications into a single unifying framework. The eventual goal is to define a global third generation mobile radio standard called the Future Public Land Mobile Telecommunications System (FPLMTS).

The success of the European second generation system, GSM, has created a mass market for mobile communications, reaching high terminal penetration in global markets. At the end of June 1998, there were 293 members of the GSM memorandum of understanding (MoU) association from 120 different countries worldwide. There are currently 278 GSM networks in operation serving 95 million subscribers, and these are still growing. A further boost to the mass market will be the introduction of multi-mode multi-band terminals, such as GSM/DCS 1800/PCS 1900, GSM/satellite and many other handset combinations. The penetration for mobile communications in developed countries is expected to rise to 50%-80% within the time frame from the introduction of Universal Mobile Telecommunication System (UMTS) [8, 9]. The UMTS system is only one of many new third generation systems being developed around the world, and serves as illustration for our current discussion.

UMTS cannot be developed as a completely isolated network with minimal interface and service interconnection to existing networks. Both UMTS and existing networks will need to develop along parallel, even convergent paths, if service transparency is to be achieved to any degree. This would then, in the end, allow UMTS services to be supported, although at different levels of functionality, across all networks. Another important requirement for seamless operation of the two standards is GSM-UMTS hand-over in both directions. Restrictions on the applicability of hand-over may be necessary for particular services and when services are different between the systems. This will require modifications of existing GSM specifications. GSM networks also need to be protected from unwanted side-effects caused by functions needed to support cross handovers.

1.1.2 *Universal Mobile Telecommunications System*

UMTS wideband code division multiple access (WCDMA) is one of the major new third generation (3G) mobile communication systems being developed within the FPLMTS framework. It represents a substantial advance over existing mobile communications systems. Above all else it is being designed with flexibility for users, network operators and service developers in mind and embodies many new and different concepts and technologies. UMTS seeks to build on and extend the capabilities of today's mobile, cordless and satellite technologies by providing increased capacity, data capability and a far greater range of services using an innovative radio access scheme and an enhanced, evolving core network.

As the demand for user data rates increases in the long term, UMTS will be developed to support even higher data rates, perhaps one or two orders of magnitude greater (provided appropriate spectrum is allocated). In later phases of UMTS development there will be a convergence with even higher data rate systems, known as broadband radio access networks (BRAN), using mobile wireless local area network (LAN) technologies (microwave or infrared) providing data rates of, for example, 155 Mbit/s in indoor environments. Figure 1.1 illustrates the mobility and coverage of UMTS compared with GSM and BRAN.

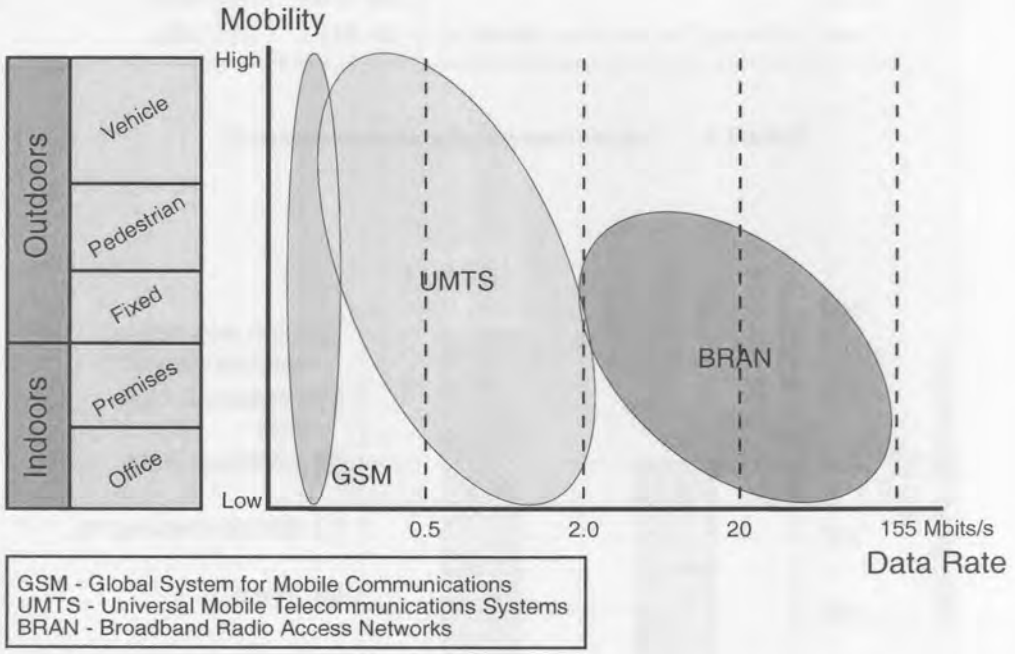

Figure 1.1. UMTS coverage versus information data bit rate.

In practical implementations of UMTS, some users may be unable to access the highest data rates at all times. For example, the physical constraint of radio propagation and the economics of operating a network will mean that the system services might only support lower data rates in remote or heavily congested areas. Therefore, in order to ensure that the subscriber is always able to use his or her terminal, services will be adaptive to different data rate availability and other quality of service (QoS) parameters. For this reason UMTS is also being designed to offer data rate on demand, where the network reacts adaptively to the user's demands, the customer's profile and the current status of the network. The use of packet-oriented transport protocols is being studied so that UMTS can enhance these abilities. Together, the combination of packet data and data rate on demand will remove technical barriers for the user and make operation of the system much cheaper – there will be no worries about how and when to connect to the network.

Table 1.1 and Figure 1.2 show the projected required frequencies per service in typical busy hours for the years 2005 and 2010. The conclusion is that roughly 580 MHz will be required in the year 2010. The requirement includes the bands currently designated for second generation (2G) systems, and the bands designated as core bands for UMTS, plus new spectrum resources fully and flexibly exploited. It is envisaged that the increase in penetration after 2010 will not be significant [8, 10]. The use of services requiring wider bandwidth, however, is expected to increase, which will lead to increasing spectrum demand.

Year	2005	2010
High interactive multimedia[1]	22 MHz	82 MHz
Medium and high multimedia[2]	113 MHz	241 MHz
Switched data	12 MHz	9 MHz
Simple messaging	2 MHz	2 MHz
Voice	220 MHz	220 MHz
Total	369 MHz[3]	554 MHz[4]
Total (allowing for spectrum division)	406 MHz	582 MHz

Table 1.1. Future terrestrial spectrum requirements [8].

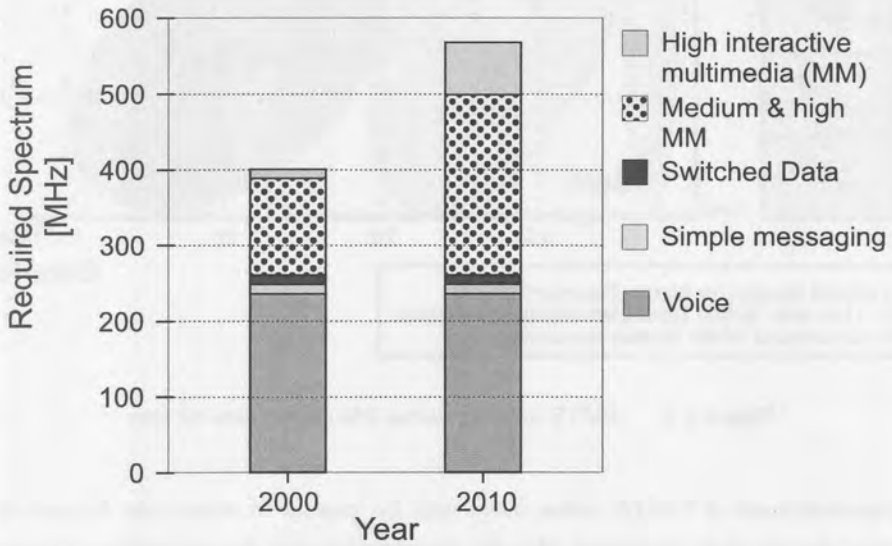

Figure 1.2. Required spectrum for terrestrial UMTS services (including second generation services) [8].

1.1.3 Third Generation and Beyond

In order to ensure that the FPLMTS vision is sustained in the long term, its capabilities will need to be progressively increased by the addition of new technologies. A selection of these are detailed below.

1.1.3.1 Re-configurable Terminals. Future mobile terminals will have to exist in a world of multiple standards – both 2G and those of other members of the FPLMTS family. Also, standards themselves are expected to evolve. In order to provide universal coverage, seamless roaming and non-standardized services, some of the elements of the radio interface (e.g. channel coder, modulator, demodulator, etc.) will no longer have fixed parameters, they will rather take the form of a "toolbox" whereby key parameters can be selected or negotiated to match the requirements of the local radio channel. In addition to the ability to adapt to different standards described above, downloadable terminals will enable network operators to distribute new communications software over the air in order to improve the terminals' performance in the network or to fix minor problems.

1.1.3.2 Application and Service Download. In using today's multimedia terminals (for example PCs), users have learned to accept the idea that the capabilities of the terminal can be modified over time by software downloading. It is now commonplace for a user to download a new "plug in" (for example a video or audio codec) to access new types of content. The introduction of multimedia services in UMTS will take this concept into the mobile domain.

1.1.3.3 Broadband Satellite Systems. Several broadband satellite systems are also planned for deployment in the post 2002 time frame (designed to offer data rates beyond 2 Mbit/s and into the Gigabits domain). Some of these systems may offer compatibility with UMTS service concepts using satellite frequency allocations in the 20/30 GHz range. The requirements of the terminal equipment and higher power consumption will necessitate larger transportable or fixed terminals.

1.1.3.4 Space-time Techniques. As will be discussed throughout this thesis, space-time techniques are a key way to enhance the capability of mobile communication services in the long term, and are currently regarded by many within the wireless communications industry as a core system component in future-generation mobile networks. For example, the current UMTS standard already provides for antenna array use. The pilot bits available in the dedicated physical channels ensure that space-time technology can be introduced in the future. As an example of a space-time processing technique, antenna arrays react intelligently to the received radio signal, continually modifying their parameters to optimize the transmitted and received signal. More detail concerning these techniques are given in Section 1.3.

1.2 GOALS OF THIS THESIS AND STATEMENT OF ORIGINALITY

Clearly radio technologies are no longer confined to serving the needs of mobile or rural telecommunications users. In fact, it can be said that radio technology has been liberated and that it is today viewed as a viable alternative to access technologies such as fiber and copper. This liberation of radio technology from its traditional role as a mobile or rural access system is further exemplified by Figure 1.1. UMTS solutions, for instance, can be applied to many different mobility and service provision scenarios, with other high speed radio access technologies like wireless local area networks and mobile broadband systems extending the applicability of radio based access solutions to almost any conceivable scenario.

In order to understand the importance of this thesis, the goals and contributions are sketched against the background of an ever increasing user population that is placing increasingly stringent demands on existing and planned communication networks for high quality, flexible services. Of particular importance in this thesis, will be those CDMA based solutions for the mobile sector and the new performance analysis issues that need to be addressed as a result of the introduction of heterogeneous services and service environments

into a single, mobile cellular access network. Furthermore, novel applications of transmit antenna diversity techniques to mobile cellular access networks aimed at increasing the efficiency of such networks will be considered.

1.2.1 *Thesis Goals*

Against the background of the rapid evolution of mobile communication systems in the areas of service provision and capacity enhancement described above and the role of smart antenna concepts therein, this thesis has the following goals:

- To establish a general spatial/temporal channel model for use in the evaluation of coded space-time processing concepts applied to CDMA networks.
- To analyze the performance of uncoded cellular CDMA systems incorporating space-time techniques using analytical methods in a number of realistic application scenarios.
- To design, implement and evaluate coding strategies for incorporation into the space-time CDMA systems. This objective can be broken down into the following items:
  - Space-time coding systems when considering multiple transmit antennas for the downlink.
  - Coded space-time systems when considering multiple receive antennas for the uplink.
- To establish the performance of coded space-time CDMA cellular networks under realistic scenarios.

1.2.2 *Statement of Originality*

This thesis examines the topic of combined diversity and turbo coding systems in CDMA. Several novel results and techniques are developed which allow significant performance improvements under a range of conditions in cellular CDMA systems.

The main contributions are summarized below.

- Turbo encoding and its applicability to transmit diversity and receive beamforming/diversity scenarios for cellular CDMA is investigated and illustrated.
- New analytical models are developed to provide a simple mechanism of evaluating the performance of the existing space-time coding proposals. These analytical models facilitate a direct comparison of various techniques.
- The field of knowledge is extended by introduction of a particular class of layered space time codes for CDMA, namely turbo transmit diversity (TTD).
- Novel TTD schemes are designed and their performance analyzed. These are:
  - Parallel concatenated TTD (PCTTD).
  - Serial concatenated TTD (SCTTD).
  - Super-orthogonal TTD (SOTTD).
- The work of previous authors in the field of space-time trellis codes is extended. The relationship between multiple trellis coded modulation (MTCM) and good space-time code design techniques is shown.

- New analytical models are developed for determining the performance of space-time trellis codes based on MTCM techniques. New metrics for measuring space time code quality and for examining the relative "goodness" of existing space-time codes are derived.
- The relationship between turbo coded space-time turbo codes in receive diversity and directional antenna (beamforming) systems is examined.

Details about the organization of this thesis are presented in Section 1.4.

1.3 CODED SPACE-TIME PROCESSING FOR CELLULAR CDMA

Theoretically, the most effective technique to mitigate flat fading in a wireless channel is transmitter power control. In addition, if the channel multipath conditions as experienced by the receiver are known at the transmitter, the transmitter can pre-distort the signal in order to compensate for the distortion introduced by the channel at the receiver. Other effective techniques are time, frequency and space diversity. When possible, wireless communication systems should be designed to encompass all forms of available diversity to ensure adequate performance [11].

From a practical point-of-view, space diversity reception in the uplink is one of the most effective and, hence, widely applied techniques for mitigating the effects of multipath fading. The classical approach is to use multiple antennae at the receiver and perform combining or selection and switching in order to improve the received signal quality. The major problem with the receive diversity approach at the mobile terminal, is cost, size and power. As a result, antenna diversity techniques have almost exclusively been applied to the base stations. In this thesis, the use of multiple transmit/receive antennas at the base station is considered, when combined with advanced forward error correcting codes to increase system capacity of cellular CDMA communication for both the uplink and downlink.

The reasoning behind the use of space-time processing techniques (which include smart antennas as a special case) is the optimization of the cellular spectral efficiency of the network. This is realized by implementing more than one antenna element to optimally transmit or receive signals by using both temporal and spatial signal processing techniques in the transceiver. Well known techniques such as antenna sectorization (spatial signal processing), diversity combining (spatial and temporal signal processing) and beamforming arrays (spatial and temporal signal processing) are considered to be examples of space-time processing. In fact, all antenna array systems can be considered to be space-time processors.

1.3.1 Channel Coding and CDMA

CDMA communications are interference-limited systems, due to the presence of self and mutual interference signals at the receiver antenna. This is because all users communicate simultaneously in the same frequency band [12, 13]. The received signal suffers multipath fading created by the reflections and diffraction by many obstacles, such as buildings and hills located between the mobile. Multiple access interference (MAI) is often produced which significantly reduces the link capacity. Thus, advanced techniques to counteract these impairments are indispensable in order to minimise MAI. Forward error correction (FEC) coding can be regarded as a time diversity technique when it is combined with interleaving of sufficient depth. Thus, FEC aims to correct errors caused by noise and interference in the CDMA communication environment.

Channel coding is an extremely complex topic to which entire books are dedicated. The reader is referred to Lin and Costello [14] or Clark and Cain [15] for detailed introductory discussions on FEC coding, and to

Viterbi and Omura [16], Petersen and Weldon [17], Gallager [18], Berlekamp [19, 20] and Biglieri *et al.* [21] for advanced discussions of both information theoretic and algebraic foundations of channel coding.

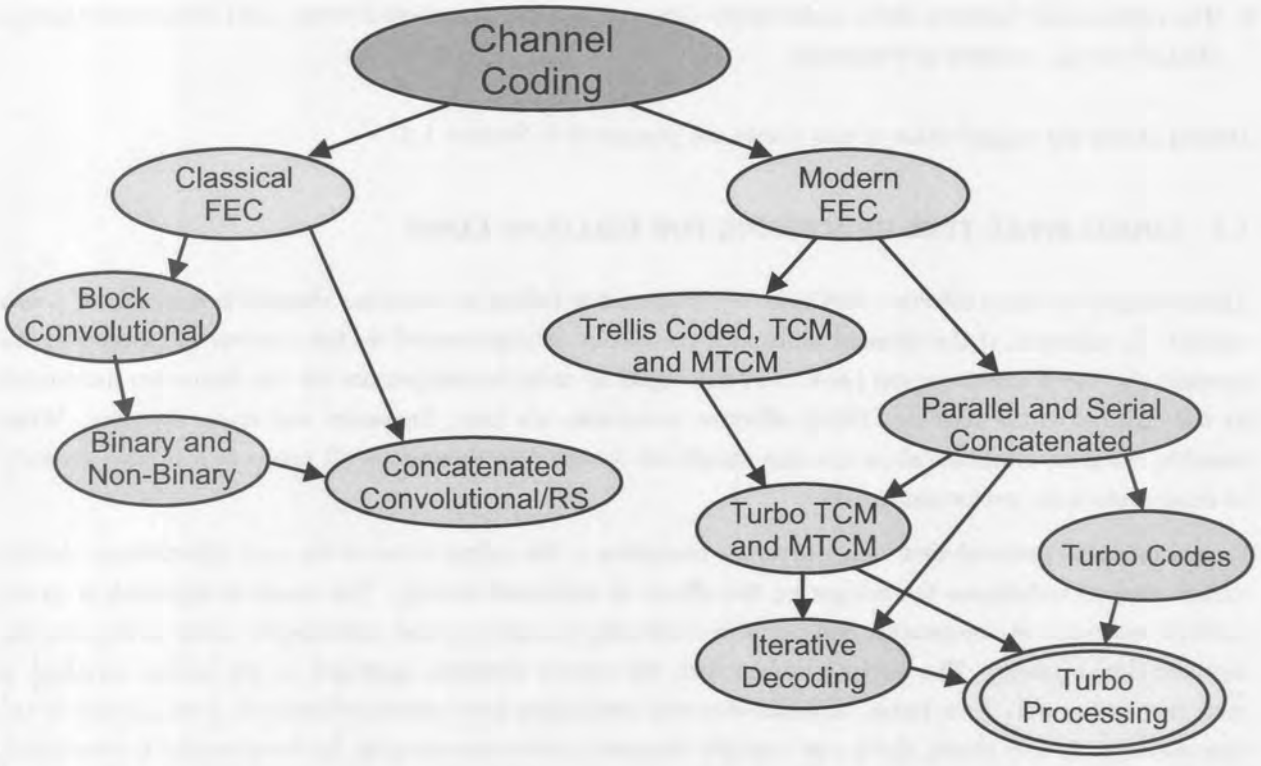

Figure 1.3. Classification of channel coding techniques.

As shown in Figure 1.3, channel coding techniques can broadly be classified as:

- Classical FEC coding, including
  - Binary (e.g., Hamming and Reed-Muller) and non-binary (e.g., Reed-Solomon) block codes,
  - Convolutional codes, and
  - Concatenated block and convolutional codes.
- Modern FEC coding, including
  - Trellis coding, encapsulating both trellis coded modulation (TCM) and multiple trellis coded modulation (MTCM), and
  - Parallel (turbo) and serial concatenated convolutional and block codes with iterative decoding, and
  - Turbo trellis coded modulation.

Turbo codes and its trellis coded variants are the parallel concatenation of two recursive systematic convolutional (RSC) codes separated by an interleaver and decoded using iterative decoding techniques. The discussion here is confined to the more general concepts of turbo processing. In Chapter 4, a more detailed discussion on turbo codes and their application to CDMA communications will be presented.

The Viterbi algorithm was introduced in 1967 as a computationally efficient method for performing maximum likelihood (ML) decoding of convolutional codes [22]. Since then, it has found numerous other applications including maximum likelihood sequence estimation (MLSE) equalizers [23], trellis-coded modulation [24], and multiuser detection [25, 26, 27, 28]. Along these lines, it was soon recognized that the iterative method of decoding turbo codes was also suitable for many other applications, and could be incorporated as a design methodology for advanced receiver design. Examples of sub-systems include source decoding [29], symbol detection [30], equalizers [31] and multiuser detectors [32, 33, 34]. Also, in line with the thesis goals, combinations with multiple transmit and receive antennas.

Communication receivers typically consist of a cascade of signal processing intensive subsystems, each optimized to perform a single task. In a "conventional" receiver, the interface between subsystems involves the passing of bits, or hard-decisions, down the stages of the chain. Whenever hard-decisions are made, information is lost and becomes unavailable to subsequent stages. Additionally, stages at the beginning of the processing chain do not benefit from information derived by stages further down the chain. The interface between stages can be greatly improved by employing the same strategy used to decode turbo codes. In [30] the term "turbo processing" was coined to describe the general strategy of iterative feedback decoding or detection. The latter processing forms the basis for the space-time turbo coded processing techniques for the downlink. These techniques are covered in detail in Chapters 5 and 6.

1.3.1.1 Coded Cellular CDMA. It is well known that CDMA systems exhibit maximum capacity potential when combined with FEC coding [13, 35, 36, 37, 38]. In fact, most FEC systems, especially those with low code rates, expand bandwidth and can be viewed as spreading systems. The positive trade-off between greater distance properties of lower rate codes and increased cross-correlation effects (due to shorter sequence length) is fundamental to the success of coded CDMA. From information theory it is known that the maximum theoretical CDMA capacity can only be achieved by employing very low rate FEC codes utilizing the entire bandwidth, without further spreading by the multiple access sequence [38, 39, 40, 41].

Viterbi [35, 38] has proposed the use of orthogonal convolutional codes as low rate code extensions for code-spreading CDMA. Recently, two new classes of low rate codes with improved performance have been proposed. Pehkonen *et al.* [42, 43] proposed a coding scheme that combines super-orthogonal turbo codes (SOTCs) with super-orthogonal convolutional codes (SOCCs) [38]. A different approach was taken by Frenger *et al.* [40, 41], where a class of nested rate-compatible convolutional codes (RCCC), with maximum free distance (MFD), was derived.

In [44], performance gains achieved in a RAKE based CDMA system with convolutional versus trellis coding were reported. Codes were constructed over an MPSK signal set by taking a standard Ungerboeck type code for MPSK modulation and multiplied by a binary pseudo-noise sequence, thereby spreading the signal over a large bandwidth. It was reported that this approach did not yield a performance advantage over standard convolutional codes, with the conclusion that it is better to exploit the low distance properties of low rate convolutional codes as opposed to using higher order modulation schemes for efficient signalling.

A different approach to trellis coded CDMA was investigated by Woerner *et al.* [45]. In this approach the trellis code is constructed over the set of possible signature sequences rather than over some $2D$ signal constellation. Instead of expanding the number of signal points in the $2D$ constellation, the signal points were expanded over a set of orthogonal spreading sequences. A carefully designed trellis then allows only certain combinations of sequences that have a large total minimum distance. By increasing the number of sequences, the actual minimum distances between sequences have been decreased. The trellis code compensates for this decrease by increasing the minimum distance of the code above that of the uncoded system.

For non-optimum multiuser receivers, such as the MF or RAKE, coding gain comes at the cost of increased MAI level. A limitation to the use of low rate coding comes when the spreading is reduced to such a level that the MAI does not appear Gaussian anymore. By using more powerful codes than those used by Boudreau *et al.* [44], the issue of spreading versus coding can be more adequately addressed. For a finite effective code rate (and hence a finite spreading ratio), the level of MAI, under AWGN equal power conditions, is fixed. If the MAI was truly Gaussian in nature, turbo codes should perform in a similar way as if applied to an AWGN channel. For a RAKE receiver with perfect channel estimation, the soft input turbo code will perform equally well in an AWGN and a fading channel. The power of turbo coding approaching the Shannon bound in narrow band systems, implies that almost optimum performance should be achievable with coded CDMA systems under similar signalling conditions.

1.3.2 Space-time Processing Techniques

The introduction of spatial aspects into the cellular problem through the innovative use of antennas now offers new possibilities to extend the receiver algorithms mentioned above. Specifically, the use of multiple antennas at both the transmitter and the receiver adds a new dimension to the CDMA receiver problem as it allows for the improved separation of users' signals. Through the use of space-time processing techniques, the levels of MAI and fading a receiver has to cope with can be significantly reduced, thereby increasing the capacity of the overall system. In the latter parts of this thesis, the above mentioned receiver structures, used in conjunction with coded space-time processing, are discussed in detail.

With this in mind, the purpose of space-time processing systems should become clearer. Essentially, space-time processing techniques provide an integrated approach to fight channel impairments on two fronts. Firstly, by introducing diversity into the system to minimize the effects of fading on the received signal and secondly by adaptively changing the radiation pattern of the antenna system to minimize the total MAI seen by the receiver. Whereas both techniques are well known, the power of space-time processing lies therein that the basic principles of beamforming and diversity are incorporated in the overall system design. Thus, space-time processing is defined as:

Space-time processing is the minimization of fading and MAI through the integrated use of multiple antennas, advanced signal processing techniques, advanced receiver structures and forward error correction.

Based on this definition, the main aim of space-time techniques for mobile systems is to maintain an acceptable level of error performance and, hence, to maximize the signal-to-interference and noise ratio (SINR) for each user in the system.

Combinations of implicit (coded) and external (i.e., multiple transmit/receive antennae) for space-time diversity and beamforming processing can be used to improve both the downlink and uplink QoS of CDMA cellular communications. As will be shown in this thesis, it is important to note that the overall system gains that can be achieved with these space-time coded systems, depend heavily on the error correction strategy employed.

Following along the lines of the discussion above, the general definition of space-time processing is extended to incorporate coding. In the context of the thesis, two concepts need to be defined, namely space-time coded processing (or simple space-time coding), and coded space-time processing. These are defined as:

Space-time coded processing refers to the combined use of adaptive antenna arrays and forward error correction coding in the downlink of a cellular network to maximize the combined space-time diversity/beamforming and coding gain.

Coded space-time processing refers to the use of adaptive antenna arrays, followed by a forward error correction coding strategy in the uplink of a cellular network to make maximum use of the available diversity/beamforming gain.

Thus, in space-time coding the signal processing involved with the use of multiple transmit antennas and coding are combined to provide a so called space-time coding gain in the downlink. For coded space-time processing systems multiple receive antennas are considered combined with coding in the uplink. For both the uplink and downlink channel diversity, beamforming or combined diversity/beamforming techniques may be considered.

In general, space-time processing techniques can be classified according to Figure 1.4. Diversity techniques require a number of signal transmission paths, called diversity branches, that carry the same information but have, ideally, uncorrelated multipath fading, and a circuit to combine the received signals or to select one of them. This definition of diversity differs from beamforming where it is normally assumed that the signals arriving at the antenna array are perfectly correlated. Whenever the signals on the various antenna elements are not perfectly correlated, the beamforming pattern is influenced in a detrimental way. At some point, due to a lack of correlation, the beam pattern will revert back to an omni-directional pattern. Lack of correlation is normally induced by the environment through which the received signal is propagated and also due to the spacing of the antenna elements. Whenever the correlation, ρ_{ij}, between branch i and j, is less than perfect, that is $\rho_{ij} < 1$, there will be some diversity gain present in the system. Diversity combining is different from antenna array processing and beamforming in that it combines signals at baseband or at a intermediate frequency to increase the signal level without affecting the individual antenna pattern. Beamforming techniques, on the other hand, exploit the differential phase between different antennas to modify the antenna pattern of the whole array. In this arrangement, once the signals are combined, the whole of the array has a single antenna pattern.

1.3.2.1 Transmit Diversity. For narrowband TDMA many techniques have been proposed to provide transmit diversity. These techniques can broadly be categorized as

- space-space transmit diversity (polarized antennas are often used to realize space-space transmit diversity),
- space-frequency transmit diversity and space-phase transmit diversity (the introduction of frequency offsets [46] and phase-sweeping [47, 48], to convert a frequency non-selective channel into a frequency selective channel is a technique used to realize such a transmit diversity scheme), and
- space-time transmit diversity (examples are FIR pulse shaping techniques imposing intentional inter-symbol interference (ISI) [49, 50, 51, 52, 53], delay diversity [54, 55, 56], and space-time antenna-hopping (also known as round-robin antenna selection [57]) diversity schemes.)

Many of these techniques can easily be extended to CDMA. A general classification of transmit diversity techniques, for TDMA and CDMA, can be summarized as follows:

Transmit Diversity with Feedback [58, 59].
In these schemes, implicit or explicit (closed loop) information is fed from the receiver to the transmitter in order to configure the transmit diversity structure. Winters [58, 60] considered switched diversity with

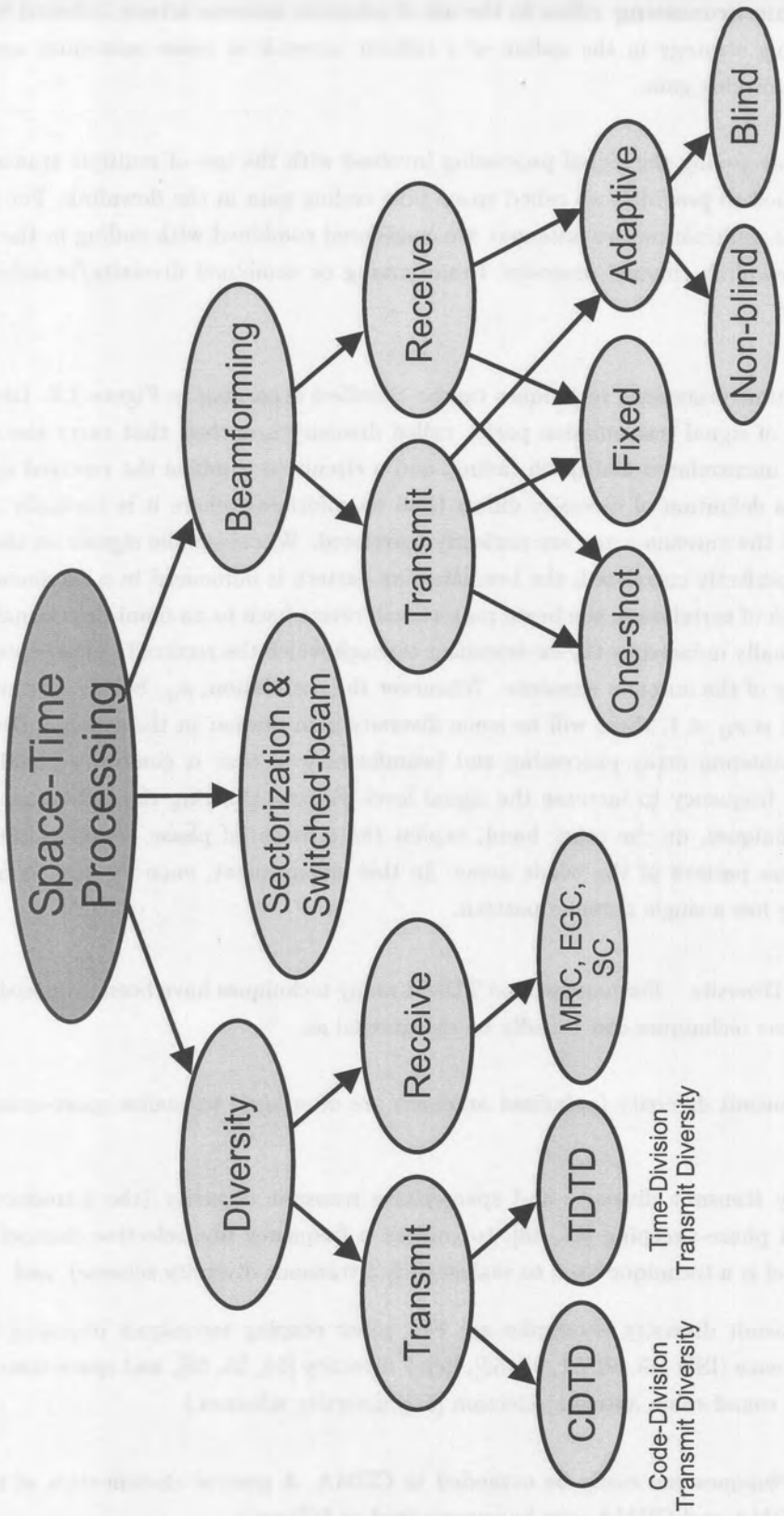

Figure 1.4. Classification of space-time processing techniques.

feedback while Raleigh et al. [59] considered spatio-temporal-frequency water pouring, a technique based on channel feedback response. These techniques are limited in practice by vehicle movements and/or interference which cause a mismatch between the state of the channel perceived by the transmitter and that perceived by the receiver.

Transmit Diversity with Training Information [49, 50, 54, 61].
Linear processing at the transmitter is used to distribute encoded and control (e.g. transmitter power) information to the antenna sub-sequences. Feed-forward or training information is utilized to estimate the link from the transmitter to the receiver. The first scheme of this type was proposed by Wittneben [50], which includes the delay diversity scheme presented by Seshadri *et al.* [54] as a special case. Lu *et al.* [61] has considered a technique where channel reciprocity was assumed by assigning the same antenna weights to the transmitter and receiver via implicit (open loop) feedback.

Hybrid Feedback/Training Transmit Diversity.
In practice, the information update rate is slow, and channel reciprocity cannot be guaranteed because of vehicle movement and/or interference. Here, the feedback and training estimates are combined to compensate for the channel response at both the transmitter and receiver. In this way the best features of both open and closed loop channel state estimation are combined.

Blind Transmit Diversity [47, 48, 54, 62, 63].
No feedback or feed-forward information is required. Instead, blind transmit diversity exploits the use of multiple transmit antennas combined with channel coding to achieve diversity. An example of this approach is to combine phase sweeping transmitter diversity [47] with channel coding [48]. Here a small frequency offset is introduced on one of the antennas to create fast fading. Another scheme is to encode the information by a channel code and then to transmit the code symbols using different antennas in an orthogonal manner. This can be achieved by either considering frequency multiplexing [62], or time multiplexing [54]. Also in the case of CDMA, orthogonal spreading sequences can be assigned to the different transmitting antennas [63]. When appropriate channel coding is employed, it is possible to relax the orthogonality requirement, with the benefit of achieving diversity and coding gain.

Two promising transmit diversity techniques well suited to CDMA are code-division transmit diversity (CDTD) and time-division transmit diversity (TDTD). These techniques will be covered in detail in Chapter 3.

1.3.2.2 Receive Diversity. With receive diversity systems, the fact that the signals arriving at different locations fade at different rates, are therefore utilized [64]. A system employing a receive diversity combiner uses signals induced on various antennas placed a few wavelengths apart at different locations and combines these signals in one of many ways [65]. These combining techniques can broadly be categorized as follows:

Selection Combining (SC) [66]. This is the simplest receive diversity technique, that simply selects the best of the available diversity branches. The selection may be based upon the power of the desired signal, the total power, or the SINR available at each antenna.

Maximal Ratio Combining (MRC) [67, 68, 69, 70, 71]. In this method the signals from all of the diversity branches are weighted according to their individual SNRs and then summed. Here, the individual signals must be co-phased before being summed to produce an output SNR equal to the sum of the individual SNRs. This technique gives the best statistical reduction of fading of any known linear diversity combiner.

Equal Gain Combining (EGC) [66]. The equal gain combiner adjusts the phases of the desired signals and combines them in-phase after equal weighting. This allows the receiver to exploit signals that are simultaneously received on each branch. The possibility of producing an acceptable signal from a number of unacceptable inputs is still retained, and performance is only marginally inferior to MRC and superior to SC.

1.3.2.3 Beamforming. Receive beamforming refers to the use of adaptive antenna arrays in the uplink of a cellular network to focus the antenna beam on a specific user, thereby increasing the antenna gain in the direction of the user and suppressing transmissions received from interfering users.

In the case of TDMA and FDMA systems the beamforming system may use pencil antenna beams [72] to focus on the active users, whereas in CDMA systems, the system can increase the SNR in the uplink by introducing nulls in the antenna pattern in the direction of strong interfering signals.

In a manner similar to receive beamforming, transmit beamforming can be used in the downlink of a cellular system to focus all the energy radiated by the base station onto a single user or cluster of users [73]. Transmit beamforming reduces the interference experienced by mobile communication systems in the downlink by concentrating all radiated electromagnetic energy in the direction of a user or group of users, avoiding geographical areas where no users are active.

Transmit and receive beamforming techniques can broadly be classified as follows [74].

Fixed Beamforming [75, 76, 77]. The first application of antenna arrays in beamforming is that of fixed beamforming networks.

One-shot Beamforming [76, 77]. A slightly more general case of a fixed beamforming network would be a one-shot beamformer. A one-shot beamformer is defined as a beamforming array where an optimal radiation pattern or antenna weights are determined using a single operation. Such beamforming techniques are also known as statistically optimal techniques as they determine a weight vector which is optimum in some statistical sense. Specifically, the weight vector is determined by minimizing a cost function. Minimizing the cost function will maximize the signal quality at the output of the beamformer. One of the most popular techniques is the minimum mean square error (MMSE) algorithm, which is widely used.

Adaptive Beamforming [77, 78, 79, 80, 81]. There are several reasons why it is not desirable to solve the optimum weight vector directly. Since the mobile environment varies with time, the solution of the weight vector must be updated periodically. Typically, the change in the channel from one adaptation cycle to the next will be small. Also, since the data required to estimate the weight vector is noisy, it is desirable to use the current weight vector to determine the next weight vector. This would result in a smoothing of the weight vector reducing the effect of noise. When a training sequence is used in the adaptation process, the beamforming method is known as non-blind beamforming, while the solution of the weight vector, without the use of training sequences, is known as blind beamforming.

Because the uplink of a cellular network is, in general, the capacity limiting factor, it might seem that receive diversity and beamforming systems will yield greater capacity advantages than the transmit diversity and beamforming systems. However, the increased downlink quality afforded by transmit space-time techniques may lead to fewer dropped calls during handovers (because of the better signal quality estimates available to the mobile), increasing the overall QoS. In addition, the downlink of a cellular system in future wireless systems will also be a limiting aspect due to for example downloading of large files to a mobile terminal

from a server and the limited possibilities to implement space-time signal processing techniques at mobile receivers.

It is therefore clear that both transmit and receive space-time processing techniques are of great importance in wireless communication systems.

1.3.2.4 Multi-beam and Switched-beam Antennas. In addition to diversity and beamforming systems, smart antenna techniques such as multi-beam and switched-beam antennas can also be used to increase the capacity of CDMA systems. In [82], experimental test results show that a multi-beam antenna array with fixed beam azimuths can increase the capacity of a CDMA system compared to a system using sectorized antennas. Furthermore, in [83, 84] it is shown that switched-beam antennas can both increase the capacity of a CDMA systems, as well as extend the radio coverage by increasing the carrier-to-interference ratio (CIR).

1.3.3 Space-time Processing Performance

This thesis will consider the performance of the cellular system in terms of parameters such as bit error rate, rather than the operation and performance of specific algorithms for the control of the antenna radiation pattern. In this regard, many algorithms exist for the adaptation of the weights associated with each radiating element (on a global or peruser basis) and for the combining of signals received on radiating elements.

The analysis of the bit error probability (BEP) and outage performance of CDMA systems have received much attention in literature. The analysis of basic asynchronous CDMA systems in Additive White Gaussian Noise (AWGN) channels using a Gaussian approximation of the interfering signal is presented in [85, 86]. In [87, 88, 89], upper and lower bounds on the average error probability for CDMA systems in AWGN channels are presented. The evaluation of CDMA systems was extended in [90] to include multipath fading channels, where the fading coefficients were either Rayleigh or Rician distributed random variables. Additionally, a detailed analysis of the performance of a CDMA system over Nakagami channels is presented in [91]. Performance analysis methodologies that utilize more accurate descriptions of specifically the MAI present in the cellular network are presented in [92], with extensions to the modeling of the MAI presented in [93, 94, 95].

All of the above mentioned performance analysis methodologies considered only basic CDMA systems with no smart antenna systems included. The basic smart antenna systems that are most often analyzed are receive diversity systems. In [67, 68], optimum diversity combining and equalization techniques for TDMA mobile radio systems are evaluated. In these references, it is clearly shown that diversity techniques can significantly increase the performance of mobile radio systems. These results are extended in [69, 96, 97] where it is shown that diversity matched filters and combining techniques such as MRC, EGC and SC can significantly increase the performance of mobile radio systems over Nakagami channels. The same is true for frequency selective fading channels, as is indicated in [98] and [99] where it is shown that space diversity techniques may improve system performance by as much as 10 dB. The system gains described for TDMA systems are also realizable in CDMA systems. In [100], the performance of a microcellular CDMA system over slow and fast Rician fading radio channels with forward error correction coding and diversity is presented. In this paper, it is clearly shown that increasing the order of the diversity system increases the system capacity, a result which is confirmed in [64, 101, 102, 103]. In addition to diversity systems, smart antenna techniques such as multibeam and switchedbeam antennas can also be used to increase the capacity of CDMA systems. In [82], experimental test results show that a multibeam antenna array with fixedbeam azimuths can increase the capacity of a CDMA system compared to a system using sectorized antennas.

The promise of increased system capacity through the use of multiple transmit and receive antenna techniques such as diversity and beamforming have lead to the detailed analysis of such systems. In [104, 105, 106], the application of antenna arrays to TDMA systems such as GSM is described. These results are extended to CDMA system in a number of papers. For example, in [78, 107, 108, 109] interference cancellation systems using antenna arrays are described as examples of CDMA systems using antenna arrays to increase system performance by limiting interference. This theme is central to a number of applications of antenna arrays in limiting MAI. In [110] for instance, a linear receiver for direct sequence spread spectrum multiple access systems with antenna arrays and blind adaptation is described.

Various other system analysis approaches to determine the gains afforded by smart antenna techniques in CDMA systems can also be found in literature. In [111, 112], simulation and experimental results are used to show the gains that can be achieved through the use of smart antennas as beamforming arrays. However, as was stated in the goals of this thesis, an analytic solution to this problem is required. Various approaches to obtaining analytical solutions have also been published. In [113], the system gain is determined based on the approach of calculating the increase in signal to interference and noise ratio (SINR) that can be achieved by transmit and receive beamforming techniques. Such an approach can yield a first order approximation of system gains, but does not take a number of physical realities, such as the distribution of users and fast/slow fading, into account. In [70, 114], the analysis is extended to include aspects such as multipath scattering, fading and, to a lesser extent, user distribution. In [115], these effects are analyzed for CDMA systems without antenna arrays and where the fading parameters are arbitrarily chosen as opposed to being calculated based on the physical scenario in which the cellular system is deployed. In [116, 117, 118], the performance of adaptive antenna array systems has been treated were the effects of fading correlation, fading and antenna array configurations are discussed respectively. In [116], a power based approach as described above is used to determine the effect of fading correlation on diversity communication systems.

1.3.4 Advantages of Space-time Processing

As has been discussed in the foregoing sections and in [119, 120, 121, 122, 123, 124, 125], (coded) space-time techniques have the ability to improve the performance of a mobile communication system in a number of ways. Specific advantages of space-time techniques are that they yield:

- Increased capacity (spectrum efficiency) by increasing the number of active users for a given BEP quality.
- Reduction of co-channel interference to improve QoS and/or increase the frequency re-use factor. This point is especially important in CDMA-based systems in which the system capacity is interference limited.
- Reduction in delay spread and fading. By beamforming and diversity techniques, the SINR of the system can be improved in a fading environment. Related to this is the reduction of the effect of angular spreading of the received signal due to scatterers around the mobile (which is close to the ground) by narrow beams being formed on the arriving signals.
- Reduction in outage probability. Outage probability is the probability of a channel being inoperative due to an increased error rate. For example, by reducing interference using space-time techniques, the outage probability can be reduced.
- Increase in transmission efficiency. Due to the high directivity and gain of the space-time system, base station range may be extended, and a mobile may be able to transmit using less power resulting in longer battery life.

- Reduction in hand-off rate. When the capacity of a cellular system is exceeded, cell splitting is used to create new cells, each with its own base station and new frequency assignment, with increased hand-off as a result. Hand-off may be reduced by space-time processors which can create independent beams.
- Improved positioning accuracy by applying multi-beam antenna arrays.
- Reduction in cost, complexity and potential network architecture simplification. There is no doubt that dynamic hand-off, dynamic channel assignment, and dynamic nulling (all features of space-time systems) require more complexity. However, careful consideration should also be given to the overall improvement of system reliability, QoS, etc. when comparing space-time systems to conventional systems.

While antenna arrays provide many advantages, these must be offset against cost and complexity factors. A number of important points to be considered are

- hardware and software requirements increase as the number of antenna elements increases; and
- in practical situations, the antenna array performance may be adversely affected by channel modeling errors, calibration errors, phase drift and noise which is correlated between antennas.

1.4 THESIS ORGANIZATION

In covering the vast topic of space-time processing, this thesis concentrates mainly on three aspects, namely the space-time channel and system models, space-time coded processing for the downlink channel, and coded space-time processing for the uplink.

- In this chapter, an introduction into some of the newest developments in mobile communications is presented. Specific emphasis is placed on the evolution of second generation mobile communication networks to third generation mobile communication networks. A literature survey of forward error correcting codes and space-time processing techniques is presented as a basis for the work presented in this thesis.
- In Chapters 2 to 3, extensive background information on channel impairments and space-time channel and system models are presented. Together these chapters provide the necessary background information required to understand specific space-time processing techniques. The two main smart antenna techniques covered are adaptive beamforming systems, transmit and receive diversity systems, as well as the derivation of the BEP performance of these techniques in cellular environments.

Up to this point, uncoded space-time processing systems have been treated.

- Chapter 4 presents a detailed discussion of the channel coding techniques. Specifically, detailed discussion of convolutional, turbo and TCM FEC are presented. Also, the performance of convolutional and turbo coding for CDMA is analyzed and, as a means of comparison, results on the AWGN channel are presented.

Given the presented material on space-time processing and FEC coding, the following three chapters focus on the combination of the latter techniques to maximize the coding and spatial diversity/beamforming gains on offer.

- In Chapter 5, the thesis introduces layered space-time coding techniques to improve the downlink capacity.

- Chapter 6 considers extensions of the layered space-time turbo coding techniques to turbo transmit diversity techniques and turbo processing.
- In Chapter 7 the layered space-time coding concepts are extended to include trellis coding.
- To improve the uplink system performance and capacity, Chapter 8 concentrates on coded space-time receive diversity, beamforming, and combined diversity and beamforming systems.

In Chapter 9, the concluding chapter, the major results and conclusions of the thesis are presented.

Notes

1. High speed data rates, symmetric and reasonably continuous transmission and minimum delays.
2. Moderate data rates, medium to large files, asymmetric and bursty transmission and tolerance to a range of delays.
3. Already identified spectrum is 395 MHz (70 MHz GSM+150 MHz GSM 1800 + 20 MHz DECT +155 MHz terrestrial UMTS).
4. Trunking inefficiency and guard-bands must be allowed for, due to multiple operators and public/private and service category segmentation. This is assumed to improve from 10% in 2005 to 5% in 2010.

2 SPATIAL/TEMPORAL CHANNEL MODEL

The gain offered by space-time processing relies on many parameters, some of which are beyond the control of the design engineer, but which should be modeled accurately when analyzing such systems. Specifically four main areas of influence can be identified, namely: (i) the propagation path of the signal, (ii) temporal fading, (iii) the scattering environment and, (iv) the angular distribution of subscribers. These factors influence the system performance and careful attention should be given to the different aspects for optimal system design [126]. For this reason a thorough understanding of the various aspects influencing space-time performance is needed.

2.1 SPACE-TIME PROCESSING PERFORMANCE ISSUES

When realistic channel models of a mobile communication system are available, efficient signal processing schemes can be devised to improve system performance, and accurate system analysis can also be performed to predict system capacity and performance. In general, models describe parameters such as received signal strength, power delay profiles and Doppler spectra, which are important for the analysis of systems with omni-directional antennas. Of high importance in space-time systems, is knowledge of the direction of arrival (DOA) of the received signals, which is not available from conventional models. In this chapter, important effects are described such as multipath fading, and models for the scattering surrounding the mobile and base station. It is of importance to note that, due to the difference in angular dispersion at the mobile and base station, the propagation characteristics in the uplink and downlink might be different (channel non-reciprocity), and this is of significance in space-time based system performance analysis. The presented channel model will be used in later chapters to evaluate the performance of space-time CDMA systems under a variety of conditions.

2.1.1 Propagation Path

The modeling of the propagation path needs to take into account a number of effects. These include

- Path (propagation) loss;
- Shadowing (The particular scattering environment (i.e. trees, buildings) along a path at a given distance will be different for every path, causing variations with respect to the nominal value given by the path loss model. Some paths will suffer increased loss, while others will be less obstructed and have an increased signal strength. This phenomenon is called shadowing or slow fading and exhibits log-normal fading statistics.);
- Number of multipath components and the distribution of their envelopes (These effects are a result of the local scattering environment around the mobile and/or base station);
- Temporal fading (Due to its fundamental importance in a mobile environment, this effect is described in detail in Section 2.1.2, with emphasis on a space-time fading environment); and
- Correlation (Multipath components generated by a single area of local scatterers may show considerable correlation, with the correlation depending heavily on assumptions made concerning the spatial distribution of local scattering elements. Correlation is a very important concept in space-time systems since it influences the antenna pattern in beamforming (see Section 3.3.1.1) and the amount of diversity gain achievable in the system. The effect of correlation is considered in detail in Section 3.3.1.1, after the discussion of appropriate channel models for space-time systems).

The above mentioned propagation characteristics influence mainly the performance of the beamforming algorithm used, as well as the performance of the combining algorithm used in the case of space-time systems relying on both beam steering and diversity techniques. Most beamforming algorithms used assume that the signals arriving at each element of the array are highly correlated (ρ_{ij} >0.8) [127]. However, this assumption depends heavily on the composition of the local scattering area surrounding the mobile.

2.1.1.1 Path Loss. If a wireless channel's propagating characteristics are not specified, it is usually inferred that the signal attenuation versus distance behaves as if propagation takes place over ideal free-space. The model of free space treats the region between the transmitting and receiving antennas as being free of all objects that might absorb or reflect RF energy. It is further assumed that, within this region, the atmosphere behaves as a perfectly uniform and non-absorbing medium. Furthermore, the earth is treated as being infinitely far away from the propagating signal. In this idealized free-space model, the attenuation of RF energy behaves according to an inverse-square law.

2.1.2 Temporal Fading

Based on experimental evidence, the cause of fading can be attributed to large-scale fading and/or small-scale fading. Large-scale fading (or shadowing) has path loss as a result with effects as described in Section 2.1.1. Small-scale fading manifests itself in two mechanisms, namely signal dispersion (time-spreading of the signal) and time-variant behavior of the channel. Due to motion between the transmitter and the receiver the channel is time-variant as a result of the propagation path changing. The rate of change of these propagation conditions accounts for the rapidness of the fading (rate of change of the fading impairments). Small-scale fading is generally statistically described by either a Rayleigh [128, 129], Rician [129, 130] or Nakagami-m [130, 131, 132] distribution. The model choice depends mainly on the operating environment of the communication system. If the multiple reflective paths are large in number and there is no line of sight (LOS) signal component, the envelope of the received signal is traditionally statistically described by a Rayleigh probability density function. When there is a dominant non-fading signal component present, such

as a LOS propagation path, the small-scale fading envelope is described by a Rician pdf. In addition to the attractive mathematical properties of the Nakagami-m fading model, it has also been shown in [133, 134] that the Nakagami model can be used to accurately describe the fading behavior of multipath signals and the varying physical scattering processes. The distribution of these multipath signal parameters is dependent on the type of environment (i.e., macro-, micro- or pico cell).

2.1.3 *Scattering Environment*

The distribution of the DOA of multipath signals is often assumed to be uniform over $(0, 2\pi]$ [135, 136]. To determine the performance of a space-time system, channel models that include the effect of the DOA need to be constructed. A critical aspect that determines the DOA at either the base station or the mobile, is the scattering environment around the transmitter and receiver.

For a detailed discussion of spatial scatterer models, the text by Ertel *et al.* [137] may be consulted. Two typical scattering models commonly used are the circular disk of scatterers model (CDSM) [138], and the Gaussian scatterer (GS) model [139]. The CDSM is the "classical" spatial model, while the GS model is more realistic in certain environments. In this section the CDSM originally proposed by Jakes [138] and used in Lee [140] is presented.

2.1.3.1 CDSM DOA [116, 138, 140, 141]. Making extensive use of the results by Van Rheeder *et al.* [141], the DOA pdf at the base station is derived here for the CDSM shown in Figure 2.1.

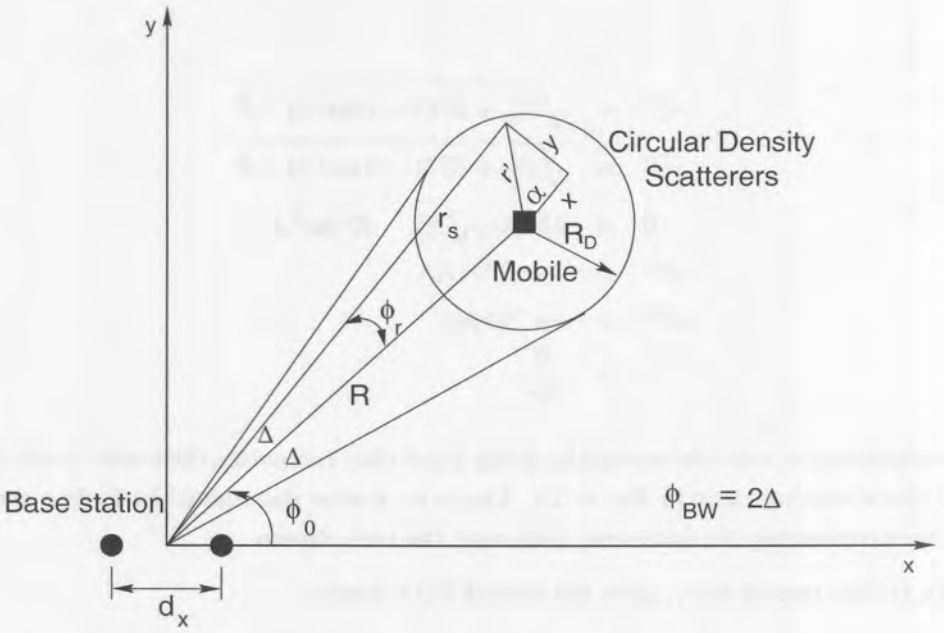

Figure 2.1. Cartesian geometry of circular disk of scatterers model.

If the mobile is located at the co-ordinates $(0, 0)$, then the pdf of the location of scatterers around the mobile is given by

$$p_{X,Y}(x,y) = \begin{cases} \frac{1}{\pi R_D^2} & , x^2 + y^2 \leq R_D^2 \\ 0 & , \text{elsewhere} \end{cases} . \tag{2.1}$$

Finding the joint density $p_{R_s,\Phi}(r_s,\phi)$ requires a transformation of the random variables (X,Y) into the random variables (R_s,Φ) via

$$p_{R_s,\Phi}(r_s,\phi) = \mid J \mid p_{X,Y}(x,y)|_{x=r_s\ \cos\phi - R, y=r_s\ \sin\phi}, \tag{2.2}$$

where $\phi = 90^o - \phi_0$.

In (2.2), J is the Jacobian of the transformation, computed as

$$J = \begin{vmatrix} \frac{\partial(r_s\ \cos\phi - R)}{\partial r_s} & \frac{\partial(r_s\ \sin\phi)}{\partial r_s} \\ \frac{\partial(r_s\ \cos\phi - R)}{\partial \phi} & \frac{\partial(r_s\ \sin\phi)}{\partial \phi} \end{vmatrix} = r_s. \tag{2.3}$$

Substituting (2.1) and (2.3) into (2.2) yields the joint density of R_s and Φ

$$p_{R_s,\Phi}(r_s,\phi) = \begin{cases} \frac{r_s}{\pi R_D^2} & , r_s^{(1)} \leq r_s \leq r_s^{(2)}, \phi^{(1)} \leq \phi \leq \phi^{(2)} \\ 0 & , \text{otherwise} \end{cases} , \tag{2.4}$$

where

$$\begin{aligned} r_s^{(1)} &= \sqrt{R_D^2 + R^2(1 - 2\sin^2\phi) - \mathcal{B}} \\ r_s^{(2)} &= \sqrt{R_D^2 + R^2(1 - 2\sin^2\phi) + \mathcal{B}} \\ \mathcal{B} &= 2R\cos\phi\sqrt{R_D^2 - R^2\sin^2\phi} \\ \phi^{(1)} &= -\sin^{-1}(1/\upsilon) \\ \phi^{(2)} &= \sin^{-1}(1/\upsilon) \\ \upsilon &= \frac{R}{R_D}. \end{aligned} \tag{2.5}$$

Limits on the parameter r_s were determined by fixing ϕ and then computing the points at which the resulting line intersect the scattering circle in Figure 2.1. Limits on ϕ were determined by finding the angles of the two tangent lines connecting the scattering circle with the base station.

Integrating (2.4) with respect to r_s, gives the desired DOA density

$$p_{\Phi,\nu}(\phi,\nu) = \begin{cases} \frac{1}{2\pi}\left(\upsilon\ \cos\ \phi + \sqrt{1 - \upsilon^2\ \sin^2\ \phi}\ \right)^2 & , 0 \leq \phi \leq 2\pi,\ 0 \leq \upsilon \leq 1 \\ \frac{2}{\pi}\ \upsilon\ \cos\ \phi\ \sqrt{1 - \upsilon^2\ \sin^2\ \phi} & , \phi^{(1)} \leq \phi \leq \phi^{(2)};\ \upsilon > 1 \\ 0 & , \text{otherwise.} \end{cases} . \tag{2.6}$$

Note that this result is valid for $\upsilon > 1$ and $0 \leq \upsilon \leq 1$, i.e., when the base station is located outside the scattering circle and when the base station is located inside the scattering circle, respectively.

Figure 2.2 depicts $p_{\Phi,\nu}(\phi, \nu)$ as a function of both ϕ and υ. From this figure, the following observations can be made. For large υ, the situation where the mobile terminal is far from the base station, and all the scatterers are close to the mobile, the pdf approaches an "impulse-like" density. Conversely, for small υ, the situation where the mobile is close to the base station and the scattering circle is large (non line of sight (NLOS) propagation), the pdf approaches a uniformly distributed density. Using (2.6) and setting υ equal to zero, the latter uniform DOA density is calculated as $1/2\pi, \forall\phi$.

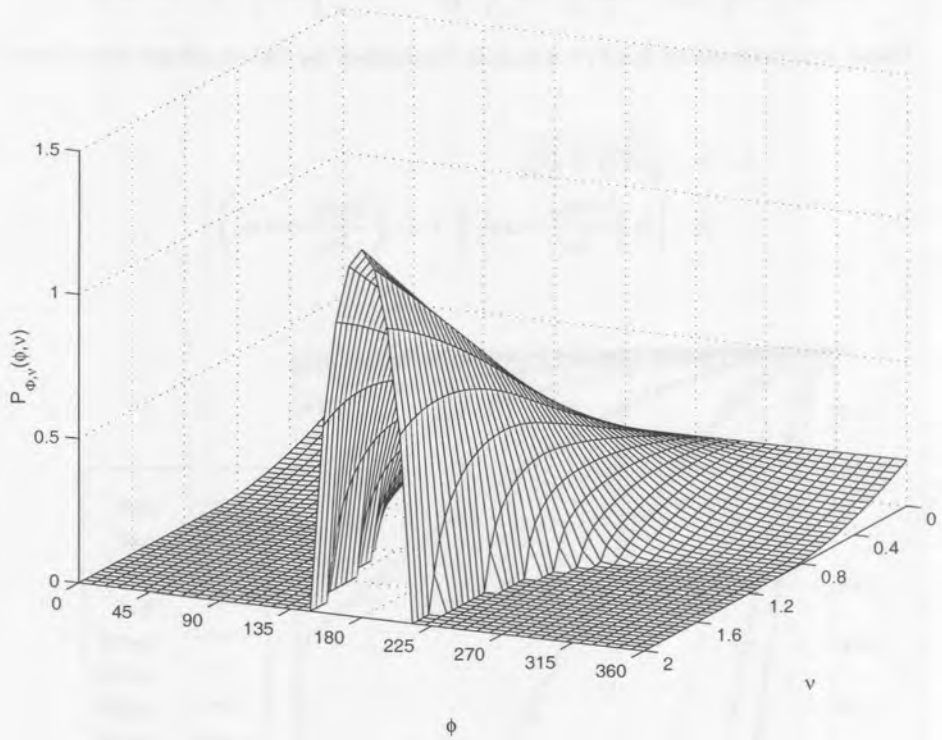

Figure 2.2. DOA as a function of ϕ and υ.

2.1.3.2 CDSM Correlation [141]. In the CDSM it is assumed that all signals arrive at the base station within $\pm\Delta$ of the angle ϕ_0, and that the ith received signal path is uniformly distributed with height $1/2\Delta$. Using the results of Lee [142], the fading correlation between two antenna elements, spaced d_x apart, can be written as two components R_{xx} and R_{xy}

$$R_{xx} = \int_{-\pi/2+\phi_0}^{+\pi/2+\phi_0} \cos[\, 2\pi(d_x/\lambda)\sin\ \phi\,]\ p_\Phi(\phi)\ d\phi \tag{2.7}$$

$$R_{xy} = \int_{-\pi/2+\phi}^{+\pi/2+\phi_0} \sin[\, 2\pi(d_x/\lambda)\sin\ \phi\,]\ p_\Phi(\phi)\ d\phi. \tag{2.8}$$

where R_{xx} denotes the correlation of the real components of the signal received at the two antennas, and R_{xy} denotes the correlation of the real component of the signal arriving at the one antenna element and the imaginary component arriving at the other antenna element.

From (2.6) with ν constant, the density $p_\Phi(\phi)$ is used to derive R_{xx} and R_{xy} as series expansions of integer order Bessel functions. Substituting (2.6) into (2.7) and (2.8), and using geometric substitutions and some numerical analysis the correlation of fading approximations is found to be [141]

$$R_{xx} \approxeq \left[J_0\left(\frac{2\pi d_x}{\lambda \upsilon}\cos\phi_0\right) + J_2\left(\frac{2\pi d_x}{\lambda \upsilon}\cos\phi_0\right)\right]\cos\left(\frac{2\pi d_x}{\lambda}\sin\phi_0\right), \tag{2.9}$$

and

$$R_{xy} \approxeq \left[J_0\left(\frac{2\pi d_x}{\lambda \upsilon}\cos\phi_0\right) + J_2\left(\frac{2\pi d_x}{\lambda \upsilon}\cos\phi_0\right)\right]\sin\left(\frac{2\pi d_x}{\lambda}\sin\phi_0\right), \tag{2.10}$$

where $\upsilon >> 1$. These approximations lead to a simple expression for the envelope correlation

$$\begin{aligned} \rho &= \sqrt{R_{xx}^2 + R_{xy}^2} \\ &\approxeq \left|J_0\left(\frac{2\pi d_x}{\lambda \upsilon}\cos\phi_0\right) + J_2\left(\frac{2\pi d_x}{\lambda \upsilon}\cos\phi_0\right)\right|. \end{aligned} \tag{2.11}$$

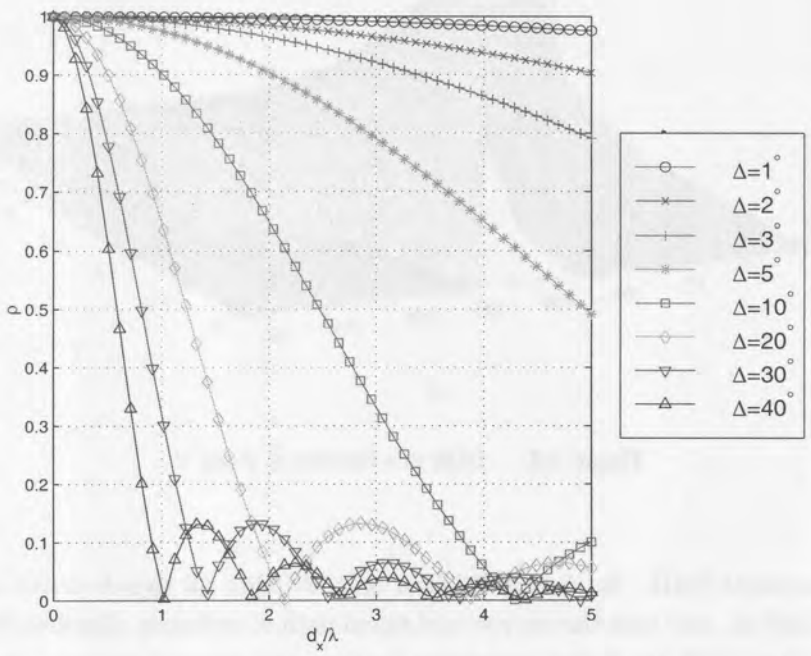

Figure 2.3. CDSM fading correlation for $\phi_0 = 45^o$.

Figure 2.3 depicts the fading correlation envelopes for the CDSM DOA when $\phi_0 = 45°$. In Figure 2.3, increasing values of Δ denote larger scattering areas (as would be found in micro-cells with NLOS propagation). Thus, whereas $\Delta = 40°$ may be used to represent a NLOS micro-cell, a value of $\Delta = 10°$ may be used to represent a macro-cell. From the figure it is then clear that the CDSM indicates that larger antenna spacing is required in macro-cellular environments to decorrelate signals received by a diversity receiver. Conversely, this would mean that with fixed antenna spacing, larger diversity gains could be achieved in an environment where severe scattering is present than in an environment where few scattering points are present.

2.1.4 *Angular Subscriber Distribution*

In addition to dependence on the distribution of scattering elements, DOA distribution of signals in a cellular system is also dependent on the distribution of subscribers in a cell. In [126], Lötter showed that the manner in which subscribers are clustered together in angle (as would be the case on a road), significantly influences the gains that may be achieved by a space-time system. For instance, if the reference user and an interfering user are co-located in angle, no antenna pattern can be formed in either the up- or downlinks to reduce the interference experienced by the reference user. Therefore, the gain offered by, for instance, a transmit beamforming system to users in the relevant cell is negligible. On the other hand, having subscribers clustered in certain areas means that antenna sectors can be narrowed, thereby reducing interference to adjacent cells and increasing the overall network performance, even if the performance of all individual cells is not increased.

A number of approaches to the modeling of user locations have been followed in literature. For example, in [143] a uniformly distributed mobile user density is proposed, with a highway traffic distribution model presented in [144] and a modified Gaussian distribution proposed in [1]. The most accurate description of user locations would be gained from practical measurements at each site of interest. These assumptions are sufficient in the intended environments. A more general pdf that describes the user distribution, and is applicable to many scenarios, has been proposed in [126].

2.2 FADING DISTRIBUTION BASED ON SCATTERING ENVIRONMENT

According to Section 2.1.2, the choice of a channel model depends mainly on the operating environment of the communication system, with Rayleigh distributions commonly used for NLOS and Rician distributions commonly used for LOS propagation environments. An alternative to these fading distributions is the Nakagami or $m$distribution [132]. This distribution is defined as

$$p_S(s) = \frac{2}{\Gamma(m)} \left(\frac{m}{\Omega}\right)^m s^{2m-1} e^{-ms^2/\Omega}, \tag{2.12}$$

where s denotes the received signal strength in volts, m is a parameter determining the fading characteristics of the signals and $\Omega = E(S^2)$.

One of the main advantages of the Nakagami distribution is its wide applicability. Specifically, the Nakagami distribution is equivalent to the Rayleigh distribution when $m = 1$, the onesided exponential distribution when $m = 0.5$, and it can also be used to model the Rician distributions with sufficient accuracy by setting [129, 130]

$$m = \left(1 - \left(\frac{\mathcal{K}}{1+\mathcal{K}}\right)\right)^{-1} \tag{2.13}$$

where $\mathcal{K}$ denotes the Rice parameter (average direct power/average scattered power). In addition to the attractive mathematical properties, it has also been shown in [133] that the Nakagami model can be used to accurately describe the fading behavior of multipath signals. Specifically it is shown that the Nakagami distribution can be used to describe varying physical scattering processes.

One of the important requirements in a spatial-temporal channel model is to incorporate the effect of the non-homogeneous geography of the cell into the temporal fading model used. Consider the case where, for

instance, each multipath echo received at the base station is subject to Rayleigh fading. The question that arises is whether it is accurate to assume that all of the received multipath echos will have the same statistical fading distribution. Is it not possible that some of the received paths may contain a LOS component changing the distribution of the fading envelope from Rayleigh to Rician, or perhaps that some paths may exhibit more severe fading, i.e., as described by a one-sided exponential distribution? Examining results from extensive measurements, this is in fact the case. For example, in the experimental study in [145], the urban propagation channel is modeled as a Rician channel with varying $\mathcal{K}$ parameter. This indicates that an accurate model would describe the fading effects on each received multipath signal at the base station.

Following the approach of Lötter [126, 146], the fading process on each of the received multipath signals can be modeled by incorporating information on the DOA of the multipath signals at the base station. Utilizing the properties of the Nakagami distribution, varying degrees of fading can be approximated by the correct choice of the m parameter. In order to develop a relationship between the fading exhibited by a signal and its DOA, the results of [145] were used in [146].

2.3 SUMMARY OF SPACE-TIME CHANNEL MODELS

Thus far, all the elements required to accurately model the cellular channel have been presented. In Section 2.1, the concepts of fading, scattering environments, subscriber distribution and correlation were introduced. These aspects were further developed in this chapter where more comprehensive treatments of the CDSM and GS model were presented. In addition, the distribution of the fading envelope of multipath signals was explained in Section 2.2. In this section, all of the aspects of the channel model described in detail in the preceding section are combined and it is shown how a comprehensive channel model for use in the evaluation of cellular system models can be constructed.

Figure 2.4 depicts the process of constructing a channel model as a simple flow diagram. Let us first turn our attention to the choice of a cellular environment. This choice between the different cellular environments can firstly be viewed as a choice between a high-rank and a low-rank channel model. Environments with very low angular spread of the received signals are deemed to be low-rank channels and, in these cases, the description of the local scattering environment becomes less important. On the other hand, when the angular spread of the received signals is expected to be larger, the channel model can be described as high-rank, and consequently the description of the local scattering environment is of higher importance. Thus, in the case of a high rank channel model (which would be the predominant case in cellular environments), a decision must be made as to whether to describe the scattering area surrounding the base station or a mobile using the CDSM or the GS model. Both models will yield accurate results, with the GS model yielding a more general description.

The choice of the scatterer model will determine three additional channel model parameters, namely the correlation between the received signal envelopes at different points in space, the pdf of the received signal at the base station subsystem (BSS) and the characteristics of the temporal fading present on each multipath signal. The correlation between the received signal envelopes at different points in space will determine the possible gains that can be achieved using diversity systems. As the possible diversity gain is significantly influenced by the correlation between the fading envelopes, this part of the channel model is extremely important in order to accurately estimate the overall system performance. Whereas the correlation characteristics of the channel model influence mainly the diversity performance of the system, the pdf of the DOA at the BSS influences the performance of a beamforming system, as well as the fading characteristics of the received signals.

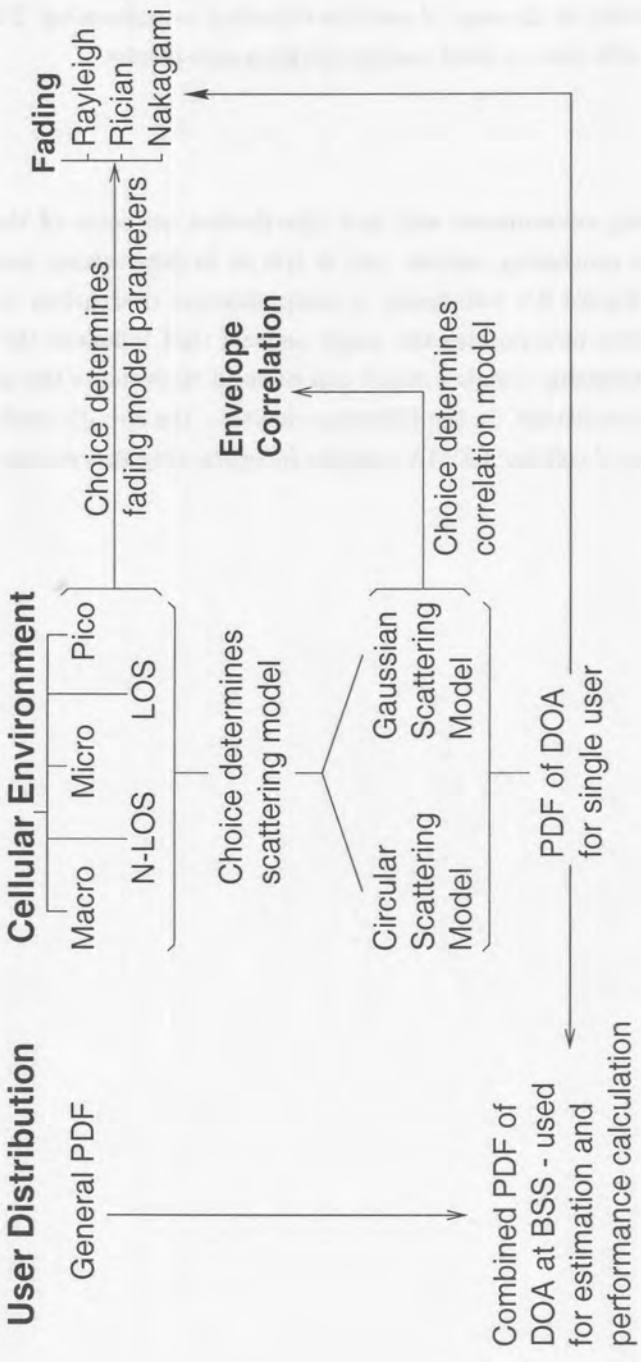

Figure 2.4. Constructing a typical cellular channel model.

Finally, the choice of cellular environment will determine the characteristics of the fading envelope of each received multipath signal. Generally, the received signal envelope is described as either Rayleigh, Rician or Nakagami. The Nakagami description provides the most general description of the fading characteristics and the use of this distribution is described in Section 2.2.

In addition to the choice of the environment, the choice of the user distribution will also significantly influence the performance of the cellular system. Thus, an estimation of the distribution of the user population based on the geographical environment where the users are active is required as one of the core ingredients of

the channel model, specifically in the case of systems including beamforming. The general assumption of a uniform user distribution will tend to yield average performance results.

2.4 SUMMARY

Path loss, fading, scattering environment and user distribution are some of the key aspects limiting the performance of space-time processing systems and is crucial in determining mitigation techniques. With the process described in Figure 2.4 completed, a comprehensive description of the cellular environment is available. This description incorporates the major aspects that influence the performance of a cellular system and therefore the resulting channel model can be used to evaluate the performance of any cellular system under a variety of conditions. In the following chapters, the specific analysis techniques required to determine the performance of cellular CDMA systems incorporating space-time processing techniques will be presented.

3 SYSTEM MODEL AND UNCODED PERFORMANCE EVALUATION

It was shown that factors such as the scattering environment, the user distribution and the fading environment, amongst others, play important roles in determining the performance of space-time mobile systems. In this chapter three smart antenna techniques, namely beamforming, transmit and receive diversity, are considered in more detail to mitigate the effects due to the inherent impairments of the mobile communication channel. These techniques are especially applicable to mobile CDMA communications, where interference is more pronounced due to the fact that users transmit on the same frequency with unique spreading codes.

The aim of a well-designed mobile communication system is to share the common transmission medium in such a manner that

- the average overall amount of transmitted information will be as large as possible,
- the average probability of error experienced by each user will be as low as possible, and
- the average delay will be as low as possible.

In general, not all of these goals can be achieved simultaneously, and the design process involves a trade-off between these objectives. By making use of coding and smart antenna techniques, it is possible to approach these goals. For instance, beamforming can be used to decrease a system's probability of error by reducing CDMA interference. This can be achieved by intelligent combination of the received signals by multiple antenna elements at the base station or mobile. In a mobile communication system with antenna arrays, the fast fading signal component introduces a random phase and amplitude to the received signal on each antenna element, which perturbs the steering vector of the array. In the case of Rayleigh or Nakagami fading, the phase can take on any value between $(0, 2\pi]$, and the DOA of the waves may be impossible to determine from short-duration observations of the received signal. For this reason, in a fading environment it may not be useful to implement the beamformer to create lobes and nulls toward desired and interfering sources. When the fast fading is highly correlated between the elements, it may be considered as a single scalar which multiplies with the steering vector, affecting all elements equally. On the other hand, no receive

diversity gain can be obtained, since receive diversity relies on uncorrelated fading. The correlation between elements decreases with element spacing and changes according to the scattering environment in which the system operates. There is therefore a conflict between the avoidance of grating lobes and the need for receive diversity gain [127].

3.1 BACKGROUND

Thus far in this thesis, it has been shown that a variety of factors influence the performance of cellular systems incorporating smart antenna techniques. These factors have been combined into an easy to use channel model that makes the analytic evaluation of a space-time smart antenna based cellular CDMA systems possible. In this chapter, the channel model developed in Chapter 2 will be used to evaluate the performance of an uncoded cellular CDMA system.

In order to simplify the analysis of space-time processing systems, a basic model of the communication system which identifies inputs, outputs and the channel is required. For a general space-time processing system where multiple antennas are employed at both the transmitter and the receiver, such a signal model is known as a multiple-input/multiple-output (MIMO) model. Clearly this is due to the fact that the desired signal has multiple inputs into the channel (the transmit antennas) as well as multiple outputs (the receive antennas). Furthermore, a MIMO system can be viewed as multiple single-input/single-output (SISO) sub-channels. The MIMO system's channel capacity is then the sum of the individual capacities of these sub-channels. Fading correlation effects as described in Chapter 2, affects the MIMO system capacity by modifying the distributions of the gains characterizing the SISO sub-channels. As the general MIMO case is not frequently used in practice, a number of alternative channel configurations for single user (SU) and multi user (MU) scenarios are considered. These are

- Uplink and downlink (single-input/single-output - SISO)
  - SU-SISO: Single user with single antenna input/output at the base station and single antenna input/output at the mobile.
  - MU-SISO: Multiuser with single antenna input/output at the base station and single antenna input/output at each of the mobile units.
- Downlink (multi-input/single-output - MISO)
  - SU-MISO: Single user with multiple antenna inputs at the base station and single antenna output at the mobile unit.
  - MU-MISO: Multi user with multiple antenna composite inputs at the base station and single antenna output at each mobile.
- Uplink (single-input/multi-output - SIMO)
  - SU-SIMO: Single user with single antenna input at the mobile and multiple antenna outputs at the base station.
  - MU-SIMO: Multi user with single antenna input at each mobile and multiple antenna composite outputs at the base station.

This research looks at ways and means of using multiple antennas at the BSS transmitter (downlink) and the BSS receiver (uplink) to make the recovery of the transmitted data more reliable. Specifically, the use

of coding in conjunction with transmit and receive diversity combining (space-time coding), and receive beamforming arrays (coded space-time) are considered. The BEP performance analysis presented in this chapter is restricted to the performance of the uncoded space-time CDMA system. In the following chapters, these results will be extended to include the performance of the CDMA systems incorporating space-time coding techniques.

Conventional detection in a single path transmission environment is done by matched filtering and sampling of the received signal, followed by a decision device, e.g., a simple polarity check for BPSK or QPSK. The received signal is matched to the spreading code of the desired user. In a single user environment, this is optimal in the sense that the SNR is maximized which in turn corresponds to ML detection. In a multiuser environment, this is, however, not entirely true. The SNR is still maximized, but the detector is not ML due to the presence of MAI.

In a multi-path environment, the decision statistics for each multi-path component are obtained. As has been discussed in Chapter 1 there are then several strategies for receive diversity combining of these decision statistics pertaining to the same bit. Combining can, of course, also be done after individual detection of each multi-path component which does in fact provide potentially better performance. This is, however, not as common as pre-detection or RAKE combining. For this reason the receiver is restricted to a matched filter front-end followed by RAKE multipath diversity combiner.

In general, adaptive receiver structures, for instance minimum mean-square error detectors, may also be considered. With these receivers the focus is directed towards interference cancellation. In the most general terms, interference cancellation detectors have structures where an explicit estimate of the MAI component in the received signal is generated and then subtracted from the received signal in an iterative manner. In this thesis, the application of interference cancellation, and multiuser detectors in general, has not been considered. It is proposed to be addressed in future research.

Figure 3.1 depicts the basic structure of an M_D-branch diversity system, with

$$\begin{aligned} M_D &= 1 \text{ for a SISO system,} \\ M_D &= M_T \text{ for a MISO (transmit diversity) system,} \\ M_D &= M_R \text{ for a SIMO (receive diversity) system,} \\ M_D &= M_T \times M_R \text{ for a MIMO (combined transmit/receive diversity) system.} \end{aligned}$$

With reference to Figure 3.1, let the signal in the nth channel diversity system have power Ω_n, Nakagami fading parameter m_n, and correlation between the nth and $(n+1)$th branch be $\rho_{n(n+1)}$. It is assumed that each channel is frequency non-selective with channel attenuation factors $\{\beta_n\}, n = 1, \cdots, M_D$ having Nakagami-distributed envelope statistics. Making use of (2.12), the fading distribution of each diversity branch may be written as

$$p_{\beta_n}(\beta_n) = \frac{2}{\Gamma(m_n)} \left(\frac{m_n}{\Omega_n}\right)^{m_n} \beta_n^{2m_n-1} e^{-m_n\beta_n^2/\Omega_n}, \tag{3.1}$$

with $\Omega_n = E\{S_n\} = E\{\beta_n^2\}$. The fading *power*, $S_n = \beta_n^2$, therefore has a gamma distribution [147].

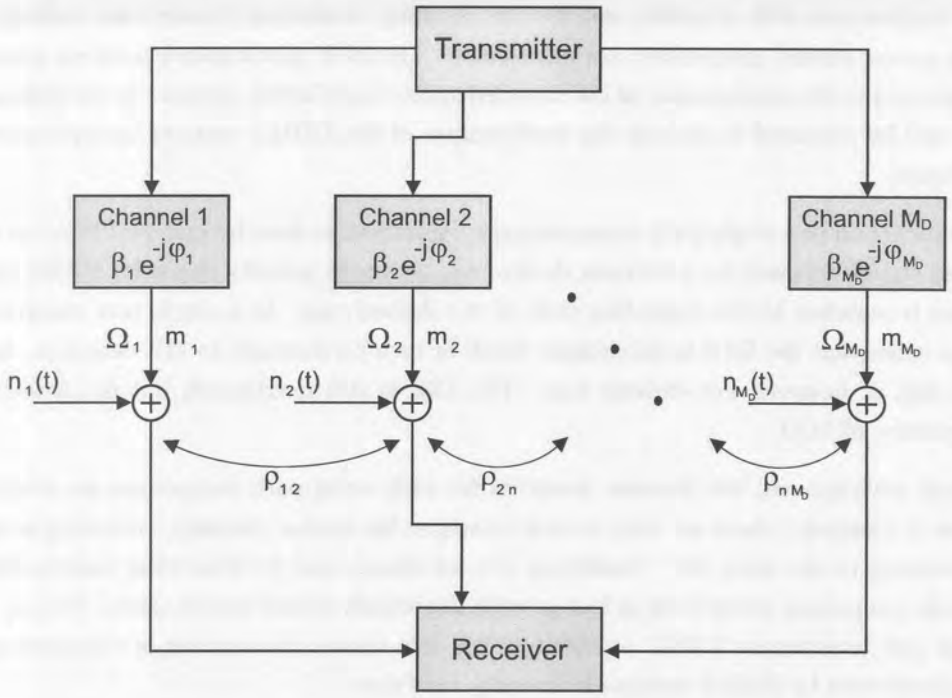

Figure 3.1. Basic structure of a diversity system.

3.2 MULTIPLE TRANSMIT/RECEIVE ANTENNA SYSTEM MODELS

In this section, the different transmit and receive diversity, and beamforming techniques for cellular CDMA are considered.

3.2.1 Transmit Diversity

Two transmit diversity techniques, namely code-division and time-division are proposed for the downlink. As with its receive diversity counterpart, transmit diversity techniques also require a number of uncorrelated diversity branches carrying the same information and a circuit to combine the received signals or to select one of them.

3.2.1.1 Code-Division Transmit Diversity (CDTD). In CDMA it is desirable to transmit orthogonal signals to different users in the downlink and to simultaneously maintain a fixed number of user channels. Clearly both these requirements cannot be met, since the number of available orthogonal channels is fixed. For this reason two main approaches are followed in transmit diversity for cellular CDMA. These are

Orthogonal CDTD (O-CDTD) [63, 148].
For O-CDTD, different complex orthogonal spreading codes are assigned to every antenna element. This maintains the orthogonality between the two output streams, and hence self-interference is eliminated in flat fading. O-CDTD should also be compared with orthogonal transmit diversity (OTD) [149, 150] and Alamouti code transmit diversity (ACTD) [151] proposed for narrowband TDMA.

Non-orthogonal CDTD (NO-CDTD) [54, 55, 152, 153].
For NO-CDTD, the same complex spreading code is assigned to every antenna with an intentional delay

between each antenna element. For this reason NO-CDTD is also known as delayed CDTD, similar to the delayed transmit diversity (DTD) scheme proposed for narrowband TDMA [54, 55, 56]. Typical non-orthogonal spreading sequences used for NO-CDTD are Gold sequences. The advantage of Gold sequences are that they maximize the number of spreading sequences, but compromises orthogonality due to self-interference.

Figure 3.2(a) illustrates the CDTD structure for a single user in the downlink. Both O-CDTD and NO-CDTD have the receive diversity property of soft-failure[1].

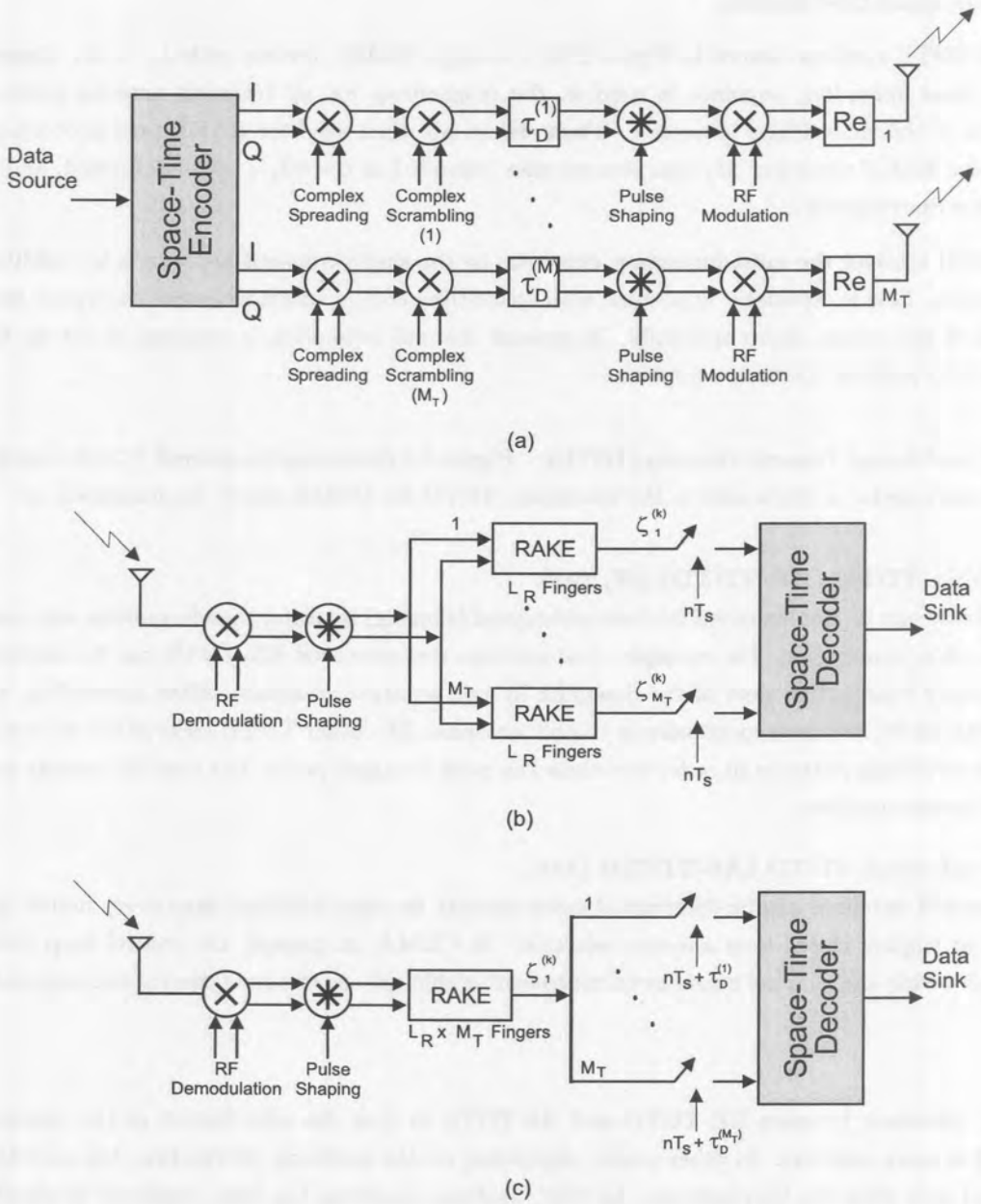

Figure 3.2. Block diagram of single user CDTD system. (a) Transmitter for O-CDTD and NO-CDTD, (b) Receiver for O-CDTD, and (c) Receiver for NO-CDTD.

The main components are the spaced-time encoder, complex spreader, modulator and transmit antennas. Data modulation per antenna is QPSK, where the spaced-time encoded downlink data is mapped to the I and Q branches. The data is spread by a combination of complex (orthogonal and non-orthogonal) variable spreading and complex scrambling codes. In both O-CDTD and NO-CDTD the symbol rate on each transmit antenna M_T is reduced by a factor $1/M_T$ to ensure that the data bits are evenly distributed to each transmit antenna element.

The general receiver structures for O-CDTD and NO-CDTD are shown in Figure 3.2(b) and 3.2(c), respectively. With reference to Figure 3.2(b), a total of M_T RAKE receivers, each with L_R fingers, are employed for O-CDTD. Each of the M_T RAKE receivers is trained on the spreading sequence associated with the corresponding transmit antenna. The M_T complex outputs are then sampled at the symbol rate, T_s, and passed to the space-time decoder.

In the NO-CDTD receiver, shown in Figure 3.2(c), a single RAKE receiver with $L_R \times M_T$ fingers is used. Since the same spreading sequence is used at the transmitter for all transmit antenna paths, *a priori* information of the time delays is needed. These delays are then used for RAKE post-processing. At the output of the RAKE combiner M_T complex samples (sampled at $t = nT_s + \tau_D^m$) are formed, and processed by the space-time decoder.

At the CDTD receiver the most important extension to the single transmit antenna is the addition of M_T RAKE fingers. This is especially important with space-time coding which attempts to exploit the degrees-of-freedom of the system more optimally. In general channel estimation is required to set up the RAKE receiver and to perform diversity reception.

3.2.1.2 Time-Division Transmit Diversity (TDTD). Figure 3.3 illustrates the general TDTD transmitter and receiver structures for a single user in the downlink. TDTD for CDMA can be implemented as

Round-robin TDTD (RR-TDTD) [57, 148].
This scheme can be implemented by time-orthogonal (sharing) by using pseudo-random antenna hopping (round-robin) sequencing. For example, dual antenna time-switched RR-TDTD can be implemented by transmitting consecutive slots of the downlink by two separate antennas. After scrambling, the spread time slots can be switched consecutively to each antenna. The other TDTD users of the system may have different switching patterns in order to reduce the peak transmit power and peak to average power ratio in each power amplifier.

Antenna selection TDTD (AS-TDTD) [148].
The transmit antennas can be determined more optimal, by using feedback from every mobile to the base station to employ closed-loop antenna selection. In CDMA, in general, the control loop delay can be kept well within the channel coherence time to enable efficient use of power control and antenna selection loops.

The main difference between RR-TDTD and AS-TDTD is that the distribution of the encoded bits in AS-TDTD is more selective. In other words, depending on the feedback information, the encoded bits are transmitted only from the best antenna. In [148], feedback signaling has been employed to simultaneously perform fast closed loop power control for downlink diversity.

The drawbacks associated with TDTD are that

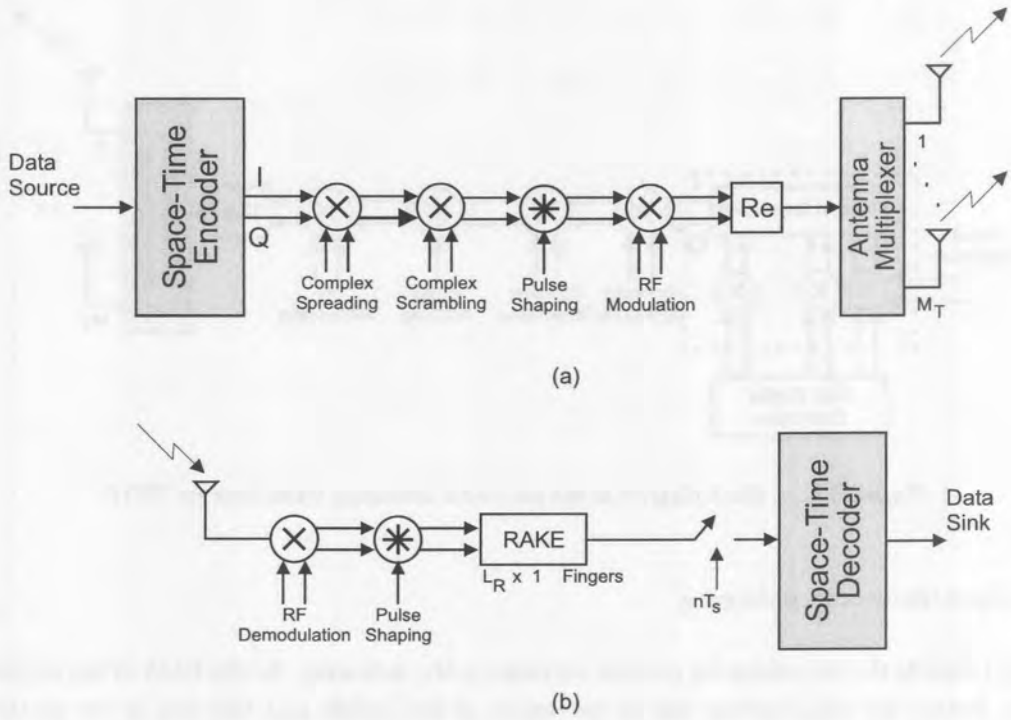

Figure 3.3. Block diagram of single user TDTD system. (a) Transmitter, and (b) Receiver.

- TDTD does not provide soft-failure, and

- the channel has to be re-estimated on a slot-by-slot basis.

3.2.1.3 CDTD and TDTD with Pre-RAKE Combining. As a interesting extension to both the CDTD and TDTD diversity schemes presented in the foregoing, a pre-RAKE configuration may be considered. Figure 3.4 illustrates a general pre-RAKE combining TDTD transmitter. This transmitter is based on the CDMA pre-RAKE combining strategy by Jeong *et al.* [154]. The principle of operation is that the transmitted pre-RAKE signal is a time-reversed replica of the channel impulse response. In this way space and path diversity is possible at the mobile receiver without any conventional receive diversity techniques. The transmitter is based on two diversity principles, pre-RAKE (realized by the tapped delay line) and space diversity (realized by the multiple transmit antennas). A similar extension to CDTD is possible.

3.2.2 Receive Diversity

As has been argued in Chapter 1, space diversity reception in the uplink is one of the effective and, hence, widely applied techniques for mitigating the effects of multipath fading. The classical approach is to use multiple antennae at the receiver and perform combining (i.e., MRC or EGC) or selection (i.e., SC) and switching in order to improve the received signal quality. The receive diversity system employing M_R antennas is shown in Figure 3.5(a) (transmitter) and 3.5(b) (receiver), respectively.

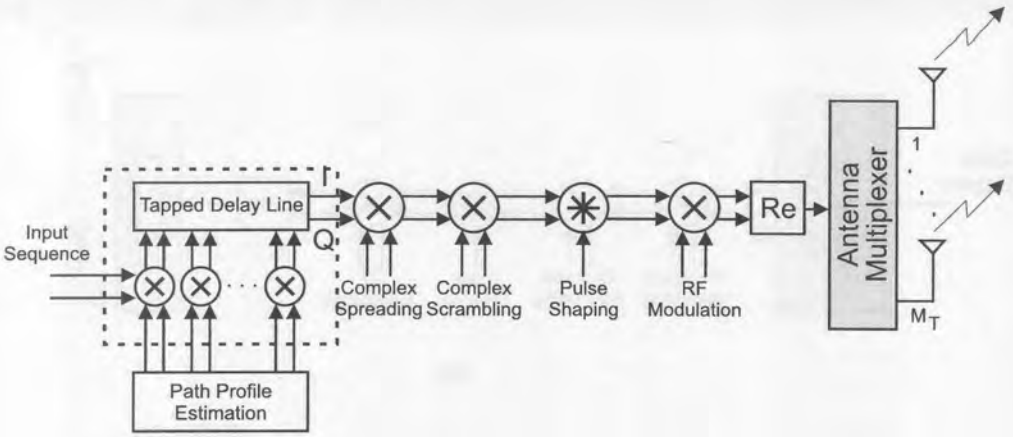

Figure 3.4. Block diagram of the pre-RAKE combining transmitter for TDTD.

3.2.3 Transmit/Receive Beamforming

Figure 3.5(c) depicts the beamforming receiver employing M_D antennas. As the DOA of the received signals at the base station are time-varying due to movement of the mobile and also due to the scattering environment, the co-channel interference, multipath components and even Doppler frequency are time varying functions. By using a beamformer, it is possible to separate signals co-located in frequency, but separated in the spatial domain and to track these time varying signals. In a CDMA system, this specifically results in reducing the interference from unwanted signals by optimizing the array pattern through the adjustment of the weights of the array according to some criteria, or cost function.

3.3 PERFORMANCE EVALUATION

The BEP performance derivation for uncoded space-time beamforming and transmit/receive diversity are considered in this section.

3.3.1 Receive Beamforming Performance

Making extensive use of the analysis carried out by Lötter [126], the BEP performance of a uniform linear array (ULA) beamformer, with M_B antenna elements is considered. Consider Figure 3.5(a), where the output of the transmitter of user k can be written as

$$s^{(k)}(t) = \sqrt{2P}a^{(k)}(t)\, b^{(k)}(t)\, \cos(\omega_c t + \phi^{(k)}), \tag{3.2}$$

where P denotes the average transmitted signal power, $b^{(k)}(t)$ denotes binary data with symbol period T_s seconds and values taken from the set $\{\pm 1\}$, $a^{(k)}(t)$ denotes a random binary spreading sequence with chip period T_c seconds and length $N = T_s/T_c$ [2] with value taken from the set $\{\pm 1\}$. N is the spreading sequence length. In addition, standard BPSK [3] modulation is used with carrier frequency ω_c rad/s and unknown carrier phase $\phi^{(k)}$, a random variable uniformly distributed over $[0, 2\pi)$. The transmitted signal propagates over a radio channel modeled as a Nakagami fading, time invariant, discrete multipath channel with equivalent lowpass response

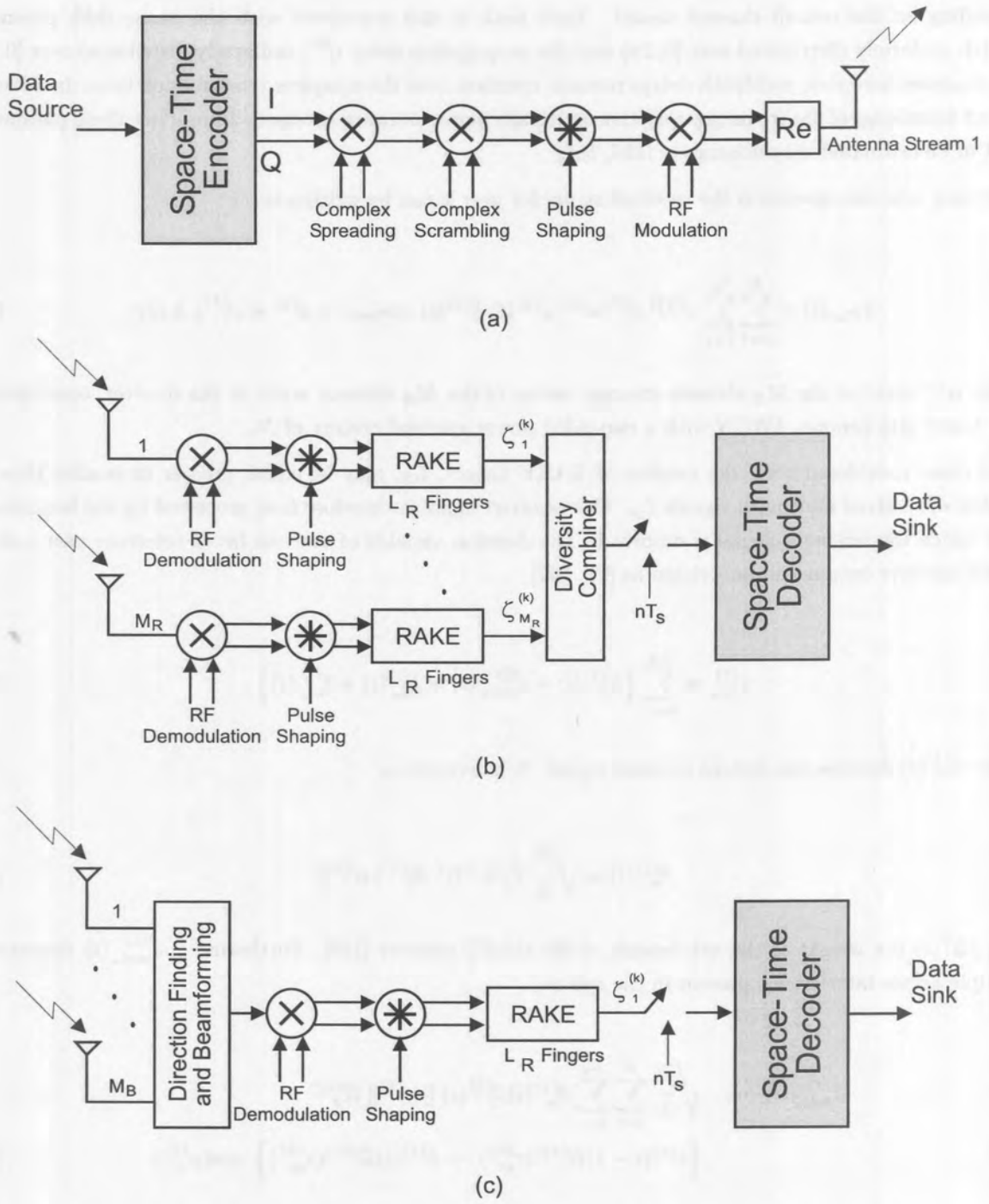

Figure 3.5. Block diagram of receive diversity and beamforming system. (a) Transmitter, (b) Diversity receiver, and (c) Beamforming receiver.

$$h^{(k)}(\tau) = \sum_{l=1}^{L_p} \beta_l^{(k)} \exp\left(j\varphi_l^{(k)}\right) \delta[\tau - \tau_l^{(k)}]. \tag{3.3}$$

Each path is characterized by the random variables $\beta_l^{(k)}(i)$ denoting the strength of path l from user k at symbol interval i. Each of these can be modeled as either Rayleigh distributed or Nakagami-m distributed,

depending on the overall channel model. Each path is also associated with the phase shift parameter $\varphi_l^{(k)}(i)$, uniformly distributed over $[0, 2\pi)$ and the propagation delay $\tau_l^{(k)}$, uniformly distributed over $[0, T_s)$. It is assumed here that multipath delays remains constant over the complete transmission time. In addition, perfect knowledge of the frequency selective multipath parameters are assumed. In practice these parameters need to be estimated very accurately [155, 156].

Assuming coherent operation the received signal for user k can be written as

$$r_{M_B}(t) = \sum_{k=1}^{K} \sum_{l=1}^{L_p} \sqrt{2P}\, \beta_l^{(k)} \mathbf{w}^{(k)}\, a^{(k)}(t)\, b^{(k)}(t)\, \cos(\omega_c t + \phi^{(k)} + \varphi_l^{(k)}) + \eta(t), \tag{3.4}$$

where $\mathbf{w}^{(k)}$ denotes the M_B element steering vector of the M_B element array at the receiver, optimized for user k and $\eta(t)$ denotes AWGN with a two sided power spectral density of N_0.

In all cases considered here, the number of RAKE fingers, L_R, may be equal, greater or smaller than the number of received multipath signals L_p. The received signal is therefore first processed by the beamformer after which the reference signal is despread. The decision variable of the i-th bit of reference user j at the RAKE receiver output can be written as [91, 157]

$$\zeta_{M_B}^{(j)} = \sum_{n=1}^{L_R} \left\{ S_n^{(j)}(i) + I_{\mathrm{mai}_n}^{(j)}(i) + I_{\mathrm{si}_n}^{(j)}(i) + I_{\mathrm{ni}_n}^{(j)}(i) \right\}, \tag{3.5}$$

where $S_n^{(j)}(i)$ denotes the desired received signal. It is written as

$$S_n^{(j)}(i) = \sqrt{\frac{P}{2}}\, T_s\, b^{(j)}(i)\, \beta_n^{(j)^2} \|\mathbf{w}^{(j)}\| \tag{3.6}$$

with $\beta_n^{(j)}(i)$ the weight of the nth branch of the RAKE receiver [129]. Furthermore, $I_{\mathrm{mai}_n}^{(j)}(i)$ denotes the multiple access interference present in the cell or,

$$\begin{aligned} I_{\mathrm{mai}_n}^{(j)}(i) \;=\; & \sqrt{\frac{P}{2}} \sum_{k=2}^{K} \sum_{l=1}^{L_p} \beta_n^{(j)}(i) \beta_l^{(k)}(i)\, \|\mathbf{w}^{(k)}\|\, \mathcal{R}_x^{(kj)} \cdot \\ & \left\{ b^{(k)}(i-1) R^{(kj)}(\tau_{nl}^{(k)}) \;+\; b^{(k)}(i) \hat{R}^{(kj)}(\tau_{nl}^{(k)}) \right\} \cos(\varphi_{nl}^{(k)}). \end{aligned} \tag{3.7}$$

$I_{\mathrm{si}_n}^{(j)}(i)$ denotes the self-interference present in the cell,

$$\begin{aligned} I_{\mathrm{si}_n}^{(j)}(i) \;=\; & \sqrt{\frac{P}{2}} \sum_{l=1}^{L_p} \beta_n^{(j)}(i) \beta_l^{(j)}(i)\, \|\mathbf{w}^{(j)}\|\, \mathcal{R}_x^{(jj)} \cdot \\ & \left\{ b^{(j)}(i-1) R^{(jj)}(\tau_{nl}^{(j)}) \;+\; b^{(j)}(i) \hat{R}^{(jj)}(\tau_{nl}^{(j)}) \right\} \cos(\varphi_{nl}^{(j)}). \end{aligned} \tag{3.8}$$

$I_{\mathrm{ni}_n}^{(j)}(i)$ denotes the AWGN interference, with variance $\sigma^2 = N_o T/2$. In (3.7) to (3.8), $b^{(j)}(i)$ denotes the information bit to be detected, and $b^{(j)}(i-1)$ the preceding bit. In addition, $\tau_{nl}^{(k)} = \tau_l^{(k)} - \tau_n^{(j)}$, $\varphi_{nl}^{(k)} = \varphi_l^{(k)} - \varphi_n^{(j)}$,

$$R^{(kj)}(\tau) = \int_0^{\tau} a^{(k)}(t-\tau)\, a^{(j)}(t)\, dt$$
$$\hat{R}^{(kj)}(\tau) = \int_{\tau}^{T} a^{(k)}(t-\tau)\, a^{(j)}(t)\, dt, \tag{3.9}$$

and, the spatial correlation parameter

$$\mathcal{R}_x^{(kj)} = \frac{Re[\mathbf{w}^{(j)^H}\mathbf{w}^{(k)}]}{\|\mathbf{w}^{(j)}\|\,\|\mathbf{w}^{(k)}\|}. \tag{3.10}$$

In (3.10), $(\cdot)^H$ denotes the Hermitian transpose and $\mathbf{w}^{(k)}$ the array steering vector optimizing the response of the antenna array for user j, or

$$\mathbf{w}^{(j)} = (w_1, w_2, \cdots, w_{M_B})^T. \tag{3.11}$$

From (3.10) it should be clear that $\mathcal{R}_x^{(kk)} = 1$ for all k, and independent of n, the specific diversity branch (or multipath signal). This means that the array response has been optimized in such a way that the antenna radiation pattern is a maximum in the direction of each of the L_p multipath components. Clearly this assumption assumes that the DOA of each multipath component has been perfectly estimated[4]. Furthermore, the antenna array elements are assumed to be sufficiently closely spaced to ensure that the signals received at each antenna element is highly correlated. More specifically, it is assumed that the correlation between the signals received at each element of the antenna array is greater than 0.8. If this correlation factor is lower, the antenna pattern synthesized by the adaptive antenna array will exhibit grating lobes [127]. The high correlation levels would enable digital beamforming techniques to be used to implement a spatial filter.

3.3.1.1 Correlation Influence on Beam Pattern. It is well known that lack of correlation influences the beamforming capabilities of an antenna array, but increases the receive diversity gain.

Figures 3.6 and 3.7 show the beam pattern for a $M_B = 12$ element uniform linear array (ULA) with antenna element spacing of $\lambda/2$. For each correlation value, 1000 snapshots were simulated and the corresponding radiation patterns generated.

Shown in these figures are the maximum beam pattern, the minimum beam pattern and the average beam pattern. A correlation of $\rho_{ij} = 0.8$ already degrades the beamforming characteristics and the beam pattern tends towards an omni-directional antenna pattern. However, the main beam is still at 0° with the side lobe levels altered. With the correlation between the antenna elements equal to $\rho_{ij} = 0.3$, it is clear that the antenna array cannot be used as a beamformer – the antenna pattern tends toward an omni-directional pattern, with very little gain relative to the side lobes in the desired direction of 0°.

3.3.1.2 BEP Performance. To arrive at an expression for the BEP of a beamforming system with a RAKE receiver, the signal power, U_S^2, and the total interference power, σ_T^2 need to be calculated. With these variables known, the received SNR is

$$\text{SNR} = \frac{U_S^2}{\sigma_T^2}. \tag{3.12}$$

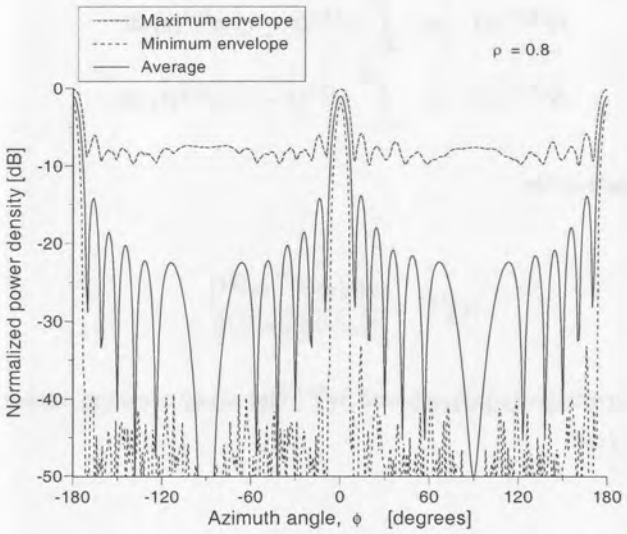

Figure 3.6. ULA beam pattern with envelope correlation of $\rho_{ij} = 0.8$.

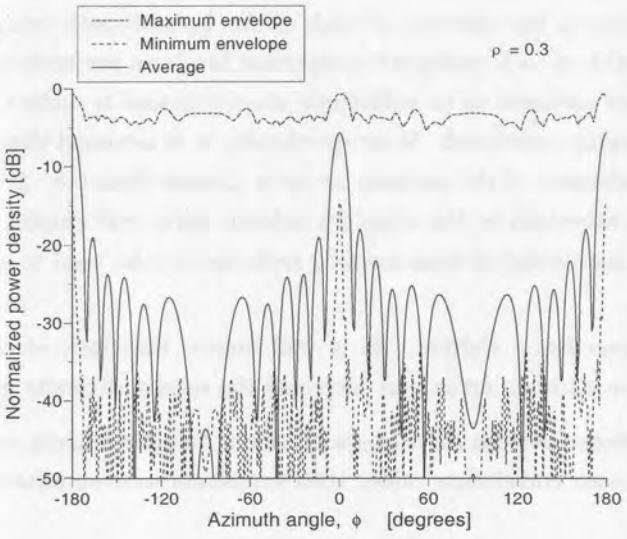

Figure 3.7. ULA beam pattern with envelope correlation of $\rho_{ij} = 0.3$.

From (3.11), the ULA beamformer for the reference user (j), will calculate [126]

$$\|\mathbf{w}^{(j)}\|^2 = (\mathbf{w}^{(j)})^H \mathbf{w}^{(j)} = \sum_{i=1}^{M_B} w_i^* w_i = M_B. \tag{3.13}$$

To simplify the analysis, it is assumed that the sum of all interference terms of (3.5) are Gaussian distributed [70, 85, 91, 115]. This assumption has been shown to be accurate, even for a small number of users K when the BEP is 10^{-3} or greater. Therefore, expanding on the results of [91, 115] to include beamforming, the variance of each interference term (equations (3.6), 3.7) and (3.8)) on the n^{th} RAKE tap, conditioned on the fading parameter, $\beta_n^{(j)}$, can be written as

$$\left(\sigma_{\mathrm{si}_n}^{(j)}\right)^2 = \frac{E_b T_s}{4N} \sum_{\substack{l=1 \\ l \neq n}}^{L} \left(\beta_n^{(j)} \|\mathbf{w}^{(j)}\| E\left\{\mathcal{R}^{(jj)}\right\}\right)^2 \Omega_l^{(j)}, \tag{3.14}$$

$$\left(\sigma_{\mathrm{mai}_n}^{(j)}\right)^2 = \frac{E_b T_s}{6N} \sum_{\substack{k=1 \\ k \neq j}}^{K} \sum_{l=1}^{L} \left(\beta_n^{(j)} \|\mathbf{w}^{(k)}\| E\left\{\mathcal{R}^{(jk)}\right\}\right)^2 \Omega_l^{(k)}, \tag{3.15}$$

$$\sigma^2 = \frac{T_s N_0}{4} \cdot \left(\beta_n^{(j)}\right)^2, \tag{3.16}$$

where $\Omega_l^{(k)}$ denotes the average signal power of path l received from user k. This in turn yields a total interference term of

$$\sigma_T^2 = \sum_{n=1}^{L_R} \left(\left(\sigma_{si_n}^{(j)}\right)^2 + \left(\sigma_{mai_n}^{(j)}\right)^2 + \sigma^2 \right), \tag{3.17}$$

where L_R denotes the number of branches in the RAKE receiver. Furthermore, the desired signal output of the RAKE combining receiver can be written as

$$U_S = \sqrt{\frac{E_b T_s}{2}} \sum_{n=1}^{L_R} \|\mathbf{w}^{(j)}\| (\beta_n^{(j)})^2. \tag{3.18}$$

In (3.18), it is assumed that the RAKE receiver will recover the strongest (i.e. largest average received signal power) L_R multipath components. For convenience, and without loss of generality, the strongest multipath components are assumed to be the L_R components that arrive at the receiver first.

The variance of the fading parameters of each interfering user, $E\left\{(\beta_l^{(k)})^2\right\}$ is equal to the average signal power received from that user, $\Omega_l^{(k)}$. This variance is not a function of the antenna array or steering vector, as the fading process is caused by physical scattering processes that occur at the mobile. The effect of the array is contained in the spatial correlation parameter (given by (3.10)), which will be a minimum if the array has a null in the direction of a specific interfering multipath signal arriving at the base station.

For coherent demodulation, the BEP conditioned on the instantaneous SNR, S, can be expressed as [126, 158]

$$P_{e|S} = Q\left(\sqrt{\Gamma_0 \cdot s}\right), \tag{3.19}$$

where $Q(x) = \frac{1}{\sqrt{2\pi}} \int_x^\infty e^{-t^2/2} dt$ is the Q-function [147]. The output SNR (as defined in (3.12)), can be written in the form required by (3.19) as

$$S = \sum_{n=1}^{L_R} \left(\beta_n^{(j)}\right)^2, \tag{3.20}$$

and

$$\Gamma_0 = \left(\frac{1}{2N} \sum_{\substack{l=1 \\ l \neq n}}^{L} \left(E\left\{ \mathcal{R}^{(jj)} \right\} \right)^2 \Omega_l^{(j)} + \frac{1}{3N} \sum_{\substack{k=1 \\ k \neq j}}^{K} \sum_{l=1}^{L} \left(E\left\{ \mathcal{R}^{(jk)} \right\} \right)^2 \Omega_l^{(k)} + \frac{N_0}{2E_b \|\mathbf{w}^{(j)}\|^2} \right)^{-1}, \tag{3.21}$$

assuming that $\|\mathbf{w}^{(k)}\|^2$ is equal for all k [126].

To obtain the average BER, (3.19) must be averaged over the pdf of S. As discussed in Chapter 2, the distribution of S should accommodate different values of the fading parameter m for the different received paths. If it is assumed that the fading amplitude, $\beta_n^{(j)}$, is Nakagami distributed, the *power*, $\left(\beta_n^{(j)}\right)^2$, of the received fading amplitude will be gamma distributed. From (3.20) it is clear that the pdf of the sum of L_R gamma distributed random variables is required to obtain the average error rate. In Appendix A a general pdf for the sum of an arbitrary number of correlated gamma distributed random variables are derived, and repeated here in terms of the characteristic function

$$p_S(s) = \frac{1}{2\pi} \int_{-\infty}^{\infty} \Phi_S(t) e^{-its} dt, \tag{3.22}$$

where $\Phi_S(t)$ is the characteristic function defined in Appendix A. The BEP for a beamforming system with a RAKE receiver can now be written as

$$P_e = \int_{-\infty}^{\infty} P_{e|S} p_S(s) ds, \tag{3.23}$$

which can be solved using numerical methods [126].

3.3.2 *Transmit/Receive Diversity Performance*

In this section, the BEP performance of a CDTD transmit and MRC receive diversity system with arbitrary correlated fading on each of the transmit/receive diversity branches will be determined.

In beamforming applications it is assumed that the beamforming antenna array receives L_p multipath components, with the received signal envelope correlation at each of the array elements equal to one. The same signal is therefore received by all elements of the beamformer. In the case of diversity, the situation changes since the elements of the diversity array are separated by a larger physical distance. This means that the L_p uncorrelated multipath signals arriving at the first element in the diversity array is no longer the exact same set of multipath components received by the other elements in the array. In fact, when some of the elements of the diversity array are separated by a large distance (typically 20λ or more), the L_p uncorrelated multipath signals received at one element in the diversity array are completely different to the L_p multipath signals received at any other element in the diversity array.

Moving on from the conceptual discussion above, the decision variable of a M_D-branch diversity system can be written as

$$\zeta_{M_D}^{(j)} = \sum_{m=1}^{M_D} \zeta_{m_D}^{(j)}, \tag{3.24}$$

where each

$$\zeta_{m_D}^{(j)} = S_n^{(j)} + I_{\mathrm{si}_n}^{(j)} + I_{\mathrm{mai}_n}^{(j)} + I_{\mathrm{ni}_n}^{(j)}, \tag{3.25}$$

and represents the output of the RAKE receiver on a specific diversity branch. In 3.25, S_n, I_{mai_n} and I_{si_n} are defined in (3.6), (3.7) and (3.8), respectively, with the weight vector, $\mathbf{w}$ unity. As before, $I_{\mathrm{ni}_n}^{(j)}$ is the AWGN sample.

3.3.2.1 BEP Performance. In order to determine the BEP of a CDTD or MRC diversity system, it is necessary to determine the pdf of the SNR at the output of the combiner at the receiver. The SNR pdf is a function of

- The characteristics of the composite signal transmitted/received at each diversity branch (the effective value of the Nakagami fading parameter m). It has been shown [115, 158] that coherently combined, uncorrelated multipath components result in a composite signal envelope with effective Nakagami fading parameter, m_{eff}, given by

$$m_{eff} = \sum_{l=1}^{L_R} m_l. \tag{3.26}$$

  For instance, if an antenna element in a diversity array receives three multipath echoes, each with a Nakagami fading parameter $m_l = 1$ and coherently combines these signals using a RAKE combiner, the composite fading signal will have an effective Nakagami parameter $m_{eff} = 3$.

- The relation (correlation) between the signals received at each branch. The correlation between the composite fading envelopes received at each diversity branch is a function of the antenna height and also of the scattering environment as described in Chapter 2.

From [158] and (3.19) it follows readily that the conditional BEP of a M_D-branch diversity system is also

$$P_{e|S} = Q\left(\sqrt{\Gamma_0 \cdot s}\right), \tag{3.27}$$

where the received signal power random variable, S, will have a different pdf in (3.27) than in (3.19). Specifically for receive diversity with MRC, the pdf of S is given in Appendix A, with the transformation of $M_D = M_R$ and $m = m_{eff}$. For Rayleigh fading (Nakagami fading parameter $m = 1$) with equal path strength ($\Omega_l = \Omega$) and equal correlation, a special case for the pdf of S follows as (see Appendix A)

$$\begin{aligned} p_S(s) &= \frac{1}{\Omega^2\Gamma(M_R)}\left(\frac{s}{\Omega^2}\right)^{M_R-1} \\ &\times \frac{\exp\left(-\frac{s}{(1-\rho)\Omega^2}\right) \cdot {}_1F_1\left(1, M_R, \frac{\rho M_R s}{(1-\rho)(1-\rho+\rho M_R)\Omega^2}\right)}{(1-\rho)^{(M_R-1)}(1-\rho+\rho M_R)}, \end{aligned} \tag{3.28}$$

where M_R denotes the number of MRC receive diversity branches.

A similar expression for the pdf of S for a $M_D = M_T$ CDTD transmit diversity scheme with equal powered transmissions, with $m = m_{eff} = 1$, and with constant correlation between the branches, and transmitted over a Rayleigh fading channel, can be written. Specifically, the components of the received power vector for the transmit diversity system can be written as

$$\begin{aligned} p_{\mathbf{S_n}}(\mathbf{s_n}) &= \frac{1}{\Omega^2\Gamma(M_T \cdot L_R)} \left(\frac{\mathbf{s_n}}{\Omega^2}\right)^{M_T \cdot L_R - 1} \\ &\times \frac{\exp\left(-\frac{\mathbf{s_n}}{(1-\rho)\Omega^2}\right) \cdot {}_1F_1\left(1, M_T \cdot L_R, \frac{\rho M_T \cdot L_R \mathbf{s_n}}{(1-\rho)(1-\rho+\rho M_T \cdot L_R)\Omega^2}\right)}{(1-\rho)^{(M_T \cdot L_R - 1)}(1-\rho+\rho M_T \cdot L_R)}. \end{aligned} \tag{3.29}$$

With reference to (3.27), the unknown variables required to determine the BEP performance of a diversity system are the interference term Γ_0 and the correlation matrix given in Appendix A. The interference term has been defined in (3.21) for CDMA with beamforming. However, as has been shown by Lötter [126], the analysis is equally valid for diversity with $M_B = 1$ elements.

3.3.3 Numerical Results

Using (3.23), (3.28), (3.29) and the system parameters outlined in Table 3.1, the BEP performance of a CDMA system using beamforming, together with transmit and receive diversity can be determined numerically under various physical and implementation conditions. The BEP performance of the space-time systems will be presented as a function of system load, $V = N/K$, with operating point taken as $E_b/N_0 = 20$ dB. Figures 3.8 to 3.10 compare the (uncoded) performance of the different space-time processing techniques covered in this chapter.

Parameter	**Simulation value**
Spreading sequence length	$N = 32$
Operating environment	2-Path, equal strength.
User distribution	uniform
Number of multipath signals	$L_p = 2$
Number of users	$K = 1, 2, \ldots, N$
Number of RAKE fingers	$L_R = 2$
Beamforming elements	$M_B = 1, 2, 3;\ \rho = 1, 0.5$
Transmit diversity elements	$M_T = 1, 2, 3\ \rho = 0, 0.5$
Receive diversity elements	$M_R = 1, 2, 3\ \rho = 0, 0.5$

Table 3.1. System parameters for numerical evaluation of BEP performance.

In Figure 3.8, the influence of the beamforming antenna array size on the capacity of a cellular CDMA system is shown assuming a constant correlation model. As would be expected, the BEP performance of the system improves with increasing beamformer size. This is due to the fact that larger beamforming arrays can synthesize narrower beams and thereby reduce the MAI seen by the reference user. As the BER

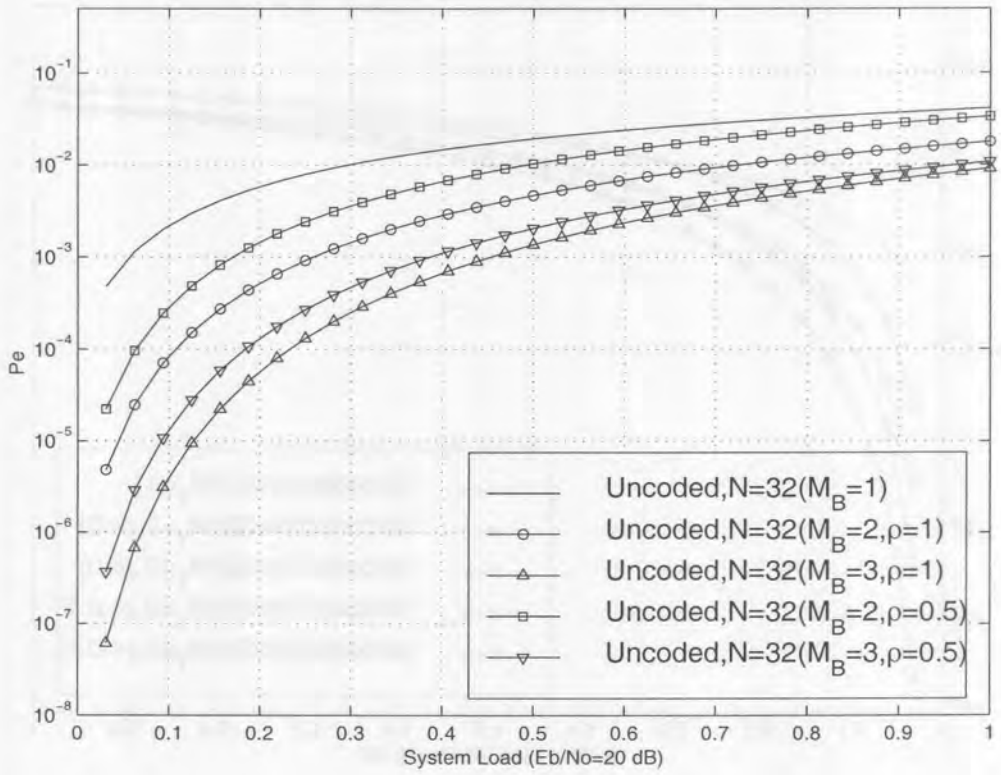

Figure 3.8. Uncoded receive beamforming performance.

probability is reduced by increasing the number of elements in the beamformer, the capacity of the cellular system is also increased.

In the beamforming system the signal processor performs the calculation of the direction of the desired signal, as well as the set of antenna weights required to focus the antenna radiation pattern in the direction of the desired signal. Typically, the radiating elements of an adaptive antenna array are separated by $\lambda/2$ where λ denotes the wavelength of the carrier frequency. Transmission from the target mobiles occurs at the same time instant, and the beam of the base station antenna is formed to maximize the received signal power from these target mobiles, while the received power from other interfering mobiles (inside this particular cell, as well as in adjacent cells) is minimized through the introduction of nulls in the antenna radiation pattern.

Note that in the case of systems using CDMA, the situation changes as follows. In general, it can be assumed that the number of subscribers active in a cell will be larger than the number of elements in an array, that is greater than the freedom levels of the adaptive system. All of these subscribers are transmitting in the same frequency band at the same time, meaning null steering cannot be used to cancel all interfering signals. Therefore, in the case of CDMA, at best beamsteering techniques in conjunction with limited null steering can be used to point the main beam of the antenna array in the direction of a desired user or group of users [112] and to place nulls in the direction of the main interfering signals.

Also shown in Figure 3.8, is the effects of correlation (or lack thereof), indicating the reduced effectiveness of the beamformer to "remove" unwanted users from the system under conditions of reduced correlation.

The uncoded BEP performance of transmit O-CDTD and receive MRC diversity systems under different constant correlation conditions are shown in Figure 3.9 and 3.10, respectively.

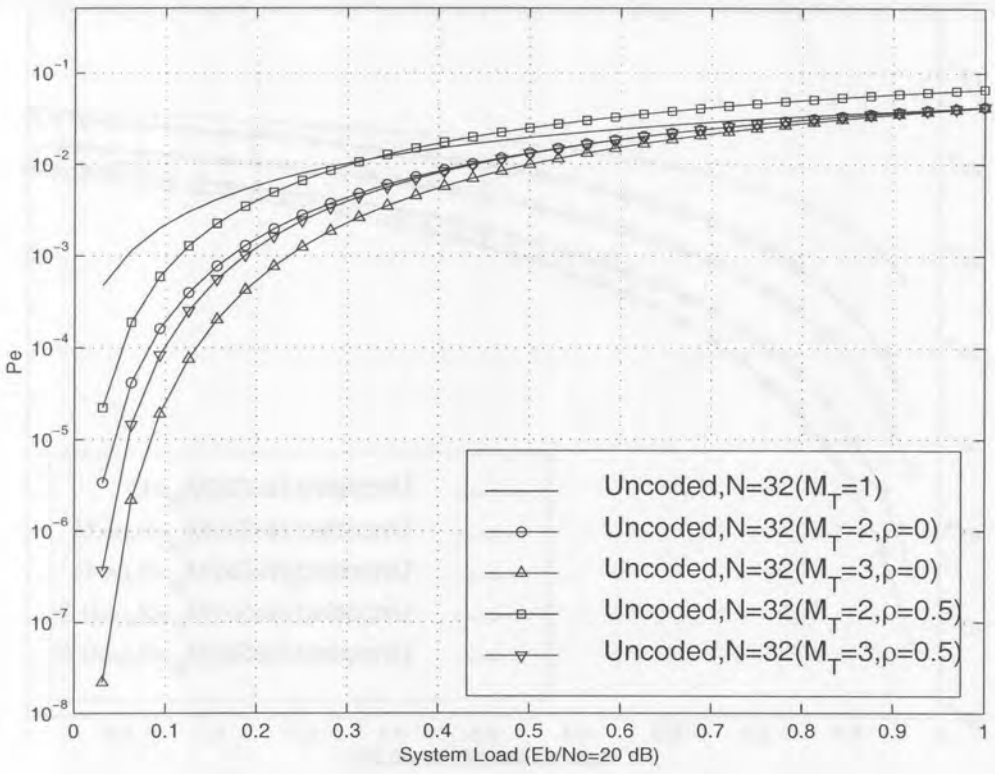

Figure 3.9. Uncoded O-CDTD transmit diversity performance.

In both cases it is clear that the correlation between the transmitted/received signals on the diversity branches has a significant impact on the BEP performance of the system. This is evident from the figures where the influence of the number of diversity branches, as well as the correlation between the signals at the various branches is clearly shown. The results indicate that variations in the correlation between received signal envelopes as a function of the user's position or other spatial parameters must be taken into account when determining the capacity of a diversity system.

It is also important to note that even when employing orthogonal spreading sequences (as in O-CDTD), the downlink will not be perfectly orthogonal due to multipath propagation. In [159, 160], the downlink orthogonality factor has been calculated for different environments. This factor, expressed as a percentage and shown in Table 3.2, is the fraction of the total output power that will be experienced as intra-cell interference. An orthogonality factor of zero corresponds to a perfectly orthogonal downlink, while a factor of one is a completely non-orthogonal downlink. As shown in Table 3.2, 40% of the power transmitted from the reference cell will act as intra-cell interference in a vehicular environment.

Propagation model	Orthogonality factor (%)
Indoor office	10 %
Outdoor to indoor and pedestrian	6 %
Vehicular	40 %

Table 3.2. Orthogonality factor for the different WCDMA channel environments.

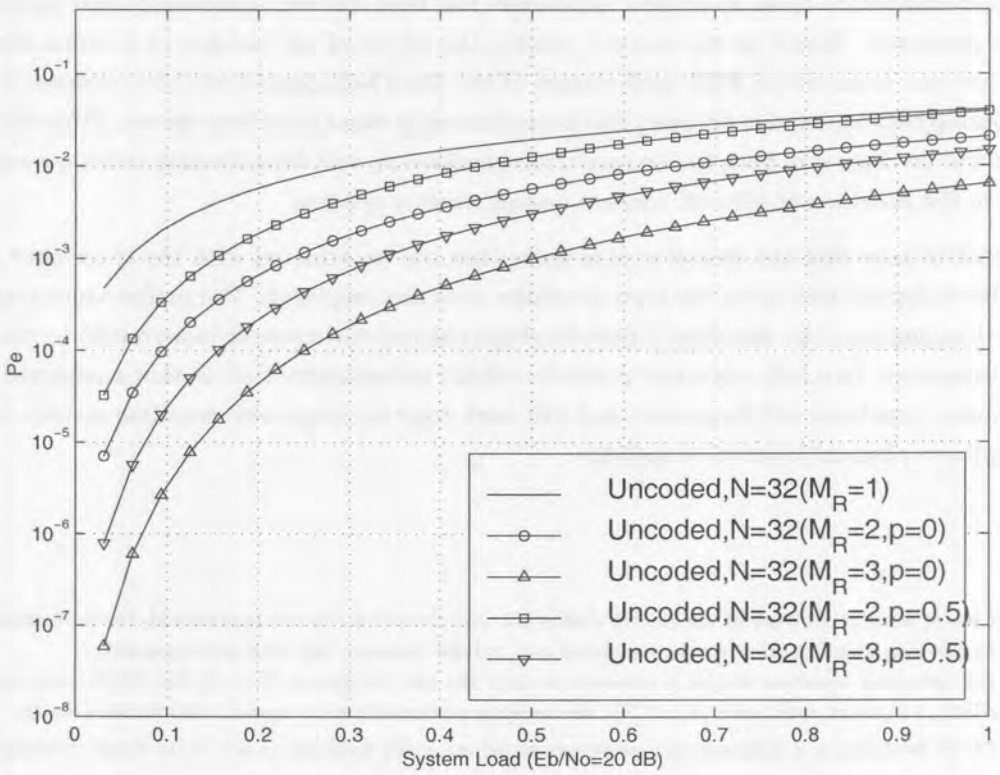

Figure 3.10. Uncoded MRC receive diversity performance.

Orthogonality, therefore, removes 60% of the interference or, stated differently, an orthogonality factor of 0.4 is obtained (40% of orthogonality remains). Under these conditions, the effectiveness of O-CDTD transmit diversity system is reduced, and it is expected that NO-CDTD should provide improved performance.

Also, from Figures 3.9 and 3.10 it is clear that the performance of the transmit diversity is inferior to that of receive diversity employing the same number of diversity branches. This is also attributed to the loss of orthogonality in the downlink.

Receive beamforming provided the best performance of all the techniques considered. Since the antenna beam is focused on a specific user, the antenna gain (or SNR) in the direction of the user is increased, and the transmissions received from interfering users are suppressed by the introduction of nulls in antenna pattern.

From the results presented in Figure 3.8 and 3.10 it can be seen that the performance of perfect beamforming ($\rho = 1$) and perfect receive diversity ($\rho = 0$) is similar as has been shown in [126].

3.4 SUMMARY

The reasoning behind the use of space-time processing techniques is the optimization of the cellular spectral efficiency of the network. This is realized by implementing more than one antenna element to optimally transmit or receive signals by using both temporal and spatial signal processing techniques in the transceiver. This chapter considered in detail the main smart antenna techniques, namely transmit and receive diversity, and beamforming.

The BEP performance of these space-time processors has been derived analytically and some numerical results were presented. Based on the analytic results, the effects of the number of antenna elements and correlation between branches on BEP performance of the three techniques have been addressed. Also, the close relationship between receive diversity and beamforming systems have been shown. From the presented results it should be clear that both the transmit/receive diversity and beamforming techniques are of great importance in the provision of efficient wireless communication systems.

It is important to note that the overall system gains that can be achieved with the space-time techniques described above, depend heavily on the type of cellular structure employed. The performance may therefore differ when changing from the described 2-path Rayleigh channel environment (macro-cell) to micro- or pico cellular environments. In a fully operational mobile cellular environment, such as that envisioned in UMTS, all these cellular structures will be present and will work together to provide seamless service, irrespective of the subscriber's physical location or mobility.

Notes

1. Soft-failure states that, should one of the receive chains fail, and the other chain is operational, the performance loss is of the order of the diversity gain. In other words, the signal may still be detected, but with inferior quality.
2. Although the spreading sequence length is assumed to span the the bit period ($T = T_b$ for BPSK) and symbol period ($T = T_s$ for QPSK), i.e., short codes with $N = T/T_c$, the analysis presented here is equally valid for long codes.
3. Although BPSK modulation is assumed, the results presented are easily extended to any other linear modulation scheme.
4. The estimation of the DOA of multipath signals fall outside the scope of this thesis.

4 CHANNEL CODING FOR CDMA

Following the derivation of the uncoded system performance in Chapter 3, based on the presented channel model of Chapter 2, this chapter shifts the focus to channel coding techniques and their performance. Specifically, the use and performance of classical convolutional, turbo codes and trellis codes for cellular CDMA will be addressed.

4.1 FEC BACKGROUND

4.1.1 Block Codes

The approach to error correction coding taken by modern digital communication systems started in the late 1940's with the ground breaking work of Shannon [161], Hamming [162], and Golay [163]. The next main class of linear block codes to be discovered were the Reed-Muller (RM) codes in 1954 [164]. The latter codes provided a significant improvement on the Hamming and Golay codes because they allowed more flexibility in the size of the code word and the number of correctable errors per code word [165, 166]. Following the discovery of RM codes came the discovery of cyclic codes [164, 165].

An important subclass of the cyclic codes was discovered simultaneously by Hocquenghem in 1959 and by the team of Bose and Ray-Chaudhuri in 1960 [15, 164], known as BCH codes. BCH codes were extended to the non-binary case ($q > 2$) by Reed and Solomon in 1960 [167]. Reed Solomon (RS) codes constituted a major improvement since their non-binary nature allows for protection against bursts of errors.

Despite the success of block codes, there are several fundamental drawbacks to their use. Firstly, due to the frame (block) oriented nature of block codes, the entire code word must be received before decoding can be completed. This can introduce an intolerable latency into the system, particularly for large block lengths. A second drawback is that block codes require precise frame synchronization. A third drawback is that algebraic-based decoders for block codes usually employ hard-decision decoding (HDD), rather than the unquantized, or "soft", outputs of the demodulator. It is actually possible to perform soft-decision decoding of block codes, although until recently soft-decision decoding has been regarded as too complex. Recent

work in the area of errors-and-erasures decoding for RS codes [165] and trellis-based soft-decision decoding algorithms for other classes of block codes, swung the interest and approach towards soft-decision decoding (SDD) [168].

4.1.2 *Convolutional Codes*

The drawbacks of block codes can be avoided by taking a different approach to coding, namely that of convolutional coding, which was first introduced in 1955 by Elias [164]. Rather than segmenting data into distinct blocks, convolutional encoders add redundancy to a continuous stream of input data by using a linear shift register. Each set of n output bits is a linear combination of the current set of k input bits and the m bits stored in the shift register. The total number of bits that each output depends on is called the constraint length, denoted by K_{cc}[1]. Just as the data is continuously encoded, it can also be continuously decoded with only nominal latency. Furthermore, the decoding algorithms based on the Viterbi and maximum *a posteriori* (MAP) algorithms, can make full use of soft-decision information from the demodulator.

A key weakness of convolutional codes is that they are very susceptible to burst errors. This weakness can be alleviated by using an interleaver, which scrambles the order of the code bits prior to transmission. By scrambling the code bits' order at the transmitter and then reversing the process at the receiver, burst error patterns can be broken up so that they appear independent to the decoder. All of the 2G and 3G digital cellular standards use some form of block interleaving.

It should be noted that in many ways convolutional codes have properties that are complimentary to those of RS codes. While convolutional codes are susceptible to burst errors, RS codes handle burst errors quite well. However, convolutional codes with soft-decision decoding generally outperform RS codes of similar complexity at low SNRs [165]. In severely power limited channels, an interesting and efficient system design can be obtained by using the concatenation of a RS "outer" code and a convolutional "inner" code [169].

4.1.3 *Concatenated Codes and Iterative Decoding*

Since conventional block- and convolutional codes are highly structured, encoders and decoders with reasonable implementation complexity are possible. However, the very same structure that facilitates practical implementation, results in significantly inferior performance gains relative to the random coding bounds predicted by Shannon.

With this in mind, perhaps the most exiting and potentially important development in coding theory in recent years has been the introduction of parallel concatenated convolutional codes by Berrou *et al.* [170]. The term "turbo code" was adopted to describe this new class of code. The introduction of turbo coding has opened a whole new way of looking at the problem of constructing good codes with low complexity decoding. Although turbo codes possess random-like properties, they still contain enough structure to admit practical encoding and decoding algorithms. As a consequence, the performance of turbo codes comes much closer to the Shannon bound than conventional block and convolutional codes.

4.1.3.1 Turbo Encoding.

Turbo codes are iteratively decoded parallel concatenated convolutional codes (referred to here as PCCC) which consist of two convolutional encoders, one of which encodes the information bits directly, while the other encodes the information bits following interleaving. The key to solving the decoding complexity of PCCC schemes is the existence of a sub-optimal decoding algorithm which achieves performance very close to that of a maximum likelihood decoder. This algorithm iteratively decodes each code separately using soft-input/soft-output algorithms such as MAP or SOVA [166, 171].

In [172] the serial dual of turbo codes were introduced. These iteratively decoded serially concatenated convolutional codes (SCCC) are constructed from the same constituent codes and interleaver elements as PCCC, but are concatenated in a serial rather than a parallel fashion. Again, an iterative decoding algorithm is used which achieves near-optimum results. SCCC achieve comparable performance to PCCC, and in some cases can offer superior performance [172, 173, 174, 175].

The turbo or PCCC encoder is composed of two or more recursive systematic convolutional (RSC) encoders, which are in general identical. The constituent encoders receive the "same" data, the only difference is that the stream to each encoder is permuted by an interleaver, with the result that turbo codes appear random. Because the interleaver must have a fixed structure and generally works on data in a block-wise manner, turbo codes are by nature block codes.

Recall that the minimum distance of a linear block code is a good first order estimate of the code's performance. For linear block codes, the minimum distance is the smallest non-zero Hamming weight of all valid code words. The combination of interleaving and RSC encoding ensures that most code words produced by a turbo coder have a high Hamming weight. Because of its infinite impulse response properties, the output of an RSC encoder generally has a high Hamming weight. There are, however, some input sequences which cause an RSC encoder to produce low weight outputs. Because of the interleaver, the two RSC encoders do not receive their inputs in the same order. Thus, if one encoder receives an input that causes a low weight output, then it is improbable that the other encoder also receives an input that produces a low weight output. Unfortunately, since there will always be a few input messages that cause both RSC encoders to produce low weight outputs, the minimum distance of a turbo code may, in general, not be particularly high. But the *multiplicity* of low weight code words in well designed turbo codes is low. It is because of the relatively small number of low weight code words that turbo codes can perform well at low SNR [176, 166].

However, the performance of turbo codes at higher SNRs becomes limited by the relatively small minimum distance of the code. While the goal of traditional code design is to increase the minimum distance of the code, the objective of turbo code design is to reduce the multiplicity of low weight code words.

4.1.3.2 Turbo Decoding. The problem of estimating the states of a Markov process in the presence of noise has two well known trellis-based solutions — the Viterbi algorithm [177] and the (symbol-by-symbol) MAP algorithm [178, 179]. The two algorithms differ in their optimality criterion. The Viterbi algorithm finds the most probable transmitted sequence, while the MAP algorithm, on the other hand, attempts to find the most likely transmitted symbol, given the received sequence [166, 180, 181].

One drawback of both PCCC and SCCC is decoder complexity. For some applications, such as hand-held mobile handsets, it may be desirable to tradeoff some of the high coding gain of SCCC for lower decoder complexity. Several types of algorithms can be used within a turbo decoder to perform soft/input soft-output decoding of the constituent codes. An excellent overview of the trellis-based soft-input soft-output decoding algorithms has been presented in [166]. Shown in Figure 4.1 are the trellis based algorithms. These algorithms can be partitioned into two main classes, depending on whether they were derived from the Viterbi algorithm or from the MAP algorithm. Generally speaking, the algorithms at the bottom of the diagram are more computationally complex and perform better than the algorithms at the top of the diagram. Also, the MAP-based algorithms are generally more computational intensive and perform better than the algorithms based on the Viterbi algorithm.

The soft output Viterbi algorithm (SOVA) is an extension of the classic Viterbi algorithm that provides the reliability of the bit estimates [180, 182, 183, 184]. In addition, the improved SOVA algorithm, utilizing a multiplicative correction factor to improve the reliability estimates, may also be considered.

The MAP algorithm calculates the *a posteriori* probabilities directly. However, the algorithm suffers from a high computational complexity and numerical sensitivity. The Max-Log-MAP and Log-MAP algorithms perform the MAP algorithm in the log domain, which significantly reduces complexity and numerical sensitivity [171].

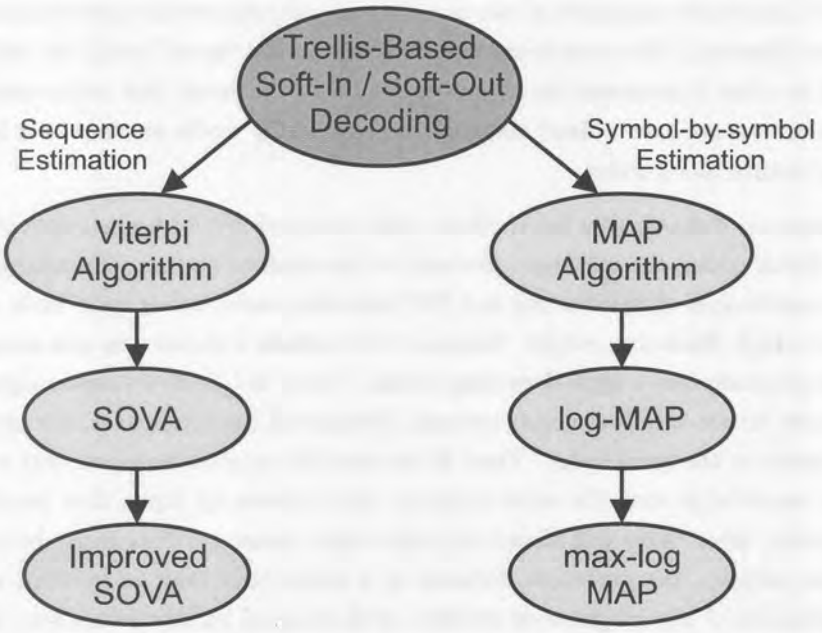

Figure 4.1. Trellis-based soft-input soft-output algorithms.

4.1.4 *Turbo Codes Performance*

Figure 4.2 depicts the turbo code design space [185]. The design space can be grouped into service dependent and implementation dependent components. The service dependent components influence typically the quality of service and the data rate. The implementation dependent components influence the maximum decoding delay, the implementation complexity, system flexibility, modularity and integratability.

Below, a short description of the more important blocks of Figure 4.2 is given.

Turbo Interleaver/Permuter. The interleaver (or permuter) component of the turbo encoder directly defines the service dependent part of the system design space. The weight distribution of the codewords produced by the turbo decoder depends on how the codewords from one of the basic codes are teamed with codewords from the other encoder(s). Stated differently, the performance of the turbo code depends on how effectively the data sequences that produce low encoded weights at the output of one encoder, are matched with permutations of the same data sequence that yield higher encoded weights at the outputs of the others. Two characteristics of the interleaver is of particular importance

- Interleaver size, N_{tc}. This is the most important factor influencing the turbo code performance, and it is well known that performance improves as the interleaver size increases [186]. The gain, in terms of error performance, with increased interleaver size is formally known as the *interleaver gain*. However, as the interleaver size (gain) increases, so does decoding delay, and a balance must be found between

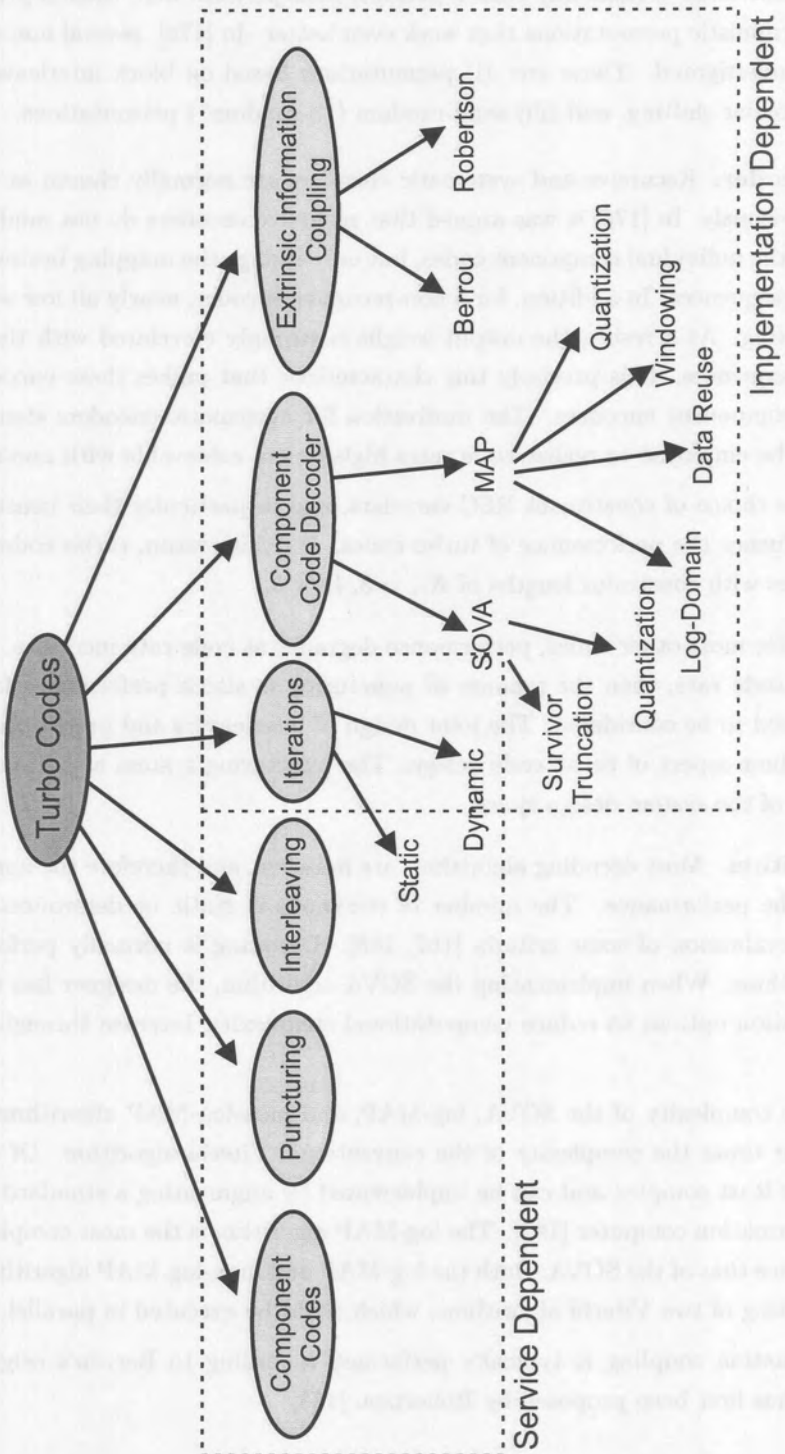

Figure 4.2. Turbo coded system design space [185].

acceptable performance and tolerable latency. At high SNRs, the interleaver design becomes critical [173], where the performance is dominated by the low weight code words. At low SNRs, turbo codes perform well with almost any (randomly permutated) interleaver, provided that the inputs at the RSC encoders are sufficiently uncorrelated.

- Interleaver selection. If randomly chosen permutations perform well, then in principle it is possible to design deterministic permutations that work even better. In [176], several non-random permutations have been investigated. These are: (i) permutations based on block interleavers, (ii) permutations based on circular shifting, and (iii) semi-random ("S-random") permutations.

Constituent Encoder. Recursive and systematic encoders are normally chosen as constituent encoders, as discussed previously. In [176] it was argued that recursive encoders do not modify the output weight distributions of the individual component codes, but only change the mapping between the input data and output encoded sequences. In addition, for a non-recursive encoder, nearly all low weight input sequences are self-terminating. As a result, the output weight is strongly correlated with the input weight for all possible input sequences. It is precisely this characteristic that makes these encoders very undesirable as constituent component encoders. The motivation for systematic encoders stems from the fact that puncturing can be employed to realize code rates higher than achievable with non-systematic encoders.

Surprisingly, the choice of constituent RSC encoders, and in particular their constraint lengths, do not significantly influence the performance of turbo codes. For this reason, turbo codes typically use simple constituent codes with constraint lengths of $K_{tc} = 3, 4$, or 5.

Puncturing. As for most other codes, performance degrades as code rate increases. If puncturing is used to increase the code rate, then the manner of puncturing is also a performance factor and puncturing matrices may need to be considered. The joint design of interleavers and puncturing matrices is perhaps the most important aspect of turbo code design. The puncturing system also directly define the service dependent part of the system design space.

Decoding Algorithm. Most decoding algorithms are iterative, and therefore the number of iterations has an impact on the performance. The number of iterations is static or determined dynamically during decoding after evaluation of some criteria [187, 188]. Decoding is normally performed with the MAP or SOVA algorithms. When implementing the SOVA algorithm, the designer has to choose among several implementation options to reduce computational complexity, increase throughput, or reduce power consumption.

The algorithmic complexity of the SOVA, log-MAP, and max-log-MAP algorithms are similar, ranging from two to four times the complexity of the conventional Viterbi algorithm. Of the three algorithms, the SOVA is the least complex and can be implemented by augmenting a standard Viterbi decoder with a reliability information computer [182]. The log-MAP algorithm is the most complex, with a complexity that is about twice that of the SOVA. Both the log-MAP and max-log-MAP algorithms have an attractive structure consisting of two Viterbi algorithms, which could be executed in parallel.

Extrinsic information coupling is typically performed according to Berrou's original method [170] or directly, which has first been proposed by Robertson [188].

4.1.5 Trellis Coded Modulation

Up until the mid 1970's, coding and modulation were regarded as two separate processes. Ungerboeck changed this thinking in 1976 with the introduction of trellis coded modulation (TCM) [189, 190]. The

main advantage of TCM over classical coding schemes is the fact that trellis coding, and the resulting data-transmission strategy, does not expand the transmission bandwidth. It is both a power- and a bandwidth-efficient modulation scheme.

In the application of trellis coding techniques to cellular CDMA communication, two different approaches have been considered. The first approach is based on classical TCM techniques which combines coding and modulation into a single entity [44]. It has been shown that for a given complexity, chip rate and throughput, these codes provide no advantage over medium to low rate convolutional codes. The second technique uses a different approach and combines coding and spreading, instead of combining coding and modulation. This technique, referred to as trellis coded spreading (TCS), performs better than standard error control techniques for the same complexity and code rate [45].

TCM for CDMA. Boudreau *et al.* [44] considered the use of trellis codes in a DS/CDMA system and compared their performance with that of convolutionally coded DS/CDMA. Their codes were constructed over an M-PSK signal set by taking a standard Ungerboeck type code for M-PSK modulation and then spreading this M-PSK signal with a binary m-sequence, over a large bandwidth. The authors in [44] reported that this approach did not yield a performance advantage over standard convolutional codes when combined in a CDMA system. It was argued that this is mainly due to the fact that a convolutional code can be employed without any bandwidth expansion or decrease in processing gain in a CDMA system. The latter directs one to rather exploit the lower distance properties of lower rate convolutional codes.

TCS for CDMA. A different approach to the idea of trellis coded CDMA was investigated by Woerner and Stark [45]. In this approach the trellis code is constructed over the set of possible signature sequences rather, than over some $2D$ signal constellation. Instead of expanding the number of signal points in the $2D$ constellation, the number of possible spreading sequences used is expanded. A carefully designed trellis then allows only certain combinations of sequences that have a large total minimum distance. Now since the number of sequences has been increased, the actual minimum distances between sequences decrease, but fortunately the trellis code more than compensates for this by increasing the minimum distance of the code above that of the uncoded system.

Coded performance can be calculated by extending the space-time mathematical model derived in Chapter 2 and using well known error control bounding techniques. In the remainder of this chapter, the performance of classical convolutional (including orthogonal extensions), turbo and trellis coded CDMA is considered.

4.2 PERFORMANCE EVALUATION

4.2.1 Convolutional Code (CC) Performance

The bounds presented here are based on block error probability bounds, originally derived by Shannon [161]. Specifically, to determine upper bounds on BEP with convolutional encoding and ML decoding represented by an equivalent (n, k) linear block code, it is useful to recall the state diagram and associated generating function approach. Due to code linearity, it is assumed that the all-zero message has been transmitted, and the upper bound on the word error probability can be written as

$$P_w \leq \sum_{d=d_{free}}^{n} A_d \, P_d(\mathbf{c} \rightarrow \hat{\mathbf{c}}), \tag{4.1}$$

where A_d is the number of codewords with Hamming weight d, obtained from the series expanded transfer function $T(L, I, D)$, and given by (for path length, $L = 1$)

$$\left.\frac{\delta T(I,D)}{\delta I}\right|_{I=1} = \sum_{d=1}^{n} A_d D^d, \tag{4.2}$$

where D is the channel parameter. By setting $I = 1$ after differentiation, the number of bit errors, corresponding to an error event of length d, equals the multiplicity of term D^d, where $D = e^{-R_c E_b/N_o}$.

The *free distance*, denoted by d_{free}, of any code is the minimum Hamming distance between any two distinct code sequences. D is a function of the channel transition probabilities and the message decoding metric only.

The conditional pairwise error probability, $P_d(\mathbf{c} \to \hat{\mathbf{c}})$, is the probability of incorrectly choosing a codeword with weight d, that is, the probability that the incorrectly encoded sequence $\hat{\mathbf{c}}_n = (c_1, c_2, \ldots, c_n)$ is chosen instead of the correctly encoded sequence $\mathbf{c}_n = (c_1, c_2, \ldots, c_n)$.

For the continuous output soft-decision AWGN channel it can be shown that the single user $P_d(\mathbf{c} \to \hat{\mathbf{c}})$ is given by [22, 16, 13]

$$P_d(\mathbf{c} \to \hat{\mathbf{c}}) \;=\; Q\left(\sqrt{\frac{2dR_cE_b}{N_o}}\right). \tag{4.3}$$

From [176], the more general expression for the average weight distribution can be written as

$$A_d = \sum_{i=1}^{k} \binom{n}{i} p(d \mid i), \tag{4.4}$$

where $\binom{k}{i}$ is the number of input words with Hamming weight i and $p(d \mid i)$ is the probability that an input word with Hamming weight i produces a codeword with Hamming weight d. Substituting (4.4) into (4.1), the upper bound on the word and bit error rate can be expressed as

$$\begin{aligned} P_w \;&\leq\; \sum_{d=d_{free}}^{n} A_d \, P_d(\mathbf{c} \to \hat{\mathbf{c}}) \\ &=\; \sum_{d=d_{free}}^{n} \sum_{i=1}^{k} \binom{k}{i} p(d \mid i) \, P_d(\mathbf{c} \to \hat{\mathbf{c}}) \\ &=\; \sum_{i=1}^{k} \binom{k}{i} E_{d|i} \left\{ P_d(\mathbf{c} \to \hat{\mathbf{c}}) \right\}, \end{aligned} \tag{4.5}$$

and

$$P_e \leq \sum_{i=1}^{k} \frac{i}{k} \binom{k}{i} E_{d|i} \left\{ P_d(\mathbf{c} \to \hat{\mathbf{c}}) \right\}. \tag{4.6}$$

In (4.5) and (4.6), $E_{d|i}\{\cdot\}$ is an expectation with respect to the distribution $p(d \mid i)$. This average upper bound is attractive because relatively simple schemes exist for computing $p(d \mid i)$ from the state transition matrix of the RSC [191, 176]. This information is implicit to the generating function $T(I, D)$ associated with the particular code employed.

4.2.1.1 Evaluation of $P_d(\mathbf{c} \to \hat{\mathbf{c}})$. Under conditions of fast fading, it is generally assumed that the fading is independent in successive signaling intervals. As a result, the sequence of fading amplitudes β_i constitutes an independent and identically distributed (i.i.d.) sequence[2].

Consider the situation where the all-zeros codeword $\mathbf{c} = \mathbf{0} = \mathbf{c_0}$, is transmitted and codeword $\hat{\mathbf{c}} = \mathbf{c_n}$ is received. In addition, a trellis path which re-emerges with the correct all-zero path is considered, having diverged at some point in the past, and differing from the all-zero path in exactly d symbol positions. Define the n-vector

$$\mathbf{S_n} = (S_{n1}, S_{n2}, \ldots, S_{nd}), \tag{4.7}$$

where $S_{ni}, (i = 1, 2, \ldots, d)$ represents the value of the resulting envelope power process in the ith signaling interval where the path differs from the all-zero path. Assuming perfect phase tracking of the phase perturbation process and channel state information (CSI) at either the transmitter or receiver, the conditional pairwise error probability for an incorrect sequence with d error symbols is [191]

$$P_d(\mathbf{c} \to \hat{\mathbf{c}} \mid \mathbf{S_n}) = Q\left(\sqrt{\Gamma_{0c} \sum_{i=1}^{d} s_{ni}}\right), \tag{4.8}$$

where Γ_{0c} is proportional to the effective output signal-to-noise ratio of the coded system (Γ_{0c} should be compared with its uncoded counterpart, Γ_0 defined in Chapter 3). The average error event probability can then be determined by averaging over the random n-vector $\mathbf{S_n}$, resulting in

$$P_d(\mathbf{c} \to \hat{\mathbf{c}}) = E_{\mathbf{S_n}}\left\{Q\left(\sqrt{\Gamma_{0c} \sum_{i=1}^{d} s_{ni}}\right)\right\}, \tag{4.9}$$

where the expectation operator $E_{\mathbf{S_n}}\{\cdot\}$ represents joint expectation with respect to the received signal power components.

Fast fading. For fast fading with perfect CSI, the pairwise error probability is given by

$$P_d(\mathbf{c} \to \hat{\mathbf{c}} \mid \mathbf{S_n}) = Q\left(\sqrt{\Gamma_{0c} \sum_{i=1}^{d} s_{ni}}\right). \tag{4.10}$$

When the pairwise error probability, (4.10), is averaged over (3.28), a multi-dimensional integral given by

$$\begin{aligned} P_d(\mathbf{c} \to \hat{\mathbf{c}}) &= \int_{s_1}\int_{s_2}\cdots\int_{s_d} Q\left(\sqrt{\Gamma_{0c} \sum_{i=1}^{d} s_{ni}}\right) \\ &\times \; p_{S_{n1}}(s_{n1})\, p_{S_{n2}}(s_{n2}) \cdots p_{S_{nd}}(s_{nd})\, ds_{n1}\, ds_{n2} \cdots ds_{nd}, \end{aligned} \tag{4.11}$$

has to be evaluated.

If the fading powers are independent, the indexes of the differing bit positions are of no importance, since only the incorrect codeword weight matters [191]. The exact evaluation of (4.11) is very difficult. To solve this problem, Hall *et al.*, examined four options [191]. The first option is to simplify (4.11) to a form that can be evaluated through numerical integration [192]. The other three options examined, avoids the problem of numerical integration by seeking closed form upper bounds for $P_d(\mathbf{c} \to \hat{\mathbf{c}})$.

The first option proposed by Hall *et al.* was employed to obtain analytical results. From [192], $Q(x)$ can be expressed in the alternative form written as

$$Q(x) = \frac{1}{\pi} \int_0^{\pi/2} e^{-x^2/(2\sin^2\psi_h)}\, d\psi_h. \tag{4.12}$$

Substituting (4.12) into (4.10), the following expression for the pairwise error probability is found

$$P_d(\mathbf{c} \to \hat{\mathbf{c}} \mid \mathbf{S_n}) = \frac{1}{\pi} \int_0^{\pi/2} \exp\left(-\frac{\Gamma_{0c} \sum_{i=1}^{d} s_{ni}}{2 \sin^2 \phi} \right) d\phi. \tag{4.13}$$

Since all the fading powers are independent, the d-dimensional integral of (4.11) reduces to a product of integrals over each S_{ni}.

Slow fading. Slow fading occurs when the symbol signalling rate is greater than the fading rate. That is, when the effective fading amplitude is assumed to be constant throughout the message sequence, $S_{ni} = \beta_{ni}^2 = \beta^2 = S$. The pdf of the received signal power S is again given by (3.28), where, for slow fading, $\mathbf{S_n} = S$.

It follows from (4.8) that

$$P_d\left(\mathbf{c} \to \hat{\mathbf{c}} \mid S\right) = Q\left(\sqrt{d\, \Gamma_{0c}\, s}\right). \tag{4.14}$$

Using the inequality

$$Q(x) \leq \frac{1}{2} e^{-x^2/2}, \;\; x >> 1, \tag{4.15}$$

the upper bound for the pairwise error probability can be written as

$$P_d(\mathbf{c} \to \hat{\mathbf{c}}) \leq E_{\mathbf{S}} \left\{ \frac{1}{2} \exp\left(-\frac{1}{2}\, d\, \Gamma_{0c} s \right) \right\}. \tag{4.16}$$

Then, from (4.9), the pairwise error probability, averaged over the fading statistics can be written as

$$P_d(\mathbf{c} \to \hat{\mathbf{c}}) \leq \frac{1}{2} \int_s \exp\left(-\frac{1}{2}\, d\, \Gamma_{0c} s \right) p_S(s)\, ds. \tag{4.17}$$

Using (4.6) and (4.13) for fast fading and (4.17) for slow fading, the performance of a space-time convolutional coded system can now be readily calculated.

4.2.2 PCCC Performance

For a turbo code with a fixed interleaver, the construction of A_d (using (4.4)) can only be accomplished through exhaustive search. The latter leads to the proposition of an average upper bound constructed by averaging over all possible interleavers [176]. Therefore, to derive this average performance bound a superfluous interleaver, called the *uniform interleaver*, is used. This interleaver, for a given input block of n bits with input weight i, outputs all $\binom{n}{i}$ distinct permutations with equal probability.

The hyper-trellis transfer function $T(I, D)$ determined by Benedetto *et al.* [193] for turbo codes in three co-decoding configurations has been evaluated in conjunction with continuous, trellis truncated and trellis terminated co-decoding. The latter showed that the performance of the truncated encoder is significantly worse than that of continuous decoding, whereas trellis termination is only slightly worse.

Using (4.6), with $p(d \mid i)$ known, the performance of space-time turbo codes can be evaluated for various channels and transceivers by formulating the conditional pairwise error probability, $P_d(\mathbf{c} \rightarrow \hat{\mathbf{c}})$, for the configuration of interest [194, 195].

The expressions for $P_d(\mathbf{c} \rightarrow \hat{\mathbf{c}})$ derived for convolutional codes, are limited to the case where the output codeword weight, d is fixed. Here, the results is extended to include the performance of turbo codes where the code weight is described in terms of an input-output conditional probability density function (cpdf), $p(d \mid i)$. In Appendix B, the Divsalar cpdf and binomial cpdf have been derived from the constituent encoder state transition matrix, $t(l, i, d)$.

Figure 4.3 shows examples of the Binomial cpdfs given by (B.15) for different code rates, R_c and turbo interleaver size, $N_{tc} = 100$.

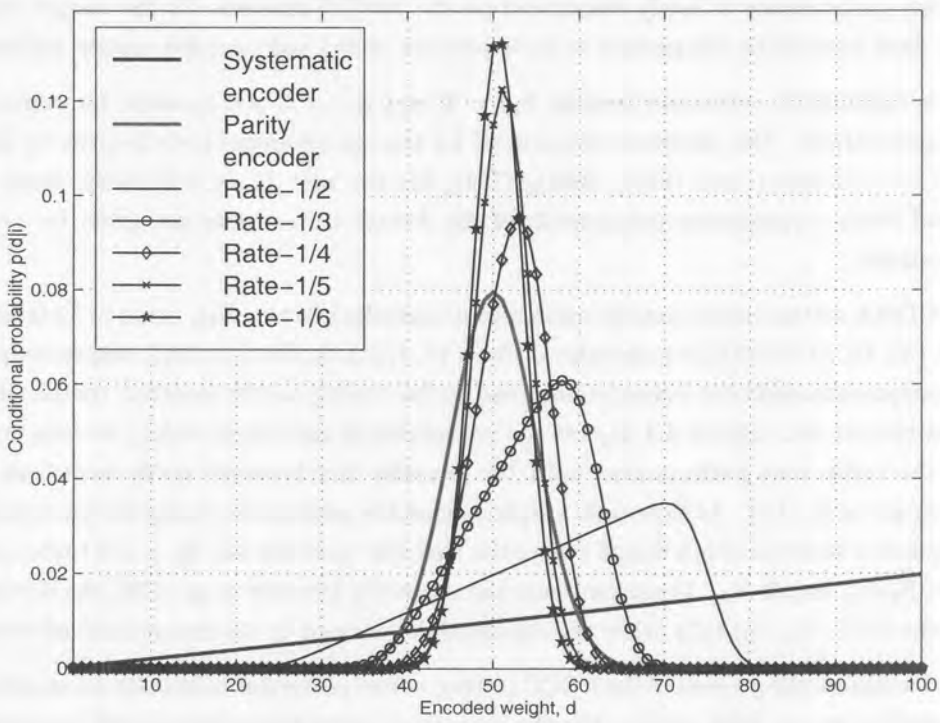

Figure 4.3. Binomial cpdfs, $p(d \mid i)$ for code rate, R_c and turbo interleaver size, $N_{tc} = 100$. (The x-axis is normalized by R_c).

Assuming an AWGN channel, the pairwise BEP of turbo codes may be written as

$$P_d(\mathbf{c} \to \hat{\mathbf{c}}) = E_{d|i}\left\{Q\left(\sqrt{d\,\Gamma_{0c}}\right)\right\}, \tag{4.18}$$

where the conditional expectation $E_{d|i}\{\cdot\}$ is over the evaluated cpdf, $\tilde{p}(d \mid i)$, as explained in Appendix B.

Employing similar arguments to that used in Section 4.2.1.1, the bound given by (4.18) can be extended to include the transmit diversity signalling and multi-path fading channel effects.

From (4.16), for the slow fading channel, the upper bound for the pairwise error probability can be written as

$$P_d(\mathbf{c} \to \hat{\mathbf{c}}) \leq E_{\mathbf{S}}\left\{E_{d|i}\left\{\frac{1}{2}\exp\left(-\frac{1}{2}\,d\,\Gamma_{0c}s\right)\right\}\right\}. \tag{4.19}$$

The conditional expectations, $E_{\mathbf{S}}$ and $E_{d|i}\{\cdot\}$ is calculated over the instantaneous fading power pdf, and the cpdf ($\tilde{p}(d \mid i)$), respectively.

Using (4.13), the bounds of (4.19) can be extended to include fast fading.

4.2.3 Numerical Results

As a benchmark and to illustrate the effect of the interference limited region associated with turbo codes, coded single user performance is firstly considered on the AWGN channel. In the results that follow an approximately fixed bandwidth comparison is made between coded and uncoded system performance.

When coding is considered, constraint lengths $L_{cc} = 9$ and $L_{tc} = 3$ are assumed for convolutional and turbo coding, respectively. The generator polynomial for the convolutional code is given by $(561)_8, (753)_8$ for the rate $R_c = 1/2$ codes, and $(557)_8, (663)_8, (711)_8$ for the rate $R_c = 1/3$ codes, respectively. The feedforward and feedback generator polynomials of the 4-state turbo codes are given by $g_{ff} = 5_8$, and $g_{fb} = 7_8$, respectively.

For the coded CDMA system under consideration a total spreading factor, N_{tot} equal to 32 is assumed. This results in $N = \{32, 16, 10, 8, 6, 5\}$ for code rates of $R_c = \{1, 1/2, 1/3, 1/4, 1/5, 1/6\}$, respectively. Single user performance comparisons between convolutional and turbo coding under identical complexity constraint requirements is carried out. Figure 4.4 depicts the convolutional and turbo coding bounds on the AWGN channel. For the turbo code performance, both the Divsalar and binomial cpdfs have been used in the calculation of P_e given in (4.6). As expected, a tighter bound is achieved by using the binomial cpdf. From Figure 4.4, it is noted that the union bound (using the Divsalar cpdf) for the $R_c = 1/2$ turbo code, diverges at low values of E_b/N_o, for all N_{tc}. Consistent with the results by Divsaler *et al.* [176], the divergence occurs roughly when the SNR (E_b/N_0) falls below the threshold determined by the computational cutoff rate R_o[3].

In an attempt to evaluate the gooness of the PCCC (turbo) codes' performance bounds a computer simulation program was used to obtain BER results. For the simulation performance the system parameters outlined in Table 4.1 were assumed. The BER performance result is also shown on Figure 4.4. In addition to the parameters outlined below, perfect synchronization, channel estimation and CSI are also assumed.

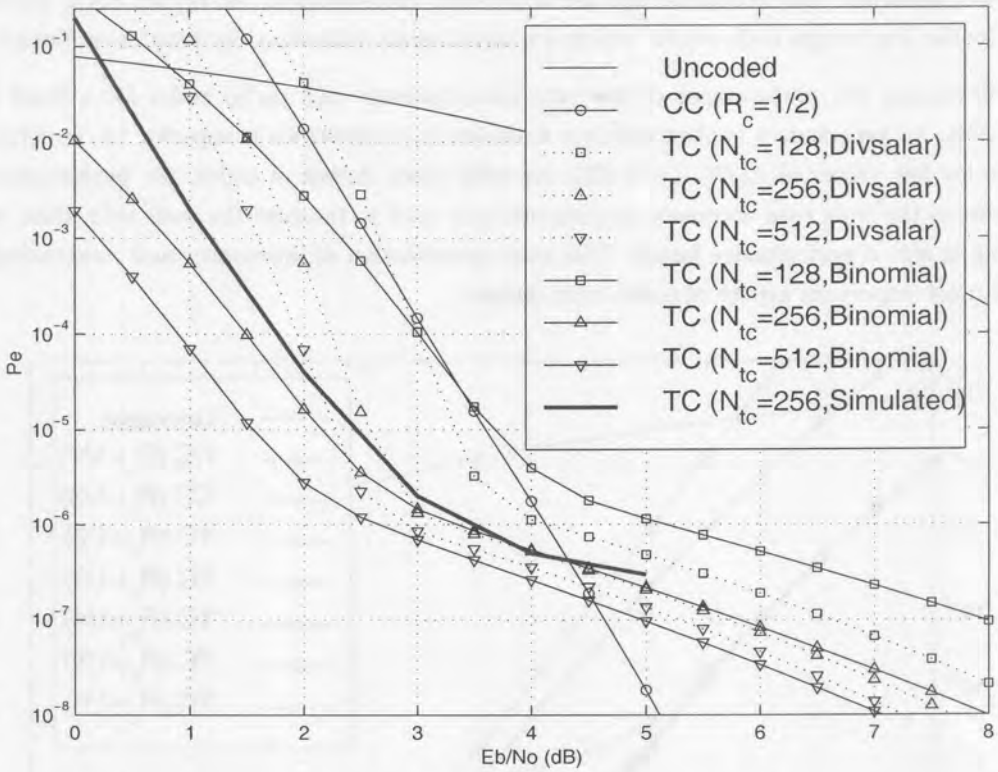

Figure 4.4. CC and TC bounds on AWGN channel with $R_c = 1/2$ and $K = 1$, as a function of turbo interleaver size, N_{tc}.

Parameter	Simulation value
Spreading sequence length	No spreading
Operating environment	AWGN channel
Code type and rate	4-state TC, $R_c = 1/2$
Interleaver	S-type, $N_{tc} = 256$
Decoder	Iterated MAP, serial configuration

Table 4.1. System parameters for BER simulation of PCCC.

Comparing the simulation curve with the performance bound, it is clear that the binomial cpdf results in an improved bound, with a slight divergence around the cutoff rate threshold. Care should be taken for values of E_b/N_o less than the cutoff rate, the performance bounds based on the binomial cpdf behaves as a lower bound to the code's simulated performance. At high SNR rations, the performance bounds based on the binomial cpdf and Divsalal cpdf become converge and both compares well with the simulated BER curve.

Focusing the attention back to the theoretical bounds, the turbo code performance reflects the expected interleaver gain in the waterfall region[4] of the performance curve. This provides an effective way to decrease the BEP without invoking any changes in the system configuration.

At high SNR ratios, the design of the interleaver in a practical system is therefore of great importance. At high values of SNR, turbo codes will perform well with almost any interleaver provided that the two

(or more) RSC encoders receive inputs that are sufficiently uncorrelated. At higher SNR, performance is dominated by the low weight code words, which are significantly influenced by interleaver design

Figure 4.5 illustrates the performance of low rate convolutional- and turbo codes for a fixed interleaver size, $N_{tc} = 256$. As expected, it is observed that turbo code performance is superior to convolutional code performance for low values of E_b/N_o (< 5 dB). As with other classes of codes, the performance of turbo codes improve as the code rate decreases. If puncturing is used to increase the code rate, then the manner of puncturing is also a performance factor. The joint optimization of interleaver and puncturing matrix is perhaps the most important aspect of turbo code design.

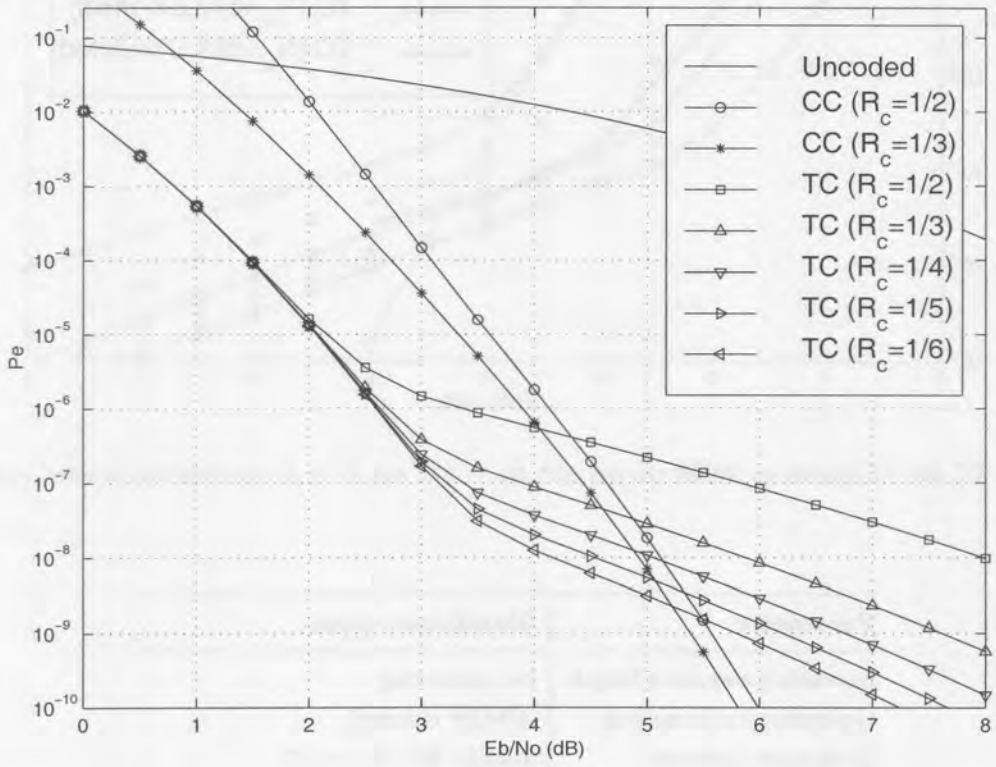

Figure 4.5. CC and TC bounds on AWGN channel with $N_{tc} = 256$ and $K = 1$, as a function of code rate.

It is noted that for a fixed interleaver size, decreasing the code rate does not significantly affect the waterfall performance region. Decreasing the code rate, however, causes the error floor region to be lowered, which may be attributed to the stronger code structure of the low rate codes. Since this region occurs at higher SNR values, the actual weight spectrum becomes more important in influencing the performance.

Since the performance of a MF-based CDMA receiver is interference limited, the uncoded BEP region of importance for a turbo code is roughly $10^{-4} < P_e < 10^{-2}$. This is the focus BEP range and coding should provide acceptable performance in this region.

For a fair comparison to an uncoded system under equal throughput and bandwidth conditions, the spreading sequence length, N, of the coded system must be shortened by a factor of $1/R_c$. This results in a degradation due to the MAI since it is well-known that the normalized cross-correlation between any two spreading sequences is proportional to the Welsh-bound, given as $1/\sqrt{N}$. A trade-off between the greater distance properties of low rate codes and increased cross-correlation effects (due to shorter sequence lengths) is fundamental to the success of coded CDMA.

As another means to investigate multiuser performance, let us define the system load as the quantity $V = K/N_{tot}$, where $N_{tot} = N/R_c$. The system load is therefore the number of active users normalized to the overall spreading factor. Figure 4.6 depicts the system load for low rate convolutional- and turbo coding. It is clear that the system load using turbo codes are substantially higher than for convolutional coding. Another interesting effect is that the coding gain for low rate turbo codes are reduced as the system load increases. This is due to the error floor effect as seen in Figures 4.4 and 4.5. It should be noted that low rate turbo coding will only exhibit this behavior at relatively high E_b/N_0. If the system is operated at low E_b/N_0, low rate turbo coding provides an increase in system capacity.

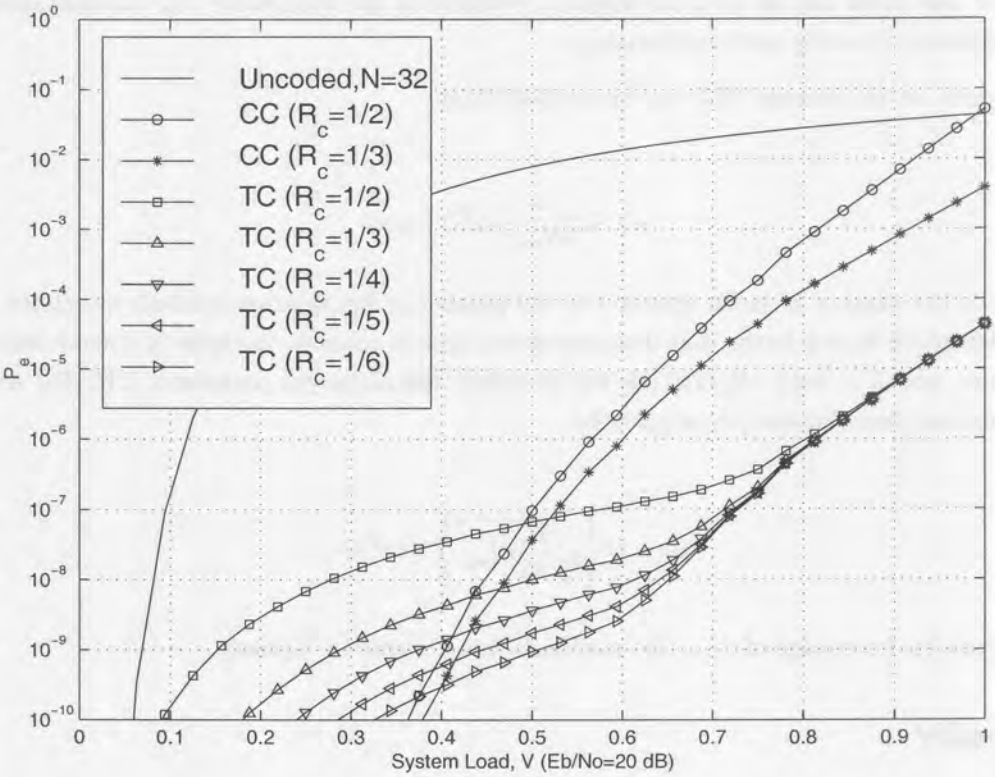

Figure 4.6. Analytical AWGN system load – low rate convolutional and turbo coding ($N_{tc} = 256$).

4.2.4 *Trellis Coded Modulation (TCM) Performance*

The sequence of trellis encoder output symbols has a very carefully controlled structure which enables the detection and correction of transmission errors in a multiple transmit/receive antenna signalling scenario. For the space-time encoder, these symbols should be designed in such a way that the combined spatial and temporal properties will guarantee maximum diversity. The channel coding may be either convolutional or turbo coded. In Chapter 6, details concerning the application and performance of space-time trellis coded modulation to cellular CDMA will be given.

In the analysis of uncoded and coded systems in multiple antenna transmission scenarios two measures of performance are commonly employed, namely SNR improvement and mutual information [196, 197]. While the two metrics are closely related, they have important differences. SNR characterizes the performance of typical uncoded systems, while mutual information measures the maximum rate of reliable communication achievable with coded systems.

In the case of ideal CSI, the transmitter or receiver is assumed to have exact knowledge of the fading channel conditions, and the decoding metric is then ML. On the other hand, when no CSI is available at the receiver, the decoding metric is no longer ML and this introduces an additional weakness into the generalized bounding procedure for TCM [21, 198, 199]. The latter situation occurs when the transmitter arrays are used in point-to-point scenarios in which the transmitter has no knowledge of the channel parameters.

It has been shown by Narula *et al.* [196], that when no information about the channel parameters is provided, beamforming cannot be used to achieve channel capacity. In addition, it was shown that when the CSI is perfect, the SNR-based design and mutual-information-based design become equivalent. All the analysis carried out in this thesis rely on accurate channel knowledge at the transmitter (for transmit diversity) and receiver (for receive diversity and beamforming).

An upper bound on the average BEP can be obtained from

$$P_e \leq \frac{k_0}{bN_{trel}} T(D) \mid_{D=Z}, \tag{4.20}$$

where N_{trel} is the number of trellis states; b is the number of information symbols associated with each branch in the trellis; k_0 is a factor that depends on the type of channel, the type of demodulation and the code structure; and $Z = \exp\{-E_s/4N_o\}$ is the so-called Bhattacharyya parameter [21]. For AWGN with optimum coherent demodulation, k_0 is given by

$$k_0 = Q\left\{\sqrt{\frac{E_s}{N_0} d_{free}^2}\right\} D^{-d_{free}^2}, \tag{4.21}$$

i.e., to compute k_0, knowledge of d_{free} the minimum free distance is required.

4.3 SUMMARY

This chapter classified, defined and discussed forward error correction techniques, including classical convolutional and turbo, and trellis codes for cellular CDMA.

The BEP performance of these codes has been addressed by the derivation of analytical average upper bounds based on the union bound and code weight distributions. Some numerical results were presented. In the following sections, the derived upper bounds will be used to evaluate the performance of space-time coded cellular CDMA systems over the channels with independent and correlated fading.

Notes

1. In this thesis the 'cc' refers to a convolutional code constraint length, the subscript 'tc' will be used to denote the turbo codes' constraint lengths.
2. In an fully interleaved scheme, fast fading is created as the de-interleaving mechanism creates a virtually memoryless channel [200].
3. The cutoff rate is defined as $E_s/N_o = R_c E_b/N_o < -\ln(2^{1-R_c} - 1)$ for a code with rate R_c [129].
4. The "waterfall region" is defined, as the part of the performance curve where the BEP decreases rapidly with increased SNR. The region where the BEP performance changes very slowly, with increased SNR, is defined as the "error floor region". (It is actually incorrect to call this a error floor, as the BEP still improves as the SNR increases).

5 LAYERED SPACE-TIME CODED TRANSMIT DIVERSITY

In Chapters 3 it was shown that space-time processing can improve uplink performance and capacity of a cellular CDMA communication systems. In particular, techniques based on multi-antenna receive diversity and beamforming were considered. In Chapter 1 it was argued that techniques to improve the downlink performance have not been developed with the same intensity to date, but is of increasing importance due to the fact that the capacity demand imposed by the projected data services, for instance internet, burdens (more heavily) the downlink channel. It is therefore of importance to find techniques that improve the downlink capacity.

Transmit diversity (see also Section 3.2) is an effective method to combat fading when multiple receive antennas are not available. Techniques such as diversity, antenna-selection, frequency-offset, phase sweeping, and delay diversity have been studied extensively in the past [46, 47, 48, 54]. Recently, space-time coding was proposed as an alternative solution for high rate data transmission in TDMA wireless communication systems [201, 202, 203, 204].

Recent studies have explored the limit of multiple antenna system performance in a Rayleigh fading environment from an information-theoretic point-of-view [104, 205, 206]. It has been shown that, with perfect receiver channel state (side) information (CSI), and independent fading between pairs of transmit-receive antennas, the situation of total capacity may be achieved.

Foschini [104] has considered a particular layered space-time architecture with the potential to achieve higher capacity. This layered architecture forms the basis for the class of orthogonal decomposable coded space-time decoders. The chapter will focus on the construction and performance evaluation of space-time coded CDMA employing multiple transmit antennas. The classification of space-time coded transmit diversity structures is illustrated in Figure 5.1. The techniques for transmit diversity suitable for CDMA can be divided into two distinct classes, CDTD and TDTD (see Sections 3.2.1.1 and 3.2.1.2). These two coded space-time transmit diversity classes will be discussed by looking at

- the suitability of classical convolutional- and turbo codes. (The application of low rate codes, including orthogonal- and super-orthogonal convolutional codes (SOCC), is also investigated); and

- extensions of the CDTD scheme to space-time turbo diversity codes, viz. turbo transmit diversity (TTD) is considered in detail in the next chapter.

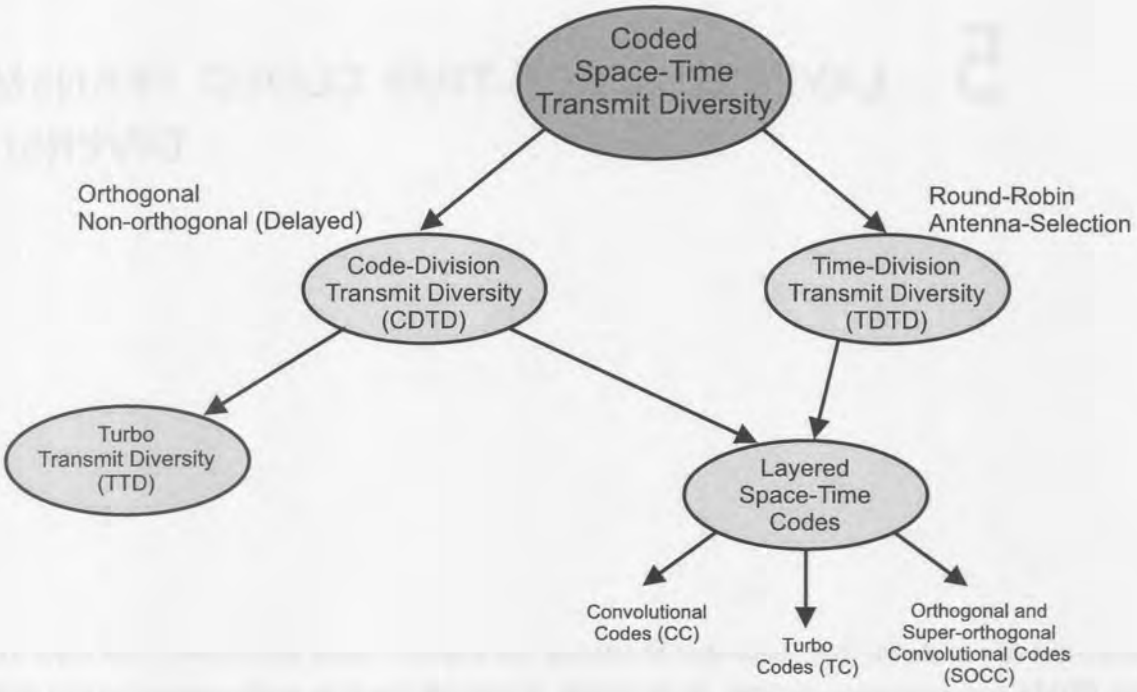

Figure 5.1. Coded transmit diversity space.

5.1 TRANSMIT DIVERSITY MULTIPLE ACCESS CHANNELS

As has been discussed earlier, the use of coded transmit diversity is an attractive solution for improving the performance and downlink capacity of CDMA communication systems.

In CDMA the channel is allocated implicitly by assigning to each information stream a unique finite length binary or non-binary (e.g., complex) signature or spreading sequence. Spreading sequences of different information streams have the same length and are almost orthogonal and, hence, messages from different users are quasi-separable by means of projections. This scheme introduces interference amongst information streams associated with different users, and this coupling between users requires a very complex receiver.

Information theoretic aspects of transmit diversity were addressed by Foschini and Gans in [206] and Telatar in [205]. Telatar derived the expressions for capacity and error exponents for multiple transmit antenna systems in the presence of Gaussian noise. Here, capacity has been derived under the assumption that the fading is statistically independent from one channel use to the other. In [206], Foschini and Gans derived the outage capacity under the assumption that the fading is quasi-static; i.e., constant over a long period of time, and then changed in an independent manner. In [104], a particular layered space-time architecture was shown to have the potential to achieve a substantial fraction of capacity.

Following the work by Urbanke [207] on multiple access communications employing coding, it is clear that the application of transmit diversity to CDMA closely resembles the classical multiple access communications problem. In the classic multiple access channel (MACH) environment there are several users competing for the available channel resources. When multiple transmit antennas are employed, the allocation of resources

is more problematic since a fair and efficient allocation of the resources among all users requires a large amount of co-ordination. This co-ordination is made more difficult by the fact that there are no direct links between the sources and the channels available and also because of the additional MAI interference.

5.1.0.1 Capacity region of transmit diversity MACH. The capacity region $\Re$ for MACHs is generally described as a polytope, i.e. a multi-dimensional figure whose faces are hyperplanes, or informal multidimensional solids with flat sides. Figure 5.2 depicts the typical region for $K \cdot M_T = 2$, the best known case since most multiple access papers focus on this special case [208].

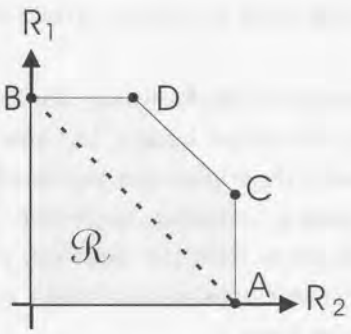

Figure 5.2. Block diagram of the dual transmit antenna single user decoder, employing an optimum successive cancellation decoder.

The reason for interest in this capacity region (besides that it is of interest in its own right) is the various operational results that follow elegantly from the particular properties of capacity region $\Re$ [207, 208]. These are described in the following.

A simple strategy to share the channel between antenna streams is time sharing. In Figure 5.2, the line AB corresponds to this scenario. Here the channel is accessed through multiple transmit antennas at disjoint moments in time, and a common time reference is needed for this scheme to work.

Following Urbanke [207], the rate tuples achievable by timesharing are those which lie on or below the line AB in Figure 5.2. The point A corresponds to the extreme case where the first transmit antenna stream of a specific user is used permanently and the second transmit antenna is never used (idle state), whereas in point B the roles of the transmit antennas are reversed. As can be seen from this example, not all points in the capacity region are achievable by means of timesharing. Hence, in order to fully utilize the given channel resources, both transmit antennas will have to access the channel concurrently. Of course, this introduces coupling among the users and, therefore, an optimum receiver (a receiver which results in the minimum achievable error probability) has to decode both users jointly. This results in high decoding complexity. Of special importance are the vertices C and D shown in Figure 5.2. It has been shown in [207], that these rate points can be achieved through *single user coding*. The latter will be addressed in more detail in the following section.

The result obtained by Wyner [209] is of particularly interest, stating that the vertices in $\Re$ are achievable by sequentially decoding one information (signature) waveform at a time. This successive decoder avoids the largest practical concern associated with multiple access communication, namely the complexity of decoders that jointly decode all waveforms at once.

This brings us to a very interesting situation. Depending on whether or not the transmitter has information on the instantaneous state of the channel, the design of space-time codes for CDMA systems can be grouped into two categories. Specifically, if the transmitter has CSI, considering the conditions of orthogonal spreading, the MACH can be decomposed into several nearly independent sub-channels. Under these conditions, the capacity region of the (frame and symbol) asynchronous MACH equals the one of the synchronous channel.

For systems in which the transmitter does not have CSI, or when the rate of information fed back from the receiver is slow, the channel cannot be decomposed as described in the foregoing. Although the lack of CSI does not imply much loss of channel capacity, the single user coding principles cannot be applied. The result is an inherently multiple space-time dimensional channel decoder, in which the redundancy embedded along the spatial as well as temporal dimensions, must be used to extract the data sources.

5.1.0.2 Single user decoding. As discussed in the foregoing, the decomposition of the MACH into independent sub-channels provides not only theoretical insight, but also potentially efficient strategies for implementing practical systems. Importantly, these strategies can be efficiently employed by a method called single user coding (also called onion peeling, stripping, successive cancellation, or superposition coding) [207, 210]. The name single user coding stems from the fact that, in the case of a dual antenna transmit scheme, the joint codeword is decoded in two steps, each of which corresponds to the decoding of a single user antenna information waveform at any time.

Consider as a special case, the single user coded dual ($M_T = 2$) antenna diversity system. The general structure for the decoder of this system is illustrated in Figure 5.3 [211].

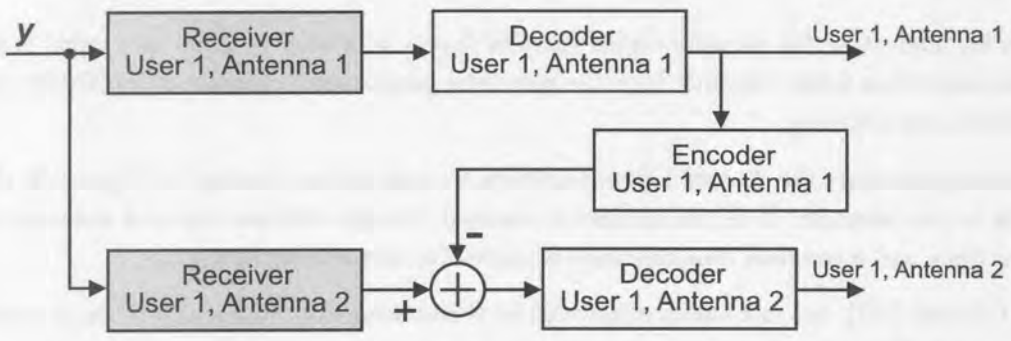

Figure 5.3. Block diagram of the dual transmit antenna single user decoder, based on optimum successive cancellation decoder.

Under these assumptions, the decoder can first decode the first antenna stream (viewing the second antenna stream as Gaussian noise). Once the correct contribution of this antenna stream is known, it can be subtracted from the received codeword and then the second antenna stream can be decoded. It has been shown in [212] that the total capacity (points C and D of Figure 5.2) can be achieved by the optimum successive cancellation decoder.

5.2 LAYERED SPACE-TIME CODES

The construction of layered space-time convolutional- and turbo coding configurations applied to multiple transmit antenna signaling is considered.

Figure 5.4 illustrates the general block diagrams of the layered space-time encoder and decoder. In this model the data source produces a sequence of N_{cc} data bits, $\mathbf{b}_k$, which enters a rate R_c encoder. The encoded sequence, $\mathbf{x}^{(j)}$ of length N_{cc}, is passed to the M_T symbol interleavers and to the multiple access transmit diversity sub-system. Recall from Figure 5.1, that this coding scenario supports both the CDTD and TDTD signalling configurations.

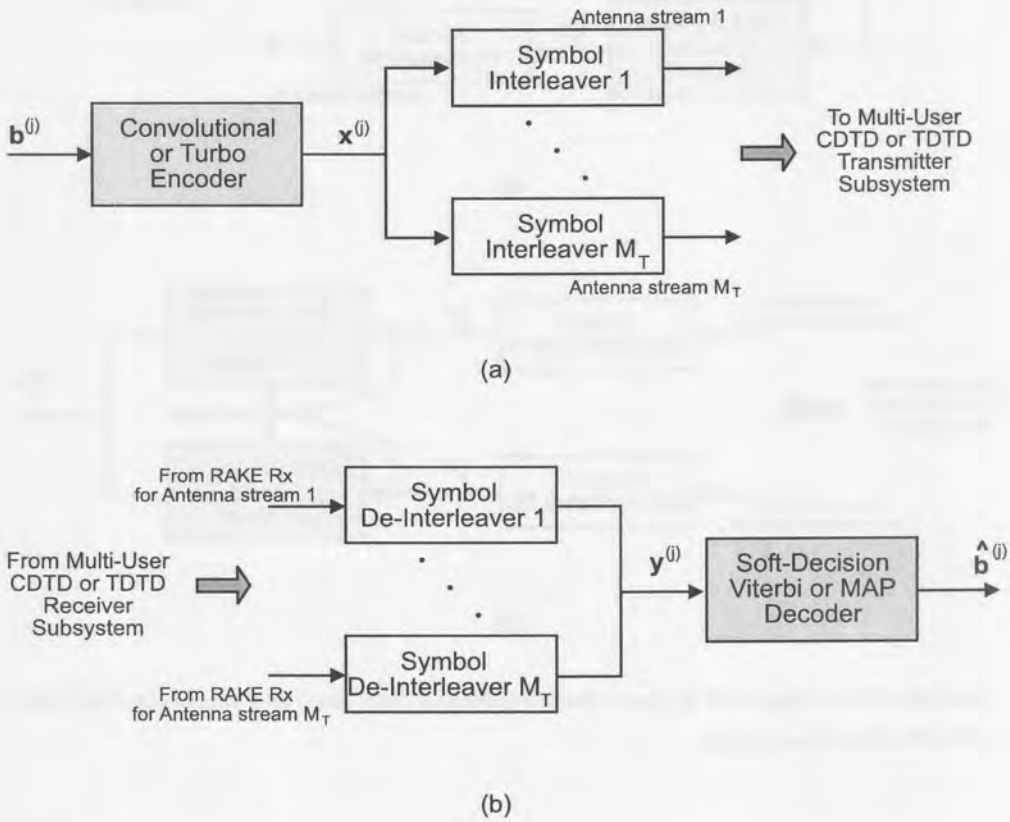

Figure 5.4. Generalized block diagram of the space-time convolutional coder based on a sub-optimum configuration. (a) Encoder, (b) Decoder.

In the receiver subsystem, the received signal is correlated with the complex scrambling/spreading sequence associated with each of the individual antenna sub-streams. With the decoding configuration, shown in Figure 5.4(b), nearly optimal decoding can be achieved by employing the Viterbi or MAP algorithm. This decoding is suboptimal since the correlator receiver is matched to the AWGN channel, and not to the MAI. It has been shown that when CSI information is available at the receiver, using soft-decision decoding and coherent detection, the coding gain on fading channels can be quite high [21].

It should be noted that for TDTD signalling, the configuration presented in Figure 5.4 can accomplish a significant portion of the theoretical system capacity, although it is a suboptimal implementation.

In contrast to the suboptimal TDTD configuration, in CDTD the M_T orthogonal streams are recovered from the receiver sub-system by means of a decorrelation process. During a specific decoding stage, the decorrelation detector only considers a single user entity for the spreading sequences associated with the M_T transmit antennas associated with the reference user. The CDTD scheme may be extended to a single user multiple antenna decoder based on a optimum successive decoder (OSD). Figure 5.5 illustrates a possible

implementation of this decoder for convolutional codes, where each user is decoded on a per-user channel basis.

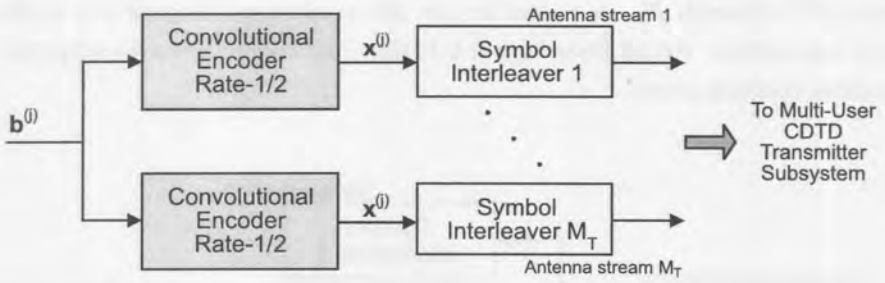

(a)

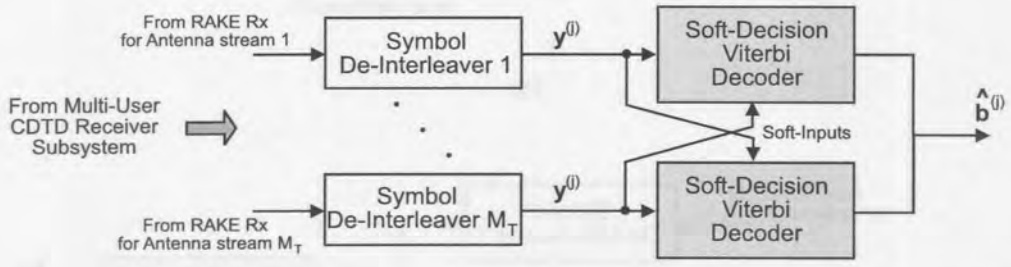

(b)

Figure 5.5. Generalized block diagram of the space-time convolutional coder based on a per-user configuration. (a) Encoder, (b) Decoder, with soft-information transfer.

In order to maintain soft failure diversity and to provide additional soft-decision information to the different decoders operating in parallel, systematic convolutional encoders are generally utilized at the encoder and decoder. In this way, the full benefits of soft-decision decoding are realized. In [211, 213], a group metric decoding scheme has been proposed that exploits the nature of the multiuser decoding problem. This decoder may be considered as a single user, single antenna decoding scheme, that will utilize information from all the user and antenna matched-filter outputs to the decoding metrics.

5.2.1 Low Rate Code Extension

The low rate codes proposed in [35, 214, 215] for CDMA, can be directly applied to configurations depicted in Figures 5.4 and 5.5. The use of orthogonal and super-orthogonal convolutional codes (SOCC) is considered.

Orthogonal block codes are known to perform well on very noisy channels. In [35], Viterbi presented a method to find orthogonal convolutional codes having similar properties. However, orthogonal convolutional codes imply a large bandwidth expansion. Along these lines, several related coding schemes with good distance properties, but less bandwidth requirements, have been proposed in [214, 215].

A rate $R_c = 1/n$ orthogonal convolutional encoder with constrained length, L_{oc}, can be constructed from a shift register and a block orthogonal encoder or signal selector [35]. One in $2^{L_{oc}}$ orthogonal waveforms is chosen based on the state of the shift register. The weight of any trellis branch (not the all-zero path)

is $2^{L_{oc}-1} = n/2$. For an orthogonal convolutional code the rate is then related to the constraint length by $R_c = 2^{L_{oc}}$. One way of implementing an orthogonal convolutional encoder is for the orthogonal code selector to choose rows from a Walsh-Hadamard matrix.

A rate $R_c = 2^{-(L_{oc}-2)}$ super-orthogonal code is obtained by modifying the orthogonal codes as follows [13]

- Let the inner $L_{oc} - 2$ stages of the shift register be used for the orthogonal waveform selection; then
- add the first and last bits of the register modulo-2 to each bit in the orthogonal waveform.

Transfer functions and upper bounds on the BEP for orthogonal and super-orthogonal convolutional codes are derived in Appendix B. Section 6.3 will consider the application of super-orthogonal turbo codes to space-time transmit diversity.

5.3 LAYERED SPACE-TIME CODES PERFORMANCE

Using (3.23), (3.29), (4.6) and the system parameters outlined in Table 5.1, the BEP performance of a cellular CDMA system employing space-time coded transmit diversity can be determined numerically.

Parameter	Simulation value
Spreading sequence length	$N = 32$
Operating environment	2-Path, equal strength.
User distribution	uniform
Number of multi-path signals	$L_p = 2$
Number of users	$K = 1, 2, \ldots, N$
Number of RAKE fingers	$L_R = 2$
Transmit diversity elements	$M_T = 1, 2, 3$
Transmit diversity technique	CDTD and AS-TDTD
FEC code type	CC and TC
FEC code rate	$R_c = 1, 1/2, \ldots, 1/6$

Table 5.1. System parameters for numerical evaluation of BEP performance.

In order to calculate the BEP of the coded CDTD and TDTD systems, the output SNR should include the transmit diversity interference term. Assuming that the cellular system is employing omni-directional antennas, the total output SNR can be determined as

$$\Gamma_{0c} = \left(\frac{1}{R_c} \frac{N_o}{2\,E_b} + \frac{(K \cdot M_T - 1)}{3N} \right)^{-1}, \tag{5.1}$$

for CDTD, and

$$\Gamma_{0c} = \left(\frac{1}{R_c} \frac{N_o}{2\,E_b} + \frac{(K - 1)}{3N} \right)^{-1}, \tag{5.2}$$

for TDTD. With reference to (3.21), it can be seen that (6.29) and (5.2) are extensions of our previous analysis and includes the code rate R_c.

It is important to note that P_e as defined in Chapter 4 represents the BEP for one spatial snapshot of the state of the cellular system. This is due to the fact that the channel model used represents one snapshot of the spatial state of the system, as described in Chapter 2. To calculate the BEP performance of the system for the average spatial state of the system P_e must be calculated a number of times and the average of these calculations determined.

5.3.1 Fading Channel Multiuser Performance

Using (4.17), (4.11) and (4.19), Figures 5.6 and 5.7 depict the BEP performance of Orthogonal CDTD (O-CDTD) under 2-path Rayleigh fast- and slow fading conditions, respectively, with rate $R_c = 1/2$ convolutional and turbo ($N_{tc} = 256, 2048$) coding. For both graphs, the number of users $K = 5$ with $M_T = 1, 2$ and 3 transmit antenna elements.

By introducing multiple transmit antennas, the diversity order is increased, and thereby the probability of coding gain is increased. This is especially true for turbo coded transmit diversity which is better suited for Gaussian-like MAI. From the graphs it clear that turbo coded transmit diversity increases the performance substantially.

Using the bounds on BEP performance derived in Section 4.2, Figures 5.8 to 5.12 depict the performance as a function of system load, V for coded O-CDTD CDMA. The analysis is restricted to a fully interleaved (i.e., fast fading) two path Rayleigh fading channel. The operating point has been taken as $E_b/N_0 = 20$ dB. Figures 5.8 and 5.9 compare coded ($R_c = 1/2$) and uncoded O-CDTD BEP performance as a function of interleaver size and transmit diversity order, with $M_T = 1, 2$. Results for single transmit diversity ($M_T = 1$) are included in an attempt to isolate the performance improvement achieved with temporal diversity from the total space-time diversity gain. From the curves it is clear that the introduction of coded transmit diversity has improved the capacity of all the coded systems quite substantially. For regions of high system load, the best performance is achieved by the turbo coded systems.

Figures 5.10 and 5.11 compare the performance of different low code rates and transmit diversity order, $M_T = 1, 2$. For the turbo coded systems the interleaver size was 256. The low rate codes provide improved performance over the complete range. This illustrates the effectiveness of low rate codes to overcome loss in processing gain under equal bandwidth conditions.

Figure 5.12 compares the performance of coded O-CDTD with $R_c = 1/2$ and transmit diversity order, $M_T = 1, 3$. From the graphs it can be seen that the best performance is always achieved with the highest order diversity.

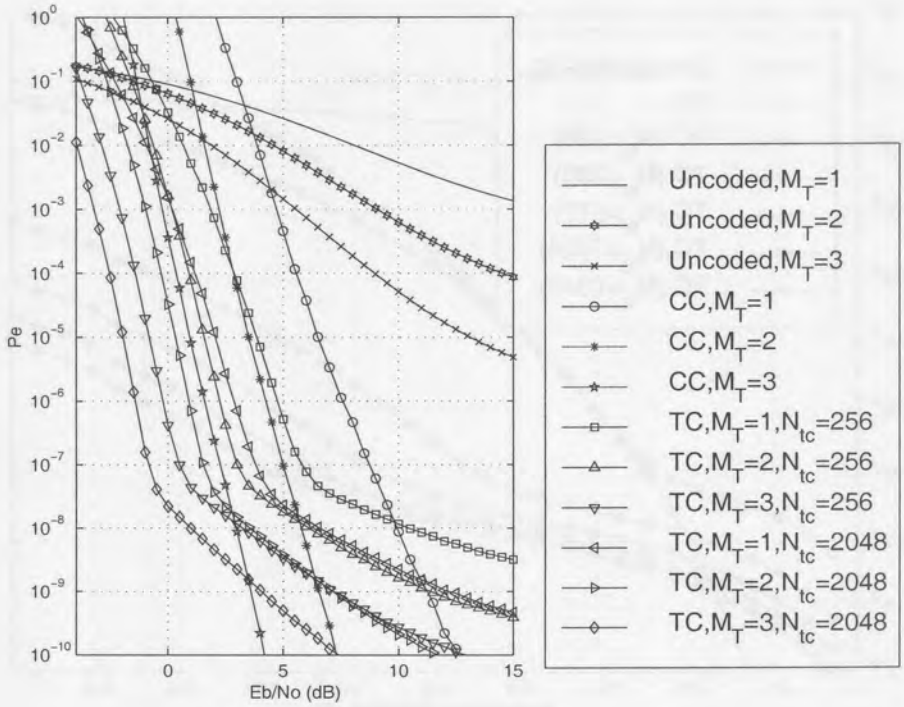

Figure 5.6. Analytical BEP performance of coded O-CDTD, with $R_c = 1/2$, $K = 5$, and $M_T = 1, 2, 3$, on a fast fading 2-path channel.

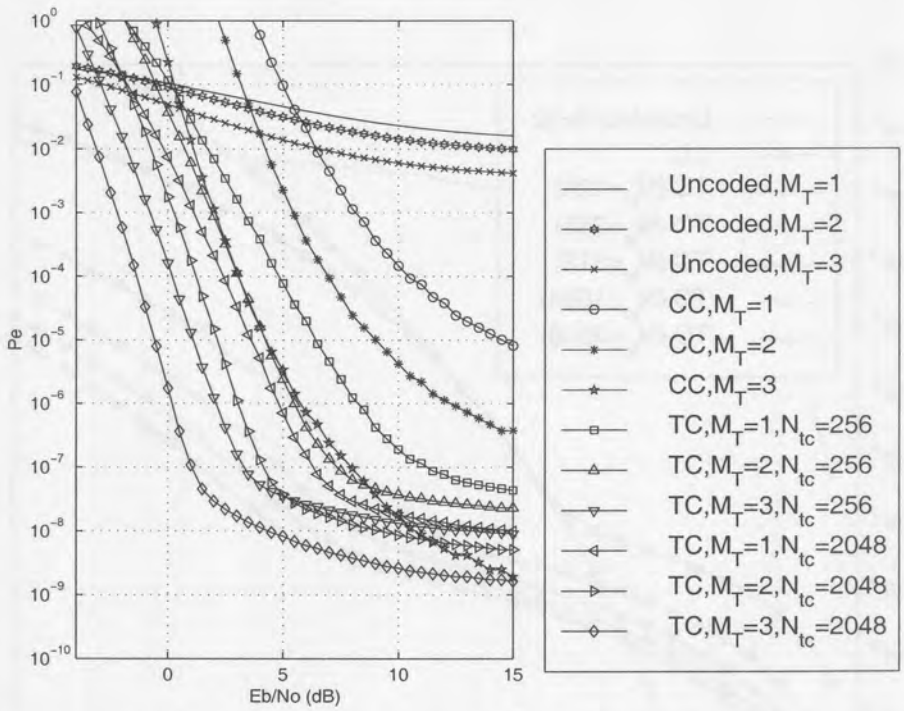

Figure 5.7. Analytical BEP performance of coded O-CDTD, with $R_c = 1/2$, $K = 5$, and $M_T = 1, 2, 3$, on a slow fading 2-path channel.

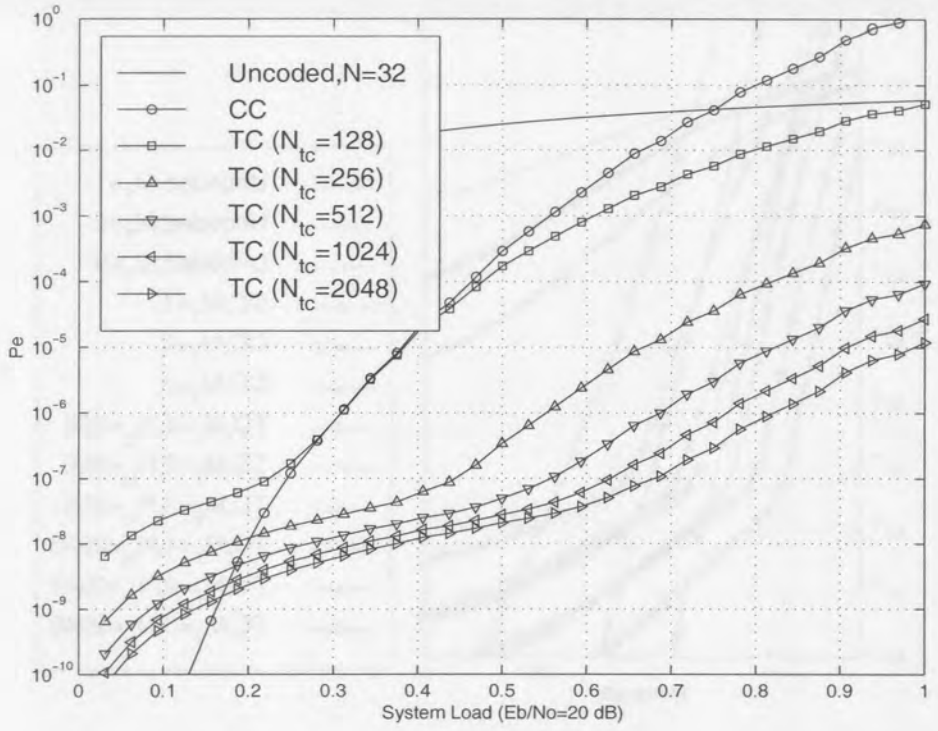

Figure 5.8. Coded O-CDTD BEP performance on a 2-path fading channel with $R_c = 1/2$ and $M_T = 1$.

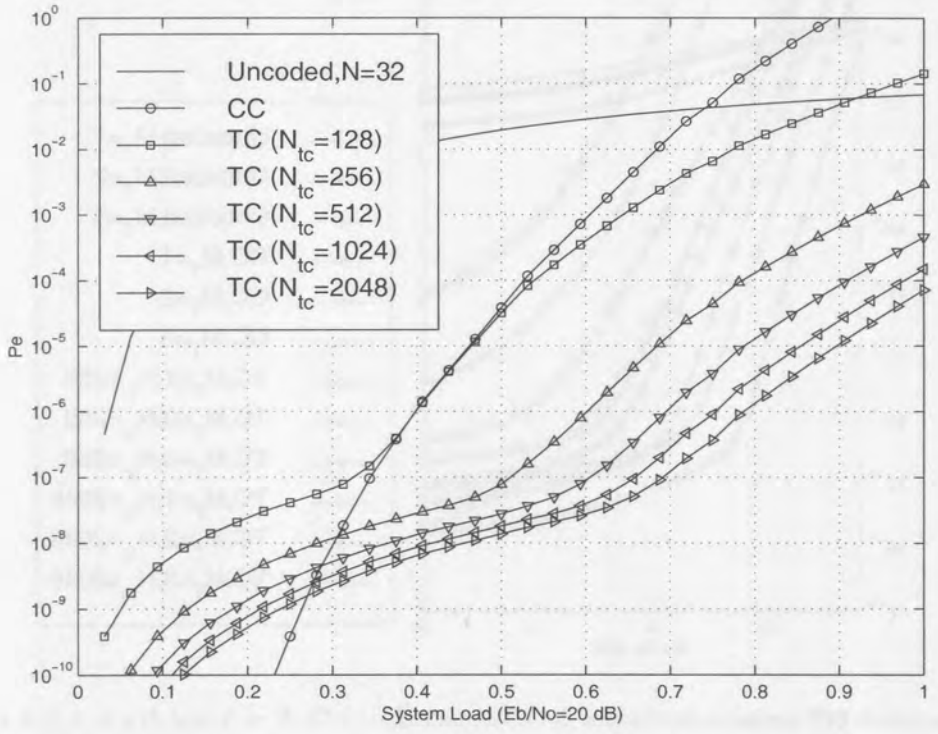

Figure 5.9. Coded O-CDTD BEP performance on a 2-path fading channel with $R_c = 1/2$ and $M_T = 2$.

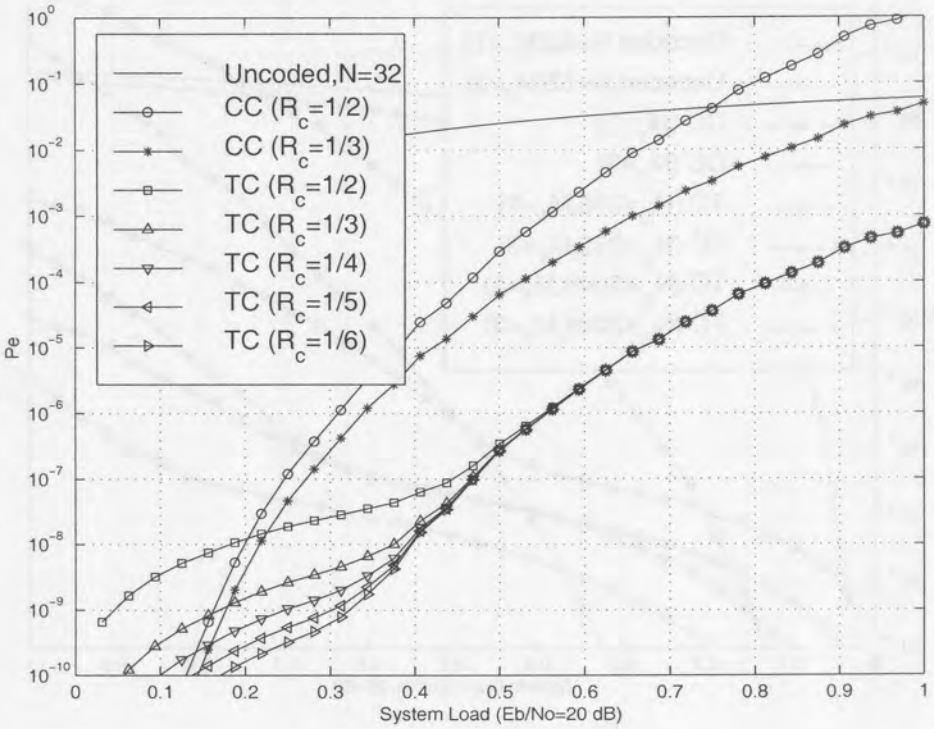

Figure 5.10. Coded O-CDTD BEP performance on a 2-path fading channel with $N_{tc} = 256$ and $M_T = 1$.

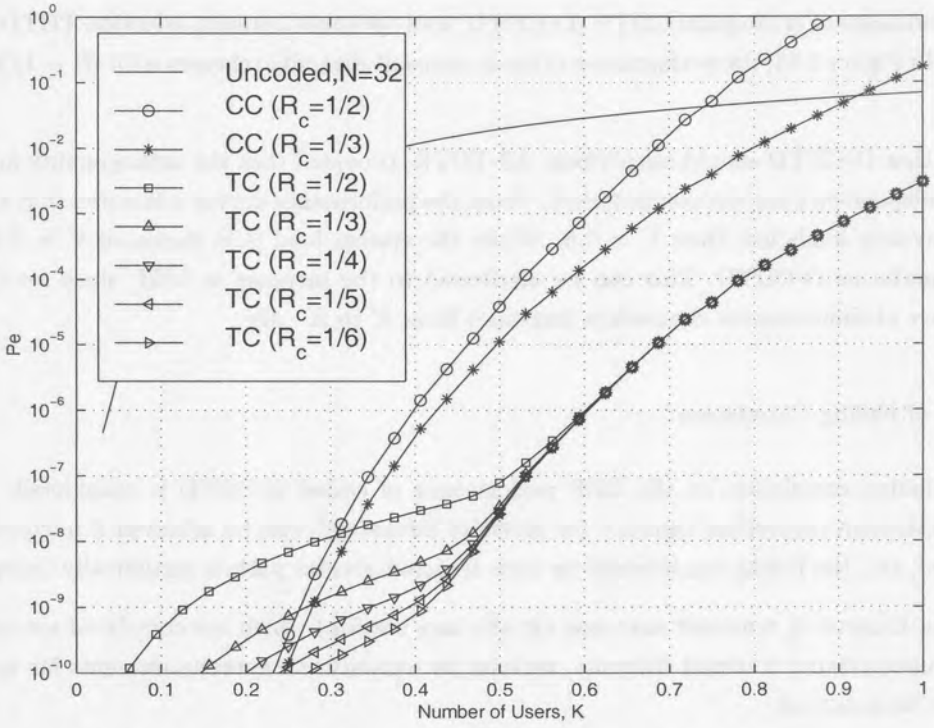

Figure 5.11. Coded O-CDTD BEP performance on a 2-path fading channel with $N_{tc} = 256$ and $M_T = 2$.

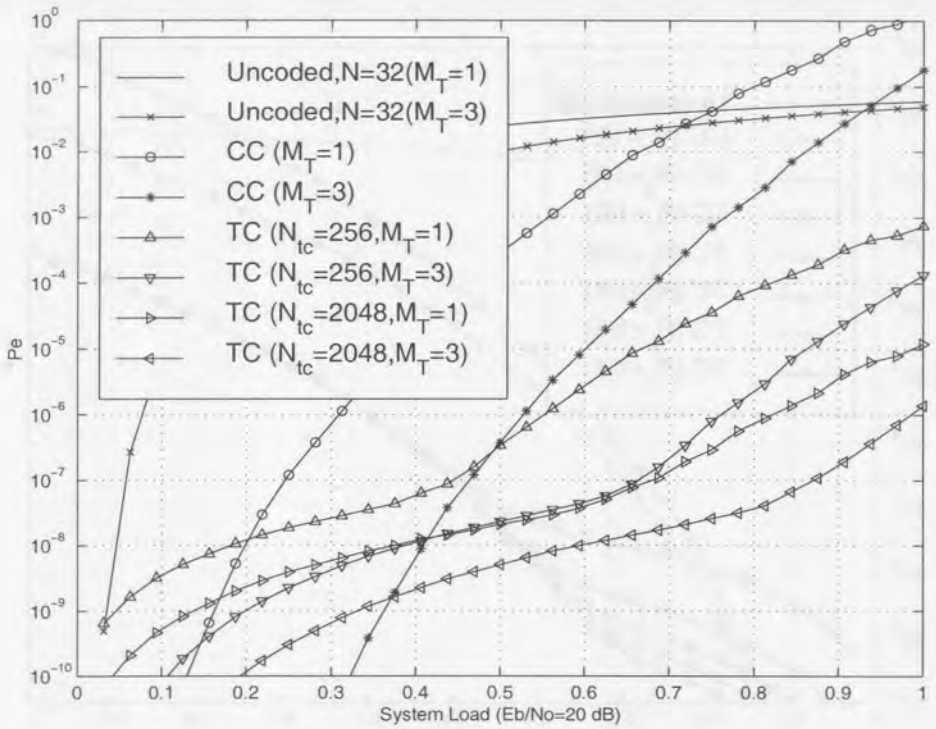

Figure 5.12. Coded O-CDTD performance comparison with $R_c = 1/2$, $N_{tc} = 256, 2048$ and $M_T = 1, 3$.

5.3.2 CDTD and TDTD Comparison

The BEP performance of orthogonal CDTD (O-CDTD) and optimum antenna-selection TDTD (AS-TDTD) is considered. In Figure 5.13, the performance of these transmit diversity schemes with $R_c = 1/2$ and $M_T = 3$ is compared.

It is expected that O-CDTD should outperform AS-TDTD, provided that the orthogonality and conditions of statistical independence are not compromised. From the performance curves it is noted that this argument is correct for system loads less than $V = 0.5$. When the system load is in excess of $V = 0.5$, AS-TDTD signalling outperforms O-CDTD. This can be attributed to the increase in MAI, since for O-CDTD the effective number of simultaneous channels is increased from K to $K \cdot M_T$.

5.3.3 Effects of Fading Correlation

The effect of fading correlation on the BEP performance of coded O-CDTD is considered. It has been argued that maximum theoretical capacity (or diversity advantage) can be achieved if uncorrelated signals are transmitted, i.e., the fading experienced by each transmit-receive path is statistically independent.

As explained in Chapter 3, transmit antennas (at the base station) which are correlated are considered. In order to have uncorrelated transmit diversity, we have to separate the antenna elements far apart ($\approx 40\lambda$), which may not be practical.

To investigate the influence of correlation, Figure 5.14 depicts the O-CDTD performance with $R_c = 1/2$, $M_T = 3$, and constant fading correlation coefficients, $\rho = 0.0, 0.5$ and 0.99. The performance degradation due to correlation is not that significant if ρ is restricted to 0.5. However, the performance is severely

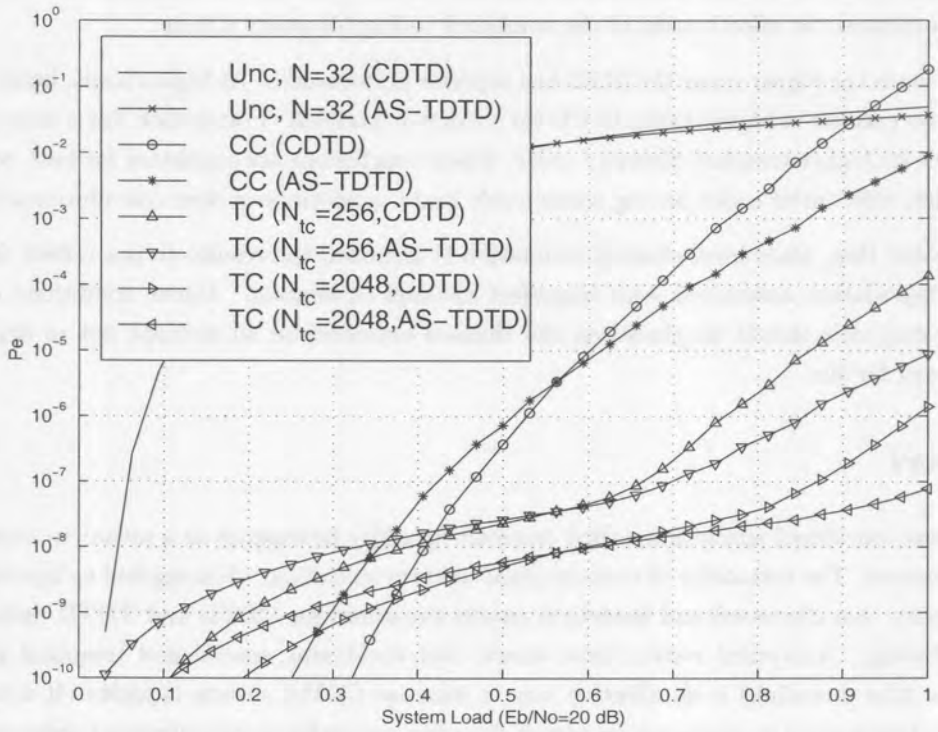

Figure 5.13. Comparison of $R_c = 1/2$ convolutional and turbo coding ($N_{tc} = 256, 2048$) CDTD and AS-TDTD.

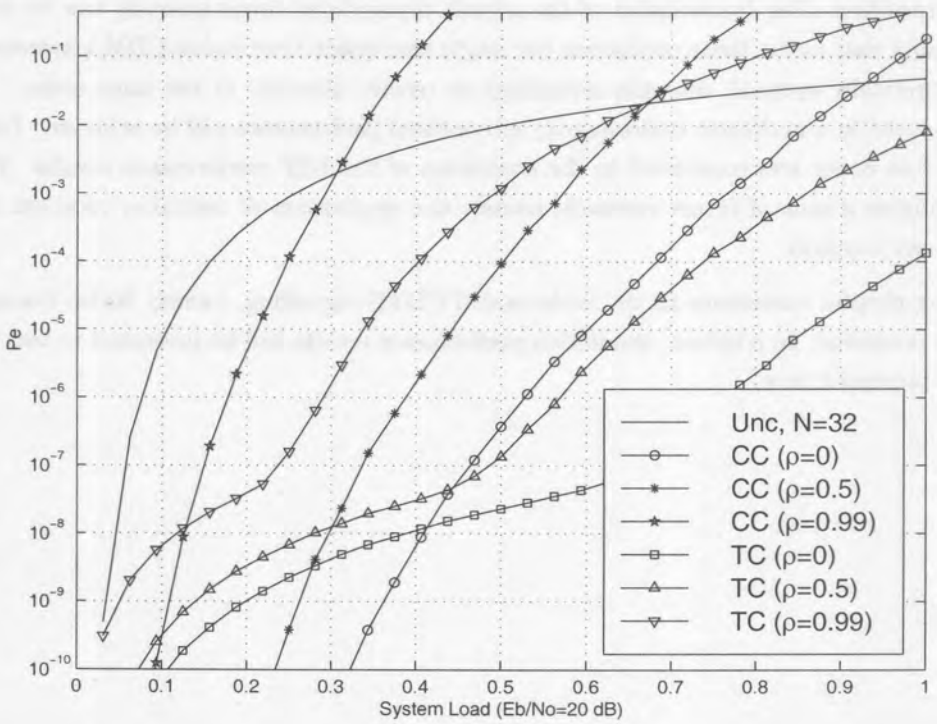

Figure 5.14. Comparison of $R_c = 1/2$ convolutional and turbo coding ($N_{tc} = 256, 2048$), with $M_T = 3$ and $\rho = 0, 0.5, 0.99$.

degraded when $\rho \geq 0.5$. The latter can be attributed to the fact that the correlated multi-path channel has memory which reduces the effectiveness of the combined coding/diversity scheme.

At low system loads the higher order O-CDTD has superior performance. At higher loads, however, the MAI increases and no gain for a higher order O-CDTD scheme is possible. Correlation has a more pronounced degrading effect for higher transmit diversity order. These conclusions are consistent for both convolutional- and turbo codes, with turbo codes having consistently better performance than convolutional codes.

It should be noted that, since ideal channel estimation is assumed, the results do not reflect the additional performance degradation associated with imperfect channel estimation. Under conditions of correlated fading, strong emphasis should be placed on the channel estimator in an attempt not to degrade system performance even further.

5.4 SUMMARY

This chapter has considered space-time coded transmit diversity techniques as a means to improve cellular CDMA performance. The suitability of convolutional- and turbo coding, when applied to layered space-time transmit diversity, was discussed and analytical results presented for CDTD and TDTD under conditions of multipath fading. Analytical results have shown that combining spatial and temporal processing at the transmitter (the downlink) is an effective way to increase CDMA system capacity. It was shown that turbo coding, when applied to space-time transmit diversity, outperforms convolutional codes with the same code rate and comparable complexity. In general, the average performance of the CDTD and TDTD is comparable.

It was argued that when orthogonal spreading is combined with the multiple transmit antennas the destructive superposition after combination of the signals transmitted simultaneously can be avoided. It is important to note that under these conditions the single user space-time coded CDMA system will achieve the same, theoretically optimal, diversity advantage as receive diversity of the same order. When a MF receiver is employed in a multiuser environment, sub-optimal performance will be achieved. For this reason the use of random codes was considered in the derivation of the BEP performance results. The foregoing argument highlights a area of future research, namely the application of multiuser receivers in the coded transmit diversity scenario.

In the following chapter extensions to the turbo coded CDTD signalling, namely turbo transmit diversity (TTD) will be presented. In addition, simulation performance results will be presented to test the goodness of the bounds presented here.

6 SPACE-TIME TURBO CODED TRANSMIT DIVERSITY

In the foregoing chapter the superior performance achieved with space-time turbo coded CDTD systems have been presented. In this chapter extensions to layered space-time coding are considered. In this chapter different turbo transmit diversity (TTD) scenarios are considered. The classification of the three TTD scenarios is illustrated in Figure 6.1. These are parallel concatenated turbo transmit diversity (PCTTD) [216, 217, 218], serial concatenated turbo transmit diversity (SCTTD)[1] [219], and super-orthogonal turbo transmit diversity (SOTTD) [220, 221, 222].

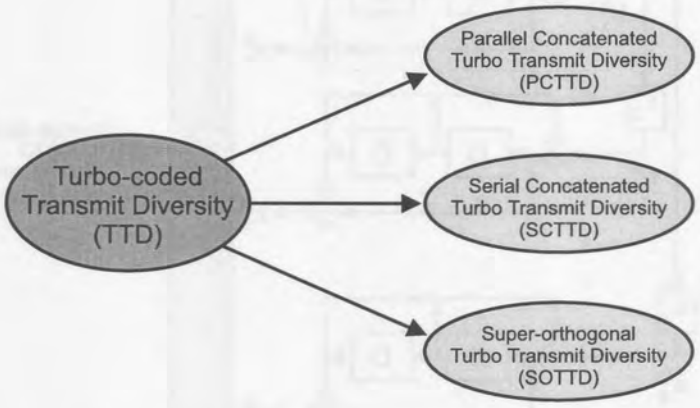

Figure 6.1. Turbo transmit diversity space.

Both PCTDD and SCTTD offer a sub-optimal, but practical implementation of the turbo coded CDTD system. The principle of operation is to transmit the coded bits, stemming from the constituent encoders, via the spatial domain rather than via the time, code or frequency domain. The received data stream is then iteratively decoded using turbo decoding principles. The way the turbo coder is configured fits naturally into the CDTD schemes described in the previous chapter.

SOTTD provides a flexible architecture for the generation of variable low rate coded transmit diversity. Here, techniques of spreading and coding at low-rate are married with the code-division transmit diversity and iterative "turbo" processing. In very general terms SOTTD can be considered as a special case of orthogonal turbo-coded CDTD, employing codes of very low rate.

Detail concerning the design, realization and BEP performance of the three TTD scenarios will be presented in the following sections.

6.1 PARALLEL CONCATENATED TURBO TRANSMIT DIVERSITY (PCTTD)

In the layered space-time turbo coded CDTD signalling, a turbo encoder (and its associated iterative decoder) is required for every transmit diversity branch available. In PCTDD a single turbo encoder-decoder pair is required, with the only requirement being that the number of constituent RSC encoders Z, should be greater or equal to the transmit diversity order M_T. By applying appropriate puncturing the original single antenna rate $R_c = 1/2$ code is transformed into a more powerful space-time rate $R_c = 1/(Z+1)$ code. The way the turbo coder is configured fits naturally into the transmit diversity schemes described above.

PCTTD can be implemented as orthogonal or non-orthogonal CDTD, and is an novel extension of the work by Barbalescu [223]. The principle of operation is to transmit the coded bits, stemming from the constituent RSC encoders, via the spatial domain rather than via the time, code or frequency domain. The received data stream is then iteratively decoded using turbo decoding principles. The power of PCTTD lies in the principle that a single-antenna rate $R_c = 1/2$ coder is transformed into a more powerful turbo code with rate $R_c = 1/(Z+1)$, where Z is the number of constituent encoders as shown in Figure 6.2.

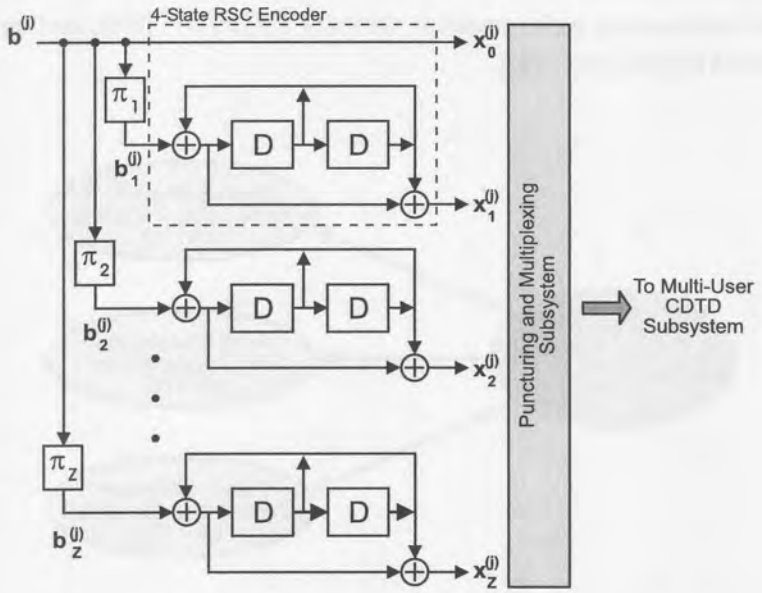

Figure 6.2. Generalized block diagram of PCTDD encoder.

The PCTTD scheme is based on three underlying principles. These are the

- rate $R_c = 1/(Z+1)$ turbo encoding,
- puncturing and multiplexing, and

- the iterative decoding.

These principles are described in detail below.

6.1.1 Rate-$1/(Z+1)$ Turbo Encoding

The constituent turbo encoder of Figure 6.2 produces one uncoded output systematic stream $\mathbf{x}_0^{(j)}$ and Z encoded output parity streams, denoted by $\mathbf{x}_1^{(j)}, \ldots, \mathbf{x}_Z^{(j)}$. Here

$$\mathbf{x}_Z^{(j)} = \{x_{0,z}^{(j)}, x_{1,z}^{(j)}, x_{2,z}^{(j)}, \ldots, x_{i,z}^{(j)}, \ldots, x_{(N_{tc}-1),z}^{(j)}\}, \ (z = 0, 1, \ldots, Z), \tag{6.1}$$

where i is the discretized time index, and j denotes the reference user. The parity streams are produced by Z identical RSC encoders with constraint length L_{tc}. In the discussion that follows the constrained length $L_{tc} = 3$.

The first component encoder operates directly (or through interleaver π_1) on the information sequence, $\mathbf{b}_1^{(j)}$ of length N_{tc}, producing two output sequences $\mathbf{x}_0^{(j)}$ and $\mathbf{x}_1^{(j)}$. The second component encoder operates on a re-ordered sequence of information bits, $\mathbf{b}_2^{(j)}$, produced by interleaver π_2, also of length N_{tc}, and outputs the sequence $\mathbf{x}_2^{(j)}$. The systematic information bit stream of this RSC encoder is discarded. Subsequent component encoders operate on a re-ordered sequence of information bits, $\mathbf{b}_Z^{(j)}$, produced by interleaver π_Z, and output the sequence $\mathbf{x}_Z^{(j)}$.

6.1.2 Puncturing and Multiplexing

The puncturing and multiplexing procedures form the heart of PCTTD. As an example, to show how a rate $R_c = 1/2$ code is being transformed into a rate $R_c = 1/(Z+1)$ code by appropriate puncturing and multiplexing, consider a turbo encoder with Z constituent RSC encoders and a single transmit antenna $M_T = 1$. Assuming further for our example QPSK modulation, the information and coded sequences of user j can be arranged in terms of the in-phase and quadrature phase components. The in-phase component of the QPSK modulator (I branch) transmits the systematic bits, while the quadrature component (Q branch) transmits the parity bits formed by the constituent encoders. Beginning at discrete time $i = 0$, the in-phase component is modulated by

$$I: \left\{x_{0,0}^{(j)}, x_{1,0}^{(j)}, \ldots, x_{(Z-1),0}^{(j)}, x_{Z,0}^{(j)}, x_{(Z+1),0}^{(j)}, \ldots, x_{(N_{tc}-2),0}^{(j)}, x_{(N_{tc}-1),0}^{(j)}\right\}, \tag{6.2}$$

while the quadrature component is modulated by

$$Q: \quad \left\{x_{0,1}^{(j)}, x_{1,2}^{(j)}, \ldots, x_{(Z-1),Z}^{(j)}, x_{Z,(Z+1)}^{(j)}, x_{(Z+1),(Z+2)}^{(j)}, \cdots, x_{(N_{tc}-2),(Z-1)}^{(j)}, x_{(N_{tc}-1),Z}^{(j)}\right\}. \tag{6.3}$$

This puncturing and multiplexing procedure is illustrated in Figure 6.3(a), using the notation $x_{i,Z}^{(j)}$. It should be pointed out that, due to the puncturing procedure, some of the coded sequences are not transmitted to maintain the $R_c = 1/2$ coding rate.

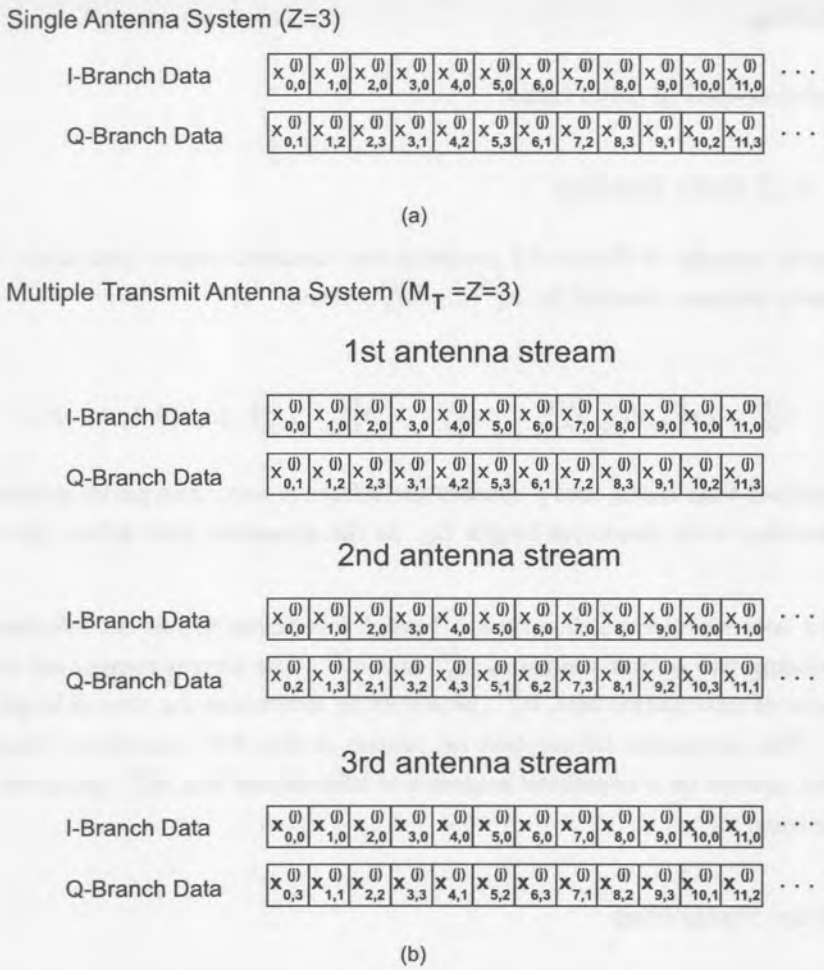

Figure 6.3. Puncturing and multiplexing procedure for a rate $R_c = 1/2$ turbo encoder with Z constituent RSC encoders. (a) Single transmit antenna, $M_T = 1$ (b) $M_T = 3$ transmit antennas.

The single transmit antenna $M_T = 1$ example can easily be extended to $M_T = Z$ transmit antennas. In PCTTD with $(M_T > 1)$, the systematic information sequences are repeatedly transmitted on the I branches of all the available transmit antennas. This is done to guarantee soft failure in order to achieve maximum space-time diversity gain. In addition, smart puncturing and multiplexing is employed to assign the parity information sequences to the different Q branches available for transmission. This puncturing and multiplexing procedure is shown in Figure 6.3(b) for $M_T = Z = 3$. Note that the information and coded sequences transmitted by the I and Q branches of the first antenna element for $M_T > 1$, agrees with the single antenna transmission of Figure 6.3(a).

The I and Q sequences transmitted by the second antenna can be written as

$$\begin{aligned} I: &\quad \left\{x_{0,0}^{(j)}, x_{1,0}^{(j)}, \cdots, x_{Z,0}^{(j)}, x_{(Z+1),0}^{(j)}, \cdots\right\} \\ Q: &\quad \left\{x_{0,2}^{(j)}, x_{1,3}^{(j)}, \cdots, x_{(Z-2),Z}^{(j)}, x_{(Z-1),1}^{(j)}, x_{Z,2}^{(j)}, \cdots\right\}. \end{aligned} \tag{6.4}$$

In general, the sequences transmitted by the zth antenna element can be written as

$$
\begin{aligned}
I: &\quad \left\{x_{0,0}^{(j)}, x_{1,0}^{(j)}, x_{2,0}^{(j)}, x_{3,0}^{(j)}, x_{4,0}^{(j)}, x_{5,0}^{(j)}, \cdots\right\} \\
Q: &\quad \left\{x_{0,z}^{(j)}, x_{1,(z+1)}^{(j)}, \cdots, x_{(Z-z-1),Z}^{(j)}, x_{(Z-z),1}^{(j)}, \cdots\right\}.
\end{aligned} \tag{6.5}
$$

It should be noted that none of the encoded information bits are lost by the puncturing and multiplexing operations, while the effective transmission per constituent QPSK transmission rate remains one half.

6.1.3 *Iterative Decoding*

Figure 6.4 depicts the iterative decoding configuration. Before the decoding is performed, the demodulated signal streams are de-multiplexed. For the punctured symbols values are obtained from the $Z-1$ received antenna streams. For a PCTTD system with $M_T < Z$, zero values are inserted in the punctured bit positions. The decoder therefore regards the punctured bits as erasures.

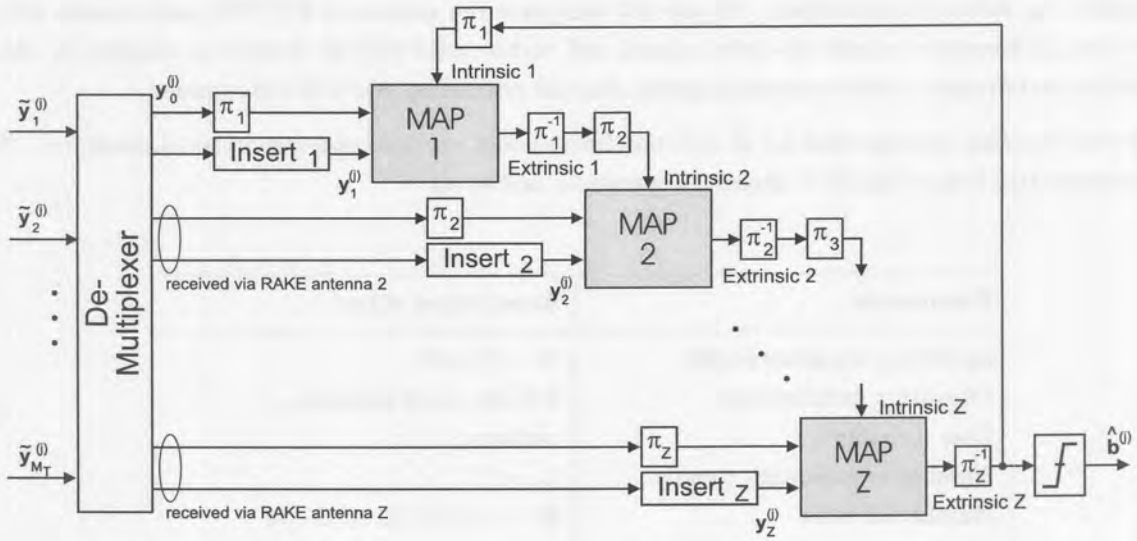

Figure 6.4. Generalized block diagram of PCTTD decoder operating in the serial mode.

From our previous single antenna PCTTD example, the following sequences are inputs to the zth decoder

$$
\begin{aligned}
I: &\quad \left\{y_{0,0}^{(j)}, y_{1,0}^{(j)}, \cdots, y_{Z,0}^{(j)}, y_{(Z+1),0}^{(j)}, \cdots\right\} \\
Q: &\quad \left\{y_{0,z}^{(j)}, 0, 0, \ldots, 0, y_{Z,z}^{(j)}, \cdots\right\}.
\end{aligned} \tag{6.6}
$$

The iterative decoding procedure requires Z component decoders using soft inputs and providing soft outputs, based on the MAP algorithm. The decoding configuration operates in *serial mode*, i.e. decoder 1 processes data before decoder 2 starts its operation, and so on [224]. Many different configurations exist, especially for the case where $Z \geq 3$.

With reference to Figure 6.4, extrinsic information (related to a data symbol) is obtained from surrounding symbols in the codeword sequence imposed by the code constraints only. The extrinsic information is obtained without any information concerning the symbol itself, and is provided as soft outputs by the

component decoders. The soft outputs, obtained from the MAP, are internal variables of the decoder, and is a measure of the reliability of the decoding of single bits and do not provide hard bit decisions.

In addition, intrinsic information related to a data symbol is *a priori* information attached to the symbol without using any code constraints. This information is used by the component decoders as additional information related to each code symbol. In iterative decoding, the extrinsic information provided by the previous decoding step becomes the *a priori* information of the current decoding process.

6.1.4 *Performance Considerations*

In this section the performance of the proposed PCTTD scheme is considered. Since PCTTD exhibits the closest resemblance to turbo coded CDTD, the performance of PCTTD should be compared with that of the turbo coded CDTD signalling. Monte-Carlo simulations are conducted to verify the goodness of the BEP bounds presented in Chapter 5.

Using the system parameters outlined in Table 6.1, the BER performance of a PCTTD CDMA has been determined by means of simulation. Figure 6.5 compares the simulated PCTTD performance with the theoretical performance bounds of convolutional and turbo coded CDTD derived in Chapter 5. For the simulation performance perfect synchronization, channel estimation and CSI are assumed.

The turbo decoding configuration for $Z = 3$ constituent codes operates operates in serial mode, i.e., "MAP 1" processes data before "MAP 2" starts its operation, and so on.

Parameter	**Simulation value**
Spreading sequence length	$N = 32 \times R_c$
Operating environment	2-Path, equal strength.
User distribution	uniform
Number of multipath signals	$L_p = 2$
Number of users	$K = 1, 5, 10, 15, 20, 25, 30$
Number of RAKE fingers	$L_R = 2$
PCTTD Parameters	
Transmit antenna elements	$M_T = 1, 3$ $\rho = 0$
Code rate	$R_c = 1/2$
Constituent encoders	$Z = 3$
Interleaver	S-type, $N_{tc} = 256$
Decoder	Iterated MAP, serial configuration.

Table 6.1. System parameters for BER simulation of PCTTD.

Concentrating on the BER curves of the PCTTD system, slight disparities between the simulation results and performance bounds can be identified for target BER of 10^{-6} or worse. As can be seen from the curves, the simulation curves are very close the the simulation bounds, for normalized user loads less than 0.75. For the conditions of low load ($P_b < 10^{-6}$), the performance of the simulated system is dominated by the performance of the sub-optimal (non ML) decoder and practical interleaver utilized.

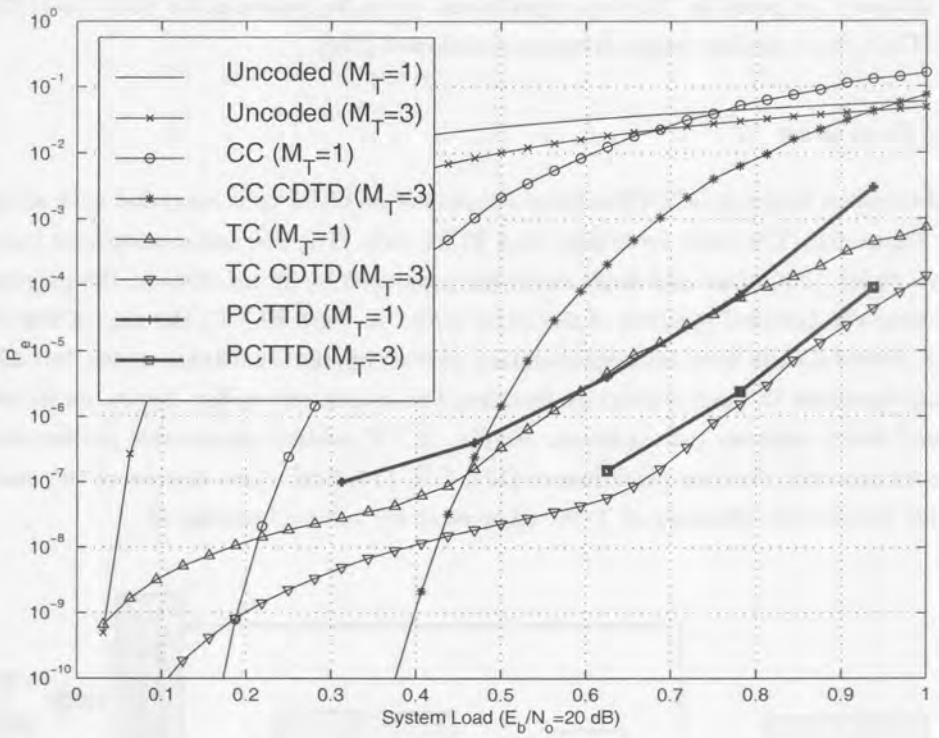

Figure 6.5. Performance comparison of the simulated BER performance of PCTTD and theoretical BEP of CDTD, as a function of the normalized system load, with operating point of $E_b/N_o = 20$ dB.

For the higher load conditions, the simulation results are also worse of than the bounding performance. From the discussion presented in Section 4.2.3, this is attributed to the fact that at low value of SNR, the PCCC bounds resulting from the use of the binomial cpdf should actually be considered as a lower bound to the code's performance. This is a matter of concern when target BER of 10^{-3} and worse. However, most practical systems operate in the BER target range of 10^{-8} (data) to 10^{-3} (voice).

6.2 SERIAL CONCATENATED TURBO TRANSMIT DIVERSITY (SCTTD)

This section deals with the natural extension of the parallel concatenation approach to the SCCTD scenario. SCCCs have drawn interest recently as the serial analogues of turbo codes, which are PCCC. The performance of the SCCC is dominated by terms with an input Hamming weight from the inner code equal to the free distance of the outer code. Many authors have concluded that these terms are made up of the concatenation of inner decoder error events with information weight 2, and it is the Hamming distance of these error events, the "effective free distance", which should be minimized.

Later in this section performance bounds for SCTTD are derived and used to conduct a search for rate-1/2 coded QPSK employing a dual-transmit antenna ($M_T = 2$) signalling scenario. In general, the SCTTD can be extended to accommodate any number of transmit antennas.

In [172] design criteria for SCCC has been developed based on the performance bounds for SCCC. These criteria were used as the basis for code searches to find the best constituent codes for SCCC. The authors of [172] conclude that the outer code in a SCCC should be a traditional convolutional code with as large a free distance as possible, and that the inner code should be a recursive convolutional code with as large an

"effective free distance" as possible. The best constituent codes for proposed for SCCC in [172], will also be optimal for SCTDD, since similar design criteria are followed [219].

6.2.1 *Encoder Description*

The basic dual-transmit antenna SCCTD scheme consists of an outer code cascaded with an inner code, as depicted in in Figure 6.6. The inner code may be a TCM code. The discussion presented here is restricted to convolutional codes. The inner and outer codes are separated by an interleaver, the purpose of which is to permute in time the encoded symbols of the outer code. As with PCCC, the aim of the SCCC scheme is to generate a powerful code from the concatenation of two simpler constituent codes, but which admits a simple decoding algorithm through separately decoding the constituent codes. Again, an iterative decoding algorithm is used which achieves near-optimum results. SCCC achieve comparable performance to PCCC, and in some cases can offer superior performance [172, 173, 174, 175]. Also, the use of the inner TCM code allows the higher bandwidth efficiency of TCM schemes to be taken advantage of.

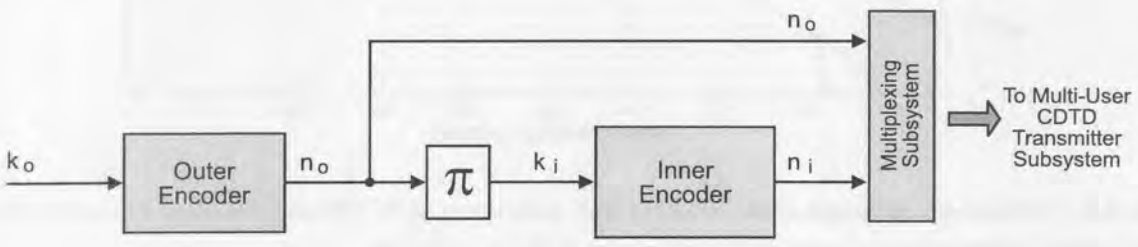

Figure 6.6. Generalized block diagram of SCTDD encoder.

The encoder for a SCCC is depicted in Figure 6.6. Both encoders are convolutional codes; the outer encoder has rate $\frac{k_o}{n_o}$ and the inner encoder has rate $\frac{k_i}{n_i}$. The information bits are encoded by the outer encoder and the resulting code bits are interleaved by the bit-wise random interleaver (π) and become the information bits of the inner encoder. This interleaver applies an N_{tc} bit random permutation to the sequence of code bits coming from the outer encoder. There is a corresponding de-interleaver in the decoder, and both the interleaver and de-interleaver must be synchronized. This means that, as in the case of PCCC and PCTTD, some form of framing information header must be transmitted. The most straight-forward implementation of a SCCC is with frames of information bits which, after encoding by the outer encoder, are equal in size to the interleaver. As for PCCCs the SCCC can be analyzed as a block code, with a code word with $N_{tc}\,\frac{k_o}{n_o}$ information bits and $N_{tc}\,\frac{n_i}{k_i}$ code bits [175]. The overall SCCC code rate is $\frac{k_i}{n_i}\,\frac{k_o}{n_o}$. It is usual, although not essential, to have $n_o = k_i$, resulting in an overall code rate of $\frac{k_o}{n_i}$.

As in single antenna SCCC, the interleaver is an essential feature of the SCCTD scheme, and the performance improves with increasing N_{tc}. However, as the interleaver is random, the transmission of the codeword cannot commence until the interleaver has been filled, and decoding cannot be completed until the entire codeword is received. The PCCC encoding latency was N_{tc} information bits, but the SCCC encoding latency is $N_{tc}\,\frac{k_o}{n_o}$ information bits, due to the action of the outer code. This results in an overall latency of $2\,N_{tc}\,\frac{k_o}{n_o}$ information bits (plus propagation delay and decoding delay). This difference in latency between PCCC and SCCC means that two schemes should be compared not with identical interleaver sizes, but with identical latency.

In [172, 175] it is concluded that the inner constituent code of a SCCC scheme should be a RSC code and that of the outer constituent code should be a traditional convolutional with maximum free distance. It

is also concluded that the effective free distance of the inner code should be maximized, and as such the constituent codes found for PCCC can be used as the inner codes of a SCCC scheme.

6.2.2 *Decoder Description*

The near-optimal iterative decoding structure for the PCTTD scheme can be readily adapted for the decoding of SCTTD scheme. In the decoder structure for the SCTTD the soft outputs of the inner code bits from the demodulator are decoded to produce soft decisions of the inner information bits. These are, after de-interleaving, also the soft decisions of the outer code bits. These are in turn decoded to produce improved soft decisions of the outer code bits, which, when interleaved, are improved soft decisions of the inner information bits. This process is iterated a number of times, before finally the outer decoder produces a hard decision of the outer information bits.

Both the inner and outer encoders are "connected" to the channel, the M_T outputs of the demodulator along with an estimate of the noise variance are used to calculate the probabilities of the code symbols for both the inner and outer codes. The decoder output corresponding the to first antenna is input to the inner MAP module, along with the interleaved code symbol probabilities of the outer code from the previous iteration (because outer code symbols are inner information symbols). Only the updated inner code information symbol probabilities are used, which is de-interleaved to become the outer code code symbol probabilities. The outer code code symbol probabilities are interleaved and input to the inner code MAP module during the next iteration, and, if it is the final iteration, the updated outer code information symbol probabilities is used to make the final decision.

6.2.3 *Performance of SCCC*

Consider the concatenation of two linear convolutional constituent codes C_o and C_i, joined by a bit-wise random interleaver defined by the permutation π. The outer code C_o has rate $R_o = k/p$ and the inner code C_i has rate $R_i = p/n$, resulting in an overall SCCC with rate $R_c = k/n$. The interleaver is of length N, which is an integer multiple of p (actually, the inner and outer codes can have rates $R_i = k_i/n_i$ and $R_o = k_o/n_o$, respectively, constraining the interleaver length to $N_{tc} = \text{lcm}(n_o, k_i)$. However, this complicates the bound expressions and is not considered here). The block size of the SCCC is NR_o bits.

There are N_{tc} interleavers of length N_{tc}, many of which will yield different performance when used in the SCCC. Rather than exhaustively enumerating the performance for all possible interleavers, an uniform interleaver is assumed. Any interleaver will permute an input word with Hamming weight h into an output word which also has Hamming weight h, and there are $\binom{N_{tc}}{h}$ of such permutations.

If the trellis is terminated at both the beginning and the end of a frame then the weight enumerating function (WEF) of the constituent codes can be determined from the equivalent block code. In the case of continuous transmission and decoding the analysis is much more complex. It involves the use of a hyper-trellis having as hyper-states pairs of states of the outer and inner codes. Each hyper-branch represents all the paths taken through both the inner and outer trellises for one interleaver block. Each hyper-branch represents all the paths taken through both the inner and outer trellises for one interleaver block. The WEF for each hyper-branch can be determined by treating the constituent codes as equivalent block codes, starting and finishing at these known states. The upper bound to the BEP can then be found by applying the standard transfer function bound approach [16] to the hyper-trellis.

However, for codes with a reasonable number of states and for large interleavers this technique becomes prohibitively complex. In [174] an approximation is introduced which is accurate when the interleaver

length is larger than the constituent code's memory. This approximation involves replacing the complete transfer function of the hyper-trellis by the WEF which labels the hyper-branch joining the zero states of the hyper-trellis. This of course is the WEF found from the equivalent block codes of the constituent codes when they both start start and finish in the all-zero state. This means that for the case of continuous transmission and decoding an accurate approximation to the bit error probability bound is that of the case of a terminated trellis.

Define the WEF of any code C as

$$A^C(I,D) = \sum_{i,d} A^C_{i,d}\, I^i\, D^d, \tag{6.7}$$

a polynomial in the dummy variables I and D, where $A^C_{i,d}$ is the number of codewords of C with input Hamming weight i, and output Hamming weight d. WEFs can also be expressed for all codewords with input Hamming weight i, and for all codewords with Hamming weight d.

The WEFs of the outer and inner constituent convolutional codes, $A^{C_o}(I,D)$ and $A^{C_i}(I,D)$, can be found from knowledge of their respective trellises [225]. Any specific codeword of C_o with output Hamming weight h will, through the action of the uniform interleaver, generate a codeword of C_i of input Hamming weight h with probability $1/\binom{N_{tc}}{h}$. There are a total of $A^{C_o}_{i,h}$ of these codewords with input Hamming weight i in C_o, and a total of $A^{C_i}_{h,d}$ of these codewords with input Hamming weight d in C_i. Thus the total number of codewords of the SCCC with input Hamming weight i and output Hamming weight d is

$$A^C_{i,d} = \sum_{h=0}^{N_{tc}} \frac{A^{C_o}_{i,h} \times A^{C_i}_{h,d}}{\binom{N_{tc}}{h}}. \tag{6.8}$$

The upper bound to the BEP of the SCCC is [174]

$$P_b \leq \sum_{i=1}^{NR_o} \sum_{d=1}^{N_{tc}/R_i} A^C_{i,d}\, \frac{i}{2\, N_{tc}\, R_o}\, Q\left(\sqrt{d\, R_o\, R_i\, \frac{E_b}{N_o}}\right). \tag{6.9}$$

For large interleavers this expression will contain a very large number of terms, however it can be evaluated more quickly by only including those terms which make a significant contribution to the bound, i.e., the d summation may be truncated.

6.2.3.1 The WEF of the Equivalent Block Code. The coefficients $A^{C_o}_{i,h}$ and $A^{C_i}_{h,d}$ of the equivalent blocks codes to the constituent convolutional codes can be found by concatenating the error events of the convolutional codes. The error events of the convolutional codes can be found by modifying the techniques of [225] to allow remergings with the all-zero state. Let $T(L,I,D,J)$ be the transfer function of the convolutional code which enumerates all paths in the trellis remerging with the zero state at or before step M, with possible remergings with the zero state for just one step before this.

$$T(L,I,D,J) = \sum l,i,d,j\; T_{l,i,d,j} L^l\, I^i\, D^d\, J^j\,, \tag{6.10}$$

where $T_{l,i,d,j}$ is the number of paths in the trellis of length l, input Hamming weight of i, an output Hamming weight of d, and j remergings with the zero state (i.e., the concatenation of j error events). The codewords of the equivalent block code can be determined by observing that each error path of length l and number of remergings j gives rise to $\binom{M-l-j}{j}$ codewords [174].

The weight enumerating coefficients of the equivalent block code are given by [174]

$$A^C_{l,D} = \sum_j \binom{M-l-j}{j} T_{l,i,d,j} \ . \tag{6.11}$$

By defining

$$T_{i,d,j} = \sum_l T_{l,i,d,j} \ , \tag{6.12}$$

and noting that $\binom{M-l-j}{j} \approx \binom{M}{j}$, the coefficient $A^{C_o}_{i,h}$ of the outer code can be approximated by

$$A^{C_o}_{i,h} \approx \sum_j \binom{N_{tc}/p}{j} T^{C_o}_{i,h,j} \ , \tag{6.13}$$

and the coefficient $A^{C_i}_{h,d}$ of the inner code can be approximated by

$$A^{C_i}_{h,d} \approx \sum_j \binom{N_{tc}/p}{j} T^{C_i}_{h,d,j} \ , \tag{6.14}$$

recall that $p = n_o = k_i$.
Using (6.8) the weight enumerating coefficient of the SCCC is then

$$A^C_{i,d} \approx \sum_{h=d^o_H}^{N_{tc}} \sum_{j^o} \sum_{j^i} \frac{\binom{N_{tc}/p}{j^o}\binom{N_{tc}/p}{j^o}}{\binom{N_{tc}}{h}} T^{C_o}_{i,h,j^o} T^{C_i}_{i,h,j^i} \ , \tag{6.15}$$

where d^o_H is the free Hamming distance of the outer code.

This expression can be simplified further by using the asymptotic approximation to the binomial coefficient for large M,

$$\binom{M}{m} \approx \frac{M^m}{m!} \ . \tag{6.16}$$

Substituting (6.16) and (6.15) into (6.9) yields

$$Pb \leq \sum_d D_d \, Q\left(\sqrt{d \, R_o \, R_i \, \frac{E_b}{N_o}}\right) \ , \tag{6.17}$$

where

$$D_d = \sum_{i=1}^{N_{tc}\,R_o} \sum_{h=d_H^o}^{N_{tc}} \sum_{j^o} \sum_{j^i} \frac{i}{2\,N_{tc}\,R_o} N_{tc}^{j^o+j^i-h-1} \frac{h}{p^{j^o+j^i}\,j^o!j^i!} T^{C_o}_{i,h,j^o}\,T^{C_i}_{i,h,j^i}\,. \tag{6.18}$$

For large N_{tc} the dominant coefficient of d will be the one for which the exponent of N_{tc} is maximum. Define this maximum exponent for each d as

$$\alpha(d) = \max_{i,h}\{j^o + j^i - h - 1\}\,. \tag{6.19}$$

In [172] design criteria for SCCC are developed by examining both the overall maximum of the exponent given in (6.19), and the value of the exponent corresponding to minimum output Hamming weight h. The maximum exponent allows the dominant contribution to P_b to be found as $N_{tc} \to \infty$. The exponent for the minimum weight allows the BEP to be evaluated as $E_b/N_o \to \infty$.

6.2.3.2 SCCC design criteria. In this paragraph the design criteria for SCCC is revisited.

Outer code. From the discussions presented in [172, 175], the outer code should have as large a free distance as possible. This will be achieved with a non-recursive convolutional code. In general, the SCCC BEP bound is dominated by error events for which $h = d_H^o$, i.e., error event from the inner decoder which generate errors in the outer code with Hamming weight equal to the free distance of the outer code. In addition, as $E_b/N_o \to \infty$ the performance of the SCCC will be dominated by the minimum value of d in the bound, which is the free distance of the SCCC.

Inner code. The authors of [175] conclude that the inner code in a SCCC should be chosen to be recursive, and to have as large a Hamming weight as possible for a weight 2 input codeword.With a recursive convolutional inner code there are error events with $h = d_H^o$ which are more likely than this. Thus the inner convolutional code in an SCCC should be designed to minimise the contribution of error events with $h = d_H^o$. This is the same criteria used for PCCC, and the codes found in [176] can be used.

Interleaver. A random bit-wise interleaver should be used. As with PCCC, S-type random interleavers give best performance with SCCC. The interleaver should be as large as possible. As with PCCC this latency means that in delay sensitive applications, such as voice transmissions, a trade-off must be made between delay and performance.

6.2.4 SCTTD Performance Approximation

The performance of a rate 1/3 SCTTD CDMA system with $M_T = 2$ antennas is considered. The system parameters outlined in Table 6.2 are assumed. The general system parameters, e.g., spreading length, are similar to the parameters given in Table 6.1.

The outer code is a 4-state rate 1/2 non-systematic convolutional code taken from [14] (Table 11.1(c)), with generator polynomials $g_1 = 5_8$ and $g_2 = 7_8$. The minimum Hamming distance of this code is 5. The inner code is a 4-state rate 2/3 RSC code taken from [176] (Table 1), with generator polynomials $h_0 = 7_8$, $h_1 = 3_8$ and $h_2 = 5_8$. The minimum Hamming weight for a weight 2 input word for this code is 4.

Parameter	Simulation value
PCTTD Parameters	
Transmit antenna elements	$M_T = 1, 2$ $\rho = 0$
Code type and rate	
Outer Code	4-state, $R_c = 1/2$
Inner Code	4-state, $R_c = 2/3$
Effective Code Rate	$R_c = 1/3$
Interleaver	Uniform , $N_{tc} = 256$

Table 6.2. System parameters for numerical evaluation of BEP performance.

Using (3.29), (4.6), (6.17), (6.18), and the system parameters outlined in Table 6.2, the approximate BEP performance of the SCTTD cellular CDMA system can been determined numerically. The results are shown in Figure 6.7.

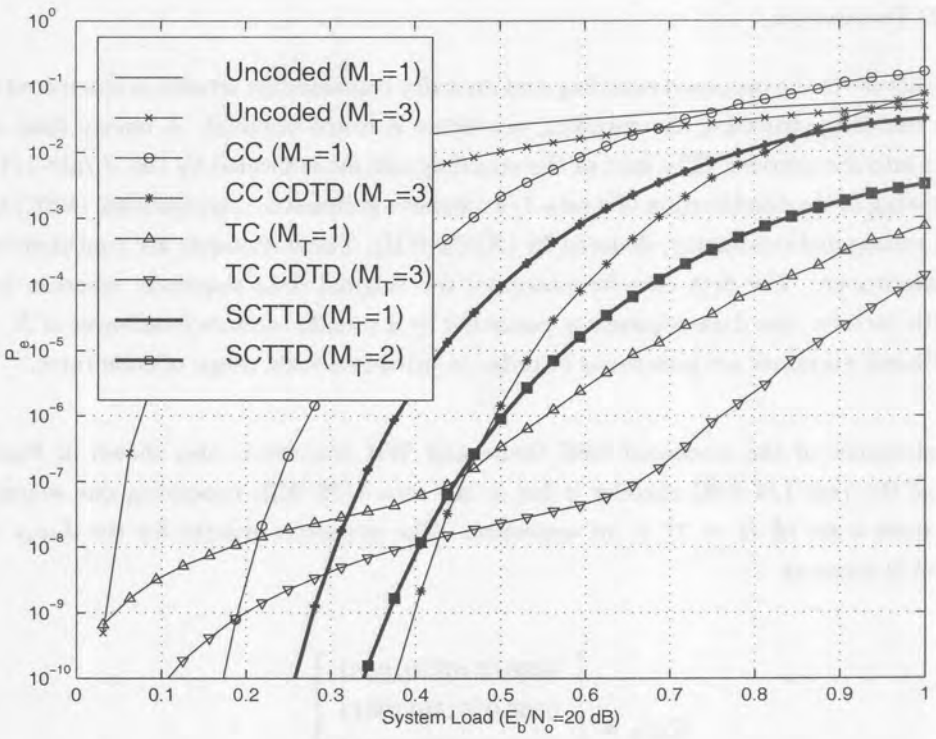

Figure 6.7. BEP performance of SCTTD as a function of the normalized system load, with operating point of $E_b/N_o = 20$ dB.

Shown on the figure are the performance of single and $M_T = 2$ transmit diversity systems' performance. The performance degradation of SCTDD system as opposed to the turbo coded CDTD (essentially PCTTD) system at average to high system loads is evident. The promising effect is the excellent performance exhibited at low system loads, implying that given a large interleaver, excellent performance may be achieved over

the complete user range. As interleaver size (gain), however, increases so does decoding delay, and thus a balance must be found between acceptable performance and tolerable latency.

6.3 SUPER-ORTHOGONAL TURBO TRANSMIT DIVERSITY (SOTTD)

This section presents the SOTTD signaling scenario for spread-spectrum CDMA communication systems. SOTTD extends layered turbo coded transmit diversity to include Z component decoders, and is roughly based in the work by Pehkonen *et al.* [42, 43]. The techniques of spreading and coding at low-rate are married with the code-division transmit diversity and iterative "turbo" processing [222]. The principle of operation is to transmit the coded bits, stemming from the constituent encoders, via the spatial domain rather than via the time and code domain. The received data stream is then iteratively decoded using turbo decoding principles.

A synchronous CDMA mobile communications system is considered where the transmitter is equipped with M_T antennas at the base station and a single receiving antenna at the mobile. The signals on the matrix channel, i.e. the $M_T \times 1$ transmission paths between transmitter and receiver, are supposed to undergo independent frequency selective Rayleigh fading. It is assumed that the path gains are constant during one frame and change independently from one frame to another (quasi-static fading).

6.3.1 SOTTD Transmitter

The general structure of the proposed encoding and diversity transmission scheme is illustrated in Figure 6.8. Owing to this encoding structure, the encoding procedure is frame oriented. A binary data sequence $\mathbf{b}$ of length N is fed into the encoder. The hart of the encoding scheme is formed by the Z rate-1/16 constituent encoders, consisting of the combination of a rate-1/4 recursive systematic convolutional (RSC) encoder and a rate-4/16 WH orthogonal modulator, denoted by (RSC&WH). These encoders are concatenated in parallel applying an interleaver. The first encoder processes the original data sequence, whereas before passing through the Zth encoder, the data sequence is permuted by a pseudo random interleaver of N. The outputs of the Z constituent encoders are punctured in order to provide a wide range of code rates.

The detailed structure of the combined RSC turbo and WH encoder is also shown in Figure 6.8. The state outputs of the rate-1/4 RSC encoder is fed to the rate-4/16 WH, producing one sequence of length ($L_{WH} = 16$) from a set of $H = 2^4 = 16$ sequences. The generator matrix for the $L_{WH} = 16$ WH in systematic form is given as

$$G_{WH} = \begin{bmatrix} 1000\,011011010101 \\ 0100\,010110110011 \\ 0010\,001110001111 \\ 0001\,000001111111 \end{bmatrix}$$

Recall from coding theory, that the most important characteristic of a codeword is its minimum free distance. Owing to the orthogonality characteristics of the WH codewords, the minimum distance of the encoded sequences for both constituent encoders is equal to $d^{WH} = L_{WH}/2 = 8$. In addition, full-rank transmit diversity may be achieved provided that the transmit antennas are sufficiently spaced.

After encoding, the output sequences are obtained by appropriate puncturing according to puncturing patterns $P^{(i)} = \{p_1^i, p_2^i, \ldots, p_N^i\}$, where $i = 1$ and 2, for the first and second puncturer, respectively. With

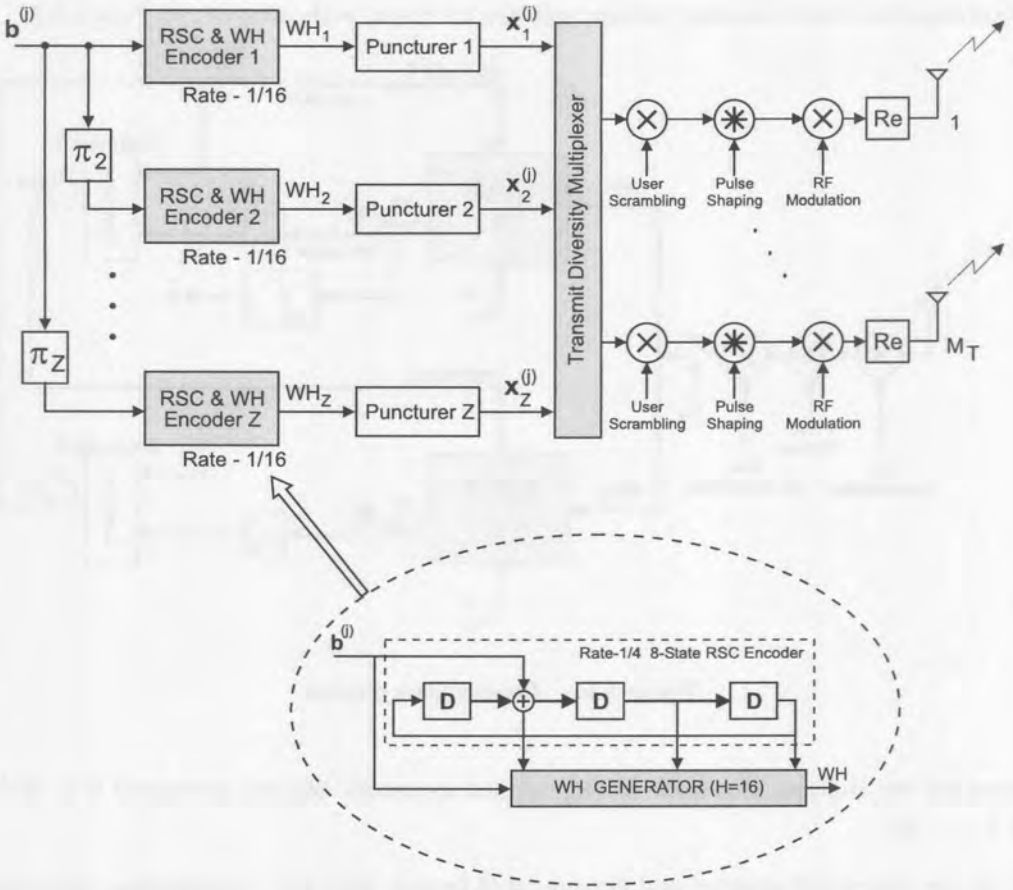

Figure 6.8. Transmitter block diagram.

$W_{P(1)}$ and $W_{P(2)}$, the weights of the first and second puncturers, respectively, the resulting overall encoder rate (R_c) is given by:

$$R_c = \frac{1}{W_{P(1)} + W_{P(2)}} \tag{6.20}$$

Therefore, for the case when none of the output sequences' bits are punctured the overall code rate of the combined turbo and WH encoding strategy is given as $R_c = 1/(16+16) = 1/32$.

After encoding, the Z encoded streams are multiplexed to the M_T available transmit antenna section, encapsulating the user specific scrambling, spreading and chip shaping.

6.3.2 SOTTD Receiver and Iterative Decoder

For description a dual transmit, $M_T = 2$ and single receive antenna, $M_R = 1$ system is assumed. Without loss of generality, the number of constituent encoders Z is taken as 2, i.e. $M_T = Z = 2$. Figure 6.9 shows general receiver for the SOTTD system, as well as the iterative turbo decoding strategy.

Before the actual decoding takes place, for those bits that were punctured, zero values are inserted. Therefore the decoder regards the punctured bits as erasures. The iterative decoding of the turbo coding scheme requires two component decoders using soft inputs and providing soft outputs. The soft output Viterbi algorithm (SOVA) or maximum *a posteriori* (MAP) algorithm may be employed.

Detail concerning the actual decoding process will now be given, with reference to Figure 6.9.

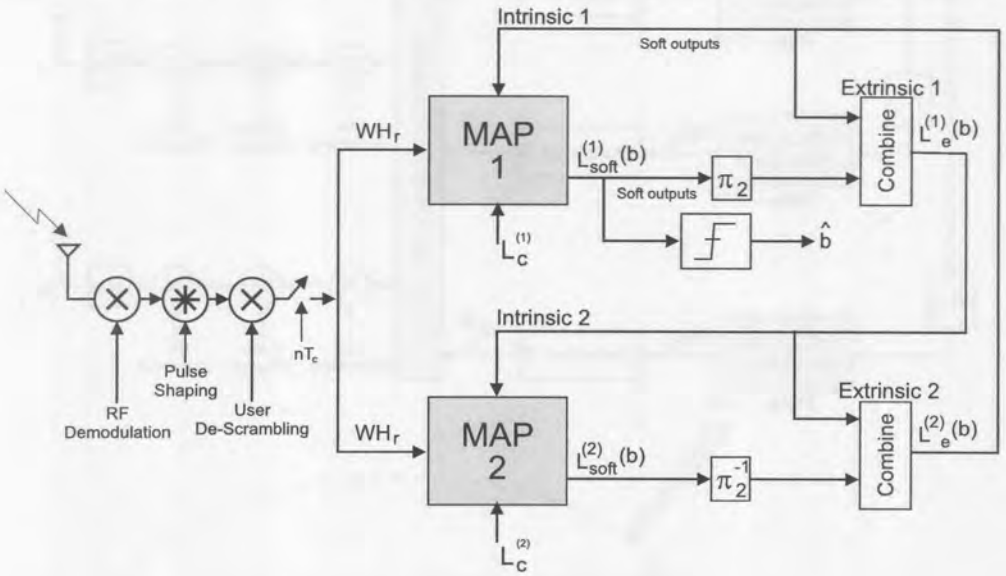

Figure 6.9. Receiver block diagram.

It is assumed for the analysis, that none of the encoded sequences' bits are punctured (i.e., $WH_z = \bar{WH}_z$, where $i = 1, \ldots, Z$).

Let WH_r be the associated received and demodulated branch with the corresponding reliability values of the channel, $L_c^{(z)}$, $z = 1, 2$, depending on whether decoder 1 or 2 is being used. The decoder accepts a priori values $L_i(b)$ for all the information bit sequences and soft-channel outputs $L_c^{(z)} \cdot WH_r$

The branch metric calculation is performed very efficiently by using soft-output inverse WH (SO-IWH) transformation, which basically correlates the received WH sequence with the branch WH sequences terminating in a specific node. Then, by discarding the branch with the lowest accumulated path metric, the maximum likelihood branch is retained.

The soft-input soft-output delivers *a posteriori* soft outputs $L(\hat{b})$ for all the information bits and extrinsic information $L_e(b)$, which for the current bit is only determined by its surrounding bits and the code constraints. It is therefore independent of the intrinsic information and the soft output values of the current bit. It is important to note that all the above mentioned sequences are vectors of length $L_{WH} = 16$.

Ideally, the log-likelihood ratio (LLR) soft-output of the decoder for the information bit b is written as

$$L(\hat{b}) = (L_c \cdot WH_r + L_i(b)) + L_e(\hat{b}) \tag{6.21}$$

implying that there are three independent estimates, which determine the LLR of the information bits: the a priori values, $L_i(b)$, the soft-channel outputs of the received sequences $L_c \cdot WH_r$, and the extrinsic LLR's $L_e(\hat{b})$.

At the commencement of the iterative decoding process there usually are no a priori values $L_i(b)$, hence the only available inputs to the first decoder are the soft-channel outputs obtained during the actual decoding process.

After the first decoding process the intrinsic information on b is used as independent[2] *a priori* information at the second decoder. The second decoder also delivers *a posteriori* information, which is used to derive the extrinsic information, which is – for its part – used in the subsequent decoding process at the first decoder in the next iteration step. The final decision is, of course, based on the *a posteriori* information, output from the second decoder. Note, that initially the LLRs are statistically independent, however, since the decoders use indirectly the same information, the improvement through the iterative process becomes marginal, as the LLR's become more and more correlated.

6.3.3 *Points to Ponder*

Various authors have stated that the design of a optimal interleaver helps to avoid low weights of encoded sequences in many cases, which leads to improved bit error rate performance. In our context, the weight of the encoded sequences (excluding the all-zeros codeword) also equals $d^{WH} = 8$. This is an important observation since it removes the requirement to design an optimal interleaver. For this reason a simple pseudo random interleaver is utilized.

The size of the interleaver, however, and not its design (for our application), determines the performance of the coded system. The larger the interleaver size (N), the larger the "interleaver gain" and greater the potential to increase the temporal spread of successive bits of the original data sequence.

It is important to note that the constituent RSC&WH encoders may produce similar WH codewords. Since these codewords are transmitter over different antennas the full-rank characteristic of the system is still guaranteed. Under multipath fading scenarios, some of the orthogonality will be destroyed. The latter is not a function of the specific WH codeword transmitted at the different antennas, but rather dependent on the delay spread of the channel. Transmitting the same WH codewords over the different antennas will have an effect on the channel estimation and initial system synchronization procedures.

The performance of the SOTTD system depends not on the distance properties of the WH code, but actually on the distance properties of the combined RSC&WH code. In this context, the most important single measure of the code's ability to combat interference is d_{min}.

Figure 6.10 depicts the modified state diagram of the RSC&WH constituent code under consideration. The state diagram provides an effective tool for determining the transfer function, $T(L, I, D)$, and consequently d_{min} of the code. The exponent of D on a branch describes the Hamming weight of the encoder corresponding to that branch. The exponent of I describes the Hamming weight of the corresponding input word. L denotes the length of the specific path.

Through visual inspection the minimum distance path, of length $L = 4$ can be identified as: $a_0 \rightarrow c \rightarrow b \rightarrow d \rightarrow a_1$. This path has a minimum distance of $d_{min} = 4 \times d^{WH} = 32$ from the all-zero path, and differs from the all-zero path in 2 bit inputs.

6.3.4 *Performance Evaluation*

In this section it is attempted to shed some light on the theoretical comprehension of parallel concatenated WH codes. In particular, an upper bound to the average performance of the parallel concatenated codes, stemming from characteristics of the combined RSC&WH (where $L_{WH} = 32$) constituent code, will be defined and evaluated.

Given an (n, k) RSC&WH constituent code, C_z, its input redundancy weight enumerating function (IRWEF) is given by [174]:

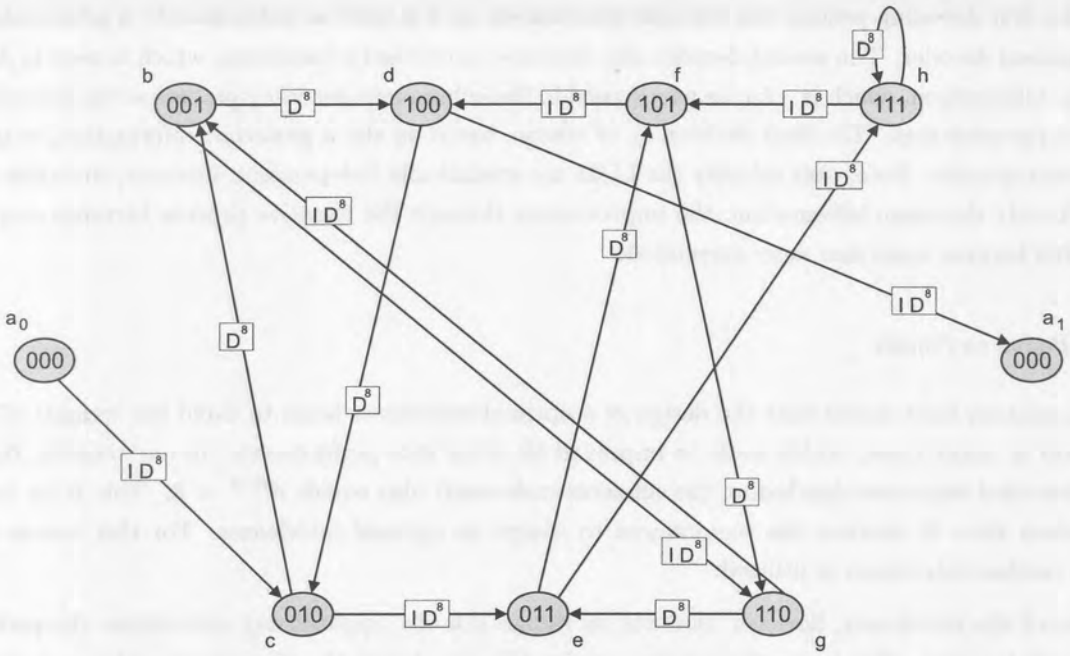

Figure 6.10. Trellis diagram of RSC&WH constituent encoder.

$$A^{C_z}(I,D) \doteq \sum_{i,d_p} A_{i,d_p} I^i D^{d_p}, \tag{6.22}$$

where A_{i,d_p} is the integer number of codewords generated by an input word with Hamming weight i whose parity check bits have Hamming weight d_p. Therefore, the overall Hamming weight is $d = i + d_p$. The IRWEF characterizes the whole encoder, as its depends on both the input information words and codewords.

The IRWEF makes implicit in each term of the normal weight enumerating function (WEF) the separate contributions of the information and the parity-check bits to the total Hamming weight of the codewords.

When the contributions of the information and redundancy bits to the total codeword weight is split, the IRWEF for the constituent WH code is obtained as

$$A^{C_z}(I,D) = 1 + 4ID^7 + 6I^2D^2 + 4I^3D^5 + I^4D^4 \tag{6.23}$$

When employing a turbo interleaver of length kN, the IRWEF of the new constituent (nN, kN) code C_z^N is given by

$$A^{C_z^N}(I,D) = \left[A^{C_z}(I,D)\right]^N, \tag{6.24}$$

for all Z the constituent codes.

Using (6.24) the conditional WEF, $A_i^{C_z^N}(D)$ of the constituent codes can be obtained from the IRWEF as

$$A_i^{C_z^N}(D) = \frac{1}{i!} \cdot \frac{\delta^i A^{C_z^N}(I,D)}{\delta I^i}\bigg|_{I=0}. \tag{6.25}$$

From the conditional WEF, owing to the property of the uniform interleaver of length kN, the conditional WEF of the two-constituent ($Z = 2$) parallel concatenated code of length $((2n - k)N, kN)$ is obtained as

$$A_i^{C_P^N}(D) = \frac{A_i^{C_z^N} \cdot A_i^{C_z^N}}{\binom{kN}{i}}. \tag{6.26}$$

The IRWEF of the parallel concatenated code using the the following inverse relationship can be obtained as

$$A^{C_P^N}(I, D) = \sum_i I^i A_i^{C_P^N}(D). \tag{6.27}$$

To compute an upper bound to the bit error probability (BEP), the IRWEF can be used with the union bound assuming maximum likelihood (ML) soft decoding. The BEP, including the fading statistics (assumed to be slow fading), assumes the form

$$\begin{aligned} P_{b|\mathbf{s}} &\leq \frac{I}{k} Q\left(\sqrt{d_{min}\sigma_{0c}\mathbf{s}}\right) \\ &\cdot \; e^{d_{min}\sigma_{0c}\,\mathbf{s}} \cdot \frac{\delta A(I, D)}{\delta I}\bigg|_{I=D=e^{-\sigma_{0c}\mathbf{s}}}, \end{aligned} \tag{6.28}$$

where σ_{0c} denotes the effective signal-to-noise ratio (SNR), and S denotes the power of the received signal.

Assuming that the cellular system is employing omni-directional antennas, the total output SNR term used in (6.27) can be determined as

$$\sigma_{0c} = \left(\frac{1}{R_c}\frac{N_o}{2\,E_b} + \frac{(K \cdot M_T - 1)}{3N}\right)^{-1}. \tag{6.29}$$

Also, if it is assumed that the M_T transmit diversity transmissions are equal powered, with constant correlation between the branches, and transmitted over a Rayleigh fading channel, the components of the received power vector S are identically distributed, with pdf given by

$$\begin{aligned} p_{\mathbf{S}}(\mathbf{s}) &= \frac{1}{\Omega^2\Gamma(M_T \cdot L_R)}\left(\frac{\mathbf{s}}{\Omega^2}\right)^{M_T \cdot L_R - 1} \\ &\times \frac{\exp\left(-\frac{\mathbf{s}}{(1-\rho)\Omega^2}\right) \cdot {}_1F_1\left(1, M_T \cdot L_R, \frac{\rho M_T \cdot L_R \mathbf{s}}{\zeta(1-\rho)\Omega^2}\right)}{\zeta\,(1-\rho)^{(M_T \cdot L_R - 1)}}, \end{aligned} \tag{6.30}$$

with $\zeta = 1 - \rho + \rho M_T \cdot L_R$.

From (6.29), ${}_1F_1(\cdot)$ is the confluent hyper geometric function, Ω^2 is the average received path strength (assumed equal), ρ the correlation between transmit or receive branches, and L_R is the number of RAKE receiver fingers.

Using a finite number of terms in (6.27) transforms the upper bound into the approximation

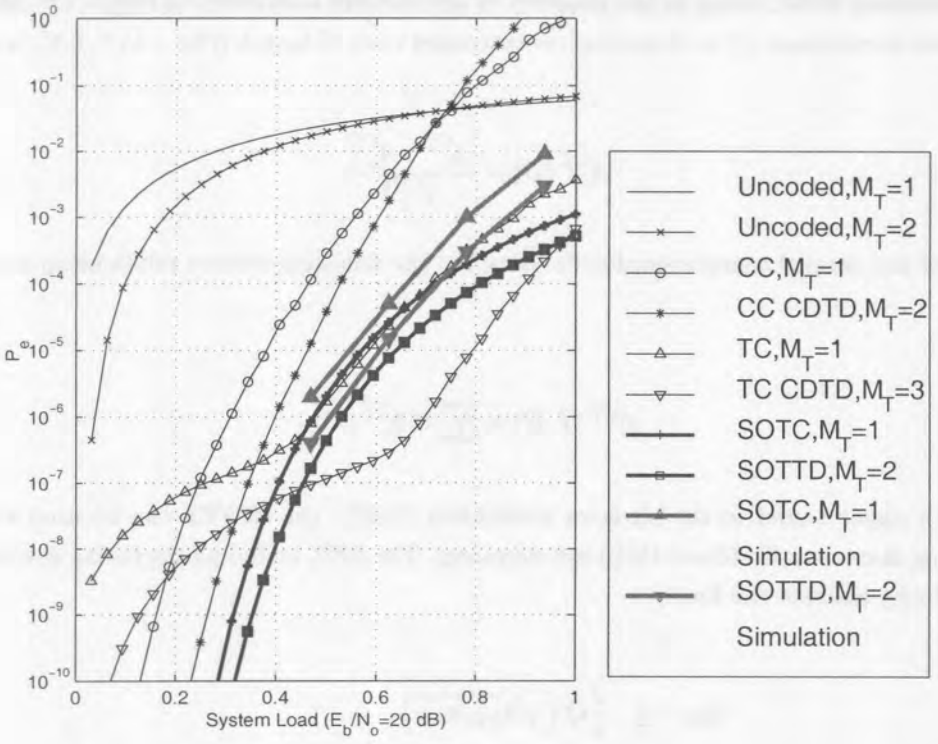

Figure 6.11. Bit error probability as a function of the load (number of users/total spreading), with operating point of $E_b/N_o = 20$ dB.

$$P_{b|\mathbf{S}} \approx \sum_m D_m Q\left(\sqrt{m\sigma_{0c}\,\mathbf{s}}\right), \tag{6.31}$$

where

$$D_m = \sum_{i+d_p=m} \frac{i}{k} A_{i,d_p}, \tag{6.32}$$

where A_{i,d_p} is obtained from the IRWEF of parallel concatenated code (compare (6.22)).

Finally, the BEP is computed using (6.31) and (6.32), when averaged over the fading statistics.

6.3.5 *Analytical and Simulation Results*

The performance of the ($M_T = Z = 2$) super-orthogonal transmit diversity (SOTTD) CDMA system is compared to that of an uncoded, and convolutional- and turbo coded code-division transmit diversity (CDTD) CDMA systems. Table 6.3 presents a summary of the techniques of importance in the performance evaluation.

Using the system parameters outlined in Table 6.4, the BEP performance of a cellular CDMA system employing the different techniques has been determined numerically. The results are shown in Figure 6.11.

Shown on the figure are the performance of single and $M_T = 2, 3$ transmit diversity systems' performance. From the curves it is clear that the superior performance predicted for TC CDTD may achieved with the

Acronym	Definition	Conditions
Uncoded	Uncoded system	$N_{spread} = N = 32$
CC	Convolutional	S=256, $R_c = 1/2$
	Coder	$N_{spread} = N/2$
TC	Turbo Coder	S=4, $R_c = 1/2$
		$N_{spread} = N/2$
SOTC	Super-Orthogonal	S=8, $R_c = 1/32$
	Turbo Coder	$N_{spread} = N/32$
CDTD	Code-Division	Uncoded, CC/TC
	Transmit Diversity	$M_T = 2, 3$
SOTTD	Super-Orthogonal	SOTC
	TTD	$M_T = 2$

Table 6.3. Summary of Techniques.

Parameter	Simulation value
Spreading sequence length	$N = 32 \times R_c$
Operating environment	2-Path, equal strength
User distribution	uniform
Number of MP signals	$L_p = 2$
Number of users	$K = 1, 2, \ldots, N$
Number of RAKE fingers	$L_R = 2$
FEC code type and rate	CC, TC ($R_c = 1/2$)
	SOTC ($R_c = 1/32$)
Turbo Interleaver Length	$N = 256$
TD elements	$M_T = 1, 2, 3$
TD technique	CDTD and SOTTD

Table 6.4. System parameters for numerical evaluation of BEP performance.

SOTTD system over the complete capacity range. Also of importance is the fact that the performance degradation of TC CDTD at low system loads (due to inherent TC error floor), is alleviated by the SOTC system, therefore the superior performance of SOTTD. This is explained in terms of the higher minimum free distance on offer by the rate-1/16 constituent encoders, as opposed to the use of rate-1/2 constituent encoders in turbo coded systems.

6.4 SUMMARY

This chapter has considered layered space-time turbo coded transmit diversity techniques for cellular CDMA. Novel extensions of CDTD have been presented in the form of PSTTD, SCTTD and SOTTD. Analytical performance results for these schemes were presented.

In addition to the three general turbo transmit diversity scenarios discussed in this chapter, many parametric investigations can still be performed. This is necessary to form a complete picture of the performance gains on offer by the different TTD schemes. Some ideas of these future investigations are listed below:

PCTTD. When the number of constituent encoders Z is more than 2, different decoding configurations may be considered. In general the advantage of using more than three or more constituent codes is that the corresponding two or more interleavers have a better chance to break sequences that were not broken by another interleaver. The disadvantage is that, for an overall desired code rate, each code must be punctured more, resulting in weaker constituent codes.

Obvious extensions of the serial mode of decoding are the master-slave, parallel and mixed serial-parallel decoding configurations [176].

SCTTD. It has been shown in [172] that the performance of SCCC schemes can be improved at low SNRs by swapping the inner and outer codes. For instance, rather than using a rate 1/2 outer code and a rate 2/3 inner code, a rate 1/3 SCTTD scheme can be constructed from a rate 2/3 outer code and a rate 1/2 inner code. This arrangement has advantages at low SNRs because the more powerful rate 1/2 code is now decoded first.

The use of non-systematic feed-forward outer convolutional codes have been considered in the SCTTD scheme. However, it is known that systematic feedback codes provide improved performance at low SNRs [226]. Therefore the use of systematic codes as the outer codes of SCTTD schemes may be investigated.

SOTTD. One natural extension to the SOTTD scheme that may be considered, is the use of different spreading sequences. In a typical mobile multiple access communication channel, the multiple access interference experienced by any user in a CDMA system will be complex-valued due to independent phase offsets between signals received from different users. For this reason complex spreading codes may also be employed, in which case the MAI is complex-valued, even without phase offsets, and improved performance can be achieved under practical conditions.

In conclusion, there are a number of important notes which must be made about the performance bounds presented in this chapter and in Chapter 5. These bounds are upper limits on the performance of the codes derived from the use of the union bound. As such the bounds are only valid for the case of ML decoding, and they will diverge significantly from the true performance at low values of E_b/N_o. Also, in practice a sub-optimal decoding algorithm is used which is not ML, and furthermore, the bounds are based upon the uniform interleaver, rather than a real random interleaver. The performance of practical systems is also strongly influenced by the available CSI. Clearly, the lack of CSI shall produce a noticeable degradation in system performance. However, there is much heuristic evidence to suggest that, despite this apparent inconsistency, these bounds do make good design and selection criteria for transmit diversity signalling scenarios.

Notes

1. For sake of notation "cleanliness" in defining the different TTD scenarios, the term serial concatenated turbo transmit diversity is adopted, although the "turbo" term normally refers to parallel concatenation.
2. Interleaving between the two decoders reduces the statistical dependencies effectively.

7 SPACE-TIME TRELLIS CODED TRANSMIT DIVERSITY

In the foregoing chapters layered space-time coded transmit diversity techniques have been proposed to benefit from antenna diversity in the downlink, while putting the diversity burden on the BSS. Recall, the usefulness of the space-time processing hinges on the separation of the spatial and temporal signatures of the signal of interest. In [201, 202] space-time trellis coding has been introduced proposing joint design of coding, modulation, transmit diversity and optional receive diversity.

In line with the goals of this thesis, this chapter investigates the extension of the classical convolutional and turbo coded transmit diversity techniques to incorporate trellis (TCM) and turbo trellis coded modulation (TTCM). When higher modulation formats are considered for cellular CDMA, for instance changing from BPSK/QPSK to multi-dimensional modulation (e.g. multi-dimensional Q^2PSK [227, 228]), the use of TCM and TTCM techniques will be indispensable.

TCM has evolved over the past two decades as a combined coding and modulation technique for digital transmission over band-limited channels. The main advantage of TCM over classical coding schemes is the fact that trellis coding, and the resulting data-transmission strategy, does not expand the transmission bandwidth. It is both a power- and a bandwidth-efficient modulation scheme. TCM schemes use redundant non-binary modulation in combination with a finite-state encoder that determines the corresponding signal shape to be transmitted over the channel. At the receiver, the corrupted signals are decoded by a soft-decision ML Viterbi or MAP decoder. According to Ungerboeck [24, 189, 190] simple four-state TCM schemes can improve the robustness of digital transmission against additive noise by 3 *dB*, compared to conventional uncoded modulation. With more complex TCM schemes the coding gain can reach 6 *dB* or more.

As has been discussed in Chapter 4, the use of the Ungerboeck codes do yield a performance advantage over standard convolutional codes when combined in a RAKE-receiver CDMA system [44]. It is important to note that for single-user receivers, such as the MF or RAKE used in a multiuser environment, coding gain comes at the cost of increased MAI level. A limitation to the use of low rate coding comes when the spreading is reduced to such a level that the MAI does not appear no longer Gaussian. When transmit diversity signalling is considered, codes optimized for the AWGN channel may again be considered. By

using more powerful codes than those used by Boudreau *et al.* [44], the issue of trellis coded spreading can be more adequately addressed. Specifically, when space-time turbo coded modulation is considered, the potential coding gain can be substantial.

The focus is placed on the design and evaluation of diagonally layered space-time coded modulation (STCM) schemes for cellular CDMA. The space-time encoder selects the constellation symbols to transmit such that both diversity and coding gain are maximized. Towards this goal, three STCM schemes, namely orthogonal transmit diversity (OTD) [229, 230, 231], delay transmit diversity (DTD) [232], and the Alamouti code transmit diversity (ACTD) are considered for CDMA [151]. Both OTD and ACTD have been adopted by 3G CDMA systems in the U.S. and Europe, respectively.

Here, the performance of these diversity schemes is analyzed from a coding perspective in terms of product distance comparisons. Also, a heuristic approach based on classical multiple trellis-coded modulation (MTCM) techniques is adopted for the design of STCM codes.

7.1 SPACE-TIME TRELLIS CODED MODULATION SYSTEM MODEL

Figure 7.1 illustrates the components of a CDMA space-time trellis coded modulation system. The outer channel encoder receives a sequence of input symbols $\mathbf{b}$, and outputs a sequence of symbols

$$\mathbf{x} = \ldots, x_1, x_2, x_3, \ldots, x_n \,, \tag{7.1}$$

from the alphabet $\{0, 1, \ldots, M\}$, where M is the number of symbols available for transmission. The encoded symbols are then interleaved, using a block symbol-by-symbol interleaver. The function of the interleaver/de-interleaver is to distribute channel errors randomly throughout the decoder input sequence $\mathbf{y}$, thereby enabling the use of coding, optimal for AWGN, to function well under adverse MAI and multi-path fading. As shown in Figure 7.1, the interleaver outputs the symbol sequence, $\tilde{\mathbf{x}}$.

The sequence of channel encoder output symbols has a very carefully controlled structure that enables the detection and correction of transmission errors. The inner space-time code encoder should be designed in such a way that its combined spatial and temporal properties will guarantee maximum transmit diversity, while maintaining the option to include receive diversity. The (outer or first stage) channel coding may be either convolutional or turbo coding, or their trellis coded modulation variants.

After encoding, the output is split into M_T streams and each of the streams are independently spread by the same spreading sequence. The RF modulation and demodulation operations have been omitted. The code/time division transmit diversity system generates a signalling waveform based on the combinations of data modulation, spreading modulation, trellis coding and space-time encoded transmit diversity schemes.

Since the signal at the receive antenna is a linear superposition of the $K \times M_T$ transmitted orthogonal signals, the receiver first performs chip waveform matching with reference to the M_T streams associated with the desired user. This despreading operation is the key function of any spread-spectrum system, and can be accomplished only if accurate synchronization information is available. Here, perfect spreading waveform synchronization, carrier recovery, symbol and frame synchronization are assumed. Channel estimation is performed on each resolved path, and used in the pilot symbol assisted (PSA) RAKE combiner to resolve each of the transmitted streams from the multiple transmit antennas.

After down-convertion, de-spreading and RAKE combining, the symbol spaced receive samples are first decoded by the space-time decoder. Soft values are generated by the space-time decoder using a MAP or

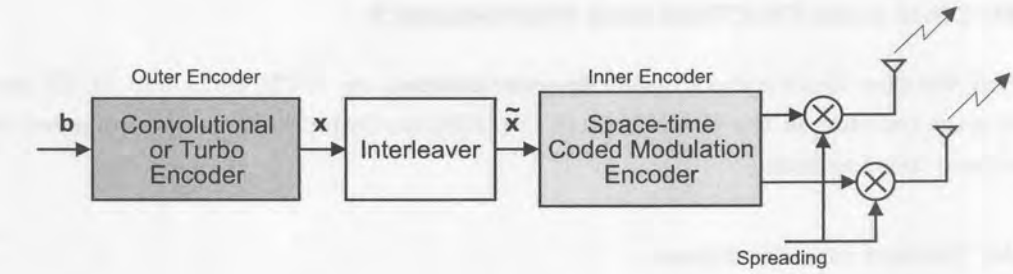

(a)

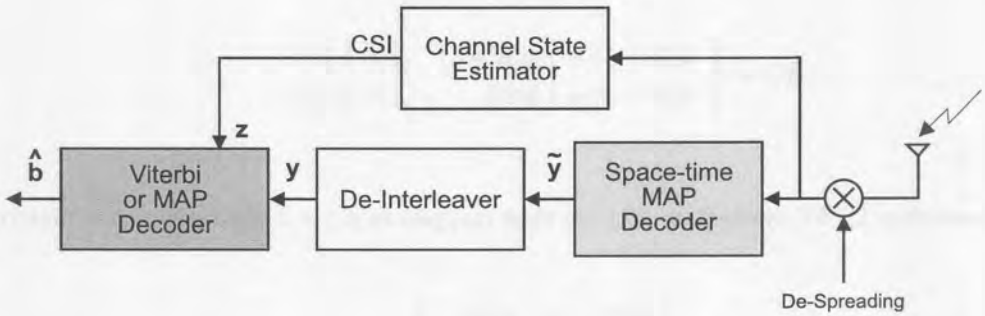

(b)

Figure 7.1. Block diagram of space-time coded transmit diversity system for CDMA.

the SOVA, and sent to the channel decoder for the outer decoding stage. To assist the channel decoder, additional reliability information can be obtained by measuring the CSI. The output of the CSI is denoted $\mathbf{z} = z_1, z_2, z_3, \ldots$ where z_j is a scaled real value.

The space-time diversity channel may be completely characterized by the probability that the channel output is $\mathbf{y}$, given that the channel input is $\mathbf{x}$ and $\mathbf{z}$ is the CSI. That is, the channel is completely characterized by

$$p(\mathbf{y} \mid \mathbf{x}, \mathbf{z}) = \prod_{i=1}^{\infty} p(y_i \mid x_i, z_i) \,, \tag{7.2}$$

where $p(y_i \mid x_i, z_i)$ is the probability that, given the input x_i and the CSI z_i, the demodulator output is y_i for channel i.

The probabilities $p(y_i \mid x_i, z_i)$ are found by analysis of the data modulation/demodulation, and the waveform channel, including transmit diversity. When the demodulator output is continuous, the probabilities of (7.2) are replaced by continuous probability density functions. Characterization of the channel using (7.2) enables decoupling of the analysis of the waveform channel from the FEC analysis.

The principle goal of the remainder of this chapter is to consider in detail the construction and performance evaluation of layered STCM codes for CDMA communication systems operating on frequency selective multiple access channels. This will be accomplished using the space-time coded system model described in this section. In the analysis perfect synchronization is assumed and it is further assumed that the MAI is Gaussian distributed (making use of the Gaussian assumption). In addition, perfect power control is assumed, implying that the base station adjusts the transmitted power such that the mobile terminal observes a prescribed SINR. Also, the analysis is restricted to QPSK ($M = 4$) modulation.

7.2 INNER CODE CONSTRUCTION AND PERFORMANCE

In this section, the three block coded transmit diversity schemes, viz. OTD, DTD, and ACTD are proposed for the first stage encoding in the STCM system. In [150], the latter schemes were proposed for TDMA based space-time coded systems.

7.2.1 Coded Transmit Diversity Schemes

7.2.1.1 Orthogonal Transmit Diversity (OTD). The channel coded bit sequence $b(i) = \pm 1$ is first mapped to QPSK symbol sequences $d(i)$, according to

$$d(i) = \begin{cases} b(2i-1) + j\, b(2i+1) & ,i = 1,3,5,\ldots \\ b(2i-2) + j\, b(2i) & ,i = 2,4,6,\ldots \end{cases}, \tag{7.3}$$

where $j = \sqrt{-1}$.

Every two consecutive QPSK symbols in $d(i)$ are then mapped to a 2×2 space-time code matrix

$$\mathbf{D}(i) = \begin{bmatrix} d(2i-1) & d(2i) \\ d(2i-2) & -d(2i) \end{bmatrix}, i = 1,2,\ldots \tag{7.4}$$

where the first column of $\mathbf{D}(i)$ is the temporal dimension and the second column is the spatial dimension.

The received samples corresponding to $\mathbf{D}(i)$ is given by

$$\begin{bmatrix} r(2i-1) \\ r(2i) \end{bmatrix} = \begin{bmatrix} d(2i-1) & d(2i) \\ b(2i-2) & -d(2i) \end{bmatrix} \cdot \begin{bmatrix} c_1 \\ c_2 \end{bmatrix} + \begin{bmatrix} \eta(2i-1) \\ \eta(2i) \end{bmatrix}, \tag{7.5}$$

where c_1 and c_2 are the independent diversity components and $\eta(2i-1)$ and $\eta(2i)$ are AWGN samples. Since the symbols are orthogonal across the antennas, the MAP decoder of an OTD code matrix simply calculates the statistics

$$\begin{aligned} \lambda(2i-1) &= c_1^* \left(r(2i-1) + r(2i)\right) \\ &= 2 \mid c_1 \mid^2 d(2i-1) + c_1^* \left(\eta(2i-1) + \eta(2i)\right), \\ \lambda(2i) &= c_2^* \left(r(2i-1) - r(2i)\right) \\ &= 2 \mid c_2 \mid^2 d(2i) + c_2^* \left(\eta(2i-1) - \eta(2i)\right), \end{aligned} \tag{7.6}$$

corresponding to $d(2i-1)$ and $d(2i)$, from $r(2i-1)$ and $r(2i)$, respectively, and determines to which quadrant in the QPSK constellation the symbols most likely belong. The likelihood (or confidence level) of this determination is the soft output passed on to the channel decoder.

Essentially, OTD sends half of the coded bits from one antenna and the other half of the coded bits from the other antenna. The diversity is achieved at the channel coding level since half of the coded bits fade independently from the other half. The space-time mapping does not provide any diversity advantage.

The OTD scheme is not restricted to two antennas. In general, any $M_T \times M_T$ unitary transformation can map M_T symbols into an $M_T \times M_T$ orthogonal code matrix.

7.2.1.2 Delay Transmit Diversity (DTD). In delay transmit diversity (DTD) the BSS transmit a delayed version of the original signal [232]. It was shown in [229] that DTD has a limited link performance gain over non-transmit diversity due to its adverse effect of degrading orthogonality and increasing the interference level at the mobile receiver.

In the DTD scheme, the first antenna sends the original QPSK sequence in (7.3) while the second antenna sends the sequence with one symbol delay. This artificially creates a dispersive channel with two equal-strength symbol-spaced channel components. As in OTD, DTD can be extended to any number of antennas with different transmit diversity delays.

7.2.1.3 Alamouti Code Transmit Diversity (ACTD). The paper by Alamouti [151], revealed a very simple yet effective block code of length 2 for a two antenna system. It maps two symbols into a 2×2 code matrix according to

$$\mathbf{D}(i) = \begin{bmatrix} d(2i-1) & d(2i) \\ -d^*(2i) & d^*(2i-1) \end{bmatrix}, i = 1, 2, \ldots . \tag{7.7}$$

Since the symbols are also orthogonal across antennas, the soft-input trellis decoder simply calculates

$$\begin{aligned} \lambda(2i-1) &= c_1^* \ (r(2i-1) + c_2 \, r^*(2i)) \\ &= \left(|\, c_1 \,|^2 + |\, c_2 \,|^2\right) d(2i-1) + c_1^* \, \eta(2i-1) + c_2 \, \eta^*(2i) \, , \\ \lambda(2i) &= c_2^* \ (r(2i-1) - c_1 \, r^*(2i)) \\ &= \left(|\, c_1 \,|^2 + |\, c_2 \,|^2\right) d(2i) + c_2^* \, \eta(2i-1) - c_1 \, \eta^*(2i) \, . \end{aligned} \tag{7.8}$$

7.2.2 *Inner Code Performance Considerations*

In an attempt to simplify the analysis, it is assumed that the channels in consideration are stationary and flat. These assumptions correspond to the condition where transmit diversity is most effective, i.e., the condition in which the terminal is moving very slowly in a single path fading environment. An indoor environment is well approximated by this model. Furthermore, it is assumed that the conditions of fading are independent (uncorrelated) across antennas.

Under conditions of the foregoing channel assumptions and assuming that the propagation delays are the same for all antennas, the received symbol-spaced samples of a transmitted "code matrix" $\mathbf{D}$ are defined as

$$\mathbf{D}(i) = \begin{bmatrix} d_1(1) & d_2(1) & \ldots & d_{M_T}(1) \\ d_1(2) & d_2(2) & \ldots & d_{M_T}(2) \\ \vdots & \vdots & . & \vdots \\ d_1(n) & d_2(n) & \ldots & d_{M_T}(n) \end{bmatrix} , \tag{7.9}$$

where $d_l(n)$, denoting the symbol transmitted by the lth antenna at time n, can be expressed in a matrix form as

$$\begin{aligned} r(1) &= \sum_{l=1}^{M_T} d_l(1)\, c_l \;+\; \eta(1)\,, \\ r(2) &= \sum_{l=1}^{M_T} d_l(2)\, c_l \;+\; \eta(2)\,, \\ &\vdots \\ r(n) &= \sum_{l=1}^{M_T} d_l(n)\, c_l \;+\; \eta(n)\,, \end{aligned} \tag{7.10}$$

where c_l denotes the i.i.d. zero-mean complex Gaussian channel component of the lth antenna, $\eta(n)$ denotes the i.i.d. AWGN at the nth symbol time, and $d_l(n)$ is the symbol transmitted by the lth antenna at the nth symbol time.

The pairwise error probability, $P_d(\mathbf{D} \to \hat{\mathbf{D}})$ of decoding a code matrix $\hat{\mathbf{D}}$, into $\mathbf{D}$ was derived in [149]. It was shown that the distance between the two code matrices is determined by the eigenvalues of $(\hat{\mathbf{D}}-\mathbf{D})^H(\hat{\mathbf{D}}-\mathbf{D})$ and that in order to achieve full diversity, the difference between any pair of code matrices must have full rank. Approximations given in [201, 202] lead to the definition of the product distance E_P [233], between two code matrices $\hat{\mathbf{D}}$, and $\mathbf{D}$ as

$$E_P = \left|(\hat{\mathbf{D}} - \mathbf{D})^H(\hat{\mathbf{D}} - \mathbf{D})\right| . \tag{7.11}$$

With (7.11), the distance properties of the three coded diversity schemes under investigation are compared. Since the channels are stationary, the interleaver is not taken into account in the inner code analysis presented here.

Making extensive use of the analysis carried out by Guey [150], the coded diversity schemes performance is considered. The product distances for OTD, DTD, ACTD, considering the difference between two distinct information sequences $\mathbf{X}$ and $\mathbf{Y}$ differing in P symbol intervals, are given by

$$E_{P_{OTD}}(\mathbf{X},\mathbf{Y}) = 4\left(\sum_{i=1}^{P/2} |\,\delta(2i-1)\,|^2\right)\cdot\left(\sum_{i=1}^{P/2} |\,\delta(2i)\,|^2\right), \tag{7.12}$$

$$E_{P_{DTD}}(\mathbf{X},\mathbf{Y}) = \left(\sum_{i=1}^{P} |\,\delta(i)\,|^2\right)^2 - \left|\sum_{i=1}^{P-1} \delta(i)\delta^*(i+1)\right|^2, \tag{7.13}$$

$$E_{P_{ACTD}}(\mathbf{X},\mathbf{Y}) = \left(\sum_{i=1}^{P} |\,\delta(i)\,|^2\right)^2, \tag{7.14}$$

where $\delta(i) = x(i) - y(i)$.

Using (7.12), (7.13) and (7.14) it can be easily shown that

$$E_{P_{ACTD}}(\mathbf{X},\mathbf{Y}) - E_{P_{DTD}}(\mathbf{X},\mathbf{Y}) = \left|\sum_{i=1}^{P-1} \delta(i)\delta^*(i+1)\right|^2 \geq 0\,, \tag{7.15}$$

and

$$E_{P_{ACTD}}(\mathbf{X},\mathbf{Y}) - E_{P_{OTD}}(\mathbf{X},\mathbf{Y}) = \left(\sum_{i=1}^{P/2} \mid \delta(2i-1) \mid^2 - \sum_{i=1}^{P/2} \mid \delta(2i) \mid^2\right)^2 \geq 2\,. \tag{7.16}$$

Therefore, for any pair of distinct information sequences, the product distance between their corresponding code matrices for the Alamouti scheme is always greater than or equal to the product distance between the code matrices associated with the other two schemes.

7.3 OUTER (CHANNEL) CODE DESIGN AND IMPLEMENTATION

The use of classical convolutional and turbo codes as the outer channel code in the STCM system is straightforward, and can readily be implemented as shown in Figure 7.1.

It is informative to note from (7.15) and (7.16) that on average for the inner codes, the ratios

$$\frac{E_{P_{ACTD}}(\mathbf{X},\mathbf{Y}) - E_{P_{OTD}}(\mathbf{X},\mathbf{Y})}{E_{P_{ACTD}}(\mathbf{X},\mathbf{Y})}\,, \tag{7.17}$$

and

$$\frac{E_{P_{ACTD}}(\mathbf{X},\mathbf{Y}) - E_{P_{DTD}}(\mathbf{X},\mathbf{Y})}{E_{P_{ACTD}}(\mathbf{X},\mathbf{Y})}, \tag{7.18}$$

decrease as P is increased. This observation indicates that the difference in performance between the Alamouti scheme and the other two schemes will be reduced by using more powerful outer channel codes having larger minimum Euclidean distances. With this objective in mind, the use of TCM and turbo TCM (TTCM) codes are proposed as outer channel codes in STCM transmit diversity.

The appropriate criterion for designing good TCM schemes for the AWGN channel is to maximize the minimum Euclidean Distance (ED) between any two distinct information sequences of the coded sequences. Several papers [234, 235] have shown that the error rate performance of TCM schemes over fading channels can be strongly influenced by the effective or shortest error event path, L_{min} and the minimum product distance, λ_L along that error event path. These parameters play a more important role than the minimum ED. For this reason MTCM codes have been designed in order to achieve superior performance on the fading channel, compared to that achievable by conventional TCM of the same throughput and decoder complexity.

A heuristic approach is adopted for the design of the outer TCM codes employing classical (MTCM) techniques. The advantage of the latter approach is that it provides a unified design procedure for these type of STCM systems, including the design of multi-level, multi-dimensional and asymmetric coded modulation schemes. In [203], Tarokh *et al.* proposed two design criteria, namely the rank and determinant criteria, for the design of STCM TDMA systems. Here, the two design criteria will be modified to be more closely related to the MTCM code construction process. Using this insight, the layered squared Euclidean distance (LSED) and layered squared Euclidean distance product (LSEDP) of the STCM system [236] are defined.

7.3.1 Code Design

In its most general form, MTCM is implemented by an encoder with b binary input bits and s binary output bits that are mapped into $\kappa\times$ QPSK symbols in each transmission interval. Figure 7.2 illustrates the proposed space-time MTCM encoder.

The parameter κ is referred to as the *multiplicity* of the code, since it represents the number of QPSK symbols allocated to each branch in the trellis diagram ($\kappa = 1$ corresponds to conventional TCM). To produce such a result, the s binary encoder output bits are partitioned into κ groups containing $m_1, m_2, \ldots, m_k$ symbols. Each of these groups, through a suitable mapping function, results in a QPSK output symbol.

Recall that with conventional trellis coding (i.e., one symbol per trellis branch), the length L_{min} of the shortest error event path is equal to the number of trellis branches along that path. A trellis diagram with parallel paths is constrained to have the shortest error event path of one branch, $L_{min} = 1$. This implies that the asymptotic region of the graph of average BEP will vary inverse linearly with $\overline{E_s}/N_o$ or E_s/N_o, since $\overline{E_s} = E_s$ [21]. Therefore, from an error probability viewpoint it is undesirable to design conventional TCM codes to have parallel paths in their trellis diagrams.

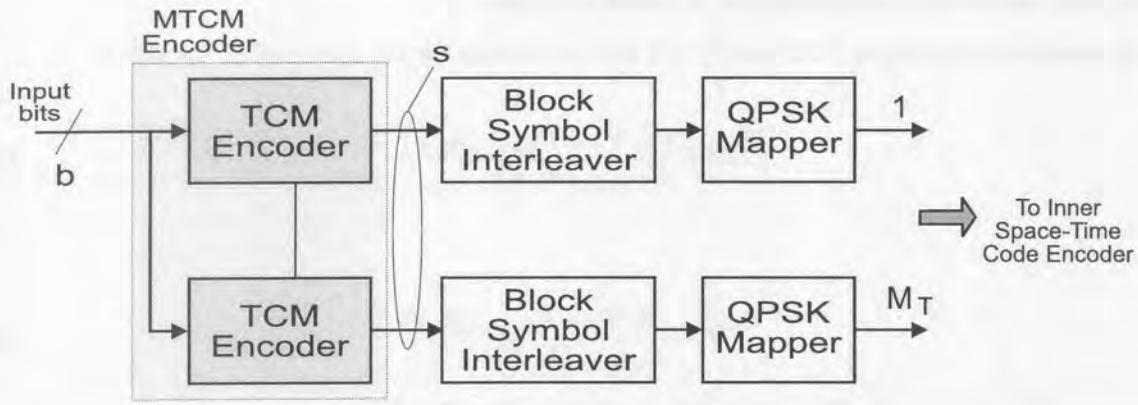

Figure 7.2. Space-time MTCM encoder and multiple transmit antenna diagram.

When the MTCM approach is employed for space-time code designs, the option of designing a trellis diagram with parallel paths may again be considered, since it offers more flexibility in selecting higher effective code lengths (or error event paths). The reason behind this lies in the fact that even if parallel paths exist in the trellis, it is now possible to have more than one coded symbol with non-zero ED associated with an error event path branch of length, $L_{min} = 1$.

In the design of the space-time codes a procedure similar to that presented in [21], known as the *Ungerboeck: From Root-to-Leaf* approach, has been followed. The set partitioning method, makes use of κ-fold Cartesian products of the sets found in Ungerboeck's original set-partitioning method for conventional trellis codes [24]. The set-partitioning procedure is started with a κ-fold Cartesian product of the complete QPSK signal set.

The latter multiplicity factor is the most important parameter in the space-time coding design procedure. In general, the design criteria do not include any direct considerations on the choice of multiplicity factor, κ, as a function of the channel parameters. In [237], it has been shown how the general design criteria for MTCM codes for fading channels, can be augmented by including an analysis of the lengths of burst errors. For the space-time transmission system under consideration the choice of κ is naturally determined by the number of available transmit antennas, n_T.

7.3.1.1 Ungerboeck Set Partitioning. Considering the code design for $M_T = 2$, the first step is to partition $A_0 \otimes A_0$ into M_c signal sets defined by the ordered Cartesian product $\{A_0 \otimes B_i\}$, $i = 0, 1, \ldots, M_c - 1$. The second element $\{j_2\}$ of B_i is defined by $nj + i \mod M_c$. In terms of the space-time mapping it is

appropriate to define a new design parameter, that will be called the LSED. Specifically, since the LSED between any pair of $\kappa = 2$-tuples is the sum of the distances between corresponding symbols in the 2-tuples, the set partitioning guarantees that the *intra-distance* (i.e., distance between pairs within a specific set or partition) of all of the partitions $A_0 \otimes B_i$ is identical. In addition, as a result of the possible existence of parallel paths in the decoding trellis, the minimum product of LSEDs must be maximized. This parameter is referred to as the LSEDP, is given by $\prod d_{ij}^2$.

Therefore, for the generating set $A_0 \otimes B_0$, the minimum LSEDP over all pairs of 2-tuples must be maximized. This is done by choosing the odd integer multiplier, n such that it produces the desired *maximin* solution. A computer search for possible values of n, revealed the solution to be $n = 1$. The sets, $A_0 \otimes B_i$, $i = 0, \ldots, M_c - 1$ for $M_T = \kappa = 2$, are illustrated below for QPSK.

$$A_0 \otimes B_0 = \begin{bmatrix} 0 & 0 & 1 & 1 \\ 2 & 2 & 3 & 3 \end{bmatrix}$$

$$A_0 \otimes B_1 = \begin{bmatrix} 0 & 1 & 1 & 2 \\ 2 & 3 & 3 & 0 \end{bmatrix}$$

$$A_0 \otimes B_2 = \begin{bmatrix} 0 & 2 & 1 & 3 \\ 2 & 0 & 3 & 1 \end{bmatrix}$$

$$A_0 \otimes B_3 = \begin{bmatrix} 0 & 3 & 1 & 0 \\ 2 & 1 & 3 & 2 \end{bmatrix}$$

Note that each set has a minimum intra-distance of $4E_b$. The *inter-distances* (i.e., minimum distances between pairs of 2-tuples from different sets), for these sets are summarized in Table 7.1.

Table 7.1. Inter-distances between partitioned subsets, with $A_0 \otimes B_0$ used as reference.

Subset	Distance	Subset	Distance
$A_0 \otimes B_0$	—	$A_0 \otimes B_1$	$4E_b$
$A_0 \otimes B_2$	$8E_b$	$A_0 \otimes B_3$	$4E_b$

Following tradition, the subsequent steps in the set-partitioning procedure are to partition each of the M sets $A_0 \otimes B_i$, into two sets $C_0 \otimes D_{i0}$ and $C_0 \otimes D_{i1}$, with the first containing the even elements ($j = 0, 2, \ldots, M_c - 2$) and the other containing the odd elements ($j = 1, 3, \ldots, M_c - 1$).

The sets, $C_0 \otimes D_{ij}$, using the procedure described in the foregoing are illustrated below.

$$C_0 \otimes D_{00} = C_0 \otimes D_{20} = \begin{bmatrix} 0 & 0 \\ 2 & 2 \end{bmatrix}$$

$$C_0 \otimes D_{01} = C_0 \otimes D_{21} = \begin{bmatrix} 1 & 1 \\ 3 & 3 \end{bmatrix}$$

$$C_0 \otimes D_{10} = C_0 \otimes D_{30} = \begin{bmatrix} 0 & 2 \\ 2 & 0 \end{bmatrix}$$

$$C_0 \otimes D_{11} = C_0 \otimes D_{31} = \begin{bmatrix} 1 & 3 \\ 3 & 1 \end{bmatrix}$$

Note that each set has a minimum intra-distance of $8E_b$ and the inter-distances for these sets are $8E_b$.

7.3.1.2 Outer Coder Implementation. The encoder and decoder configuration can be easily derived from the trellis diagram. The output channel signals are directly expressed in terms of a sliding block of input bits, with the intermediate step of output coded bits being irrelevant for analytically described trellis codes.

The realization of a rate-2/4 space-time trellis code of multiplicity $M_T = \kappa = 2$ is considered. Thus, two QPSK symbols are transmitted over the channel for every 2 bits accepted by the encoder. The input/output/state connection diagram for this coding system is shown in Figure 7.3 ((a) 2-state, (b) 4-state). It defines the sliding block of source variables $(b_1, b_2, b_3^{(1)}, b_4^{(1)}, b_3^{(2)}, b_4^{(2)})$. Note that the output bits $(b_3^{(z)}, b_4^{(z)})$, $z = 1, 2$ are mapped into the QPSK symbols output from the antenna elements.

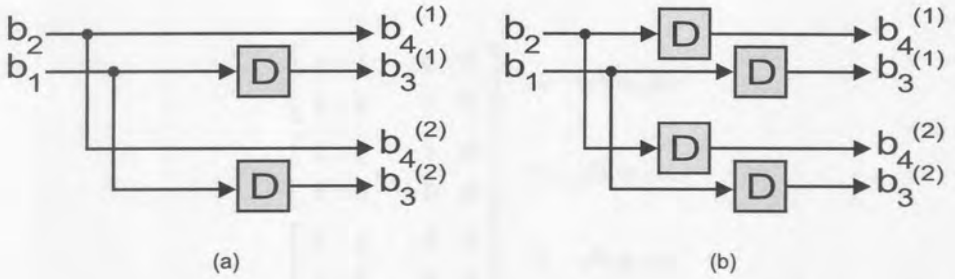

Figure 7.3. Space-time outer encoder input/output/state connection diagram (a) 2-state, (b) 4-state.

The code structure for the half-connected rate-2/4 space-time outer code is presented in Figure 7.4, for a cardinality of 2. The number of branches associated with each state (i.e., emanating from or terminating in a node) equals $2^2 = 4$.

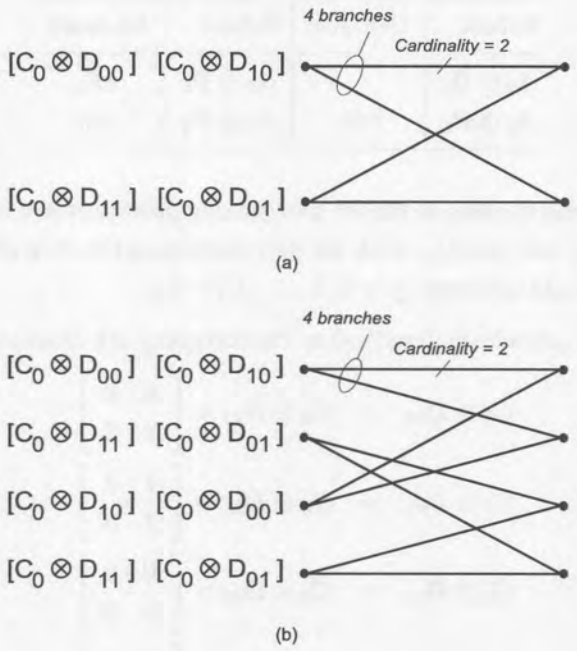

Figure 7.4. Trellis diagram of 4-state space-time code ($M_T = 2$) (a) 2-state, (b) 4-state.

7.3.2 *Extension to Space-time Turbo-Coded Modulation*

From the discussion in the previous section, it seems to be quite natural to combine bandwidth efficient MTCM with the ideas and concepts of space-time turbo codes. In [238, 239], Robertson has presented a straight forward approach of combining the two ideas of TCM and turbo codes into turbo TCM (TTCM for short). Here, the concepts of the latter are extended to turbo MTCM (T-MTCM) coded outer codes for the STCM transmit diversity scenario.

7.3.2.1 Turbo MTCM Encoder. Figure 7.5 shows the modified turbo MTCM (T-MTCM) encoder structure. The main difference between this encoder and the binary space-time turbo coding scheme is that the T-MTCM encoder operates on (multiple) symbols instead of bits.

The input of the encoder is now a block of N_{tc} information symbols with each symbol consisting of b information bits at a time. The information symbol sequence is directly processed by a rate-b/s MTCM encoder, and then by a second one after intermediate symbol-wise interleaving.

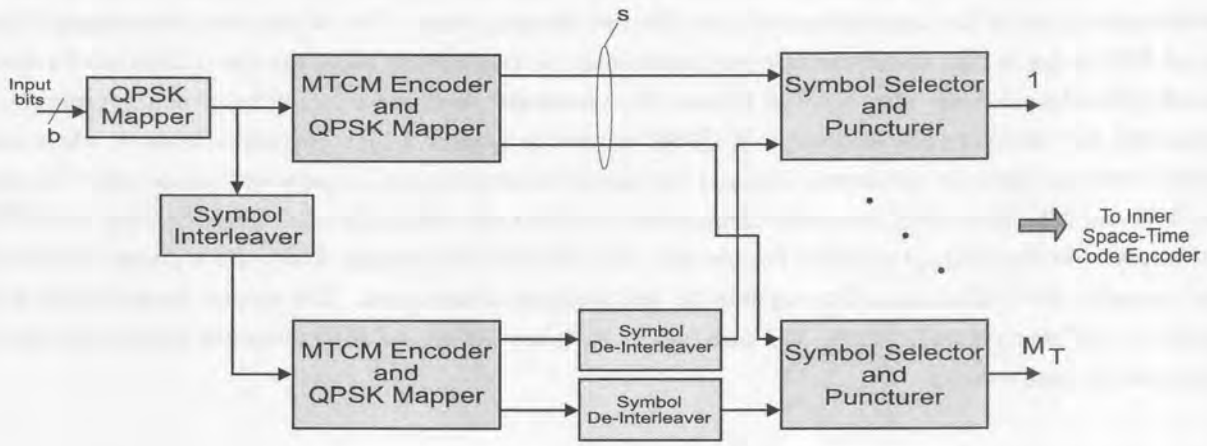

Figure 7.5. Space-time turbo MTCM encoder.

The MTCM encoders, forming the constituent turbo encoders, are designed as discussed in Section 7.3. Each encoder is immediately followed by a QPSK symbol mapper, that maps the code words onto the two-dimensional symbol plane. These output symbols of the two encoders are then alternately punctured to form the symbol streams to be transmitted at the different antennas.

From the figure it is noted that puncturing of the second encoder output takes place after previous de-interleaving, in order to restore the original order of the systematic part of the code symbols. This procedure ensures that each information symbol is only contained in one of the transmitted symbols, and the parity bit is alternately chosen from the first and second encoder. Thus, the complete code can be seen as systematic.

Interleaver (De-Interleaver) Structure. Interleaving should be performed similarly to the binary turbo coding scheme, with one exception: for T-MTCM, the input sequence is interleaved symbol-wise instead of bit-wise. All other characteristics remain the same, in particular the sub-interleaving according to the puncturing pattern of the two constituent encoder outputs as discussed earlier. The latter ensures, that the parity bits are uniformly distributed for each interleaver/de-interleaver combination.

QPSK Mapper. The mapper acts in exactly the same way as in conventional TCM schemes and assigns the non-binary code symbols to the set-partitioned phasors.

Puncturing. Normally puncturing is performed such that every second output symbol of the two constituent encoders is punctured alternately. In general any other code rates are achievable by applying different puncturing patterns to the encoder outputs.

7.3.2.2 Turbo MTCM Decoder. The iterative T-MTCM decoder is similar to the binary turbo decoder, except that there is a difference in the nature of the information passed from one decoder to another, and in the treatment of the first decoding step. This is due to the fact that – in contrast to the binary case – the systematic information is transmitted together with the parity information in the same modulation symbol. Therefore, the systematic component cannot be separated from the extrinsic one. And again, the decoder now processes symbols instead of bits.

In the binary turbo coding scheme, the constituent decoders' output is split into three additive parts for each information bit: the intrinsic or systematic component that corresponds to the received systematic value for the bit concerned, the *a priori* component that is the information given by the other decoder for the bit, and the extrinsic component that is derived by the decoder itself, depending on all the other inputs. Only the extrinsic component may be passed to the next decoder, that uses it as the *a priori* component, in order to avoid multiple use of the same information in different decoding steps. One of the great advantages of the use of RSC codes is that the systematic part needs only be transmitted once, since it is identical for both encoder/decoder combinations. If BPSK is used, the systematic and the parity information are transmitted separately and therefore are separable. If QPSK is used to achieve a high spectral efficiency, where one symbol contains both the systematic bits and the parity information, this separation is impossible because the MAI and noise that affect the parity component also affect the systematic one. Therefore, the T-MTCM component decoders' output can only be split into two different components: firstly the *a priori* component and secondly the combination of the systematic and extrinsic components. The second component is now passed to the next decoding stage, and care has to be taken not to use the systematic information more than once in each decoder.

7.3.3 Outer Code Performance

Thus far the BEP performance discussion has focused on the performance gain as measured by the improvement in minimum free Euclidean distance of the inner trellis code. Using superstate diagrams and upper bounds on the BEP performance computed from the transfer functions of these diagrams, the outer coder performance gains are evaluated.

Analogous to the analytical techniques discussed in Chapter 4, an upper bound on the BEP performance of MTCM is given by [21, 234, 235, 240]

$$P_e \leq \frac{1}{b} Q\left(\sqrt{\frac{bE_b}{\kappa N_0}\frac{d_{free}^2}{4}}\right) Z^{-d_{free}^2} \frac{\delta}{\delta I} T(I,D)\,|_{I=1,D=Z}\,, \tag{7.19}$$

where Z is the Bhttacharyya parameter defined by

$$Z = \exp\left(-\frac{1}{4}\frac{E_s}{N_0}\right) = \exp\left(-\frac{1}{4}\frac{bE_b}{\kappa N_0}\right)\,, \tag{7.20}$$

with E_s the energy per trellis code symbol, and $T(I,D)$ the transfer function of the superstate diagram associated with the multiple trellis code.

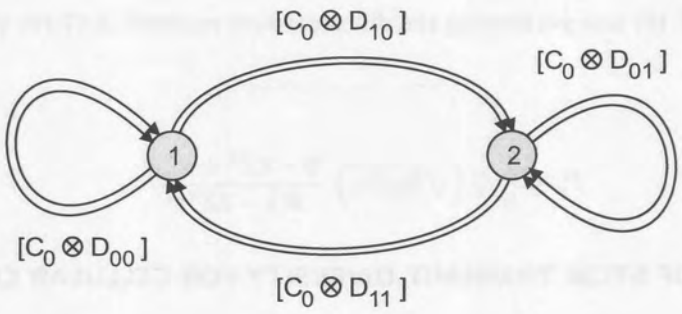

(a)

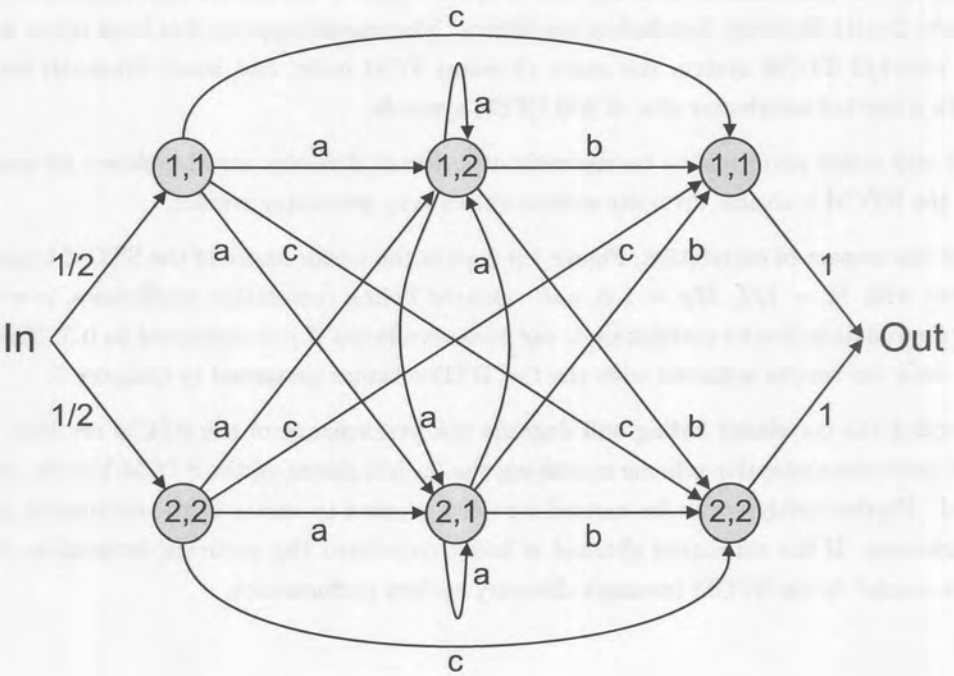

(b)

Figure 7.6. (a) State and, (b) Superstate diagram for rate-$2/4$ space-time outer code.

The performance of the 2-state rate-2/4 TCM inner code with trellis diagram as in Figure 7.4(a) is considered. The corresponding state diagram is illustrated 7.6(a), and the equivalent superstate diagram for computing $T(I, D)$ is shown in Figure 7.6(b). The branch labels are

$$a = \frac{1}{2}(I + I^2)\, D^4, \quad b = \frac{1}{2}(1 + I)\, D^4, \quad c = \frac{1}{2} I\, D^4 \,. \tag{7.21}$$

From Figure 7.6(b), in the absence of fading, the transfer function is easily computed as

$$\begin{aligned} T(I, D) &= 2c + \frac{4ab}{1 - 2a} \\ &= \frac{(2I + 2I^2 + I^3)\, D^8 - I^2 + I^3)\, D^{12}}{1 - (I + I^2)\, D^4} \,. \end{aligned} \tag{7.22}$$

Substituting (7.21) into (7.19) and performing the differentiation required in (7.19) yields the desired upper bound on the BEP

$$P_e \leq \frac{1}{8} Q\left(\sqrt{E_b/N_0}\right) \frac{9 - 8Z^4 + 4Z^8}{9(1-2Z^4)^2} . \tag{7.23}$$

7.4 PERFORMANCE OF STCM TRANSMIT DIVERSITY FOR CELLULAR CDMA

Making use of (7.23), (3.29), (4.6), the approximated BEP performance of a cellular CDMA system employing space-time trellis coded transmit diversity can be determined numerically.

Figure 7.7 depicts the performance as a function of system load, V for the STCM transmit diversity system operating under 2-path Rayleigh fast-fading conditions. The operating point has been taken as $E_b/N_0 = 20$ dB. For the rate-1/2 STCM system the outer (2-state) TCM code, and inner Alamouti code have been assumed, with a symbol interleaver size of 200 QPSK symbols.

The uncoded and coded performance curves without transmit diversity are also shown for comparison. As can be seen, the STCM transmit diversity system shows very promising results.

To investigate the impact of correlation, Figure 7.8 depicts the performance of the STCM transmit diversity CDMA system with $R_c = 1/2$, $M_T = 1, 3$, and constant fading correlation coefficients, $\rho = 0.0, 0.5$. The performance degradation due to correlation is not that significant if ρ is restricted to 0.5. This observation is consistent with the results achieved with the O-CDTD schemes presented in Chapter 5.

If left unattended the correlated fading will degrade the performance of the STCM receiver. Under these conditions, a space-time adaptive scheme modifying the branch metric of the STCM Viterbi decoder should be considered. Further analysis can be carried out with respect to errors in the estimation process of the channel parameters. If the estimated channel is badly correlated the accurate estimation of the channel parameters is crucial to the STCM transmit diversity system performance.

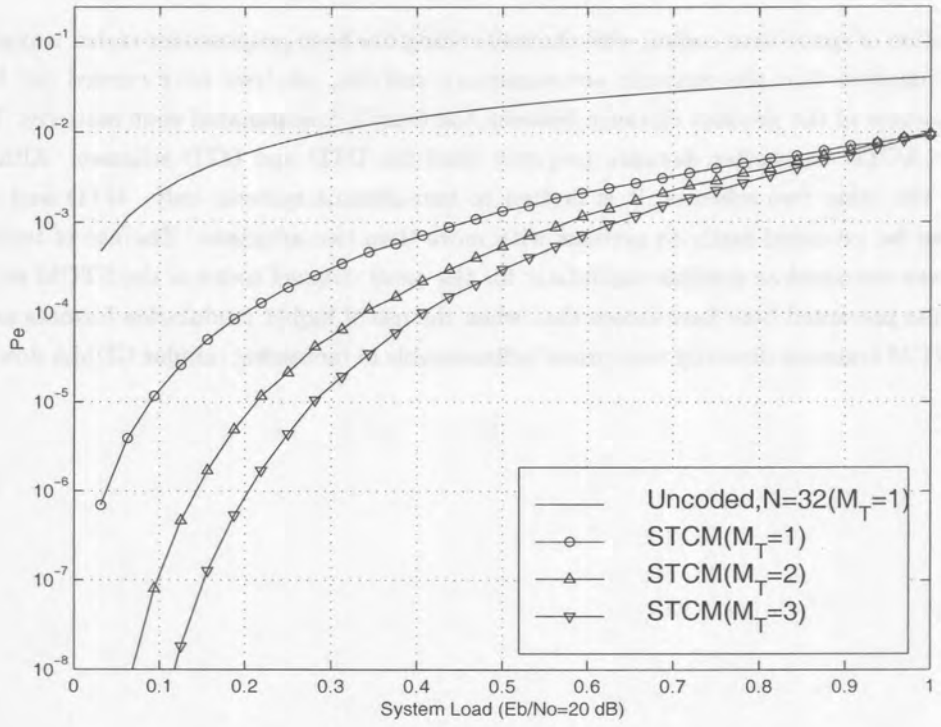

Figure 7.7. STCM transmit diversity performance on a 2-path fading channel with $R_c = 1/2$ and $M_T = 1, 2, 3$.

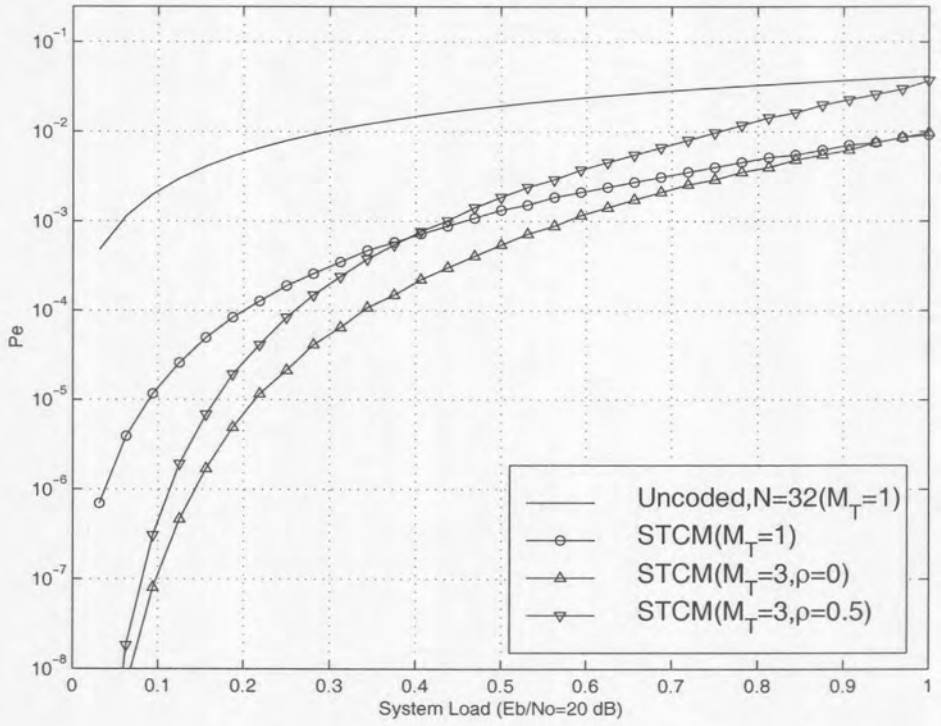

Figure 7.8. STCM transmit diversity performance on a correlated 2-path fading channel with $R_c = 1/2$ and $M_T = 1, 3$.

7.5 SUMMARY

The concatenation of space-time coding with channel coding has been proposed for coded transmit diversity. Under the assumption that the channels are stationary and flat, analysis were carried out based on the pairwise comparison of the product distance between the overall concatenated code matrices. It was shown that the inner ACTD has better distance property than the DTD and OTD schemes. Although ACTD is superior to the other two schemes, it is limited to two-antenna systems only. OTD and DTD on the other hand, can be extended easily to systems with more than two antennas. The use of trellis and turbo trellis codes were discussed as possible candidates for the outer channel coder in the STCM strategies. The analytical results presented here have shown that when the use of higher modulation formats are considered for CDMA, STCM transmit diversity may prove indispensable in increasing cellular CDMA downlink system capacity.

8 CODED SPACE-TIME RECEIVE DIVERSITY AND BEAMFORMING

In the previous three chapters the performance of space-time coded multiple transmit antenna diversity systems have been evaluated for improving the downlink capacity. In this chapter coded space-time processing for the uplink, namely receive diversity and beamforming, are discussed.

Recall, any mapping of information carrying symbol (or bit) sequences into a spatial-temporal code matrix is referred to as a space-time code. Following this convention, it should be clear that the coding techniques to be used with multiple receive antenna cannot be regarded as "true" space-time coding. For this reason these are referred to as coded space-time processing since the type of space-time receiver will influence the choice of FEC coder.

This chapter uses the system model and analysis presented in Chapter 3 in conjunction with the space-time channel model presented in Chapter 2 and the coding bounds derived in Chapter 4 to evaluate the performance of the space-time CDMA systems. Specifically, the performance of a convolutional and turbo coded CDMA system in a receive diversity environment, and a beamforming environment is considered.

8.1 CODED SPACE-TIME RECEIVE DIVERSITY PERFORMANCE

Making use of (3.23), (3.28), (3.29) and (4.6) the BEP performance of a CDMA system using coded space-time receive diversity are considered here, The assumed system parameters as outlined in Table 8.1.

Figure 8.1 depicts the BEP performance of MRC receive diversity CDMA under 2-path Rayleigh fast fading conditions, with rate $R_c = 1/2$ convolutional and turbo ($N_{tc} = 256, 2048$) coding. The number of users are taken as $K = 5$ with $M_T = 1, 2$ and 3 receive antenna elements.

Figures 8.2 and 8.3 depict the performance as a function of system load, V for coded CDMA employing MRC receive diversity. The operating point has been taken as $E_b/N_0 = 20$ dB.

By introducing multiple receive antennas, the diversity order is increased, resulting in a improvement in the composite fading signal. Thus, the probability of coding gain is increased. From the graphs it clear that turbo coded transmit diversity increases the performance substantially.

Parameter	Simulation value
Spreading sequence length	$N = 32$
Operating environment	2-Path, equal strength.
User distribution	uniform
Number of multi-path signals	$L_p = 2$
Number of users	$K = 1, 2, \ldots, N$
Number of RAKE fingers	$L_R = 2$
Transmit diversity elements	$M_T = 1$
Receive diversity elements	$M_R = 1, 2, 3\ \rho = 0, 0.5$

Table 8.1. System parameters for numerical evaluation of coded receive diversity CDMA BEP performance.

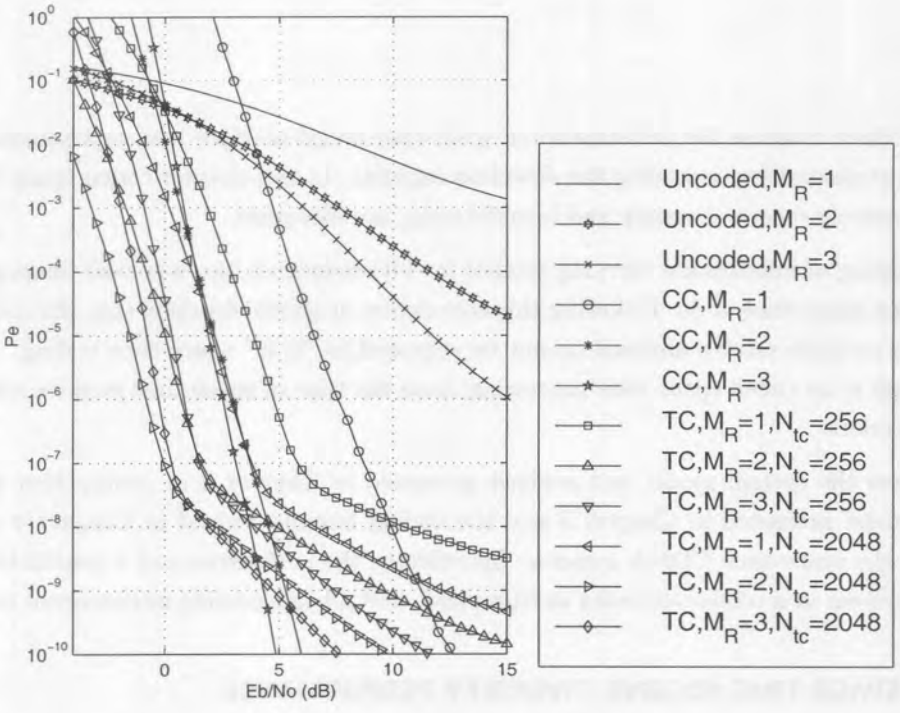

Figure 8.1. Analytical BEP performance of coded MRC receive diversity, with $R_c = 1/2$, $K = 5$, and $M_R = 1, 2, 3$, on a fast fading 2-path channel.

With reference to Figure 8.3, it is clear that the correlation between the M_R diversity elements influences the achievable BEP performance. Thus, when designing the diversity system, the assumption that the signals received at each element are uncorrelated cannot be used in BEP computations. Specifically, the presence of correlation between the fading envelopes of signals received at the various diversity branches will increase the BEP.

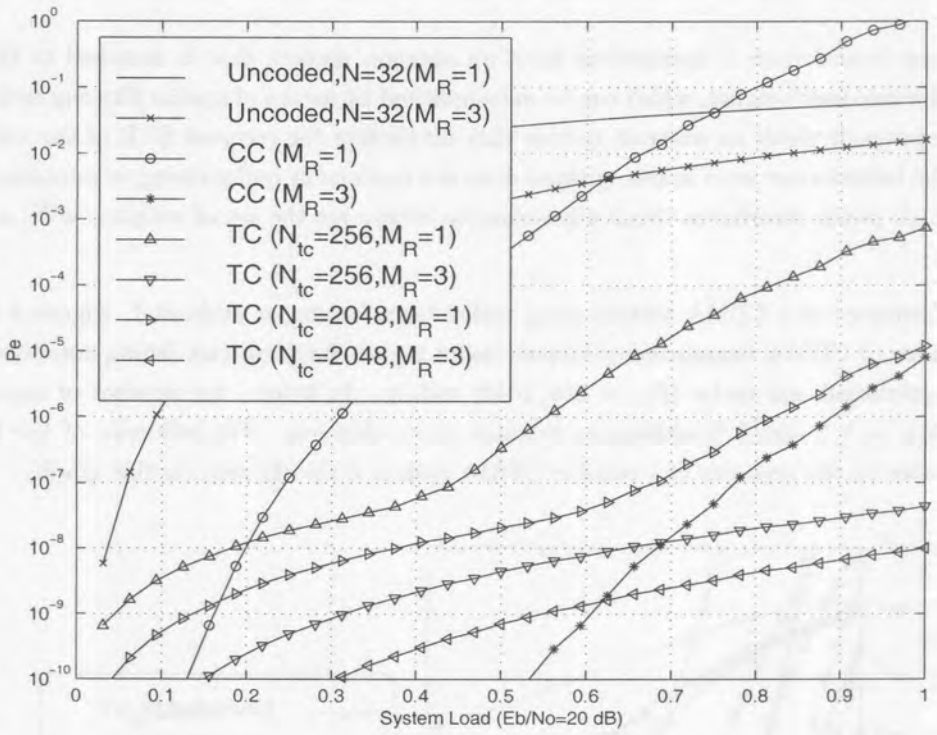

Figure 8.2. Coded O-CDTD performance comparison with $R_c = 1/2$, $N_{tc} = 256, 2048$ and $M_R = 1, 3$.

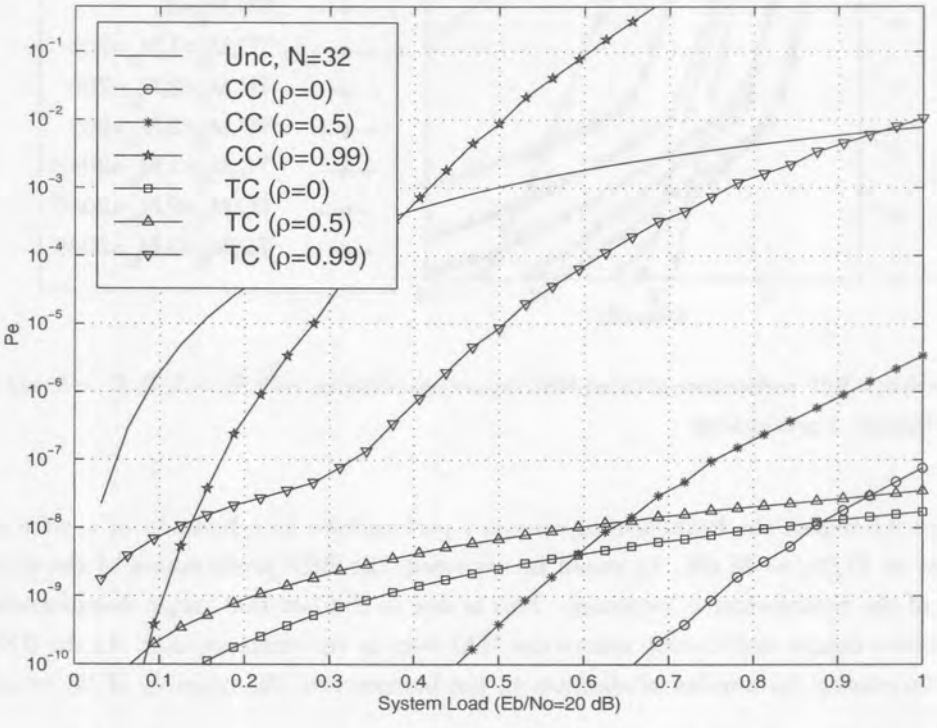

Figure 8.3. Comparison of $R_c = 1/2$ convolutional and turbo coding ($N_{tc} = 256, 2048$), with $M_R = 3$ and $\rho = 0, 0.5, 0.99$.

8.2 CODED SPACE-TIME BEAMFORMING ARRAY PERFORMANCE

The M_B element beamformer is assumed to form an antenna pattern that is matched to the pdf of the DOA of the reference user's signal, which can be accomplished by means of spatial filtering techniques. This beamforming approach yields an antenna system that maximizes the received SNR of the reference user's signal. Also, the beamformer used in this analysis does not implement null-steering to minimize interference from specific high power interferers. Such algorithms to determine the set of weights, $\mathbf{w}^{(k)}$, are treated in [126].

The BEP performance of a CDMA system using coded beamforming is evaluated. Figure 8.4 depicts the BEP performance of CDMA beamforming system under 2-path Rayleigh fast fading conditions, with rate $R_c = 1/2$ convolutional and turbo ($N_{tc} = 256, 2048$) coding. As before, the number of users is taken as $K = 5$ with $M_B = 1, 2$ and 3 beamforming antenna array elements. The influence of the beamforming antenna array size on the capacity of a cellular CDMA system is clearly seen on this graph.

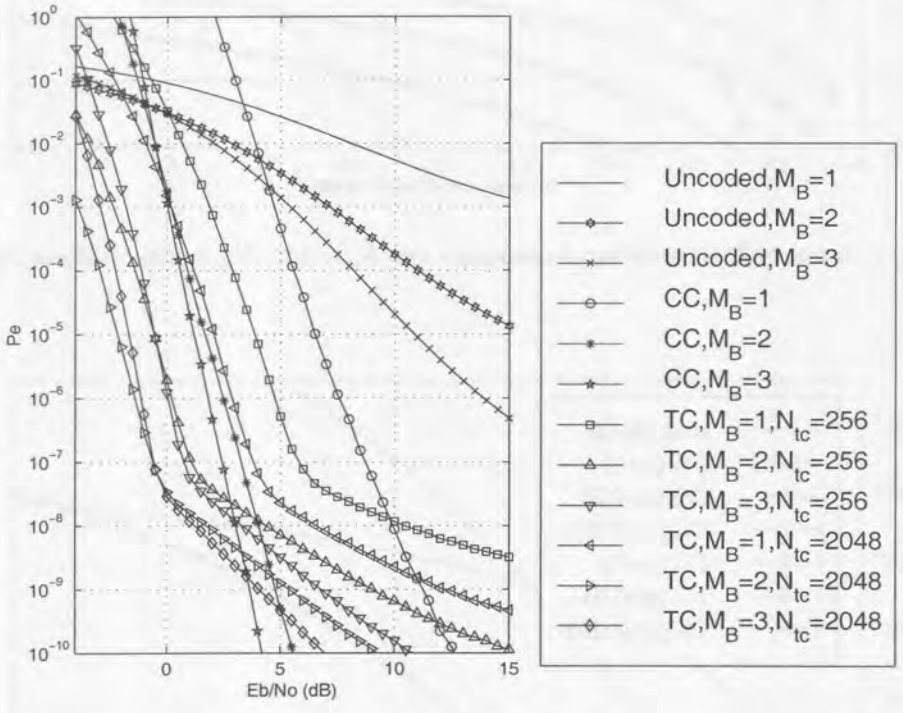

Figure 8.4. Analytical BEP performance of coded MRC receive beamforming, with $R_c = 1/2$, $K = 5$, and $M_B = 1, 2, 3$, on a fast fading Rayleigh 2-path channel.

Figures 8.5 and 8.6 depict the beamforming system's performance as a function of system load, V, at a operating point of $E_b/N_0 = 20$ dB. As would be expected, the BEP performance of the system is better when the size of the beamformer is increased. This is due to the fact that larger beamforming arrays can synthesize narrower beams and thereby reduce the MAI seen by the reference user. As the BEP probability is reduced by increasing the number of elements in the beamformer, the capacity of the cellular system is also increased.

Comparing the BEP performance of the beamforming (Figures 8.5 and 8.5) system with that of the receive diversity system (Figures 8.2 and 8.2), it can be seen that the beamformer BEP results are significantly better. As would be expected, the absolute BEP performance is worse as a result of the fading that is

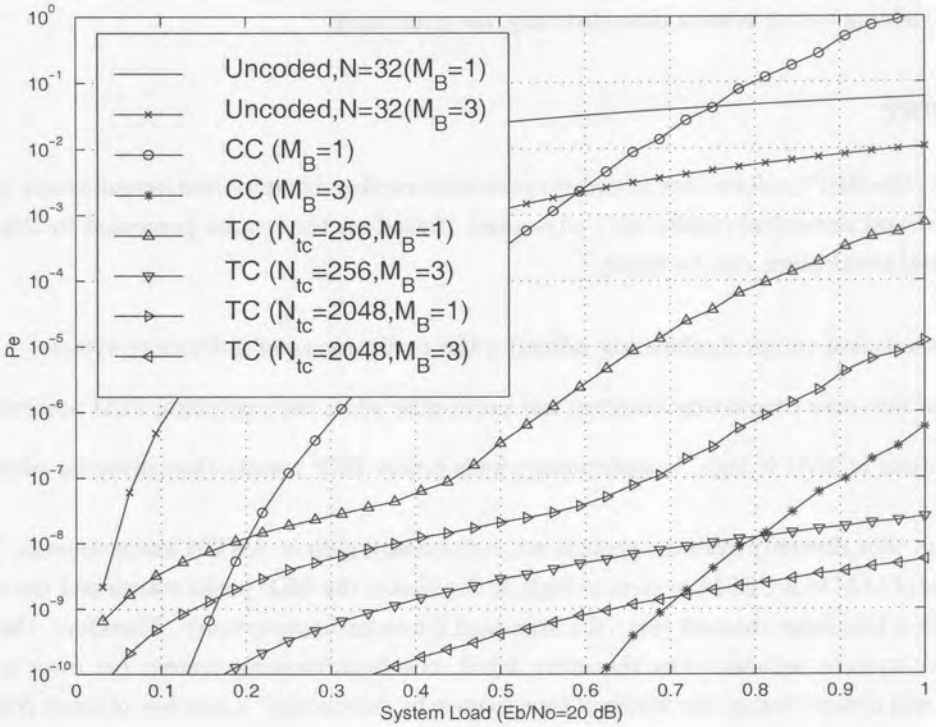

Figure 8.5. Coded MRC receive diversity performance comparison with $R_c = 1/2$, $N_{tc} = 256, 2048$ and $M_B = 1, 3$.

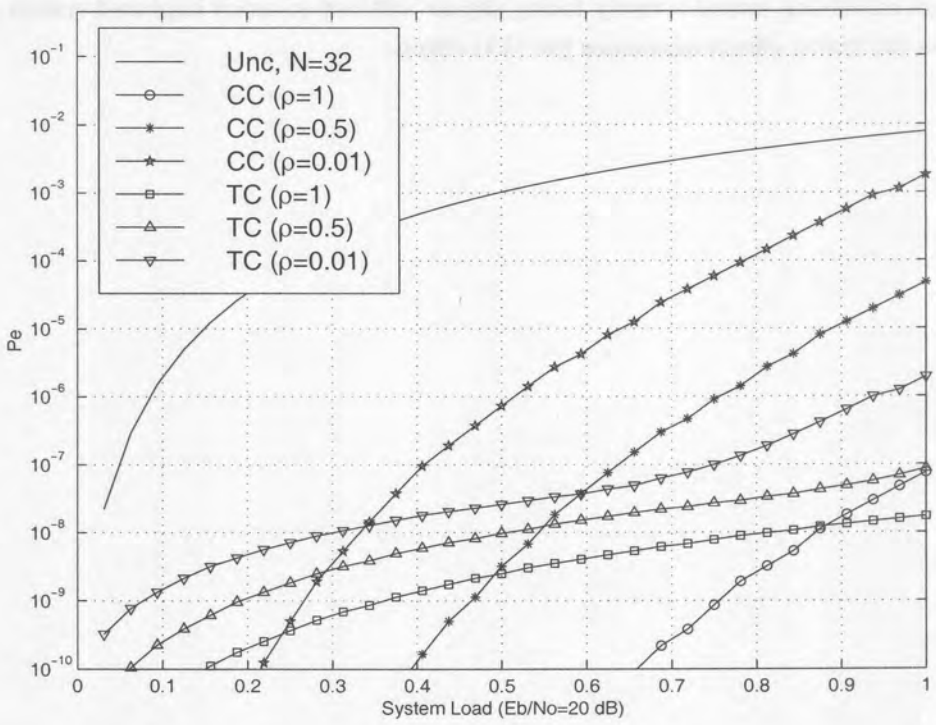

Figure 8.6. Comparison of $R_c = 1/2$ convolutional and turbo coding ($N_{tc} = 256, 2048$), with $M_B = 3$ and $\rho = 0, 0.5, 0.99$.

more severe, however, the general trends of correlation negatively influencing diversity performance and beamforming yielding better results than diversity, are continued.

8.3 SUMMARY

In this chapter, the BEP performance of coded space-time receive diversity and beamforming processors has been addressed and numerical results were presented. Based on the results presented in this chapter, the following general conclusions can be made

- Non-zero correlation values significantly influence the performance of a diversity system.
- The effect of non-zero correlation becomes less noticeable when the prevailing MAI present is high.
- When the levels of MAI is high, beamforming yields better BEP results than diversity alone.

It is well known that diversity systems provide no performance gain in AWGN environments. Furthermore, when the levels of MAI in a CDMA system is high, it dominates the BEP performance and the channel starts to approximate a Gaussian channel (viz. the standard Gaussian assumption). Therefore, the effectiveness of the diversity system reduces. On the other hand, the beamforming system (or even a system with sectorization) will always reduce the levels of interference by "removing" a number of users from the system resulting in better BEP performance. The contrary is also true. When the number of users are low, and the channel is severely fading (as in the NLOS case), the beamforming system cannot improve the receive signal as it does not add any new information to the received signal, but merely limits the MAI. Thus, beamforming systems do not achieve high performance gains. In severe fading, on the other hand, a diversity system combining several severely fading signals will lead to much improved system performance, especially when the fading effects dominates the MAI effects.

9 SUMMARY AND CONCLUSIONS

In this final chapter, a summary of the most important results and conclusions of this thesis is given. The goals of the thesis as outlined in the introductory chapter are revisited and it is stated whether the goals have been reached. In addition future areas of research yet to be explored are also highlighted.

9.1 GOALS OF THE THESIS

The main focus of the research has been on coded space-time processing techniques, which were presented in the context of designing mobile communication systems where the two core areas of spatial processing and error coding have to be integrated in an optimum way. The main goals of the thesis are given below and it is shown whether these have been met.

- To establish a general spatial/temporal channel model for use in the evaluation of coded space-time processing concepts applied to CDMA networks.
  - A spatial/temporal channel model for the evaluation of cellular systems incorporating smart antenna techniques has been developed (see Chapter 2). Amongst the many parameters incorporated in this model, the ability to model the influence of local scatters on the fading envelope correlation has been shown to be of utmost importance in the performance evaluation of space-time coded systems.
- To analyze the performance of uncoded cellular CDMA systems incorporating space-time techniques using analytical methods under a number of realistic application scenarios.
  - BEP performance has been determined in integral form, where the integral is easily evaluated using numeric integration techniques, based on the above mentioned channel model.
- To design, implement and evaluate coding strategies for incorporation into the space-time CDMA systems. This objective has been broken down into
  - Space-time coding systems when considering multiple transmit antennas for the downlink.

    - * Layered space-time convolutional and turbo coded transmit diversity systems have been considered. The techniques included CDTD and TDTD.
    - * Novel extensions to layered space-time configurations, viz. PSTTD, SCTTD and SOTTD, have been proposed.
    - * The application of trellis codes and turbo trellis codes have been considered in Chapter 7.
  - Coded space-time systems when considering multiple receive antennas for the uplink.
    - * Classical convolutional and turbo coded space-time receive diversity and beamforming have been considered.

- To establish the performance of coded space-time CDMA cellular networks under realistic scenarios.
- Underpinned by a comprehensive chapter on the derivation of FEC coding upper bounds, the BEP performances of all the above mentioned space-time coding techniques have been carried out.

9.2 SUMMARY

In order to establish a frame of reference for the evaluation of the contribution of this work, a brief overview of some emerging wireless technology application has been given in Section 1.1. In this overview, it has been shown that many new wireless access solutions, such as UMTS, will incorporate space-time techniques as one method of increasing overall system capacity. A literature survey of forward error correcting codes and space-time processing techniques has been presented as basis for the work covered in this thesis.

In Chapters 2 to 3, extensive background information on channel impairments and space-time channel and system models have been presented. It has been shown that path loss, fading, scattering environment and user distribution are some of the key aspects limiting the performance of space-time processing systems and is crucial in determining mitigation techniques. Together, these chapters provided the necessary background information required to understand the specifics of the two main space-time techniques covered, namely adaptive beamforming, and transmit/receive diversity. The BEP performance of these space-time processors has been derived analytically and numerical results were presented. Based on the analytic results, the effects of the number of antenna elements and correlation between branches on BEP performance of the space-time processing techniques have been addressed. The BEP sensitivity of all the space-time techniques to fading correlation (or lack of it for the beamforming case) were illustrated.

Chapter 4 presented a detailed discussion of the channel coding techniques, including classical convolutional and turbo, and trellis codes for cellular CDMA systems. The BEP performance of these codes has been addressed by the derivation of analytical average upper bounds based on the union bound and code weight distributions. Numerical results were presented.

In Chapter 5 space-time coded transmit diversity techniques have been introduced as a means to improve cellular CDMA performance. The suitability of convolutional- and turbo coding, when applied to layered space-time transmit diversity, has been discussed and analytical results presented for CDTD and TDTD under conditions of multipath fading. The analytical results have shown that the combining of spatial and temporal processing at the transmitter provides an effective way to increase CDMA system capacity in the downlink. In Chapter 6 extensions of CDTD have been presented in the form of TTD, including PCTTD, SCTTD and SOTTD. These schemes have the ability to improve the cellular capacity even further.

In Chapter 7 the concatenation of space-time coding with channel coding has been proposed for coded transmit diversity. The novel use of trellis and turbo trellis codes have been discussed as possible candidates

for the outer channel coder in the STCM strategies. It was shown that the inner ACTD has better distance property than the DTD and OTD schemes.

As a means of improving cellular CDMA uplink system performance and capacity, Chapter 8 has presented the BEP performance of coded space-time receive diversity and beamforming processors. Numerical results were presented and basic guidelines for choosing between diversity, beamforming and combined diversity and beamforming systems have been discussed.

9.3 AREAS FOR FUTURE RESEARCH

This research has highlighted a number of avenues yet to be explored. These avenues fall into two broad categories, namely further parametric and performance investigations of the existing transmit diversity schemes, and the investigation of new space-time coding structures for CDMA.

Parametric and Performance Investigation. Many space-time transmit diversity schemes have been introduced in this thesis. For all of these schemes only the most general descriptions were given, and limited performance evaluations were carried out. In this regard many parametric and performance investigations can and should still be performed. This is necessary to form a complete picture of all the issues involved and performance gains over a wide range of operating conditions.

Some ideas of these future investigations are listed below:

Performance investigations. In the performance analysis carried out in this thesis perfect power control has been assumed. By perfect power control it is implied that all signals received at the base station (or mobile terminal) are of equal power. Fortunately, when considering the performance of the downlink, the assumption of perfect power control is not necessarily bad, since the near-far problem is more common to the uplink. In practice, when the number of users is large and the power control is not perfect, the performance loss can be substantial. For this reason, future work should address the situation of non perfect power control on the space-time systems for both the uplink and downlink.

Parametric investigations. In the practical implementations of space-time transmit/receive and beamforming systems, many configurations and parameter selections may be considered. In order to form a complete assessment of the advantages on offer by the different space-time coded schemes the crossover point between complexity and performance improvement should be determined. For instance, it is possible to improve the performance of all the turbo coded systems simply by choosing a different interleaver, or by employing a different decoding configuration. Also, the performance of these schemes will vary significantly according to the size of the interleaver, and comparisons between the different schemes should be performed as a function of decoding complexity and desired transmission delay.

New space-time coding structures. The conventional matched filter receiver is optimal in a single user scenario with only AWGN. In a multiuser CDMA system with MAI, the performance is degraded and its only acceptable with accurate power control, error correction coding and relatively low load. It fails terribly in a near-far situation or if the number of simultaneous users is large. One way to improve the performance of cellular CDMA systems is to use interference cancellation and multiuser detection techniques to exploit the structure of the MAI and jointly detect (and decode) the users. It is important to note that multiuser detection does not necessarily mean that the system ceases to be interference limited but it improves the performance and removes the immense sensitivity to MAI.

There are two possible approaches to the use of space-time coding and multiuser detection in a receiver:

- The multiuser detection algorithm is applied first, and the soft/hard outputs are processed by the space-time decoding algorithm.
- The space-time decoding is performed if possible within the multiuser detection algorithm, so that the data estimates that are used to estimate the MAI components are those which have been error-corrected and are thus more reliable.

In [26], the optimal ML receiver for joint decoding is proposed. As both the CDMA channel and the FEC encoders are described by finite state machines, they each impose a trellis structure on the transmission. The joint effect can be described by a joint finite state machine with a corresponding super trellis. A linear approach is taken in [241] to accommodate joint detection and decoding based on the decorrelator. This decoder is based on incorporating the linear decorrelating process into the FEC decoder by modifying the metric. In effect, the projection receiver in [241] is a decorrelating detector followed by an FEC detector based on the Mahalanobis distance [242] rather than the Euclidean distance normally used. In [243] FEC decoding is incorporated into an interference structure. By embedding Viterbi decoding within the cancellation structure, significant improvements are achieved at the expense of a substantially increased detection delay. Even further improvements can be achieved by letting the bandwidth expansion be done entirely through low-rate error control coding.

With the current developments in digital signal processing technology these techniques may be considered for inclusion into the mobile handset. As a matter of fact, the present WCDMA proposal supports interference cancellation at the mobile terminals. Therefore, future research should be focused on the combination of multiuser detection and space-time coding processing. Along these lines turbo processing may again be considered, with the combined strategy of iterative feedback decoding, diversity combining and multiuser detection.

9.4 CONCLUSION

This thesis has introduced many (some novel) space-time turbo coded techniques to increase the downlink capacity of a cellular CDMA network using multiple transmit antennas. For improving the uplink capacity, coded space-time diversity and beamforming techniques, employing multiple receive antennas, have been considered. In order to quantify the performance improvements that may be achieved, a framework for the evaluation of these systems has been constructed. Using this framework the BEP of all the space-time coding systems have been derived analytically, and evaluated under identical propagation scenarios.

The results of this thesis have shown that the use of space-time turbo coded processing is an attractive solution since it can improve system performance significantly under conditions of multipath fading for both the uplink and downlink. It was shown that the two core areas of spatial processing and channel coding can be integrated in an optimum way to increase the capacity of existing cellular CDMA networks. It is envisioned that designers of future CDMA systems and networks will work towards the goal of the optimal combination of the processing involved with iterative (turbo) decoding, diversity signalling and multiuser detection. In line with this vision, the work presented in this thesis may be used as basis for the design and evaluation of these future multiuser space-time cellular CDMA networks.

Appendix A

CORRELATED MULTIVARIATE GAMMA DISTRIBUTION

In mobile communication systems the most frequently used statistical models to describe the amplitude fading process are Rayleigh, Rician and Nakagami distributions. When the *power* of the fading amplitude is of interrest, these statistical fading models are all related to the gamma distribution. In diversity based systems the correlated multivariate gamma distribution is of interrest. With reference to Figure 3.1, this appendix presents a very general result when arbitrary Nakagami fading, arbitrary correlation and arbitrary signal powers are present on each MRC receive diversity branch.

A.1 CORRELATED MULTIVARIATE GAMMA DISTRIBUTION

With reference to Figure 3.1, the following assumptions are made in deriving the model

- arbitrary signal power, Ω_l, on branch l,
- arbitrary correlation, $\rho_{k,l}$, between branches k and l, and
- arbitrary Nakagami fading, m_l, on each branch.

Two well-known correlation models are the constant correlation model, where

$$\rho_{i,j} = \rho \qquad \forall \qquad i,j = 1,2,\cdots,M_D, \tag{A.1}$$

and the exponential correlation model where

$$\rho_{i,j} = \rho^{|i-j|} \qquad \forall \qquad i,j = 1,2,\cdots,M_D. \tag{A.2}$$

The constant correlation model is applicable to closely spaced diversity antennas. When the diversity signals are taken from a configuration which, in some physical sense, is equi-spaced (either in space, time, frequency, etc), the correlation model can be exponential. The validity of this model stems from the assumption that, given the stationary nature of the overall diversity process (assuming statistical equivalence of the signals),

the correlation between a pair of signals decreases as the separation between them increases (see Chapter 2 for a more detailed discussion on this issue).

For a fixed set of received fading amplitudes $\{\beta^{(k)}\}$, the random variables X_{ck} and X_{sk} are normally assumed Gaussian, with received power given by

$$S = \sum_{k=1}^{M_D} \beta_k^2 = \sum_{k=1}^{M_D} \{X_{ck}^2 + X_{sk}^2\} = \sum_{k=1}^{M_D} S_k, \tag{A.3}$$

with S_k the instantaneous power of the kth channel. It is noted that

$$E\{\beta_k^2\} = E\{S_k\} = \Omega_k. \tag{A.4}$$

The received instantaneous SNR per bit can be written as

$$\gamma_b = \frac{E_b}{N_0} \sum_{k=1}^{M_D} \beta_k^2 = \sum_{k=1}^{M_D} \gamma_k, \tag{A.5}$$

and

$$\overline{\gamma}_k = \frac{E_b}{N_0} E\{\beta_k^2\} = \frac{E_b}{N_0} \Omega_k, \tag{A.6}$$

the average SNR of the kth diversity branch.

The general characteristic function for an M_D branch MRC diversity system can be derived as [244]

$$\Phi_S(t) = \Pi_{k=1}^{M_D} \left| \mathbf{I}_{M_{D_k} \times M_{D_k}} - i\, t \mathbf{D}_{M_{D_k}} \left(\overline{m}^{-1}\right) \mathbf{D}_{M_{D_k}}(\Omega_k) \mathbf{J}_{M_{D_k} \times M_{D_k}} \right|^{-(m_k - m_{k+1})}, \tag{A.7}$$

where $m_{M_D} + 1 = 0$, $i = \sqrt{-1}$, and

$$\begin{aligned} \mathbf{D}_{M_{D_k}}(\Omega) &= diag\{\Omega_1, \Omega_2, \cdots, \Omega_{M_{D_k}}\}, \\ \mathbf{D}_{M_{D_k}}\{\overline{m}^{-1}\} &= diag\{m_1^{-1}, m_2^{-1}, \cdots, m_{M_{D_k}}^{-1}\}, \end{aligned} \tag{A.8}$$

and $\mathbf{J}_{M_{D_k} \times M_{D_k}}$ is an $M_{D_k} \times M_{D_k}$ correlation matrix, given by

$$\begin{aligned} \mathbf{J}_{k,l} &= \rho_{k,l} \sqrt{\frac{m_l}{m_k}},\ k \geq l, \\ k &= 1, 2, \cdots, M_D. \end{aligned} \tag{A.9}$$

The restriction

$$m_1 \geq m_2 \geq \cdots \geq m_{M_D} \tag{A.10}$$

applies and the correlation matrix $\mathbf{J}$ is valid for

$$-\frac{1}{M_D-1} < \rho < 1. \tag{A.11}$$

The multivariate gamma distribution is finally obtained by taking the inverse Fourier transform of $\Phi_S(t)$ w.r.t. t,

$$p_S(s) = \frac{1}{2\pi}\int_{-\infty}^{\infty} \Phi_S(t)e^{-its}dt. \tag{A.12}$$

It is emphasized again that the characteristic function of (A.7) is very general and valid within the constraints of (A.10) and (A.11).

A.1.1 Example

In this example we show how to calculate the pdf for the sum of $M_D = 4$ MRC receive diversity signals. We begin by calculating the characteristic function given in (A.7), and then taking the inverse Fourier transform as shown in (A.12).

In our calculations it is important to adhere to the constraints given by (A.10) and (A.11). For our example the fading parameters on the k diversity branches is arbitrarily chosen as $\{m_k\} = 4$ with average received power on each branch $\{\Omega_k\} = 1$. The correlation matrix is given by

$$\mathbf{J} = \begin{pmatrix} 1 & \rho_{21}\sqrt{\frac{m_2}{m_1}} & \rho_{31}\sqrt{\frac{m_3}{m_1}} & \rho_{41}\sqrt{\frac{m_4}{m_1}} \\ \rho_{21}\sqrt{\frac{m_2}{m_1}} & 1 & \rho_{32}\sqrt{\frac{m_3}{m_2}} & \rho_{42}\sqrt{\frac{m_4}{m_2}} \\ \rho_{31}\sqrt{\frac{m_3}{m_1}} & \rho_{32}\sqrt{\frac{m_3}{m_2}} & 1 & \rho_{43}\sqrt{\frac{m_4}{m_3}} \\ \rho_{41}\sqrt{\frac{m_4}{m_1}} & \rho_{42}\sqrt{\frac{m_4}{m_2}} & \rho_{43}\sqrt{\frac{m_4}{m_3}} & 1 \end{pmatrix}. \tag{A.13}$$

In general $\rho_{ij} = \rho_{ji}$ due to symetry (i.e. $\rho_{12} = \rho_{21}$ etc.). In our example, let $\rho_{21} = \rho_{31} = \rho_{41} = \rho_{32} = \rho_{31} = \rho_{42} = \rho_{43} = 0.65$. The correlation matrix $\mathbf{J}$ therefore reduces to

$$\mathbf{J} = \begin{pmatrix} 1 & 0.65 & 0.65 & 0.65 \\ 0.65 & 1 & 0.65 & 0.65 \\ 0.65 & 0.65 & 1 & 0.65 \\ 0.65 & 0.65 & 0.65 & 1 \end{pmatrix}. \tag{A.14}$$

The calculation of $D_{M_{D_k}}(\Omega)$ and $D_{M_{D_k}}(\overline{m}^{-1})$ follows trivially from (A.8). Using the identity

$$|\mathbf{B}| = [1-a(1-b)]^{(k-1)} \cdot [1-a(1-b+bk)], \tag{A.15}$$

with

$$\mathbf{B} = \begin{pmatrix} 1-a & -ab & \cdots & -ab \\ -ab & 1-a & \cdots & -ab \\ -ab & -ab & \cdots & -ab \\ -ab & -ab & \cdots & 1-a \end{pmatrix}_{k\times k}, \tag{A.16}$$

the characteristic function is obtained with the pdf shown in Figure A.1. Figure A.1 also displays the pdf for different values of ρ.

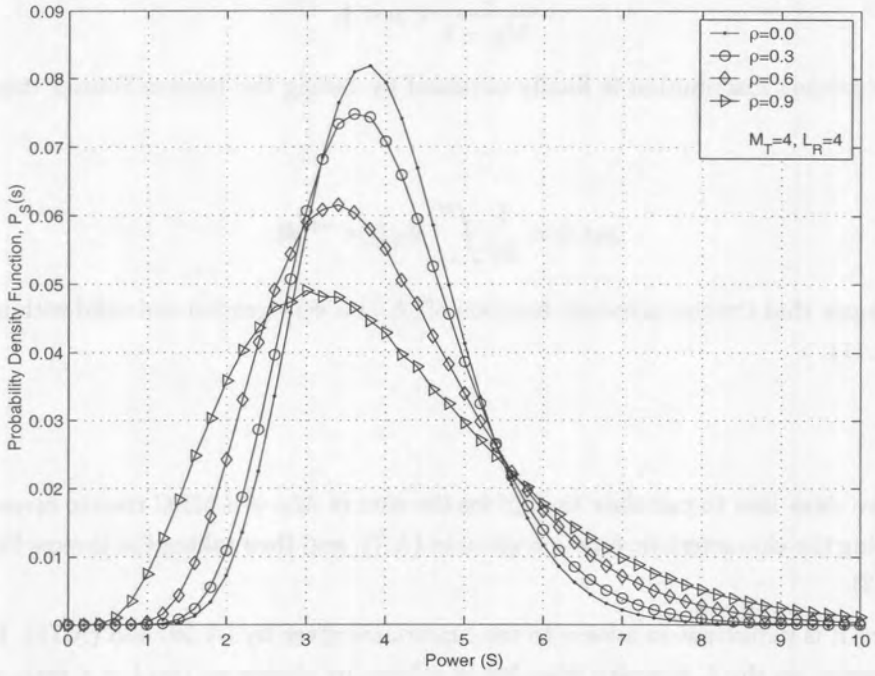

Figure A.1. Probability density function for $M = 4$ and $m = 4$.

A.1.2 Special Case

For the special case where the received signal strength is constant, i.e. $\Omega_k = \Omega$, and the fading on the branches is constant, i.e. $m_k = m = 1$, and we make use of the constant correlation model given by (A.1), the characteristic function of (A.7) reduces to

$$\Phi_S(t) = [1 - i\, t\Omega^2(1-\rho)]^{-(M-1)} \cdot [1 - i\, t\Omega^2(1-\rho+\rho M)]^{-1}. \tag{A.17}$$

Taking the inverse Fourier transform of (A.17), gives a closed form expression for the pdf of interrest as

$$\begin{aligned} p_S(s) &= \frac{1}{\Omega^2\Gamma(M)}\left(\frac{s}{\Omega^2}\right)^{M-1} \\ &\times \frac{\exp(-\frac{s}{(1-\rho)\Omega^2}) \cdot {}_1F_1(1, M, \frac{\rho M s}{(1-\rho)(1-\rho+\rho M)\Omega^2})}{(1-\rho)^{(M-1)}(1-\rho+\rho M)}, \end{aligned} \tag{A.18}$$

where ${}_1F_1(\cdot)$ is the confluent hyper geometric function [147].

Appendix B

CONVOLUTIONAL AND TURBO CODE TRANSFER FUNCTIONS

B.1 CONVOLUTIONAL CODE PERFORMANCE

B.1.1 Convolutional Codes

In this appendix, the transfer functions, $T(L, I, D)$ for the rate-1/2 and 1/3, constraint length $L_{cc} = 9$ codes are considered as required in Chapter 4. The exponents of l, i, and d of the monomial $L^l I^i D^d$ indicate, respectively, the path length, input word weight and output word weight.

For the rate-1/2 code, characterised by the generator polynomials $g_1 = (561)_8$ and $g_2 = (753)_8$, the coefficients of the transfer function have been found through computer search and they are tabulated in the literature [245]:

$$T(D) = 11D^{12} + 50D^{14} + 286D^{16} + 1630D^{18} + 9639D^{20} + \ldots,$$

where D and I are the distance and information error weight operators, respectively. Differentiating the transfer function with respect to I and setting $I = 1$, the following expression is obtained

$$\left.\frac{\delta T(I, D)}{\delta I}\right|_{I=1} = 33D^{12} + 281D^{14} + 2179D^{16} + 15035D^{18} + \ldots$$

Similarly, for the rate-1/3 code, characterised by the generator polynomials $g_1(D) = (557)_8$, $g_2 = (663)_8$ and $g_3 = (711)_8$, the coefficients of the transfer function are given by [245]:

$$T(D) = 5D^{18} + 7D^{20} + 36D^{22} + 85D^{24} + 204D^{26} + \ldots$$

with transfer function derivative written as

$$\left.\frac{\delta T(I, D)}{\delta I}\right|_{I=1} = 11D^{18} + 32D^{20} + 195D^{22} + 564D^{24} + \ldots$$

B.1.2 Orthogonal and Super-orthogonal Convolutional Codes

Now consider the transfer functions of proposed low-rate codes for combined coding and spreading are considered. These codes are the orthogonal, bi-orthogonal and super-orthogonal convolutional codes [13]. Here, $L_{oc} = L$ is used to denote the constraint length of orthogonal encoders considered.

An expression for the transfer function of orthogonal convolutional codes is given by [16]

$$T(I,D) = \frac{ID^{L2^{L-1}}(1-D^{2^{L-1}})}{1-D^{2^{L-1}}\left[1+I(1-D^{(2^{L-1})(L-1)})\right]}. \tag{B.1}$$

The corresponding expression for the transfer function derivative is [16]

$$\left.\frac{\delta T(I,D)}{\delta I}\right|_{I=1} = \frac{D^{L2^{L-1}}(1-D^{2^{L-1}})^{\,2}}{(1-2\,D^{2^{L-1}}+D^{L2^{L-1}})^{\,2}}. \tag{B.2}$$

Performing a series expansion of (B.2), the number of bit errors corresponding to an error event of length d is obtained as the multiplicity term of D^d. The results from the series expansion can then be applied to the BEP bounds discussed in Section 4.2.

When the second order terms are discarded, (B.2) can be approximated by

$$\left.\frac{\delta T(I,D)}{\delta I}\right|_{I=1} \approx D^{L\,2^{L-1}}. \tag{B.3}$$

The distance spectrum of the super-orthogonal encoder can be obtained in the same way as for the orthogonal scheme, namely through a series expansion of the differentiated transfer function. This produces [13]

$$\left.\frac{\delta T(I,D)}{\delta I}\right|_{I=1} = \frac{D^{L2^{L-1}}(1-D^{2^{L-1}})^{\,2}}{(1-2\,D^{2^{L-1}}+D^{L2^{L-1}})^{\,2}} \tag{B.4}$$

$$\approx D^{(L+2)\,2^{L-3}}. \tag{B.5}$$

The upper bounds for the BEP for the orthogonal and super-orthogonal convolutional codes can then be written, respectively, as

$$P_e \leq \frac{1}{2}\exp\left(-\sigma_{0c}\,L\,2^{L-1}\right), \tag{B.6}$$

$$P_e \leq \frac{1}{2}\exp\left(-\sigma_{0c}\,(L+2)\,2^{L-3}\right), \tag{B.7}$$

where σ_{0c} is the effective received SNR.

B.2 TURBO CODE PERFORMANCE

B.2.1 Input-Output Weight Enumerator Recursion

The notation and terminology introduced by Divsalar *et al.* in [176] are used. The turbo code is the parallel concatenation of the constituent rate $R_c = 1$ components, which is referred to as constituent code fragments.

The constituent non-trivial 4-state (2^m) code fragment is completely characterized by its state transition matrix, $\mathbf{A}(L, I, D)$, where

$$\mathbf{A}_{g_{ff}/g_{fb}} = \begin{pmatrix} L & LID & 0 & 0 \\ 0 & 0 & LD & LI \\ LID & L & 0 & 0 \\ 0 & 0 & LI & LD \end{pmatrix}. \tag{B.8}$$

For a given constituent code the number of paths of length l, input weight i, and output weight d, starting in the all-zero state, denoted by $t(l, i, d)$. Then the corresponding transfer function, or complete path enumerator, is defined by [246]

$$\begin{aligned} \mathbf{T}(L, I, D) &= \sum_{l\geq 0}\sum_{i\geq 0}\sum_{d\geq 0} L^l\, I^i\, D^d \cdot t(l, i, d) \\ &= \left[(\mathbf{I} - \mathbf{A}(L, I, D))^{-1}\right]. \end{aligned} \tag{B.9}$$

The first element of the matrix given in (B.9) produces the transfer function of the constituent code

$$T(L, I, D) = \mathbf{T}^{(1,1)}(L, I, D) = \frac{T_N}{T_D}. \tag{B.10}$$

where

$$T_N = 1 - LD - L^2 I - L^3(D^2 - I^2), \tag{B.11}$$

and

$$T_D = 1 - L(1 + I) - L^3(D^2 - I - I^2 - I^3 D^2) - L^4(D^2 - I^2 - I^2 D^4 + I^4 D^2). \tag{B.12}$$

For a constituent code, the path input/output weight index is used to determine the output weight probability distribution function. For the constituent encoder, the path input/output weight index, is

$$\begin{aligned} t(l, i, d) &= t(l-1, i-1, d) + t(l-1, i, d) + t(l-3, i-3, d-2) - t(l-3, i-2, d) \\ &- t(l-3, i-1, d) + t(l-3, i, d-2) - t(l-4, i-4, d-2) + t(l-4, i-2, d-4) \\ &+ t(l-4, i-2, d) - t(l-4, i, d-2) + \delta(l, i, d) - \delta(l-1, i-1, d) \\ &- \delta(l-2, i-1, d) - \delta(l-3, i, d-2) + \delta(l-3, i-2, d) \end{aligned} \tag{B.13}$$

with initial conditions such that $t(l, i, d) = 0$ for any negative index, where $\delta(l, i, d) = 1$ if $l = i = d = 0$ and $\delta(l, i, d) = 0$ otherwise.

B.2.2 Input-Output Conditional Probability Density Function

In this section the conditional probability of producing a codeword fragment of weight d given a randomly selected input sequence of weight i is evaluated. This is given by

$$p(d \mid i) = \frac{t(N_{tc}, i, d)}{\sum_{d'} t(N_{tc}, i, d')} = \frac{t(N_{tc}, i, d)}{\binom{N_{tc}}{i}}. \tag{B.14}$$

The conditional pdf (cpdf) of the constituent recursive convolutional encoder is shown in Figure B.1, for an interleaver size of $N_{tc} = 100$. Since the code fragment only produces even output weights, the uneven weight probabilities are not shown. Similar distributions are obtained when the interleaver size is increased. In this thesis the latter is refered to as the Divsalar cpdf. It was shown in [176] that, given a sufficiently large input codeword weight i, the cpdf approaches a binomial distribution. Given a balanced source with N_{tc} sufficiently large (typically > 100), this condition will always be met. Thus, in addition to the calculated weight distributions the cpdf, described as a binomial probability distribution with probability $1/2$ (taken over $N_{tc} = 100$ trails) is also shown for reference purposes.

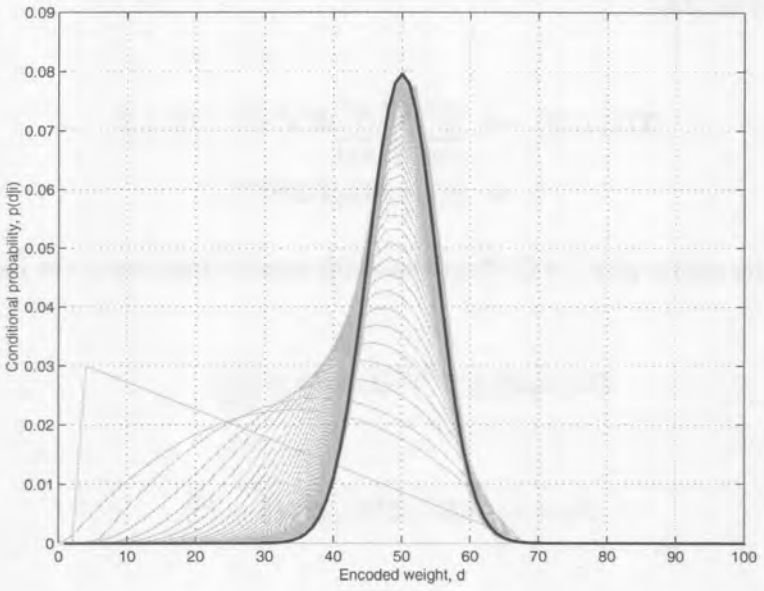

Figure B.1. Conditional probability density function (cpdf) as a function of the output weight d of the constituent recursive convolutional encoder, given input weight i, with interleaver size $N_{tc} = 100$.

If the interleavers of the encoder are selected randomly and independently, the cpdf $p(d \mid i)$ that any input sequence $\mathbf{u}$ of weight i will be mapped into code fragments of weights d^s, d^p is

$$\begin{aligned} R_c = 1/2 : p(d \mid i) &= p^s(d_s \mid i) * p^p(d_p \mid i), \\ R_c = 1/3 : p(d \mid i) &= p^s(d_s \mid i) * p^p(d_p \mid i) * p^p(d_p \mid i), \end{aligned} \tag{B.15}$$

where $*$ denotes convolution.

In (B.15), $p^s(d_s \mid i)$ corresponds to the systematic output weight probability, and $p^p(d_p \mid i)$ corresponds to the non-punctured parity output weight probability. Therefore, the total codeword output weight relative to the all-zero codeword is $d = d_s + d_p$ and $d = d_s + 2d_p$, for the rate-1/2 and rate-1/3 coders, respectively. The extension to the low-rate code, e.g. $R_c = 1/6$ follows in a similar manner.

In the calculation of the BER for turbo codes of different code rate we have to integrate over the total code input-output weight probability distribution, denoted by $\tilde{p}(d_0, d_i, \ldots, d_Z \mid i)$. This is achieved by the introduction of the conditional expectation $E_{d|i}\{\cdot\}$ which should be taken over the probability distribution $\tilde{p}(d_0, d_i, \ldots, d_Z \mid i)$. Here, Z constitutes the number of constituent code fragments.

REFERENCES

[1] R. Prasad, *CDMA for wireless personal communications.* Artech House, 1996.

[2] L. C. Godara, "Application of antenna arrays to mobile communications, part I: Performance improvement, feasibility, and system considerations," *Proceedings of the IEEE*, vol. 85, pp. 1031–1060, July 1997.

[3] L. C. Godara, "Application of antenna arrays to mobile communications, part II: Beamforming and direction-of-arrival considerations," *Proceedings of the IEEE*, vol. 85, pp. 1195–1245, August 1997.

[4] A. F. Naguib, A. Paulraj, and T. Kailath, "Capacity improvement with base-station antenna arrays in cellular cdma," *IEEE Transactions on Vehicular Technology*, vol. 43, pp. 691–698, August 1994.

[5] A. F. Naguib and A. Paulraj, "Performance enhancement and trade-offs of smart antennas in cdma cellular networks," in *VTC'95: IEEE Vehicular Technology Conference*, (Chicago, USA), pp. 40–44, July 1995.

[6] A. J. Paulraj and C. B. Papadias, "Space-time processing for wireless communications," *IEEE Signal Processing Magazine*, pp. 49–83, November 1997.

[7] A. J. Paulraj and E. Lindskog, "Taxonomy of space-time processing for wireless networks," *IEE Proceedings on Radar, Sonar and Navigation*, vol. 145, pp. 25–31, February 1998.

[8] "A Regulatory Framework for UMTS." Report #1 from the UMTS Forum, June 1997.

[9] E. Berruto, M. Gudmundson, and R. Menolascino, "Research activities on UMTS radio interface, network architectures and planning," *IEEE Communications Magazine*, vol. 36, pp. 82–95, February 1998.

[10] "UMTS 30.01 Baseline Document." ETSI SMG #23, Budapest, Hungary, October 1997.

[11] G. J. Pottie, "System design issues in personal communications," *IEEE Personal Communications Magazine*, vol. 2, pp. 50–67, October 1995.

[12] W. C. Y. Lee, "Overview of cellular CDMA," *IEEE Transactions on Vehicular Technology*, vol. 40, pp. 291–302, May 1991.

[13] A. J. Viterbi, *Principles of Spread Spectrum Communication.* Addison-Wesley Publishing Company, Massachusetts, 1995.

[14] S. Lin and D. J. Costello, Jr, *Error control coding - Fundamentals and Applications.* Prentice-Hall, 1983.

[15] G. C. Clark and J. Bibb Cain, *Error-Correction Coding for Digital Communications.* Plenum Press, 1988.

[16] A. J. Viterbi and J. K. Omura, *Principles of Digital Communication and Coding.* McGraw-Hill, 1979.

[17] W. W. Peterson and E. J. Weldon, *Error-Correcting Codes.* Cambridge Mass.: MIT Press, 1972.

[18] R. G. Gallager, *Information Theory and Reliable Communication.* Wiley: New York, 1968.

[19] E. R. Berlekamp, *Algebraic Coding Theory.* McGraw-Hill: New York, 1968.

[20] E. R. Berlekamp, R. E. Peile, and S. P. Pope, "The application of error control to communications," *Proceedings of IEEE*, vol. 25, pp. 44–57, 1987.

[21] E. Biglieri, D. Divsalar, P. J. McLane, and M. K. Simon, *Introduction to Trellis-Coded Modulation with Applications.* Macmillan, 1991.

[22] A. J. Viterbi, "Error bounds for convolutional codes and an asymptotically optimum decoding algorithm," *IEEE Transactions on Information Theory*, vol. 13, pp. 260–269, April 1967.

[23] G. D. Forney, "Maximum-likelihood sequence estimation of digital sequences in the presence of intersymbol interference," *IEEE Transactions on Information Theory*, vol. 18, pp. 368–378, May 1972.

[24] G. Ungerboeck, "Channel coding with Multilevel/Phase signals," *IEEE Transactions on Information Theory*, vol. IT-28, pp. 55–67, January 1982.

[25] S. Verdú, "Minimum probability of error for asynchronous Gaussian multiple-access channels," *IEEE Transactions on Information Theory*, vol. 32, pp. 85–96, January 1986.

[26] T. R. Giallorenzi and S. G. Wilson, "Multiuser ML sequence estimation for convolutionally coded asynchronous ds-cdma systems," *IEEE Transactions on Communications*, vol. 44, pp. 997–1008, August 1996.

[27] T. R. Giallorenzi and S. G. Wilson, "Suboptimum multiuser receivers for convolutionally coded asynchronous ds-cdma systems," *IEEE Transactions on Communications*, vol. 44, pp. 1183–1196, September 1996.

[28] P. D. Alexander, L. K. Rasmussen, and C. B. Schlegel, "A linear receiver for coded multiuser CDMA," *IEEE Transactions on Communications*, vol. 45, pp. 605–610, May 1997.

[29] J. Hagenauer, "Source-controlled channel decoding," *IEEE Transactions on Communications*, vol. 43, pp. 2449–2457, September 1995.

[30] J. Lodge and M. Gertsman, "Joint detection and decoding by turbo processing for fading channel communications," in *Proceedings of the International Symposium on Turbo Codes and Related Topics*, (Brest, France), pp. 88–95, 1997.

[31] C. Douillard, M. Jezequel, C. Berrou, A. Picart, P. Didier, and A. Glavieux, "Iterative correction of intersymbol interference," *European Transactions on Telecommunication*, vol. 6, pp. 507–511, September/October 1995.

[32] P. Hoeher, "On channel decoding and multi-user detection for DS-CDMA," in *IEEE International Conference on Universal Personal Communication (ICUPC)*, (Ottawa, Canada), pp. 641–646, 1993.

[33] M. C. Reed, C. B. Schlegel, P. D. Alexander, and J. A. Asenstorfer, "Joint multiuser detection for CDMA with FEC," in *Proceedings of the International Symposium on Turbo Codes and Related Topics*, (Brest, France), pp. 162–165, 1997.

[34] P. D. Alexander, A. J. Grant, and M. C. Reed, "Iterative detection in code-division multiple-access with error control coding," *European Transactions on Telecommunication*, vol. 9, July-August 1998.

[35] A. J. Viterbi, "Orthogonal tree codes for communication in the presence of white Gaussian noise," *IEEE Transactions on Communications*, vol. COM-15, pp. 238–242, April 1967.

[36] A. J. Viterbi, "Spread spectrum communication — myths and realities," *IEEE Communication Magazine*, pp. 11–18, July 1979.

[37] A. J. Viterbi, "When not to spread spectrum — a sequel," *IEEE Communication Magazine*, vol. 23, pp. 12–17, April 1985.

[38] A. J. Viterbi, "Very low rate convolutional codes for maximum theoretical performance of spread-spectrum multiple-access channels," *IEEE Journal on Selected Areas in Communications*, vol. 8, pp. 641–649, May 1990.

[39] J. Hui, "Throughput analysis for code division multiple accessing of the spread spectrum channel," *IEEE Journal of Selected Areas in Communications*, vol. SAC-2, July 1984.

[40] P. Frenger, P. Orten, and T. Ottosson, "Combined coding and spreading in CDMA systems using maximum free distance convolutional codes," in *48th Annual Vehicular Technology Conference*, (Ottawa, Canada), May 1998.

[41] P. Frenger, P. Orten, and T. Ottosson, "Code-spread CDMA using low-rate convolutional codes," in *Proceedings of ISSSTA '98*, (Sun City, South Africa), pp. 374–378, September 1998.

[42] K. Pehkonen and P. Komulainen, "A superorthogonal turbo-code for CDMA applications," in *ISSSTA'96: International Symposiun on Spread Spectrum Techniques & Apllications*, (Mainz, Germany), pp. 580–584, September 1996.

[43] K. Pehkonen and P. Komulainen, "Performance evaluation of superorthogonal turbo codes in AWGN and flat Rayleigh fading channels," *IEEE Journal on Selected Areas in Communications*, vol. 16, pp. 196–205, February 1998.

[44] G. D. Boudreau, D. D. Falconer, and S. A. Mahmoud, "A comparison of trellis coded versus convolutionally coded spread-spectrum multiple-access systems," *IEEE Journal on Selected Areas of Communication*, vol. 8, pp. 628–640, May 1990.

[45] B. D. Woerner and W. E. Stark, "Trellis-coded direct-sequence spread-spectrum communications," *IEEE Transactions on Communications*, vol. 42, pp. 3161–3170, December 1994.

[46] W. Y. Kuo and M. P. Fitz, "Design and analysis of transmitter diversity using intentional frequency offset for wireless communications," *IEEE Transactions on Vehicular Technology*, vol. VT-46, pp. 691–698, November 1997.

[47] T. Hattori and K. Hirade, "Multitransmitter simulcast digital signal transmission by using frequency offset strategy in land mobile radio-telephone system," *IEEE Transactions on Vehicular Technology*, vol. VT-27, pp. 170–176, May 1992.

[48] A. Hiroike, F. Adachi, and N. Nakajima, "Combined effects of phase sweeping transmitter diversity and channel coding," *IEEE Transactions on Vehicular Technology*, vol. 41, pp. 170–176, May 1992.

[49] A. Wittneben, "Base station modulation diversity for SIMULCAST," in *VTC'91: IEEE Vehicular Technology Conference*, pp. 848–853, May 1991.

[50] A. Wittneben, "A new bandwidth efficient transmit antenna modulation diversity scheme for linear digital modulation," in *ICC'93: International Conference on Communications*, (Geneva, Switzerland), pp. 1630–1634, May 1993.

[51] D. Gerlach and A. Paulraj, "Adaptive transmitting antenna array with feedback," *IEEE Signal Processing Letters*, vol. 1, October 1994.

[52] G. G. Raleigh, S. D. Diggavi, V. K. Jones, and A. Paulraj, "A blind adaptive transmit antenna algorithm for wireless communications," in *ICC'95: IEEE International Conference on Communications*, vol. 3, p. 1949, 1995.

[53] D. Gerlach and A. Paulraj, "Base station transmitting antenna arrays for multipath environments," *Signal Processing*, no. 54, pp. 59–73, 1996.

[54] N. Seshadri and J. H. Winters, "Two signalling schemes for improving the error performance of frequency-division-duplex transmission system using transmitter antenna diversity," *International Journal of Wireless Information Networks*, vol. 1, pp. 49–60, 1994.

[55] J. H. Winters, "Diversity gain of transmit diversity in wireless systems with Rayleigh fading," in *ICC'94: IEEE International Conference on Communications*, (New Orleans, LA), pp. 1121–1125, May 1994.

[56] J. H. Winters, "Diversity gain of transmit diversity in wireless systems with Rayleigh fading," *IEEE Transactions on Vehicular Technology*, vol. 47, pp. 119–123, February 1998.

[57] H. Olofsson, M. Almgren, and M. Hook, "Transmitter diversity with antenna hopping for wireless communication networks," in *IEEE VTC'97*, (Phoenix, Arizona, USA), May 1997.

[58] J. H. Winters, "Switched diversity with feedback for DPSK mobile radio systems," *IEEE Transactions on Vehicular Technology*, vol. IT-32, pp. 134–150, February 1983.

[59] G. Raleigh and J. M. Cioffi, "Spatio-temporal coding for wireless communications," in *IEEE GLOBECOM'96*, pp. 1809–1814, December 1996.

[60] J. H. Winters, "Smart antennas for wireless systems," *IEEE Personal Communication*, vol. 2, pp. 23–27, February 1998.

[61] J. Lu, K. B. Letaief, M. L. Liou, and J. C.-I. Chuang, "On the use of modulation and diversity for enhancing cellular spectrum efficiency for wireless multimedia communication networks," in *IEEE GLOBECOM'97*, (Phoenix, Arizona, USA), pp. 1168–1172, November 1997.

[62] L. J. Cimini and N. R. Sollenberger, "OFDM with diversity and coding for high bit-rate mobile data applications," in *Proceedings of 3rd Internationl Workshop on Mobile Multimedia Communications*, p. A.3.1.1, September 1996.

[63] V. Weerackody, "Diversity for direct-sequence spread spectrum system using multiple transmit antennas," in *ICC'93: International Conference on Communications*, (Geneva, Switzerland), pp. 1775–1779, May 1993.

[64] P. Diaz and R. Agusti, "The use of coding and diversity combining for mitigating fading effects in a DS/CDMA system," *IEEE Transactions on Vehicular Technology*, vol. 47, pp. 95–102, February 1998.

[65] W. Lee, *Mobile Communications Design Fundamentals*. Wiley Series in Telecommunications, 1993.

[66] T. Rappaport, *Wireless Communications*. Upper Saddle River, NJ: Prentice Hall, 1996.

[67] P. Balaban and J. Salz, "Optimum diversity combining and equalization in digital data transmission with applications to cellular mobile radio - Part I: Theoretical considerations," *IEEE Transactions on Communication*, vol. 40, pp. 885–894, May 1992.

[68] P. Balaban and J. Salz, "Optimum diversity combining and equalization in digital data transmission with applications to cellular mobile radio - Part II: Numerical results," *IEEE Transactions on Communication*, vol. 40, pp. 895–907, May 1992.

[69] M. Clark, L. Greenstein, W. Kennedy, and M. Shafi, "Matched filter performance bounds for diversity combining receivers in digital mobile radio," *IEEE Transactions on Vehicular Technology*, vol. 41, pp. 356–362, November 1992.

[70] P. van Rooyen and R. Kohno, "DS-CDMA performance with maximum ratio combining and antenna arrays in Nakagami multipath fading," in *Proceedings IEEE ISSSTA*, (Mainz, Germany), pp. 292–296, University of Kaiserslautern, 1996.

[71] P. van Rooyen, R. Kohno, and I. Oppermann, "DS-CDMA performance with maximal ratio combining and antenna arrays," *Wireless Networks*, vol. 4, pp. 479–488, October 1998.

[72] C. Balanis, *Antenna Theory - Analysis and Design*, ch. 6. USA: Wiley, second ed., 1997.

[73] F. Rashid-Farrokhi, K. R. Liu, and L. Tassiulas, "Transmit beamforming and power control for cellular wireless systems," *IEEE Journal on Selected Areas of Communication*, vol. 16, pp. 1437–1450, October 1998.

[74] J. Litva and T. Lo, *Digital Beamforming in Wireless communications*. Norwood, MA: Artech House, 1996.

[75] W. Lee and M. Bae, "Efficient interference suppression using a constrained beamformer for mobile communications," in *Proceedings IEEE ISSSTA*, (Mainz, Germany), pp. 282–286, University of Kaiserslautern, 1996.

[76] P. Zetterberg and P. L. Espensen, "A Downlink Beam Steering Technique for GSM/DCS1800/PCS1900," in *Proceedings of IEEE PIMRC*, October 1994.

[77] F. Rashid-Farrokhi, L. Tassiulas, and K. J. R. Liu, "Joint optimal power control and beamforming in wireless networks with antenna arrays," *IEEE Transactions on Communication*, 1998.

[78] S. C. Swales, M. A. Beach, and D. J. Edwards, "Multi-beam adaptive base station antennas for cellular land mobile radio systems," in *Proceedings of IEEE Vehicular Technology Conference, VTC '89*, pp. 341–348, 1989.

[79] P. L. E. P. Zetterberg and P. Mogensen, "Propagation, Beam Steering and Uplink Combining Algorithms for Cellular Systems ." ACTS Mobile Communication Summit, Garanda, Spain, November, 1996.

[80] R. Gooch and J. Lundell, "The CM array: An adaptive beamformer for constant modulus signals," in *Proceedings of IEEE ICASSP*, pp. 1523–2526, 1986.

[81] M. Jones and M. an Wickert, "Direct sequence spread spectrum using directionally constrained adaptive beamforming to null interference," *IEEE Journal on Selected Areas of Communication*, vol. 13, pp. 71–79, January 1995.

[82] Y. Li, M. Feuerstein, and D. Reudink, "Performance evaluation of a cellular base station multibeam antenna," *IEEE Transactions on Vehicular Technology*, vol. 46, pp. 1–9, February 1997.

[83] M. ju Ho, G. L. Stüber, and M. D. Austin, "Performance of switched-beam smart antennas for cellular radio systems," *IEEE Transactions on Vehicular Technology*, vol. 47, pp. 10–19, February 1998.

[84] T. Matsumoto, S. Nishioka, and D. Hodder, "Beam-selection performance analysis of switched beam multibeam antenna system in mobile communications environment," *IEEE Transactions on Vehicular Technology*, vol. 46, pp. 10–20, February 1997.

[85] M. Pursley, "Performance evaluation for phase-coded spread-spectrum multiple access communications - Part I: system analysis," *IEEE Transactions on Communication*, vol. COM-25, pp. 795–799, August 1977.

[86] M. Pursley, "Performance evaluation for phase-coded spread-spectrum multiple access communications - Part II: code sequence analysis," *IEEE Transactions on Communication*, vol. COM-25, pp. 800–803, August 1977.

[87] M. Pursley, D. Sarwate, and W. Stark, "Error probability for direct-sequence multiple access communications - Part I: upper and lower bounds," *IEEE Transactions on Communication*, vol. COM-30, pp. 975–984, May 1982.

[88] M. Pursley, D. Sarwate, and W. Stark, "Error probability for direct-sequence multiple access communications - Part I: approximations," *IEEE Transactions on Communication*, vol. COM-30, pp. 985–995, May 1982.

[89] D. Laforgia, A. Luvison, and V. Zingarelli, "Bit error rate evaluation for spread-spectrum multiple access systems," *IEEE Transactions on Communication*, vol. COM-32, pp. 660–669, June 1984.

[90] E. Geraniotis and M. Pursley, "Performance of coherent direct-sequence spread-spectrum communications over specular multipath fading channels," *IEEE Transactions on Communication*, vol. COM-33, pp. 502–508, June 1985.

[91] T. Eng and L. Milstein, "Coherent DS-CDMA performance in Nakagami multipath fading," *IEEE Transactions on Communication*, vol. 43, pp. 1134–1143, February/March/April 1995.

[92] J. Lehnert and M. Pursley, "Error probabilities for binary direct sequence spread-spectrum communications with random signature sequences," *IEEE Transactions on Communication*, vol. COM-35, pp. 87–98, January 1987.

[93] M. Kavehrad, "Performance of nondiversity receivers for spread spectrum in indoor wireless communications," *AT&T Technical Journal*, vol. 64, pp. 1181–1210, July-August 1985.

[94] J. Holtzman, "A simple, accurate method to calculate spread-spectrum multiple access error probabilities," *IEEE Transactions on Communication*, vol. 40, pp. 461–464, March 1992.

[95] K. Letaief, "Efficient evaluation of the error probabilities of spread-spectrum multiple access communications," *IEEE Transactions on Communication*, vol. 45, pp. 239–246, February 1997.

[96] A. Abu-Dayya and N. Beaulieu, "Micro- and macrodiversity NCFSK (DPSK) on shadowed Nakagami-fading channels," *IEEE Transactions on Communication*, vol. 42, pp. 2693–2702, September 1994.

[97] V. Aalo, "Performance of maximal-ratio diversity systems in a correlated Nakagami-fading environment," *IEEE Transactions on Communication*, vol. 43, pp. 2360–2369, August 1995.

[98] A. Abu-Dayya and N. Beaulieu, "Micro- and macrodiversity MDPSK on shadowed frequency selective channels," *IEEE Transactions on Communication*, vol. 43, pp. 2334–2343, August 1995.

[99] N. Benvenuto and L. Tomba, "Performance comparison of space diversity and equalization techniques for indoor radio systems," *IEEE Transactions on Vehicular Technology*, vol. 46, pp. 358–368, May 1997.

[100] C. Wijffels, H. Misser, and R. Prasad, "A micro-cellular CDMA system over slow and fast Rician fading radio channels with forward error correction coding and diversity," *IEEE Transactions on Vehicular Technology*, vol. 42, pp. 570–580, November 1993.

[101] P. Jung, B. Steiner, and B. Stilling, "Exploitation of intracell macrodiversity in mobile radio systems by deployment of remote antennas," in *Proceedings of IEEE ISSSTA*, (Mainz,Germany), pp. 302–307, University of Kaiserslautern, 1996.

[102] A. Steil and J. Blanz, "Spectral efficiency of JD-CDMA mobile radio systems applying coherent receiver antenna diversity with directional antennas," in *Proceedings IEEE ISSSTA*, (Mainz,Germany), pp. 313–319, University of Kaiserslautern, 1996.

[103] J. H. Winters, J. Salz, and R. D. Gitlin, "The impact of antenna diversity on the capacity of wireless communications systems," *IEEE Transactions on Communications*, vol. 42, pp. 1740–1751, February/March/April 1994.

[104] G. Foschini, "Layered space-time architecture for wireless communication in a fading environment when using multi-element antennas," *AT&T Bell Technical Journal*, vol. 1, 1996.

[105] M. Feuerstein, K. Blackard, T. Rappaport, S. Seidel, and H. Xia, "Path loss, delay spread and outage models as functions of antenna height for microcellular system design," *IEEE Transactions on Vehicular Technology*, vol. 43, pp. 487–498, August 1994.

[106] S. Anderson, M. Millnert, M. Viberg, and B. Wahlberg, "An adaptive array for mobile communication systems," *IEEE Transactions on Vehicular Technology*, vol. 40, pp. 230–236, 1991.

[107] V. Ghazi-Moghadam and M. Kaveh, "Interference cancellation using antenna arrays," in *Proceedings IEEE PIMRC*, (Toronto, Canada), pp. 936–939, 1995.

[108] R. Kohno, H. Imai, M. Hatori, and S. Pasupathy, "Combination of an adaptive array antenna and a canceller of interference for direct-sequence spread-spectrum multiple-access system," *IEEE Journal on Selected Areas of Communication*, vol. 8, pp. 675–681, May 1990.

[109] J. C. Liberti and T. S. Rappaport, "A Geometrically Based Model for Line of Sight Multi-path Radio Channels," in *Proceedings of IEEE VTC*, pp. 844–48, 1996.

[110] T. Wong, T. Lok, J. Lehnert, and M. Zoltowski, "A linear receiver for direct-sequence spread-spectrum multiple-access systems with antenna arrays and blind adaptation," *IEEE Trans. Inform. Theory*, vol. 44, no. 2, pp. 659–676, 1998.

[111] R. Roy, "An overview of SDMA technology." ArrayComm, April 98.

[112] E. Buracchini, F. Muratore, V. Palestini, and M. Sinibaldi, "Performance analysis of a mobile system based on combined SDMA/CDMA access techniques," in *Proceedings of ISSSTA'96*, (Mainz, Germany), pp. 370–374, University of Kaiserslautern, 1996.

[113] B. Suard, A. Naguib, G. Xu, and A. Paulraj, "Performance of CDMA mobile communication system using antenna arrays," in *Proceedings IEEE ICASSP*, pp. IV–153–IV–156, 1993.

[114] P. Grant, J. Thompson, and B. Mulgrew, "Antenna arrays for cellular cdma systems," in *CDMA Techniques for Third Generation Mobile Systems* (F. Swartz, P. van Rooyen, I. Oppermann, and M. Lötter, eds.), pp. 59–81, Kluwer Academic Publishers, 1998.

[115] G. Efthymoglou, V. Aalo, and H. Helmken, "Performance analysis of coherent DS-CDMA systems in a Nakagami fading channel with arbitrary parameters," *IEEE Transactions on Vehicular Technology*, vol. 46, pp. 289–297, May 1997.

[116] J. Salz and J. H. Winters, "Effects of correlated fading on adaptive arrays in digital mobile radio," *IEEE Transactions on Vehicular Technology*, vol. 43, pp. 1049–1057, November 1994.

[117] A. Weiss and B. Friedlander, "Fading effects on antenna arrays in cellular communications," *IEEE Trans. Sign. Proc.*, vol. 45, pp. 1109–1117, May 1997.

[118] C. Farsakh and J. Nossek, "Comparison of symmetric antenna array configurations by their spatial separation potential," in *Proceedings of IEEE ICUPC*, pp. 433–436, 1996.

[119] J. Winter, J. Salz, and R. Gitlin, "The impact of antenna diversity on the capacity of wireless communication systems," *IEEE Transactions on Communication*, vol. 42, pp. 1740–1750, February/March/April 1994.

[120] V. Barroso, M. Rendas, and J. Gomes, "Impact of array processing techniques on the design of mobile communication systems," *Proceedings IEEE MEC*, pp. 1291–1294, 1994.

[121] M. Mizuno and T. Ohgane, "Application of adaptive array antennas to radio communications," *Electron. Commun. Japan*, vol. 77, pp. 48–59, 1994.

[122] L. Godara, "Applications of antenna arrays to mobile communications, Part I: Performance Improvement, Feasibility and System Considerations," *Proceedings IEEE*, vol. 85, pp. 1031–1060, 7 1997.

[123] M. Barrett and R. Arnott, "Adaptive antennas for mobile communications," *Electron. Commun. Eng. J.*, vol. 6, pp. 203–214, 1994.

[124] S. Swales, M. Beach, D. Edwards, and J. McGeehan, "The performance enhancement of multibeam adaptive basestation antennas for cellular land mobile radio systems," *IEEE Transactions on Vehicular Technology*, vol. 39, pp. 56–67, 1990.

[125] M. Goldburg and R. Roy, "The impacts of SDMA on PCS system design," (San Diego, CA), pp. 242–246, 1994.

[126] M. Lötter, *Numerical analysis of spatial/temporal cellular CDMA systems.* PhD thesis, University of Pretoria, 1999.

[127] W. Mohr, "Impact of radio channel properties on adaptive antenna concepts for terrestrial mobile radio applications," in *Proceedings IEEE ICT*, (Melbourne, Sydney), pp. 405–410, 2-5 April 1997.

[128] B. Sklar, "Rayleigh fading channels in mobile digital communication systems Part I: characterization," *IEEE Communications Magazine*, pp. 90–100, July 1997.

[129] J. Proakis, *Digital Communications*, ch. 14. Singapore: McGraw-Hill, 1995.

[130] G. Stüber, *Fundamentals of Mobile Communications.* Kluwer Academic Publishers, 1998.

[131] T. Zwick, D. Didascalou, and W. Wiesbeck, "A broadband statistical channel model for SDMA applications," in *Proceedings IEEE ISSSTA*, (Sun City, South Africa), pp. 527–531, University of Pretoria, September 1998.

[132] M. Nakagami, "The m-distribution - a general formula of intensity distribution of rapid fading," in *Statistical Methods in Radio Wave Propagation* (W. Hoffman, ed.), Elmsford, NY: Pergamon, 1960.

[133] W. Braun and U. Dersch, "A physical mobile radio channel model," *IEEE Transactions on Vehicular Technology*, vol. 40, pp. 472–482, May 1991.

[134] H. Suzuki, "A statistical model for urban multipath channels with random delay," *IEEE Transactions on Communication*, pp. 9–16, February 1972.

[135] J. Parsons, *The mobile radio propagation channel.* McGraw Hill: New York, 1992.

[136] R. Clarke, "A statistical theory of mobile-radio reception," *Bell Sys. Tech. J.*, vol. 47, pp. 957–1000, 1968.

[137] R. Ertel, K. Sowerby, T. Rappaport, and J. Reed, "Overview of spatial channel models for antenna array communication systems," *IEEE Personal Communications Magazine*, vol. 5, pp. 10–22, February 1998.

[138] W. Jakes, *Microwave Mobile Communications.* Wiley: New York, 1974.

[139] M. Lötter and P. van Rooyen, "Modeling spatial aspects of cellular CDMA/SDMA systems.," *IEEE Commun. Let.*, vol. 3, pp. 128–131, May 1999.

[140] W. C. Y. Lee, *Mobile Communication Engineering.* McGraw Hill Publications, 1982.

[141] D. R. van Rheeden and S. C. Gupta, "A Geometric model for fading correlation in multi-path radio channels," in *Proceedings of ICC*, (Atlanta, Georgia), pp. 1655–1659, June 1998.

[142] W. C. Y. Lee, "Antenna spacing requirements for a mobile base-station diversity," *Bell Systems Technical Journal*, vol. 50, pp. 1859–1877, July-August 1971.

[143] D. Hong and S. Rappaport, "Traffic model and performance analysis for cellular mobile radio telephone systems with prioritized and non-prioritized handoff procedures," *IEEE Transactions on Vehicular Technology*, vol. VT-35, pp. 77–92, August 1986.

[144] K. Leung, W. Massey, and W. Whitt, "Traffic models for wireless communication networks," *IEEE Journal on Selected Areas of Communication*, vol. 12, pp. 1353–1364, October 1994.

[145] J. Talvitie, *Wideband radio channel measurement, characterisation and modeling for wireless local loop applications.* PhD thesis, University of Oulu, 1997.

[146] M. Lötter and P. van Rooyen, "Performance of DS/CDMA systems with antenna arrays in non-uniform environments," *IEEE Journal on Selected Areas in Communication*, 1999. Accepted for publication.

[147] M. Abramowitz and I. Stegun, *Handbook of Mathematical functions.* Dover, 1972.

[148] A. Hottinen and R. Wichman, "Transmit diversity by antenna selection in CDMA downlink," in *Proceedings of ISSSTA '98*, (Sun City, South Africa), pp. 767–770, September 1998.

[149] J.-C. Guey, M. P. Fitz, M. R. Bell, and W. Y. Kuo, "Signal design for transmitter diversity wireless communication systems over Rayleigh fading channels," in *VTC'96: Vehicular Technology Conference*, pp. 136–140, 1996.

[150] J.-C. Guey, "Concatenated coding for transmit diversity schemes," in *VTC'99: Vehicular Technology Conference*, (Amsterdam, The Netherlands), pp. 2500–2504, 1999.

[151] S. V. Alamouti, "A simple transmit diversity technique in wireless communications," *IEEE Journal on Selected Areas in Communication*, vol. 16, pp. 1451–1458, October 1998.

[152] K. Ban, M. Katayama, T. Yamazato, and A. Ogawa, "The DS/CDMA system using transmission diversity for indoor wireless communications," in *PIMRC'96: International Symposium on Personal Indoor and Mobile Radio Communications*, (Taipei, Taiwan), pp. 803–812, October 1996.

[153] K. Ban, M. Katayama, W. E. Stark, T. Yamazato, and A. Ogawa, "Multi-antenna transmission scheme for convolutionally coded DS/CDMA," *IEICE Transactions on Communication*, vol. E80-A, pp. 2437–2444, December 1997.

[154] I. Jeong and M. Nakagawa, "A novel transmission diversity system in TDD-CDMA," in *Proceedings of ISSSTA '98*, (Sun City, South Africa), pp. 771–775, September 1998.

[155] D. Hatzinakos and C. Nikias, "Estimation of multipath channel response in frequency selective channels," *IEEE Journal on Selected Areas in Communication*, vol. 7, pp. 12–19, January 1989.

[156] V. A. N. Borroso, J. M. F. Moura, and J. M. F. Xavier, "Blind array channel division multiple access (AchDMA) for mobile communications," *IEEE Transactions on Signal Processing*, vol. 46, pp. 737–752, March 1998.

[157] B. Suard, A. Naguib, G. Xu, and A. Paulraj, "Performance analysis of CDMA mobile communication systems using antenna array," in *ICASSP'93: International Conference on Acoustic, Speech and Signal Processing*, (Minneapolis, MN), pp. 153–156, April 1993.

[158] A. Wojnar, "Unknown bounds on performance in Nakagami channels," *IEEE Transactions on Communication*, vol. COM-34, pp. 22–24, January 1986.

[159] ETSI SMG2, "UTRA physical layer description FDD parts," Tech. Rep. v0.4, 1998-06-25, ETSI STC SMG2 UMTS-L1, June 1998.

[160] ETSI SMG2, "The ETSI UMTS terrestrial radio access (UTRA) ITU-R RTT candidate submission," tech. rep., ETSI STC SMG2, May/June 1998.

[161] C. E. Shannon, "A mathematical theory of communication," *Bell Systems Technical Journal*, vol. 27, pp. 379–423, 623–656, 1948.

[162] R. W. Hamming, "Error detecting and correcting codes," *Bell Systems Technical Journal*, vol. 29, pp. 147–160, 1950.

[163] M. J. E. Golay, "Notes on digital coding," *Proceedings of IEEE*, vol. 37, p. 657, 1949.

[164] M. Y. Rhee, *Error-Correcting Coding Theory*. McGraw-Hill, 1989.

[165] S. Wicker, *Error Control Systems for Digital Communication Storage*. Prentice Hall, Englewood Cliffs, NJ, USA, 1995.

[166] M. C. Valenti, *Iterative detection and decoding for wireless communications*. PhD thesis, Blackburg, Virginia, 1998.

[167] I. S. Reed and G. Solomon, "Polynomial codes over certian finite fields," *SIAM Journal on Applied Mathematics*, vol. 8, pp. 300–304, 1960.

[168] S. Lin, T. Kasami, T. Fujiwara, and M. Fossorier, *Trellises and trellis-based decoding algorithms for linear block codes*. Kluwer Academic Publishers, 1998.

[169] G. D. Forney, *Cancatenated Codes*. Cambridge, MA: MIT Press, 1966.

[170] C. Berrou, A. Clavieux, and P. Thitimasjshima, "Near Shannon limit error-correcting coding and decoding," in *ICC'93: International Conference on Communications*, (Geneva, Switzerland), pp. 1064–1070, May 1993.

[171] M. P. C. Fossorier, F. Burkert, S. Lin, and J. Hagenauer, "On the equivalance between SOVA and Max-Log-MAP decodings," *Electronics Letters*, vol. 2, pp. 137–139, May 1998.

[172] S. Benedetto, G. Montorsi, D. Divsalar, and F. Pollara, "Serial concatenation of interleaved codes: Performance analysis, design, and iterative decoding," *JPL TDA Progress Report*, vol. 42, August 1996.

[173] S. Benedetto and G. Montorsi, "Serial concatenation of block and convolutional codes," *Electronics Letters*, vol. 32, pp. 887–888, May 1996.

[174] S. Benedetto and G. Montorsi, "Unveiling turbo codes: Some results on parallel concatenated codings schemes," *IEEE Transactions on Information Theory*, vol. 42, pp. 409–428, March 1996.

[175] S. Benedetto, D. Divsalar, G. Montorsi, and F. Pollara, "Serial concatenation of interleaved codes: Performance analysis, design, and iterative decoding," *IEEE Transactions on Information Theory*, vol. 44, pp. 909–926, May 1998.

[176] D. Divsalar, F. Pollara, and R. J. McEliece, "Transfer function bounds on the performance of turbo codes," *JPL TDA Progress Report*, vol. 41, August 1995.

[177] G. D. Forney, "The Viterbi Algorithm," *Proceedings of the IEEE*, pp. 268–278, March 1973.

[178] L. Bahl, J. Cocke, F. Jeinek, and J. Raviv, "Optimal decoding of linear codes for minimizing symbol error rate," *Abstracts of papers, International Symposium on Information Theory*, p. 90, 1972.

[179] L. Bahl, J. Cocke, F. Jeinek, and J. Raviv, "Optimal decoding of linear codes for minimizing symbol error rate," *IEEE Transactions on Information Theory*, vol. 20, pp. 248–287, March 1974.

[180] J. Lodge, R. Young, P. Hoeher, and J. Hagenauer, "Separable MAP 'filters' for the decoding of product and concatenated codes," in *ICC'93: International Conference on Communications*, (Geneva, Switzerland), pp. 1740–1745, May 1993.

[181] A. J. Viterbi, "An intuitive justification and a simplified implementation of the MAP decoder for convolutional codes," *IEEE Journal of Selected Areas in Communications*, vol. 16, pp. 260–264, February 1998.

[182] J. Hagenauer and P. Hoeher, "A Viterbi algorithm with soft-decision outputs and its applications," in *IEEE GLOBECOM'89*, (Dallas, Texas), pp. 1680–1686, 1989.

[183] J. Hagenauer, "Iterative decoding of binary block and convolutional codes," *IEEE Transactions on Information Theory*, vol. 42, pp. 429–445, March 1996.

[184] J. Hagenauer and L. Papke, "Decoding turbo codes with the soft-output Viterbi algorithm SOVA," in *International Conference on Information Theory*, (Trondheim, Norway), p. 164, June 1994.

[185] F. Berens, A. Worm, H. Michel, and N. Wehn, "Implementation aspects of turbo-decoders for future radio applications," in *IEEE VTC'99: Vehicular Technology Conference*, (Amsterdam, The Netherlands), pp. 2601–2605, September 1999.

[186] S. Benedetto and D. Divsalar, "Turbo codoes: Comprehension, performance, analysis, design and iterative decoding." GLOBECOM'98 Tutorial, Sydney, Australia, November 1998.

[187] P. Robertson, "Improving decoder and code structure of parallel concatenated recursive systematic (turbo) codes," in *IEEE International Conference on Universal Personal Communication (ICUPC)*, pp. 183–187, 1994.

[188] P. Robertson, "Illuminating the structure of parallel concatenated recursive systematic (turbo) codes," in *IEEE GLOBECOM*, pp. 1298–1303, 1994.

[189] G. Ungerboeck, "Trellis-Coded Modulation with redundant signal sets - Part 1:Introduction," *IEEE Communications*, vol. 25, pp. 5–11, February 1987.

[190] G. Ungerboeck, "Trellis-Coded Modulation with redundant signal sets - Part II:State of the art," *IEEE Communications Magazine*, vol. 25, pp. 12–21, February 1987.

[191] E. Hall and S. G. Wilson, "Design and analysis of turbo codes on rayleigh fading channels," *IEEE Journal of Selected Areas in Communications*, vol. 16, pp. 160–174, February 1998.

[192] J. Craig, "A new, simple and exact result for calculating probability of two-dimensional signal constellations," *Proceedings IEEE MILCOM*, pp. 25.5.1–25.5.5, 1991.

[193] S. Benedetto and G. Montorsi, "Performance of continuous and blockwise decoded turbo codes," *IEEE Communications Letters*, vol. 1, pp. 77–79, May 1997.

[194] D. J. van Wyk, I. J. Oppermann, and L. P. Linde, "Low rate coding considerations for space-time coded DS/CDMA," in *IEEE VTC'99: Vehicular Technology Conference*, (Amsterdam, The Netherlands), pp. 2520–2524, September 1999.

[195] D. J. van Wyk and L. P. Linde, "Fading correlation and its effect on the capacity of space-time turbo coded DS/CDMA systems," in *Proceedings of IEEE MILCOM '99*, (Atlantic City, U.S.A), November 1999.

[196] A. Narula, M. D. Trott, and G. W. Wornell, "Information-theoretic analysis of multiple-antenna transmission diversity," in *ISITA'96: Proceedings of the International Symposium on Information Theory and Applications*, September 1996.

[197] A. Narula and M. D. Trott, "Multiple-antenna transmission with partial side information," in *ISIT'96: Proceedings of the International Symposium on Information Theory*, July 1996.

[198] M.-C. Lin and S.-C. Ma, "A coded modulation scheme with interblock memory," *IEEE Transactions on Communications*, vol. 42, pp. 911–916, February/March/April 1994.

[199] C.-H. Chuang and L.-S. Lee, "A coded modulation design with equal utilization of signal dimensions using a simple convolutional code," in *International Symposium on Information Theory and its Applications*, (Sydney, Australia), pp. 469–473, November 1994.

[200] D. Chase, "Digital signal design concepts for a time-varying rician channel," *IEEE Transactions on Communications*, vol. 24, pp. 164–172, February 1976.

[201] V. Tarokh, A. Naguib, N. Seshadri, and A. R. Calderbank, "Low-rate multi-dimensional space-time codes for both slow and rapid fading channels," in *PIMRC'97: International Symposium on Personal Indoor and Mobile Radio Communications*, (Helsinki, Finland), pp. 1206–1210, September 1997.

[202] N. Seshadri, V. Tarokh, and A. R. Calderbank, "Space-time codes for wireless communications: Code construction," in *VTC'97: Vehicular Technology Conference*, pp. 637–641, 1997.

[203] V. Tarokh, N. Seshadri, and A. R. Calderbank, "Space-time codes for high data rate wireless communication: Performance criterion and code construction," *IEEE Transactions on Information Theory*, vol. 44, pp. 744–765, March 1998.

[204] A. F. Naguib, V. Tarokh, N. Seshadri, and A. R. Calderbank, "A space-time coding modem for high-data-rate wireless communications," *IEEE Journal on Selected Areas in Communication*, vol. 16, pp. 1459–1478, October 1998.

[205] I. E. Telatar, "Capacity of multi-antenna Gaussian channels." submitted to IEEE Transactions on Information Theory.

[206] G. J. Foschini and M. J. Gans, "Capacity when using diversity at transmit and receive sites and the Rayleigh-faded matrix channel is unknown at the transmitter," in *WINLAB Workshop on Wireless Information Networks*, (New Brunswick, New Jersey), March 1996.

[207] R. L. Urbanke, *On multiple access communications*. PhD thesis, Washington University, Sever Institute of Technology, 1995.

[208] B. Rimoldi and R. L. Urbanke, "On the structure of the dominant face of multiple-access channels," in *IEEE Information Theory and Communications Workshop*, (Kruger National Park, South Africa), pp. 12–14, June 1999.

[209] A. D. Wyner, "Recent results in the Shannon theory," *IEEE Transactions on Information Theory*, vol. IT-20, pp. 2–10, January 1974.

[210] N. Chayat and S. Shamai (Shitz), "Convergence properties of iterative soft onion peeling," in *IEEE Information Theory and Communications Workshop*, (Kruger National Park, South Africa), pp. 9–11, June 1999.

[211] E. A. Fain and M. K. Varanasi, "Signal design to optimize the total capacity of multiuser decoders under location-invariant bandwidth constraints," in *GLOBECOM'99: Communications Theory Mini Conference*, (Sydney, Australia), pp. 100–105, November 1998.

[212] M. K. Varanasi and T. Guess, "Optimum decision feedbackmultiuser equalization with successive decoding achieves the total capacity of the Gaussian multiple-access channel," in *Proceedings of Asilomar Conference on Signals, Systems and Computers*, pp. 1405–1409, November 1997.

[213] M. K. Varanasi, "Parallel group detection for synchronous cdma communication over frequency-selective fading channels," *IEEE Transactions on Information Theory*, vol. 43, pp. 116–128, January 1996.

[214] E. Zehavi and A. J. Viterbi, "On new classes of orthogonal convolutional codes," *Communicatio, Control and Signal Processing*, pp. 257–263, 1990.

[215] K. Rikkinen, "Comparison of very low rate coding methods for CDMA radio communications systems," in *Proceedings of ISSSTA '94*, (Oulu, Finland), pp. 268–272, July 1994.

[216] D. J. van Wyk and L. P. Linde, "Turbo-coded/multi-antenna diversity combining scheme for DS/CDMA systems," in *Proceedings of ISSSTA '98*, (Sun City, South Africa), pp. 18–22, September 1998.

[217] D. J. van Wyk, L. P. Linde, and P. G. W. Van Rooyen, "On the performance of a turbo-coded/multi-antenna transmission diversity scheme for DS/CDMA systems with adaptive channel estimation," in *ICT'99: International Conference on Telecommunications*, (Cheju, Korea), June 1999.

[218] D. J. van Wyk, I. J. Oppermann, and L. P. Linde, "Performance tradeoff among spreading, coding and multiple-antenna transmit diversity for capacity space-time coded DS/CDMA," in *Proceedings of IEEE MILCOM '99*, (Atlantic City, U.S.A), November 1999.

[219] D. J. van Wyk and P. G. W. van Rooyen, "A serial concatenated turbo transmit diversity technique with unequal error protection capability." Preliminary International Patent. Sony Laboratories, Japan, 2000.

[220] D. J. van Wyk and L. P. Linde, "A turbo coded DS/CDMA system with embedded Walsh-Hadamard codewords: Coder design and performance evaluation," in *Proceedings of ISSSTA '98*, (Sun City, South Africa), pp. 359–363, September 1998.

[221] D. J. van Wyk and L. P. Linde, "Design and performance evaluation of a Turbo/Walsh-Hadamard coded DS/CDMA system," *The Transactions of the SAIEE*, vol. 88, pp. 17–27, September 1998.

[222] D. J. van Wyk and P. G. W. van Rooyen, "Super-orthogonal turbo transmit diversity." Preliminary International Patent. Sony Laboratories, Japan, 2000.

[223] S. A. Barbulescu, *Iterative decoding of turbo codes and other concatenated codes*. PhD thesis, University of South Australia, February 1996.

[224] D. Divsalar and F. Pollara, "Turbo codes for PCS applications," in *ICC'95: International Conference on Communications*, (Seatle, WA), pp. 54–59, June 1995.

[225] M. Rouanne and D. J. Costello, "An algorithm for computing the distance spectrum of trellis codes," *IEEE Journal on Selected Areas in Communications*, vol. 7, pp. 929–940, August 1989.

[226] D. Divsalar and F. Pollara, "On the design of turbo codes," *JPL TDA Progress Report*, vol. 42-123, pp. 99–121, November 1995.

[227] D. J. van Wyk, "Four-dimensional Q^2PSK modulation and coding for mobile digital communication," Master's thesis, University of Pretoria, South Africa, April 1996.

[228] J. E. Cilliers, D. J. van Wyk, and L. P. Linde, "A synchronous Q^2PSK DS-CDMA system: System conceptualisation, implementation and performance analysis," in *Proceedings of ISSSTA '98*, (Sun City, South Africa), pp. 18–22, September 1998.

[229] K. Rohani and L. M. A. Jalloul, "Orthogonal transmit diversity for direct spread CDMA," tech. rep., ETSI SMG2 Wideband Concept Group, September 1997.

[230] L. M. A. Jalloul, K. Rohani, K. Kuchi, and J. Chen, "Performance analysis of CDMA transmit diversity methods," in *IEEE VTC'99: Vehicular Technology Conference*, (Amsterdam, The Netherlands), pp. 1326–1330, September 1999.

[231] T. Instruments, "Space-time block coded transmit antenna diversity for WCDMA," tech. rep., UMTS SMG2-L1, December 1998.

[232] A. Salmasi and K. Gillhousen, "On the design aspects of code division multiple access (CDMA) applied to digital cellular and personal communication networks," in *IEEE VTC'99: Vehicular Technology Conference*, (St. Louis, MO), pp. 57–62, May 1991.

[233] J. Grimm, M. P. Fitz, and J. V. Krogmeier, "Further results on space-time coding for Rayleigh fading," in *Proceedings of 1998 Allerton Conference on Communications*, September 1998.

[234] D. Divsalar and M. K. Simon, "The design of Trellis Coded MPSK for fading channels: Performance Criteria," *IEEE Transactions on Communications*, vol. 36, pp. 1004–1012, September 1988.

[235] D. Divsalar and M. K. Simon, "The design of Trellis Coded MPSK for fading channels: Set Partitioning for optimum code design," *IEEE Transactions on Communications*, vol. 36, pp. 1013–1021, September 1988.

[236] D. J. van Wyk, I. J. Oppermann, E. Pretorius, and P. G. W. van Rooyen, "On the construction of layered space-time coded modulation STCM codes employing MTCM code design techniques," in *IEEE VTC'99: Vehicular Technology Conference*, (Amsterdam, The Netherlands), pp. 2969–2973, September 1999.

[237] D. J. van Wyk, M. P. Lötter, L. P. Linde, and P. G. W. van Rooyen, "A multiple trellis coded Q^2PSK system for wireless local loop," in *PIMRC'97: International Symposium on Personal Indoor and Mobile Radio Communications*, (Helsinki, Finland), pp. 624–628, September 1997.

[238] P. Robertson, "Coded modulation scheme employing turbo codes," *Electronics Letters*, vol. 31, no. 18, pp. 1546–1547, 1995.

[239] P. Roberston and T. Worz, "A novel bandwidth efficient coding scheme employing turbo codes," in *ICC'96: International Conference on Communications*, (Dallas, Texas, USA), pp. 962–967, June 1996.

[240] D. Divsalar and M. K. Simon, "Multiple Trellis Coded Modulation (MTCM)," *IEEE Transactions on Communications*, vol. 36, pp. 410–419, April 1988.

[241] P. D. Alexander, L. K. Rasmussen, and C. B. Schlegel, "A linear receiver for coded multiuser CDMA," *IEEE Transactions on Communications*, vol. 45, pp. 605–610, May 1997.

[242] L. L. Scharf, *Statistical Signal Processing.* Addison Wesley, 1990.

[243] M. R. Koohrangpour and A. B. Svensson, "Joint interference cancellation and Viterbi decoding in DS-CDMA," in *PIMRC'97: International Symposium on Personal Indoor and Mobile Radio Communications*, (Helsinki, Finland), pp. 1161–1165, September 1997.

[244] J. G. Proakis, *Digital Communications.* McGraw-Hill, third ed., 1989.

[245] J. S. Lee and L. E. Miller, *CDMA Systems Engineering Handbook.* Artech House Publishers, 1998.

[246] S. Haykin, *Digital Communications.* Wiley, 1988.